A Single Compound Alternative to a Buprenorphine/Naltrexone Combination

Irna Elina Ridzwan

A thesis submitted for the degree of Doctor of Philosophy

University of Bath

Department of Pharmacy and Pharmacology

May 2012

……

(IRNA ELINA RIDZWAN)

Table of contents

List of Tables

List of Figures

Acknowledgements

I would like to express my high appreciation and thankful to both of my supervisors, Prof Dr Stephen Husbands and Dr Chris Bailey for their guidance, commitment and continuous support throughout my PhD. A special thanks to Dr Gerta Cami-Kobeci, who trained me in the lab for both components of this PhD project. Also to Dr Emma Casey and Dr Janet Lowe, thanks for their time to proof read this thesis. To all the lab members (Medicinal Chemistry (5W 3.14) and Pharmacology (5W 2.50)) thanks for the precious moments. To my parents, Ridzwan Hashim and Maimun Abdul Hadi, thanks for the continuous support. Finally, I would like to acknowledge my sponsors, the Malaysia Ministry of Higher Education (MOHE) and International Islamic University Malaysia (IIUM) for funding my PhD studies.

Abstract

Relapse to drug taking is a major factor contributing to the low success rate of opioid addiction treatment programmes. Recently, studies have revealed a buprenorphine/naltrexone combination had successfully increased the treatment retention rate (compared to naltrexone alone) among heroin addicts (with history of cocaine abuse) who had undergone detoxification. However, buprenorphine and naltrexone could not be administered as a single formulation due to their different bioavailability, which could create compliance issues. Therefore, in this project, we aimed to synthesise a series of ligands each having the pharmacological profile of the buprenorphine/naltrexone combination (partial agonist (ORL-1 receptors), antagonist (μ- and κ-opioid receptors)). Based on the group's previous work, this profile can be achieved within the orvinols series. Compound BU127, a buprenorphine analogue with phenyl substituent (C_{20}) is very close to the desired profile. Therefore, in order to optimize BU127's profile, we designed and synthesised a series of aromatic analogues, including analogues with a small group attached to the aromatic system to increase the ORL-1 receptor efficacy, while retaining the low efficacy / antagonist activity at the μ-opioid receptor and antagonist activity at κ-opioid receptor. However, [^{35}S]GTPγS screening has shown a sudden increase of κ-opioid receptor efficacy with these modifications. The related compound BU10119, having a C_7-methyl, met the desired profile at all targeted receptors in the [^{35}S]GTPγS screen. A few analogues were selected for further evaluation in functional assays in the isolated tissue preparations (rat vas deferens (for the ORL-1 and μ-opioid receptors) and mouse vas deferens (for the κ-opioid receptor)) to estimate their binding affinity (K_B) and potency (pA_2) of the compounds relative to buprenorphine, using Schild analysis and Schild equation. Of the analogues synthesised, only compounds BU127 and BU10119 have met the desired profile at the targeted receptors (competitive reversible at the ORL-1 and μ-opioid receptors) and having binding affinity at each receptor similar to buprenorphine (ORL-1, μ- and κ-opioid receptors). Based on these results, at this point, the optimum features of buprenorphine analogues in order to achieve the targeted profiles are having a small group at C_7 and a 6-membered aromatic substituent at C_{20} without any substituent group attached to the aromatic ring.

LIST OF ABBREVIATIONS

A°	Angstrom
ANOVA	Analysis of variance
Arg	Arginine
ATS	Amphetamine-type stimulants
BCA	Bicinchoninic acid
Bu	Butyl
°C	Celsius
cAMP	Cyclic adenosine monophosphate
CHO	Chinese hamster ovarian
CI	Confidence interval
COSY	Correlation spectroscopy
CPM	Cyclopropylmethyl
CPP	Conditioned-placed preference
CR	Concentration ratio(s)
CRE	cAMP response element
CREB	cAMP response element binding
CTAP	H-D-Phe-Cys-Tyr-D-Trp-Arg-Thr-Pen-Thr-NH_2
CYP450	Cytochrome P450
d	Doublet
DA	Dopamine
DADLE	[D-Ala^2, D-Leu^5]-Enkephalin
DAMGO	[D-Ala^2,*N*-Me-Phe^4,Gly^5-ol]enkephalin acetate
DAT	Dopamine transporter
dd	Doublet of doublets
DCM	Dichloromethane
DEAD	Diethyl azodicarboxylate
DEPT	Distortionless Enhancement by Polarization Transfer
DIAD	Diisopropyl azodicarboxylate
DIHD	Diisopropyl hydrazinodicarboxylate
DMEM	Dulbecco's Modified Eagle Medium
DMF	Dimethylformamide
DMSO	Dimethylsulfoxide
equiv.	Molar equivalent
Et	Ethyl

EtOAc	Ethyl acetate
EtOH	Ethanol
FBS	Fetal bovine serum
g	Gram
GABA	Gamma-aminobutyric acid
GDP	Guanosine diphosphate
GPCR	G-protein-coupled receptor
GPI	Guinea pig ileum
GTP	Guanosine triphosphate
HMPA	Hexamethylphosphoramide
Hz	Hertz
i.c.v	Intracerebroventricular
i.p	Intraperitoneal
IP_3	Inositol(1,4,5)triphosphate
IP_4	Inositoltetrakiphosphate
IR	Infrared spectroscopy
J	Joule
kg	Kilogram
LC	Locus coeruleus
Leu	Leucine
LSD	Lysergic acid diethylamide
Lys	Lysine
m	Multiplet
m-	Meta
M	Molecular mass
Me	Methyl
MeOH	Methanol
Met	Methionine
mg	Miligram
MHz	Megahertz
min	Minute(s)
MOH	Ministry of Health, Malaysia
ml	Mililitre
MLCK	Myosin light-chain kinase
µM	Micromolar
mmol	Milimol

MVD	Mouse vas deferens
m/z	Mass to charge ratio
NA	Noradrenaline
NAcc	Nucleus accumbens
NIDA	National Institute on Drug Abuse
nM	Nanomolar
NMR	Nuclear magnetic resonance
nor-BNI	Norbinaltorphimine
nsb	Non-specific binding
o-	Ortho
ORL-1	Opioid receptor like
p-	Para
P	Purinergic
P	Partial
PBS	phosphate buffered saline
pCREB	Phosphorylated cAMP response element binding
Pet.Ether	Petroleum ether
PFC	Prefrontal cortex
Phe	Phenylalanine
PhMe	Toluene
PKA	Protein kinase A
ppm	Parts per million
Pr	Propyl
PrSNa	Sodium propanethiolate
psi	Pounds per square inch
q	Quadruplet
Rf	Retention factors
RVD	Rat vas deferens
SAMHSA	Substance Abuse and Mental Health Services Administration
SAR	Structure-activity relationship
s.c	Subcutaneous
S.E.M	Standard error of the mean
SPA	Scintillation proximity assay
t	Triplet
t-	Tertiary
TI	Therapeutic index

TLC	Thin Layer Chromatography
Tyr	Tyrosine
UNODC	United Nations Office on Drugs and Crime
VTA	Ventral tegmental area
wequiv.	Weight equivalent
WHO	World Health Organization
δ	Chemical shifts

CHAPTER 1.0: INTRODUCTION

1.1 General Introduction

Drug addiction is a chronic brain disorder and illness characterized by the persistent compulsive drug-seeking and drug-taking behaviours regardless of the harmful consequences (Feltenstein *et al.*, 2008; Trigo *et al.*, 2010). Substances that cause addiction usually share similar characteristics such as having reinforcing effects. According to the National Institute on Drug Abuse (NIDA), the commonly abused substances are opioids / morphine derivatives (eg: heroin), stimulants (eg: cocaine, amphetamine-type stimulants (ATS)), alcohol (ethanol), cannabinoids (eg: marijuana), dissociative drugs (eg: ketamine) and hallucinogens (eg: lysergic acid diethylamide (LSD)) (NIDA, 2010).

.

In 2008, the United Nations Office on Drugs and Crime (UNODC) estimated that 3.5-5.7% (155-250 million) of the world population aged 15-64 had used illicit substances at least once, with the highest usage reported for marijuana (2.9-4.3%), followed by ATS (0.3-1.2%), cocaine (0.3-0.4%) and opioids (0.3-0.5%) (UNODC, 2010). Alcohol was not included in this report. Based on the UNODC latest report (2010), the treatment demands for opioids ranked the highest among the list of drug problems (opioids, cannabis, cocaine-type, ATS) being treated in the European countries and Asia region in 2008, with the percentage of 57% and 62% respectively. These data which were based on delivery of treatment services for problem drug users indirectly reflects the main type of drug abuse in those regions (opioids) (UNODC, 2010).

Various treatment options for opioid addiction are available, either detoxification followed by long term maintenance on substitution therapy (usually 2 years minimum) or rapid detoxification followed by relapse prevention (WHO, 2009). The three main types of opioid dependence treatment are opioid agonist (full and partial opioid agonist), opioid antagonist and α_2-adrenergic agonist (eg: clonidine) (McLellan *et al.*, 2000; WHO, 2009). The opioid agonists and the opioid antagonist act directly on the μ-opioid receptors, the same receptor on which abused opiates such as heroin, morphine and oxycodone act (Dole, 1988). Methadone (a long full

acting μ-opioid receptor agonist) acts in a similar manner to morphine and heroin and so is used in substitutions for illicit opiates for long-term maintenance therapy. Naltrexone (a non-selective opioid receptor antagonist) is used, after successful detoxification in attempt to prevent relapse, to directly block the μ-opioid receptor responsible for the reinforcing effects of illicit opioids (Kirchmayer *et al.*, 2002). Clonidine, an α_2-adrenergic agonist acts by decreasing the noradrenaline (NA) activity in the central nervous system, which is increased during withdrawal (Gossop, 1988; Nutt *et al.*, 2008). As such, clonidine is most often used during detoxification to reduce the severity of withdrawal symptoms (Ponizovsky *et al.*, 2006; WHO, 2009). It is not widely used in the outpatient settings, especially because of the hypotension and sedation side effects (Mannelli *et al.*, 2012).

The principle behind the substitution (or maintenance therapy) with the μ-opioid agonist is to substitute and stabilize addicts with a safe and clinically controlled dose of opioid under medical supervision (MOH, 2005). Methadone and buprenorphine are equally recommended by the World Health Organization (WHO) for opioid agonist maintenance therapy (WHO, 2009). Since methadone is cheaper than buprenorphine and has been in use for longer, it is more widely used in many countries as the first line treatment for opioid-dependence (Saxena, 2010). However, there is not only a high drop-out rate from methadone maintenance treatment programmes, which was reported to be associated with concomitant use of cocaine and opioids (Montoya *et al.*, 2004), but the incidence of relapse back to taking illicit opiates is also high, with around 55-80% relapse rate within 1 year of the treatment completion (Tkacz *et al.*, 2012).

Even after receiving treatment, the majority of opioid addicts relapse back to drug-taking following a period of abstinence. Furthermore, a large proportion of opioid addicts are addicted to more than one drug of abuse, termed ‘polydrug addiction’ (addiction to multiple substances from different pharmacological groups, eg: heroin and cocaine) (Downey *et al.*, 2000; Leri *et al.*, 2003; McCann, 2008; McLellan *et al.*, 2000; Minozzi *et al.*, 2011). Various studies have shown that naltrexone was only clinically beneficial for highly motivated patients and the overall retention rate with this treatment agent was low due to the serious withdrawal side effects (Gerra *et al.*, 2006; Rothman *et al.*, 2000). Moreover, post-hoc studies to review the effectiveness

of the naltrexone alone treatment to prevent relapse have shown that this single pharmacotherapy agent has no significant effects in preventing relapse to opioid use compared to placebo (Kirchmayer *et al.*, 2002; Minozzi *et al.*, 2011). Therefore, the current treatment programmes for opioid addiction are poorly effective, and there are no current effective treatments for polydrug addiction.

Although buprenorphine is listed as one of the pharmacological options for opioid-dependence treatment, due to its cost, the use of buprenorphine is believed to be less than optimal. Buprenorphine is an opioid with partial agonist activity at the μ-opioid receptor. As such, as described above, it is used as an opioid substitution therapy. However, it has a more extensive pharmacology than methadone as it also acts as an antagonist at the κ-opioid receptor, an antagonist at the δ-opioid receptor and a partial agonist at the opioid receptor like (ORL-1) receptor (Bloms-Funke *et al.*, 2000; Gerra *et al.*, 2006; Leander, 1988; Lutfy *et al.*, 2004; Martin *et al.*, 1976; Montoya *et al.*, 2004). The mixed agonist/antagonist profile of buprenorphine has made this drug unique compared to the other opioids used for substance abuse related pharmacotherapy. Not only has it a lower dependence liability, studies have also suggested that buprenorphine may be effective in treating cocaine addiction and alcohol dependence, leading to the idea that buprenorphine-based therapies may be beneficial for polydrug addiction treatment (Ciccocioppo *et al.*, 2007; June *et al.*, 1998; Kosten *et al.*, 1989; Lutfy *et al.*, 2004; Mello *et al.*, 1993; Mello *et al.*, 1989; Montoya *et al.*, 2004).

These two problems (relapse and polydrug addiction) have become the major concern among the healthcare providers and a challenge to the scientists to find solutions to overcome these matters. In this project, our main aim is to find a new drug lead to prevent relapse following successful detoxification. The pharmacological profile targeted may also have potential for the treatment for polydrug abuse.

1.2 Neurocircuitry of Drug Addiction

All drugs of abuse exert their rewarding or euphoric effects by increasing dopamine (DA) release in the nucleus accumbens (NAcc) and frontal cortex (Figure 1.1) (Hollinger, 2008).

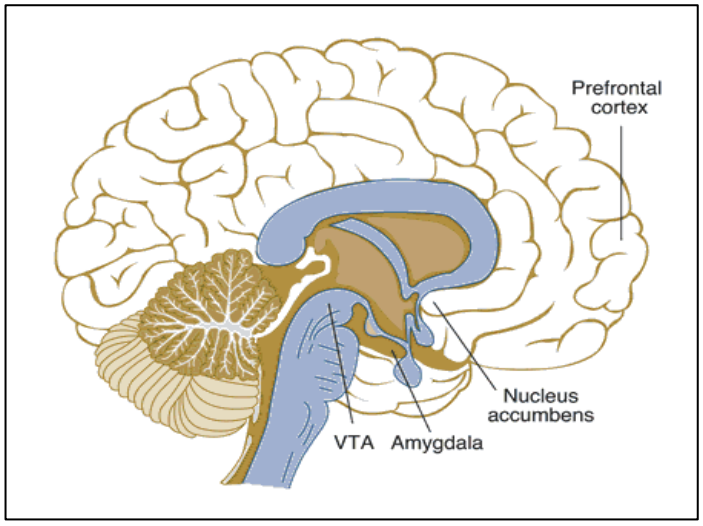

Figure 1.1: Location of brain regions related to drug addiction (Thatcher *et al.*, 2008).

The cell bodies of the dopaminergic neurons responsible for the rewarding effects are located in the ventral tegmental area (VTA) in the mid brain (Spanagel *et al.*, 1999). The corticostriatolimbic circuits, where the end terminals of the dopaminergic neurons are projected include the limbic structures (eg: amygdala, ventral pallidum, hippocampus, NAcc) and corticol areas (eg: prefrontal cortex (PFC)), which are responsible for different characteristics of addiction-related behaviours (Table 1.1) (Feltenstein *et al.*, 2008). In general, the mesolimbic pathway is responsible for the acute reinforcing effects of the addictive drugs and learning-engaged process of addiction, which in the animal models is seen as a conditional response to the environment paired with the drug-cues; while the mesocortical pathway is associated with the compulsive drug-seeking and drug-taking behaviours (Feltenstein *et al.*, 2008).

Similar to most of the other neurotransmitters, the vesicle-contained dopamine is released through Ca^{2+}-dependent exocytosis from the presynaptic nerve terminals during neuronal depolarisation (Rang *et al.*, 2007). Although the commonly abused drugs have very different pharmacologies, they act similarly in increasing the extracellular DA levels during acute exposure, mainly in the NAcc (Duvauchelle *et al.*, 2000; Pontieri *et al.*, 1995; Spanagel *et al.*, 1999). For example, stimulants (eg: cocaine, amphetamine) increase the levels of extracellular DA at presynaptic end terminals by inhibiting the dopamine transporter (DAT) in the presynaptic neurons while opioids act by inhibiting the GABAergic interneurons in the VTA of the brain (Brown *et al.*, 2009; Spanagel *et al.*, 1999). The hyperpolarization of these interneurons by μ-opioid agonists blocks the inhibitory synaptic input to the dopamine cells, thus increasing dopaminergic neurons excitatory in the VTA (Johnson *et al.*, 1992; Spanagel *et al.*, 1999). The results of this activity will cause an increase in the extracellular dopamine in the NAcc.

Table 1.1: Addiction-related function of different brain regions in the corticostriatolimbic circuits.

Brain region	Addiction-related behaviour
Nucleus accumbens (NAcc)	Primary reinforcing effects, cue-induced reinstatement
Ventral pallidum	
Amygdala	Stimulus-reward associations
Ventral hippocampus	
Dorsal hippocampus	Stimulus-stimulus associations (contextual learning)
Prefrontal cortex (PFC)	Emotional response, cognitive control

Long term exposure to abused drugs causes disruption of the neurons signalling pathway in the brain (Christie, 2008; Weiss *et al.*, 2001). Dependence and tolerance to the addictive drugs can develop following chronic drug use. The reward pathway becomes less sensitive to drug stimuli and a larger dose is required to achieve the similar euphoric experience (Hollinger, 2008). This phenomenon is known as drug 'tolerance'. Not only is the dopamine release reduced, but the opioid receptor signalling also becomes less efficient (Hollinger, 2008). The cellular neuroadaptations that slowly develop in response to the chronic drug exposures are needed to restore the homeostatic function of the cells (Christie, 2008). This

happens due to the overstimulation of neurotransmitters and neurochemicals in the brain when the drugs are present in the body system (Feltenstein *et al.*, 2008). For example, the downregulation of the dopaminergic signalling pathways is needed in order to counteract the excessive dopaminergic neurons stimulation that happen during acute phase of addiction (Trigo *et al.*, 2010). The reduction of the extracellular dopamine and also the decrease in the opioid receptor signalling, especially the μ-opioid receptor will only become visible during drug abstinence period, especially after acute drug withdrawal (Feltenstein *et al.*, 2008; Hollinger, 2008). This is manifested by the negative mood symptoms (eg: dysphoria).

1.3 Opioid Pharmacology

1.3.1 General classification of opioid receptors

Three major receptors have been identified and widely discussed for their significant interaction with opioid ligands. The classical receptors are mu-opioid receptor (μ), kappa-opioid receptor (κ) and delta-opioid receptor (δ). All of these opioid receptor subtypes differ in function, distribution and affinity towards various ligands, although there is overlap in activity responsible for producing analgesic effects (Atcheson *et al.*, 1994). Principally there are two classes of opioid ligand which compete at the same receptor; opioid agonists stimulate the activity of receptor and opioid antagonists block the activity of agonists (Casy *et al.*, 1986). There are four main endogenous (or natural) ligands, all agonists, for opioid receptors which are β-endorphin which acts non-selectively on all the opioid receptors (μ-, δ- and κ-), leu-enkephalin and met-enkephalin which act mainly on δ-opioid receptor and dynorphin (Corbett *et al.*, 1982), the main ligand that interact with the κ-opioid receptor. All the endogenous ligands may also cross-interact with other opioid receptors having different degrees of selectivity (Lord *et al.*, 1977).

Activation of the μ-opioid receptors exert the μ-agonist characteristic effects such as morphine-like analgesia, euphoria, constipation, respiratory depression, tolerance and physical dependence. Activation of the κ-opioid receptors can cause dysphoria, sedation, meiosis, diuresis and also analgesia (Johnson *et al.*, 2005). On the other hand, activation of the δ-opioid receptor can also cause analgesia as well as immune stimulation (Bidlack, 2000). Activation of the δ-opioid receptor can also induce convulsion, especially with a potent δ-opioid agonist (Broom *et al.*, 2000). Of these receptors, the μ-opioid receptor is the target receptor for most opioid drugs, including for analgesia. The μ-opioid receptors are widely distributed in the brain regions including the cortex, thalamus, hippocampus, locus coeruleus (LC), ventral tegmental area (VTA), nucleus accumbens (NAcc) and amygdala. It is the receptors located in the last three brain regions that are thought to be most responsible in mediating the rewarding and additive properties of opioid drugs (Feltenstein *et al.*, 2008).

Recently, the opioid receptor like (ORL-1) receptor has been identified as a new receptor sharing some similarities with opioid receptors (Meunier *et al.*, 1995). The endogenous ligand of the ORL-1 receptor, nociceptin (also known as orphanin FQ) has a close homology to dynorphin A (the endogenous ligand for κ-opioid receptor, which is also a 17 amino acid-containing peptide (Bignan *et al.*, 2005; Calo *et al.*, 2000). Compared to the other endogenous opioid ligands, nociceptin has a Phe^1 attached to the N-terminal of its peptide instead of Tyr^1 amino acid (Reinscheid *et al.*, 1996). Although the endogenous ligands for the classical opioid receptors do not significantly bind to the ORL-1 receptor, this receptor shares a similar mechanism of action at the cellular levels with the classical opioid receptors, by activating the G_o/G_i G protein (Bignan *et al.*, 2005; Lutfy *et al.*, 2004). The actions of nociceptin at the ORL-1 receptor were not antagonized by classical opioid receptor antagonists such as naloxone, meaning that the ORL-1 receptor has a unique profile (Nicholson *et al.*, 1998; Zaveri, 2011). Previous studies have shown that ORL-1 receptor activation caused either hyperalgesia or analgesia, depending on the route of administration and the dose. In general, the supraspinal administration of nociceptin was reported to induce hyperalgesia while spinal administration caused analgesia (Mogil *et al.*, 2001; Zeilhofer *et al.*, 2003). Nociceptin was also reported to have anxiolytic and antistress effects, believed to be due to the high distribution of ORL-1 receptors and

nociceptin in the amygdala and hippocampus in the brain region which were associated with learning ability and emotion (Bignan *et al.*, 2005).

1.3.2 Mechanism of action of opioids at the cellular level

It is important to understand the mechanism of action of opioid drugs at the cellular level in order to understand how opioid drugs change the cells' responses and produce their therapeutic effects. Besides, the knowledge about activity of opioid drugs at the cellular level also will help to better understand their side effects in different tissues expressing opioid receptors.(Connor *et al.*, 1999).

1.3.3 G-protein-coupled receptors (GPCRs)

Opioid receptors are members of the G-protein-coupled receptor family (GPCR). GPCRs are transmembrane receptors that couple with G-proteins to transmit their signals (Shaqura *et al.*, 2004). At the molecular level, the receptors have 7-transmembrane-spanning domains linked by loops with the N-terminal exposed at the outer layer and the C-terminal exposed intracellularly. There are three extracellular loops and three intracellular loops and the G-protein is thought to be linked to the third intracellular domain (Hollinger, 2008). These proteins reside on the intracellular side of the cell membrane and freely diffuse in a planar movement in the cell membranes and are called G-proteins because they interact with guanine nucleotides (guanine diphosphate (GDP) and guanine triphosphate (GTP)) to regulate their activities. There are 3 subtypes of G-protein (α, β and γ) that all generally co-exist with a single GPCR as a heterotrimer structure. These polypeptides perform their duty as a carrier between the membrane and the central system in the cell (Sheehan and Elliot, 1993). They permit the signal transduction to occur between receptor on the membrane surface and the effectors in the cell either by affecting enzymes or ion-channels.

In the resting state, G-proteins form as a αβγ trimer with an α subunit occupied by GDP, and the βγ complex. This αβγ trimer freely diffuses in the planar membrane of cells. Once the receptor is activated by an agonist, the αβγ trimer binds to the receptor causing the GDP bound to the α-subunit to exchange with intracellular GTP. α-GTP and the βγ complex then dissociate from each other and separately activate or inhibit their effectors. The signalling activities will be terminated when the α-GTP is hydrolysed back to α-GDP by GTPase. Finally, the α-GDP subunit will recombine with the βγ complex into its original trimer formation to complete the cycle (Figure 1.2) (Harrison *et al.*, 2003).

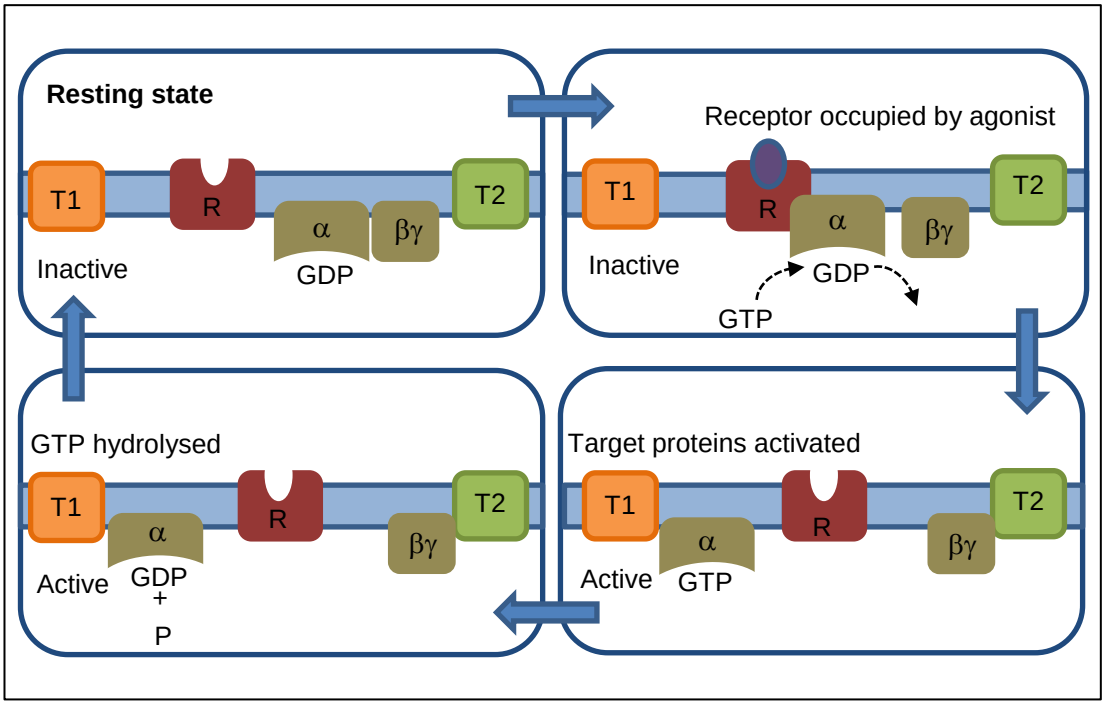

Figure 1.2: The mechanism of G-protein activation. R, receptor; T, target protein.

The G-proteins are further subdivided into three main subtypes depending on the downstream effectors that they interact with (Vauquelin *et al.*, 2007). G_s (stimulatory) or G_i (inhibitory) are named after their interaction with adenylyl cyclase; G_s G-proteins activate adenylyl cyclase and G_i G-proteins inhibit adenylyl cyclase (Vauquelin *et al.*, 2007). The third family of G-protein which is known as G_q mediates the stimulation of phospholipase C and is responsible for phosphoinositide turnover (Sheehan *et al.*, 1993). Receptors that couple to the G_i subtype of G-

protein, also generally couple to the G_o subtype of G-protein (Brody *et al.*, 1998; Dean *et al.*, 2009). As well as downstream effectors mediated by the α subunit, the $\beta\gamma$ complexes can also signal by affecting various ion channels.

Opioid and ORL-1 receptors share the same mechanism of action at the molecular level. They are all linked to $G_{i/o}$ G-proteins, and their activation causes inhibition of adenylyl cyclase, activation of certain potassium channels and inhibition of certain calcium channels (Trigo *et al.*, 2010). The different effects of activation of each opioid receptor subtypes is therefore largely dependent on their localization in the body.

1.4 The Roles of Opioid and ORL-1 Receptors in Drug Addiction

The main aim of this project is to find a new drug lead that can be used during the abstinence period, after the patient has been successfully stabilized with the tapering down dose of substituting opioid (eg: methadone). As mentioned earlier, relapse is most likely to happen during this phase, and treatment with naltrexone alone failed to reduce the relapse incidence following successful detoxification (Minozzi *et al.*, 2011). It is exacerbated by the problem of polydrug abuse (McCann, 2008), and therefore, an additional function of the new drug lead is needed in this population of patients. Therefore, the ideal pharmacological profile of drug that is suggested to achieve these purposes is having a low efficacy / antagonist at the μ-opioid receptor, antagonist at the κ-opioid receptor and partial agonist at the ORL-1 receptor (McCann, 2008).

1.4.1 Lower μ- / μ-opioid receptor antagonism to reduce dependence liability

One of the proposed pharmacological profiles of the proposed new lead is to be a low efficacy agonist, or antagonist at the μ-opioid receptor. Therefore, due to

minimal efficacy at the μ-opioid receptors, this new lead will not have a similar function as the primary substituting opioid that primarily acts as a μ-opioid receptor agonist (eg: methadone and buprenorphine) (Mattick *et al.*, 2008). Although it is indirectly suggesting that this profile is achievable by the naltrexone only treatment (opioid receptor antagonist), it is important to emphasize that this new drug lead will have a combination profiles at three targeted opioid receptors as previously described, and the overall activity is not solely reliant on one activity or another.

Although there will be a concern regarding the withdrawal side effects as the result of suppressing this receptors (Ko *et al.*, 2006; Martin *et al.*, 1976), this new drug lead is planned to replace the primary substituting opioid only after the patient has been stabilized with the lower dose of μ-opioid agonist (MOH, 2005). Considering the activity of this new drug lead on the μ-opioid receptor alone, the compliance issue will be a potential problem, if the new lead is an antagonist at the μ-opioid receptor as seen with naltrexone. By completely blocking the μ-opioid receptor, the addictive nature of any opioid agonists subsequently taken (eg: heroin) would be avoided (Crabtree, 1984; Minozzi *et al.*, 2011), but this will also block the effects of endogenous opioids which can cause aversive and negative motivational effects (Mucha, 1990; Mucha *et al.*, 1985). Besides, there is still the possibility that the patient will experience some degree of withdrawal symptoms even though the primary substituting opioid agonist is weaned-off at the lower dose. Therefore, a slight μ-opioid receptor efficacy might be an advantage compared to a complete μ-opioid receptor antagonist in order to minimize these problems, and importantly, promote compliance.

Despite the compliance issue associated with the use of a μ-opioid receptor antagonist in opioid addiction, this pharmacological approach was found to be highly beneficial in some other substance abuse-related problems (eg: alcohol and cocaine) (Lobmaier *et al.*, 2008; Schmitz *et al.*, 2001), which means by antagonizing the μ-opioid receptor, the problem of polydrug abuse also could be treated. Naltrexone is used as an adjunct therapy in alcohol-dependence patients (Lobmaier *et al.*, 2008). This was also confirmed by previous animal studies where treatment with naltrexone reduced alcohol-seeking behaviour and alcohol relapse (Boyle *et al.*,

1998; Dhaher *et al.*, 2012; Middaugh *et al.*, 2000). Pharmacologically, the similarities of opioid and alcohol dependence are the involvement of β-endorphin in the opioid system which is stimulated in both types of dependencies (Lobmaier *et al.*, 2008). Therefore the treatment principle applied for naltrexone for opioid addiction is also applied to alcohol dependency where the antagonistic activity of naltrexone is believed to block the rewarding effects of alcohol consumption (McLellan *et al.*, 2000) through competitive opioid receptor binding.

Together with the κ-opioid receptor antagonist (which will be discussed in the next paragraph) it is hopeful that the problems seen with naltrexone alone therapy, particularly in opioid dependence patient (Minozzi *et al.*, 2011) can be avoided, and the co-occurring polydrug addiction problems can be treated with this proposed new drug lead.

1.4.2 κ-antagonism to prevent relapse and drug seeking behaviour

The hyperactivity of the κ-opioid receptor system in the brain has been linked to the high tendency to relapse following drug discontinuation, and therefore one of the suggested treatment approaches to prevent relapse to drug taking is by antagonizing the κ-opioid receptor. Earlier studies had indirectly shown the involvement of the κ-opioid receptor system in mediating relapse, as activation of the receptors has been shown to increase various behavioural responses (stress, dysphoria and other psychotomimetic symptoms) (Pfeiffer *et al.*, 1986).

For example, Rothman (2000) has suggested the "κ-overdrive syndrome" phenomenon to explain the high incidence of relapse seen with heroin addicts after completing opioid detoxification (with clonidine) which was shown by negative mood symptoms (eg: dysphoria) during naltrexone maintenance therapy. The κ-overdrive syndrome relates to the body's own homeostatic system to compensate for any abnormal changes that occur within the internal environment (Rothman *et al.*, 2000).

According to this theory, a chronic exposure to a potent exogenous opioid (eg: heroin) will cause an overstimulation of the μ-opioid receptor, and therefore the drug addicts will experience excessive feeling of pleasure (euphoria). The long term effects of opioid use will cause imbalance between μ- and κ-opioid receptors stimulation. As a consequence of chronic drug exposure, the endogenous κ-agonist dynorphin will increase in order to stimulate the activity of κ-opioid receptor to compensate for overstimulation of μ-opioid receptors. However, if addicts stop consuming the drug (eg: heroin, methadone), the μ-opioid receptor will no longer be stimulated leaving the upregulated κ-opioid receptor to exert the major effect. The sudden increase in activity of the κ-opioid receptor will cause dysphoria and psychotomimetic symptoms which are unpleasant. This mood disturbance will be worst during naltrexone therapy where the μ-opioid receptor is suppressed. During this prolonged abstinence period and post-detoxification, relapse is more likely to happen because the endogenous opioid system fails to adequately compensate for the sudden loss of the exogenous opioid (Gold *et al.*, 1981; Tkacz *et al.*, 2012). One of the ways to overcome this mood breakdown is through self-medicating (usually by returning to the illicit drug-taking habits) to overcome chronic dysphoria (Rothman *et al.*, 2000). Therefore, it is believed that by suppressing the κ-opioid receptor during this abstinence period dysphoria can be overcome and prevent relapse to drug taking, which is shown by buprenorphine/naltrexone combination (a functional κ-opioid receptor antagonist) (Gerra *et al.*, 2006).

Rothman's (2000) study was based on clinical observations, where the involvement of dynorphin system cannot be determined, although the possible involvement of the κ-opioid receptor was suggested based on the clinical symptoms presented by the patients. The later studies conducted using animal models of drug reinstatement (drug seeking behaviour) had proved dynorphin is partly responsible in drug-relapse (Beardsley *et al.*, 2005). Interestingly, not only in opioid addicts (Shaham, 1996), the activity of dynorphin was also found to increase with other type of drugs dependence including cocaine (Ahmed *et al.*, 1997; Beardsley *et al.*, 2005; Redila *et al.*, 2008) and ethanol (Le *et al.*, 1998).

If the Rothman (2000) study relates the κ-opioid receptor hyperactivity with negative mood symptoms (eg: dysphoria), animal studies have linked relapse to stress (Beardsley *et al.*, 2005; McLaughlin *et al.*, 2003). Although the behavioural endpoints were quite different, the similarities between these two are the increase in dynorphin activity. A study has been conducted in mice to investigate the relation between stress and behavioural measures of drug seeking behaviour using the conditioned-place preference (CPP) model (McLaughlin *et al.*, 2003). In this model, drug-seeking behaviour can be induced by a stressful stimulus. The prodynorphin level (precursor for dynorphin) is believed to increase following a stressful event (forced swim test) which was proved using an indirect method that compared the stress induced analgesia between the wild-type mice and the dynorphin knock-out mice (McLaughlin *et al.*, 2003). In this study also, the effects of the selective κ-opioid receptor antagonist, norbinaltorphimine (nor-BNI) in reducing the cocaine-seeking behaviour in mice after exposure to the stressful event (forced swim stress) was compared to the group of stress-induced but non-pretreated mice (did not received nor-BNI). From this study, it was found that nor-BNI significantly reduced the time spent in the drug-paired compartment for the stress-induced treatment group compared to the stress-induced non-pretreated group. The differences in the time spent in the drug-paired compartment between the stress-induced non-pretreated group was also compared against the unstressed group. There was no significant difference in these two groups which indicates that nor-BNI has successfully blocked the stress-induced prodynorphin released following the forced swim test. This suggests the potential role of κ-opioid receptor antagonists in reducing relapse incidence following stressful events which is suggested to be associated with an increased in the endogenous κ-opioid agonist activity (prodynorphin) (McLaughlin *et al.*, 2003).

In both cases discussed above, it is clear that chronic drug use causes activation of the κ-opioid system, regardless of drug classes. And by selectively blocking the κ-opioid receptor, drug-relapse can be prevented. It is already known that different drugs of abuse have different modes of action, which depends on their pharmacological classification. Similar to the case of dopamine, where all the abusive drugs increased the extracellular dopamine levels during drug exposure (Duvauchelle *et al.*, 2000), this overlapping also happens with the κ-opioid receptor

system. Therefore, the downstream cellular activity following chronic drug exposure is the key to explain how κ-opioid receptor is involved.

Once dopamine is released in the nucleus accumbens (NAcc) it acts postsynaptically by activating dopamine receptors (principally D_1 and D_2 types). Following D_1 receptor activation, adenylyl cyclase (AC) is activated leading to enhanced levels of cAMP and activation of protein kinase A (PKA). One of the downstream effects of this is phosphorylation of the gene transcription factor, cAMP Response Binding Element (CREB). Indeed, phosphorylated CREB (pCREB) has been reported to increase in the NAcc following chronic drug exposure of cocaine and amphetamine (Edwards *et al.*, 2007; Yin *et al.*, 2006) and during withdrawal from opioids (Chartoff *et al.*, 2003). CREB regulates the transcription of many proteins, and pCREB has been shown to increase synthesis of prodynorphin (Briand *et al.*, 2010). In this way, as all drugs of abuse act to increase dopamine release in the NAcc, all drugs of abuse will in turn lead to enhanced synthesis of prodynorphin.

The κ-opioid receptor is expressed in distinct areas throughout the brain, including the VTA and NAcc (DePaoli *et al.*, 1994). For example, κ-opioid receptors are located on the mesocorticolimbic dopaminergic neurons themselves. As activation of the κ-opioid receptor is generally inhibitory, this leads to a general, and prolonged, decrease in dopamine release in the NAcc and frontal cortex, which is thought to lead to long-term negative mood symptoms seen in abstinent addicts, enhancing the risk of relapse to drug-taking. This explains how dynorphin is increased during chronic drug exposure, and why by blocking the κ-opioid receptor, the relapse associated with hyperactivity of the κ-opioid receptor system which was shown by negative mood symptoms and stress during drug abstinence can be prevented.

1.4.3 ORL-1 as a new target for treatment of drug addiction

The ORL-1 activity of most interest in this project was the role in the treatment of substance abuse, not only for opioid, but also including other reinforcing drugs (eg: cocaine) and also alcohol (Toll *et al.*, 2009). The anti-addiction properties shown in animal models of drug reward were limited but promising. A number of studies have demonstrated that ORL-1 receptor activation reduced the rewarding effects of reinforcing drugs (eg: morphine, cocaine) (Marquez *et al.*, 2008; Rutten *et al.*, 2010; Toll *et al.*, 2009). At the molecular level, intracerebroventricular (i.c.v) administration of nociceptin (30 nmol/10 μl) given 5 minutes before cocaine (10 mg/kg intraperitoneally) significantly decreased extracellular dopamine levels in rats, measured using dialysis samples collected from the nucleus accumbens brain region (NAcc), compared to cocaine controls (Lutfy *et al.*, 2001). In a CPP model of drug reward, the intraperitoneal (i.p) administration of Ro65-6570 (a non-peptide ORL-1 receptor agonist) was found to reduce the time spent in the drug-paired compartment in rats when administered 15 minutes prior to opioid drugs (eg: morphine, heroin) and stimulant (eg: cocaine) (Rutten *et al.*, 2010). A separate study, also conducted in rats found that the ORL-1 receptor antagonist, J-113397 reduced the dose required for morphine to induce CPP which proved that ORL-1 receptor agonist activity reduced the drug rewarding effects (Rutten *et al.*, 2011). In this study, the sensitivity of morphine to induce reinforcing effects was also found to be higher in the ORL-1 knockout rats compared to their wild-types which further proved the involvement of ORL-1 receptor in modulating drug rewards. The attenuation of the rewarding effects after acute cocaine exposures was also reported in the ORL-1 knockout mice compared to their wild-type littermates (Marquez *et al.*, 2008). When J-113397 was given 15 minutes prior to cocaine to block the ORL-1 receptors in the wild-type mice, the rewarding effects of cocaine was increased compared to the control group. All of these evidence pointed that the ORL-1 receptor agonist can be a potential target for 'polydrug addiction' with lower abusive properties due to its anti-rewarding effects compare to the μ-opioid receptor agonist.

To date, there is no single pharmacotherapy agent available in the market that has all of these listed pharmacological profiles that is suggested to be an ideal drug to

prevent relapse to drug taking, that also may be beneficial for the polydrug abusing patient population. However, buprenorphine has the closest pharmacological profile needed (κ-opioid receptor antagonist and partial ORL-1 agonist), but with a partial μ-opioid agonist activity.

1.5 Buprenorphine

Buprenorphine was first brought to market as a long-acting analgesic agent in an injectable dosage form (buprenorphine hydrochloride) (Cowan, 2007; Johnson *et al.*, 2005) but has since become better known as a treatment agent for opioid abuse (WHO, 2009). To date, buprenorphine also available in oral formulation (sublingual tablet) either contains buprenorphine alone (2 mg or 8 mg buprenorphine free base; Subutex®) or in combination of buprenorphine/naloxone in a 4:1 ratio (2 mg/0.5 mg or 8 mg/2 mg free bases; Suboxone®) (Cowan, 2007; Lacy *et al.*, 2005). For a long time it has been the long-lived partial agonist activity at the μ-opioid receptor (Cowan *et al.*, 1995; Martin *et al.*, 1974) that has attracted interest to this compound and led to its current uses. Based on the data by NIDA, buprenorphine's maximum effects are at the dose of 32 mg (base) with no further increase in response when the dose was further increased (SAMHSA, 2004). The effects are sustained for 48 hours (Walsh *et al.*, 1994) which gives advantage on dosing schedule for the patient with alternate day dosing (Amass *et al.*, 2000) compared to methadone which requires strict daily dosing (Dole, 1988; MOH, 2005). The long duration of action of buprenorphine is related to its high lipophilicity and slow dissociation from the receptor (Johnson *et al.*, 2005). Recently the κ-opioid receptor antagonist and possible ORL-1 agonist activity of buprenorphine have also been suggested as being important to its pharmacological profile (Gerra *et al.*, 2006; Rothman *et al.*, 2000). The ceiling effects which occur with buprenorphine may also be due to its activity at the ORL-1 receptor (Lutfy *et al.*, 2003a). This 'ceiling effect' also explains why buprenorphine cannot replace methadone as the first line treatment for heroin-substitution therapy because a patient with high dependence history of heroin needs higher efficacy than buprenorphine can provide (Mattick *et al.*, 2008; SAMHSA, 2004). If given parenterally and intramuscularly, buprenorphine bioavailability ranges between 40% to more than 90% and undergoes a very fast initial distribution ($t^{1/2}d$ = 2-5 minutes) based on its pharmacokinetic data (Johnson *et al.*, 2005).

Buprenorphine undergoes extensive first pass hepatic metabolism by N-dealkylation at cytochrome P450 (CYP450) to produce a polar metabolite, norbuprenorphine (Johnson *et al.*, 2005).

1.5.1 Pharmacology of buprenorphine

Buprenorphine is an opioid with a mixed agonist/antagonist profile at opioid receptors, with partial efficacy at the μ-/ORL-1 receptors and antagonist actions at the κ-opioid receptor. In receptor binding assays conducted either in rodent brain homogenates or in cloned receptors in cell lines, buprenorphine is highly bound to the classical μ-, κ- and δ-opioid receptors, and has moderate binding affinity towards the ORL-1 receptor (Huang *et al.*, 2001; Lutfy *et al.*, 2004; Spagnolo *et al.*, 2008; Toll *et al.*, 1998). Although buprenorphine is also highly bound to the δ-opioid receptor, it is believed to have no significant impact on buprenorphine pharmacological activity (Johnson *et al.*, 2005). Due to the complexity of buprenorphine's receptor profile, the discussion on its clinical and preclinical efficacy as an analgesic drug, its use in the treatment of drug addiction and also its effects on respiratory depression will be discussed separately.

1.5.1.1 **Buprenorphine and analgesia**

As an analgesic drug, buprenorphine is more potent than morphine (0.1 mg/kg/day buprenorphine = 10 mg/kg/day morphine), has a rapid onset (parenterally) and also has a longer duration of action (Martin *et al.*, 1976). The longer duration of action of buprenorphine is also believed to be due to its high lipophilicity that causes slow dissociation once buprenorphine is bound to the receptors (Boas *et al.*, 1985). The superiority in terms of buprenorphine's potency over morphine is varied, and depends on the types of stimuli and species. For example, a study conducted in mice to measure the response to visceral pain in a phenylquinone-induced writhing test has revealed subcutaneous and intraperitoneal buprenorphine were 25-40 times more potent compared to morphine (Cowan *et al.*, 1977a). In the tail-flick test

conducted in mice to measure acute pain associated with noxious stimuli (thermal), buprenorphine is only 5-9 times more potent than morphine (Christoph *et al.*, 2005; Cowan *et al.*, 1977b; Cowan *et al.*, 1971). However the differences in terms of potency between these two drugs is only 2-fold when tested in rats (Cowan *et al.*, 1977a). For a long time, buprenorphine's pharmacological profile has been described as an analgesic that produced a 'bell-shaped' (inverted u-shaped / curvilinear) dose-response curve, due to the response observed in rodents exposed to noxious stimuli (55°C) in a tail dip test (Christoph *et al.*, 2005; Cowan, 2007). Later, the preclinical studies, conducted in animal models of pain, show that the efficacy of buprenorphine depends on many factors, for example the selection of test and the nature of noxious stimuli (Cowan, 2007). Based on the commonly used animal models of pain, the bell-shaped dose response curve was reported in acute pain models (tail-flick, hot plate, and flexor reflex test) and the inflammatory pain model (formalin test) where the analgesic effects tends to decrease when the dose is increased after it reached the maximum response (1-3 mg/kg/day) (Christoph *et al.*, 2005; Cowan *et al.*, 1977b; Cowan *et al.*, 1971; Kamei *et al.*, 1995; Kamei *et al.*, 1997; Martin *et al.*, 1976). In contrast, linear dose-response relationships were observed in the animal models of visceral pain (writhing test) and in rat tail pressure test, which achieved 'ceiling effects' when the doses were further increased (Christoph *et al.*, 2005; Cowan *et al.*, 1977b). In the rat tail pressure test, buprenorphine achieved nearly full efficacy (90%) compared to morphine (100%), but the antinociceptive effects last longer with buprenorphine (Cowan *et al.*, 1977b). The 'ceiling effect' is shown by a plateau of the dose-response curve when the response remained stable after the drug reached a maximal response (Johnson *et al.*, 2005). In relation to analgesia, the 'ceiling effect' is not a barrier only if the pain is fully controlled (Johnson *et al.*, 2005; Walsh *et al.*, 1994). The previous clinical studies also have shown that buprenorphine was as effective as a full opioid agonist in controlling pain, including post-operative pain and some malignant-associated pain (Downing *et al.*, 1977; Noda *et al.*, 1989).

1.5.1.2 **Buprenorphine and respiratory depression**

Both morphine and buprenorphine have been shown to cause respiratory depression. However, the depression was significantly greater in morphine-treated

subjects compared to the buprenorphine group (measured from the arterial partial CO_2 (PCO_2) and partial O_2 (PO_2) values) (Cowan *et al.*, 1977a; Kishioka *et al.*, 2000). A clinical study conducted in non-opioid dependent healthy subjects shows a dose-dependence for the analgesic effects of buprenorphine, but not for respiratory depression (Dahan *et al.*, 2006). This shows that the 'ceiling effect' is clinically more important in relation to the respiratory depression, but not with its analgesic activity. The clinical advantage of having a ceiling effect in respiratory depression is more towards the safety margin of the drug. Respiratory depression is a life-threatening event which is usually associated with morphine and heroin toxicity. Buprenorphine has a wider therapeutic index (TI) (LD_{50}/ED_{50}) compared to morphine, which is about 12000 and 460, respectively, measured from the rat tail pressure test to determine intraperitoneal buprenorphine-induced acute toxicity (respiratory depression) (Cowan *et al.*, 1977a).

In view of the physical dependence in relation to the μ-opioid agonist activity, buprenorphine withdrawal side effects were reported as mild at best with delayed appearance after buprenorphine cessation. For example, chronic treatment with subcutaneous buprenorphine for four consecutive days (0.5 mg/kg twice daily) only produced a weak sign of withdrawal (diarrhoea) following sudden drug discontinuation in some rats, while no other symptoms were observed (Dum *et al.*, 1981). This indicates that although buprenorphine has dependence-liability, it is to a lesser extent as compared to the full μ-opioid agonists. As a partial μ-opioid agonist, buprenorphine partially precipitated withdrawal and suppressed abstinence syndrome in chronic morphine-dependent dogs (Martin *et al.*, 1976). A study conducted in morphine-dependent mice (subcutaneous (s.c) 75 mg morphine implant) shows a bell-shaped buprenorphine dose-effects in suppressing morphine-induced withdrawal symptoms, with the maximum suppressive doses seen at the lower doses (0.01-0.5 mg/kg) and at the highest dose (50 mg/kg) buprenorphine (Lizasoain *et al.*, 1991).

1.5.2 Buprenorphine for polydrug addiction

Although as mentioned above, buprenorphine is largely used currently as substitution therapy for opioid addicts, there have been studies that suggest it may also be effective against other drugs of abuse. The potential effects of buprenorphine on cocaine addiction were initially revealed when some of the patients who were in a methadone-maintenance treatment programme for their heroin addiction problems, were switched to an alternative treatment agent, buprenorphine (Kosten *et al.*, 1989). These patients had a history of both heroin and cocaine addiction prior to their enrolment into the treatment programme. However, during methadone treatment, it was noticed that cocaine use was substantially increased among these patients. This was later discovered to be associated with the longer 'speedball effects' achieved with methadone compared to heroin. It is quite common for the heroin users to take cocaine to achieve more pleasurable effects, although some patients claimed to take cocaine after methadone to overcome sedation and lethargy associated with methadone treatment. This 'speedball effect' was claimed to be ineffective during buprenorphine treatment. 'Speedball effect' is an increased feeling of pleasure or reinforcing value when an opioid (usually heroin) and cocaine are taken together (Duvauchelle *et al.*, 1998; Leri *et al.*, 2003). Therefore, the initial idea of substituting methadone (a full μ-opioid agonist) with buprenorphine (a partial μ-opioid agonist) was to reduce the increasing cocaine-abusing habit among patients during methadone treatment programme (Kosten *et al.*, 1989).

In the clinical setting, it is hard to differentiate the effects of buprenorphine on cocaine addiction on its own since cocaine usually was taken together with heroin in order to get the synergistic effects (McCann, 2008). Studies performed in cocaine-dependent rhesus monkeys have shown that intravenous buprenorphine significantly reduces cocaine self-administration in these subjects, either when buprenorphine is given alone or as a dual therapy with naltrexone (Mello *et al.*, 1993; Mello *et al.*, 1989). Since better outcomes came from the group receiving buprenorphine alone, this suggests that the agonist component of buprenorphine was important in reducing cocaine-dependence (Mello *et al.*, 1993). Buprenorphine and cocaine, not only have different drug classifications, but also have different

mechanism of actions at the cellular level, where buprenorphine acts mainly through the opioid receptor system while cocaine acts mainly through the dopaminergic system (Leri *et al.*, 2003). However, neurochemical studies have shown that both drugs could indirectly cross-interact with the other system especially during chronic drug dependence (Leri *et al.*, 2003; McLellan *et al.*, 2000).

1.5.3 Buprenorphine/naltrexone combination

The high incidence of relapse following cessation of substitution therapy with the full opioid agonist methadone (of the order of 55-85% of addicts relapse within a year of treatment) is thought to be, at least in part, due to the κ-opioid receptor system overdrive syndrome (Minozzi *et al.*, 2011; Rothman *et al.*, 2000; Tkacz *et al.*, 2012). Clinical evidence in support of this theory was provided when the buprenorphine/naltrexone combination significantly increased the treatment retention rate among patients following detoxification with clonidine compared to the group that received naltrexone treatment alone (Rothman *et al.*, 2000). A recent discovery has suggested the positive outcome could also be contributed by the ORL-1 receptor partial agonist activity of buprenorphine (Bignan *et al.*, 2005; Gerra *et al.*, 2006; McCann, 2008; Rothman *et al.*, 2000).

Since a κ-opioid antagonist is not yet available for clinical studies, naltrexone was given together with buprenorphine to leave the functional κ-opioid receptor antagonist activity of buprenorphine dominant (Gerra *et al.*, 2006; Rothman *et al.*, 2000). The objective of this combination was to unmask the κ-opioid antagonistic activity of buprenorphine by blocking the μ-opioid agonist activity of this drug, giving a functional κ-opioid antagonist. Changes of pupil diameters before and during treatment were used as a parameter to monitor the effects of μ-opioid receptor blockade in an effort to ensure that any positive outcome was not due to residual agonist activity at the μ-opioid receptor. In other words, only the κ-opioid antagonist activity of buprenorphine can be seen. Using urine analysis and retention period during 12 weeks treatment, Rothman found that the retention rate with the buprenorphine/naltrexone combination treatment was 33% (compared to 10%

retention rate as reported by Crabtree, 1984) with 5 subjects successfully completing the study and 4 of them with negative urine sample for both opiate and cocaine throughout the 12 weeks observation (Crabtree, 1984; Rothman *et al.*, 2000). However, since there was no control group used in this study, Gerra and co-workers (2006) have come out with an improved study design by introducing a naltrexone only group as a control with almost the same pretreatment procedure and duration of observation used by Rothman, but with a few modifications on the methods and with more subjects recruited. The studies by Gerra supported the findings suggested by Rothman where they found that patients stay longer in treatment with this combination drug therapy with 73.33% compared to 40% subjects completing the 12 weeks study with p values of 0.019 ($p < 0.05$) which helps substantiate the theory suggested by Rothman that the buprenorphine/naltrexone combination does indeed appear to be better than naltrexone only treatment.

1.6 Medicinal Chemistry

1.6.1 Synthesising single compounds to mimic a buprenorphine/naltrexone combination

There is growing evidence suggesting that κ-opioid antagonist activity would be important in preventing relapse and the ORL-1 receptor may also be a promising new target for drug addiction (Gerra *et al.*, 2006; McCann, 2008; Rothman *et al.*, 2000). Evidence for this was provided by the buprenorphine/naltrexone combination, compared to naltrexone alone pharmacotherapy (Gerra *et al.*, 2006). Although the suggestion of combining buprenorphine/naltrexone seems promising, pharmaceutically this combination is not ideal. This is because the bioavailability of these two drugs is very different, with buprenorphine having reasonable bioavailability via the sublingual route compared to naltrexone which can be taken orally. This may lead to non-compliance issues due to a complicated dosing requirement. Therefore a single compound that mimics this combination is desired (McCann, 2008). In this project, a series of buprenorphine analogues have been

synthesised and evaluated in the hope of developing a single compound to mimic the buprenorephine/naltrexone combination within a single compound.

Buprenorphine (Figure 1.3 (c)) is a semi synthetic drug which belongs to the orvinol series of opioids. It is synthesised from thebaine (Figure 1.3 (a), **(1)**), one of the natural alkaloids of *Papaver somniferum* (opium poppy) (Blakemore *et al.*, 2002). Compared to morphine (Figure 1.3 (b)) (the major alkaloid from opium), buprenorphine has a cyclopropylmethyl (CPM) attached at the N_{17} position while morphine retains a N-methyl as found in thebaine. There are also two major structural modifications to the morphinan C-ring. The introduction of an endoethano bridge and also the presence of an extended group at the C_7 position and these are partly responsible for the change from morphine's pharmacological profile, especially related to its potency (Loew *et al.*, 1979).

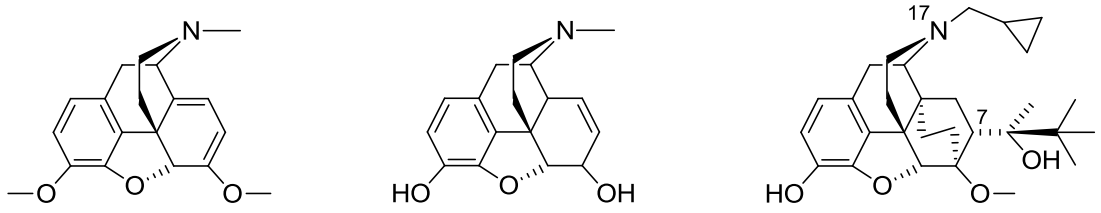

Figure 1.3: Chemical structures of thebaine (a), morphine (b) and buprenorphine (c).

In the 1960's, the investigation of the structure-activity relationship (SAR) of the opioids was initially based on their *in vivo* antinociceptive activities measured using either the tail pressure or the tail flick test which was conducted in rats (Bentley *et al.*, 1972). The antinociceptive (analgesic) activitiy of the new opioid drugs was compared against morphine by measuring the *in vivo* parameters such as the ED_{50} and tail flick withdrawal latency. During this time, the only way to differentiate pharmacological activity between opioids was by comparing their analgesic potency relative to standards. The existence of multiple opioid receptors was first postulated from Martin's study, where different pharmacological characteristics of morphine and

its analogues were identified (Martin *et al.*, 1974). This study, which was conducted in chronic spinal dog, is considered as the major evolution in the opioid field leading to more focused SAR studies based on different opioid receptor types. Later in the 1980's, *in vitro* techniques were introduced and performed in isolated tissues to evaluate opioid functional activity at the different types of opioid receptors (Huidobro-Toro *et al.*, 1981; Kajiwara *et al.*, 1986). This has been followed by other *in vitro* techniques (eg: [^{35}S]GTPγS) which used cell culture in place of isolated tissues (Chapter 1.7.2.1). The development of selective ligands, alongside the development of *in vitro* assays has allowed the terms 'efficacy', 'potency' and 'affinity' to be used with some confidence to compare pharmacological profiles between different opioid drugs.

1.6.2 Structure-Activity Relationship (SAR) of orvinols

Although morphine is widely used as an analgesic drug to control moderate to severe pain, there are many issues with this drug especially related to its side effects. Besides causing tolerance and dependence following prolonged use, an overdose of morphine can cause respiratory depression which is fatal. Therefore, an analgesic with a safer clinical profile and improved pharmacological activity (eg: more potent, longer duration of action) is needed. It was initially thought to be achievable by designing analogues of morphine with more complex and rigid chemical structures (Bentley *et al.*, 1967a). The Diels-Alder adducts of thebaine have been extensively explored by Bentley's group in order to search for the desirable morphine analogues (Bentley *et al.*, 1967a; Bentley *et al.*, 1967b; Bentley *et al.*, 1967d). The orvinols, the major products of this work will be discussed in this thesis since buprenorphine and the products synthesised in this PhD project belong to the orvinol series. The parent structures of orvinol (Figure 1.4 (a)) and buprenorphine analogues (Figure 1.4 (b)) synthesised in this project are shown in Figure 1.4 below:

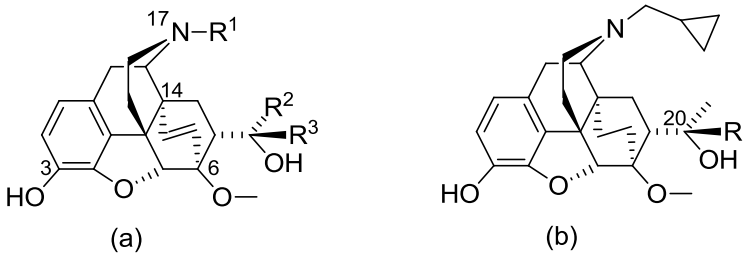

Figure 1.4: Parent structures of orvinol (a) and buprenorphine analogues (b).

The initial SAR investigations conducted by Bentley and his co-workers (1967) were mostly focussed on the orvinol (3-OH) and thevinol (3-OCH_3) with a 6,14-endoetheno bridge (Figure 1.4 (a)).

Substituting the N-methyl with N-allyl in morphine significantly changed the pharmacological profile of morphine to become a morphine antagonist (nalorphine) (Figure 1.5), in the rat tail pressure test (Martin, 1967).

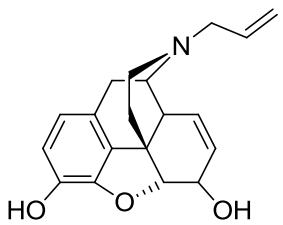

Figure 1.5: Structure of nalorphine (N-allyl normorphine), a morphine antagonist.

This prompted a similar study in the orvinol and thevinol series. Bentley discovered a similar effect with the N-allyl and N-CPM having reduced analgesic potency in the rat tail pressure test (Cowan, 1995; Lewis, 1974; Lewis *et al.*, 1971). In the tail flick test, some of the compounds that show lower analgesic potency in the previous rat tail-pressure test, antagonized morphine in the tail-flick test (Lewis, 1974). The tail-flick test is a more sensitive assay to detect opioids with mixed agonist/antagonist activity (Cowan, 1995). Therefore, it was concluded that the N-allyl and N-CPM substituted analogues of orvinols and thevinols lead to the compounds mostly

having decreased efficacy towards μ-opioid receptors, and that μ-efficacies of the orvinols were lower than their thevinol analogues (Husbands (unpublished work), (Husbands *et al.*, 2000; Lewis *et al.*, 1971; Martin *et al.*, 1974).

Replacing the N-methyl with N-CPM also increased the binding affinity of the compounds towards the opioid receptors, particularly the μ- and κ-opioid receptors (Lewis, 1985; Magnan *et al.*, 1982). While the efficacies of the analogues towards the μ-opioid receptors were greatly reduced, their efficacies at the κ-opioid receptors were only minimally affected (Katz *et al.*, 1982). Therefore, the major effect resulting from replacement of the N-methyl with N-CPM was to change the predominant intrinsic activity of the analogues from μ- to κ-opioid receptors, which was evidenced in the rhesus monkeys with the oripavine derivatives (Cowan, 1995; Katz *et al.*, 1982).

A major site of modification within the orvinol series has been at the R^3 position (Figure 1.4 (a)). SAR within the orvinol series (R^1 and R^2 = Me) (Figure 1.4 (a)), showed that alkyl manipulation at R^3 could markedly affect the potency of the analogues compared to morphine (Bentley *et al.*, 1967b). With the straight alkyl substituents (n-alkyl), the analgesic potency (ED_{50}), of the analogues increased when the size of n-alkyl was increased and achieved its peak activity between n-propyl and n-butyl. After reaching these limits, the analgesic potency of the analogues decreased if the n-alkyl chain was further lengthened. The relationship between the size of the n-alkyl substituent (R^3) and the analogues analgesic potency at the μ-opioid receptor was also seen *in vitro* in the rat vas deferens preparation (Lewis *et al.*, 2004). For the R^3 cycloalkyl substituents, cyclopentyl and cyclohexyl were reported to produce relatively higher analgesic potencies compared to morphine (70-fold and 3400-fold respectively). In conclusion, the relative order for potency in the orvinol series (Figure 1.4) with R^3 alkyl manipulation (R^1 = R^2 = Methyl (Me) is as follows (Bentley *et al.*, 1967b):

n-Butyl (n-Bu) > n-Propyl (n-Pr) > Cyclohexyl > Cyclopentyl > Ethyl (Et) > Me

Branching in the side chain adjacent to C_{20} appears to reduce efficacy, particularly at κ-opioid receptors (Lewis *et al.*, 2004). The effect of introducing a methylene spacer (n-alkyl) between the C_{20} and branched alkyl groups has also been recently investigated. As well as increasing the binding affinity of the compounds towards the μ- and κ-opioid receptors (from nanomolar to subnanomolar), introducing a methylene spacer in between the C_{20} and the branched alkyl group has increased the efficacy of the compounds at both of these opioid receptors (Husbands (unpublished work)). With this modification, the κ-opioid receptor agonist activity becomes visible. A further increase of the methylene spacer (-$(CH_2)_2$-) increased the predominant κ-opioid receptor efficacy of the compounds (Husbands (unpublished work)). For example, although both isobutyl orvinol (R = $CH_2(CHCH_3)_2$) and isopentyl orvinol (R = $(CH_2)_2(CHCH_3)_2$) (Figure 1.4 (b)) were equipotent analgesics, the analgesic activity of isobutyl orvinol was higher than the isopentyl orvinol in the presence of the selective κ-opioid receptor antagonist, nor-BNI. This suggests that the analgesic activity of the former compound was partially mediated by the μ-opioid receptors, while the analgesic activity of the latter was predominantly mediated by the κ-opioid receptors. With these recent findings, Bentley's (1967) previous results could be explained, where the analgesic potency of phenyl orvinol was greatly increased (35-fold) when an ethylene spacer was introduced between the C_{20} and the phenyl group at the R^3 position (R^1 = R^2 = Me) (Figure 1.4 (a)) (Bentley *et al.*, 1967b).

The effect of the side chain length is believed to be related to the compounds interaction with a lipophilic opioid receptor site. Since the maximum analgesic potency for the analogues as reported with the n-alkyl substituents (R^3) (Figure 1.4 (a)) was between C_3-C_4, it was concluded that this lipophilic receptor site is not more than 6 A° in distance from C_7 (Lewis *et al.*, 1971).

Early work also suggested that besides the lipophilic component, the C_{20}-hydroxyl group also has an important role in the analgesic potency of thevinols and orvinols, by forming an intramolecular hydrogen bond with the C_6-methoxy group and/or binding with the opioid receptor binding site (Figure 1.6 (a)) (Bentley *et al.*, 1972; Cowan *et al.*, 1995). This theory suggested that the intramolecular hydrogen bond

helps to fix the alkyl group (Figure 1.6 (a)) towards the lipophilic opioid receptor binding site (Cowan, 1995; Loew *et al.*, 1979). These components are not present in morphine and its close derivatives and was thought to explain the different analgesic potencies observed among these series (Figure 1.6 (b)) (Cowan, 1995).

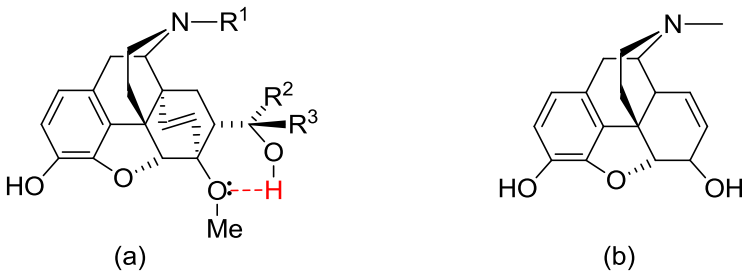

Figure 1.6: Intramolecular hydrogen bond in orvinol between C_{20}-OH and C_6-Methoxy groups (a); Morphine chemical structure shows lack of C_{20} moeity (b).

However, it was later proved that intramolecular hydrogen bonding is not crucial for the analgesic potency of these series as the C_6-demethylated analogues still managed to retain their high analgesic potency relative to morphine (Hutchins *et al.*, 1981; Knipmeyer *et al.*, 1985).

A further study conducted by Hutchins (1984) proposed the theory of synergistic hydrophilic/lipophilic opioid receptor binding sites to explain the change in analgesic potency seen when the C_{19} chiral center configuration is manipulated. Based on this study, the C_{20}-OH (hydrophilic region) is not necessarily needed in order to obtain an analogue with high analgesic potency, but it may help fix the alignment of the alkyl group (lipophilic region) to the lipophilic opioid receptor sites (Hutchins *et al.*, 1984). According to Hutchins (1984), the lipophilic alkyl chain (C_{20}) that determines the analgesic potency of the orvinol and thevinol analogues is located below C_8 (Figure 1.7) near to the 6,14-etheno bridge (Cowan *et al.*, 1995; Hutchins *et al.*, 1984; Loew *et al.*, 1979). This hypothesis was proved when the oripavine analogue (cyclohexane ring is constrained at C_7-C_8) showed 1000-fold higher potency than morphine even without the presence of C_{20}-OH (Figure 1.7) (Hutchins *et al.*, 1984).

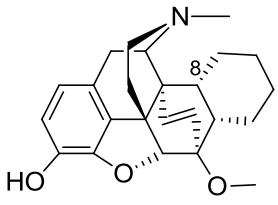

Figure 1.7: Oripavine derivatives with cyclohexane ring constrained below C_8 and near to the 6,14-etheno bridge without the presence of C_{20}-OH (1000-fold more potent than morphine).

Preliminary work by Husbands' group has found phenyl orvinol (BU127 (**15**)) to have a promising profile at the μ- and κ-opioid receptors, significantly different from all other compounds synthesised in the series, which includes branched alkyl (eg: isopropyl, isobutyl) or aryl alkyl such as benzyl and phenethenyl side chains (Figure 2.2) (Husbands (unpublished work)). BU127 (**15**) has shown low efficacy, but high affinity, at μ- and κ-opioid receptors (Figure 2.2) suggesting that the desired μ/κ profile has been achieved. Together, this evidence suggested that only direct aryl analogues of BU127 (**15**) would retain low μ/κ efficacy and that introduction of a spacer between the aryl ring and C_{20} would be detrimental to the desired profile. In addition, in the current work, the 6,14-endoetheno bridge (Figure 1.4 (a)) was reduced to 6,14-endoethano (Figure 1.4 (b)). The reduction of the bridge helps to lower the efficacy of the analogues at κ-opioid receptors (Husbands (unpublished work)), though the overall antagonist potency was only minimally affected by this reduction (Bentley *et al.*, 1972).

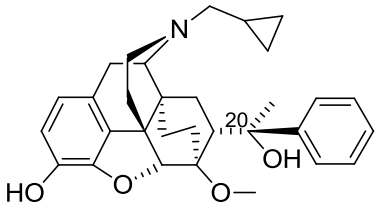

1.6.3 ORL-1 receptor pharmacophore

This PhD project also aimed to increase the efficacy and binding affinity of the buprenorphine analogues toward the ORL-1 receptor. By comparing ORL-1 ligands that have already been synthesised, it is apparent that all ORL-1 ligands share common features, which are; having a basic nitrogen, a large cyclic lipophilic group attached to the basic nitrogen and also a heterocyclic moiety at least 3 carbons

distant from the basic nitrogen (Figure 1.8) (Zaveri *et al.*, 2005). The heterocyclic group appears to play a significant role in increasing the compounds binding affinity towards the ORL-1 receptor.

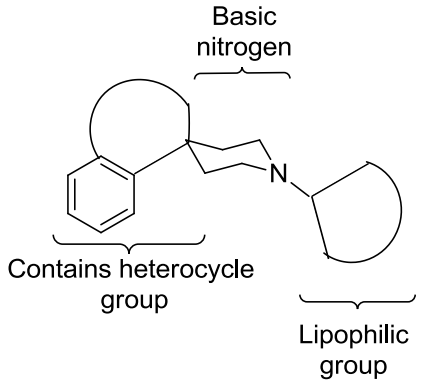

Figure 1.8: The important features of ORL-1 ligands that determine the compounds' affinities and efficacies at the ORL-1 receptors.

1.7 *In Vitro* Evaluation of Opioids (Principle and Mechanism)

There are many parameters that can be used to completely define the characteristics of opioid related drugs, starting from their physicochemical properties (*in vitro*) to their dependence liability (*in vivo*) (Leslie, 1987). However, our current work is focusing on evaluating the characteristics of the novel compounds synthesised at the receptor level and to relate their chemical structure modifications with their activities at the targeted opioid receptors, compared to the reference drug. Therefore, the parameters that are used to define the characteristics of the compounds synthesised in this project are the binding affinity, efficacy and potency (antagonist potency) at different opioid receptors type. To ease the discussion, the word 'ligand' will be used in place of drug and compound to define all the parameters used in our assay.

Binding affinity refers to the ability of a ligand to occupy a specific receptor type. The parameters that are usually used to describe the binding affinity of a ligand are IC_{50}

and K_i. Both IC_{50} and K_i are used to define the binding affinity of a ligand derived from a receptor binding assay. IC_{50} refers to the concentration of competing ligand which displaces 50% of the specific binding of the radioligand (Sheehan *et al.*, 1993). Since the IC_{50} value of the test compound varies depending on the radioligand concentration used in the assay, the binding affinity can be converted to an absolute inhibition constant, K_i using the Cheng-Prusoff equation (Kenakin, 2009). Another parameter that can be used to describe the affinity of a ligand is K_B (dissociation constant of an antagonist) (Leslie, 1987), which is derived from the functional assay for a competitive antagonist (Kenakin, 2009; Motulsky, 2007). Theoretically, the K_i and K_B value for the same antagonist is equal, provided the experimental conditions are the same (Sheehan *et al.*, 1993).

Efficacy is a term used to describe the extent of agonist activity of a ligand which has a direct proportional relationship with receptor occupancy. A high efficacy ligand only needs to occupy a low proportion of receptor to produce a maximal response, while a low efficacy ligand either needs a higher receptor occupation to produce similar response as the high efficacy ligand or sometimes only partially stimulates the receptor although all the receptor is occupied (and is therefore a partial agonist). There is no absolute value to show efficacy, except for an antagonist which has no efficacy (zero efficacy). However, theoretically, the efficacy value can be described to lie between zero and large positive value (Stephenson, 1956). For agonists, the efficacy is generally between partial to full efficacy. Since the term of efficacy is quite subjective, the efficacy of a ligand is usually described as 'relative efficacy' and compared to a standard agonist (usually a full agonist) (Sheehan *et al.*, 1993). The efficacy value is usually expressed as a percentage relative to the standard full agonist (where the full agonist is converted into 100% response).

Potency is a term used to describe the effectiveness of a ligand, either as an agonist or an antagonist. Potency is measured from a functional assay. It is important to understand that unlike efficacy and binding affinity, potency does not provide any information about receptor occupancy (Leslie, 1987). The parameters that are usually used to compare potency in a functional assay for an agonist are EC_{50} (or IC_{50}), or pEC_{50} or pIC_{50} (for an agonist) and for an antagonist, pK_B and pA_2 are commonly used. For example, EC_{50} refers to the molar concentration of an agonist

which produces 50% of the maximum possible response for that specific agonist (Sheehan *et al.*, 1993), while for a functional assay, IC_{50} refers to the molar concentration of an agonist which produces 50% of its maximum possible inhibition. pA_2 and pK_B, the parameters used to describe antagonist potency, will be discussed later in more details.

Therefore, it is important to understand the different assays and methods used to generate all these parameters before comparing the values and generalizing the results obtained by different labs.

1.7.1 Binding assay

1.7.1.1 **Receptor binding**

Receptor binding assay is used to measure the binding affinity of a drug or compound to the receptor binding sites of a particular receptor type. The cells that are usually used in this assay are cell membrane homogenates that are known to contain high population of the receptor needed. For opioids, the commonly used cells are brain cell membranes (eg: guinea pigs) or cell lines transfected with cloned receptors (eg: Chinese hamster ovarian (CHO) transfected cells) (Toll *et al.*, 1998). The receptor binding assay can measure the binding affinity of a compound regardless of its pharmacological activity (agonist or antagonist nature). For a compound with antagonist activity, the isolated tissue preparation also can be used to estimate the compound binding affinity, which will be explained in the next subchapter (Schild analysis and Schild equation).

Principle and mechanism of receptor binding assay

There are three ways of conducting binding assays which are through saturation, displacement and kinetic binding. The main principles behind these three binding assays are the same where the fraction bound of the measured ligand (specific binding) is different from the fraction unbound (non-specific binding, *nsb*) (specific binding = total binding – *nsb*). The *nsb* refers to the fraction of ligand that is bound to the sites other than the receptors, which also include the test tube and the cell membranes. The differences between saturation, displacement and kinetic binding techniques are how the tracer ligand (ligand labelled with radioactive isotope / fluorescence species) is measured (Kenakin, 2009). Saturation binding directly measures the binding of tracer ligand to the receptors. The ligand used has to be traceable which only can be done to the radioactive or fluorescence molecules. The tracer ligand in this case is the test compound. The second method, displacement binding, measures the interruption or reduction of radioactive signals through competitive binding (displacement) by a nontraceable ligand. The reduction of radioactive signal of the tracer ligand caused by the competitive activity of the nontraceable ligand at the receptor is used to measure the binding affinity of the nontraceable ligand. In this case, the tracer ligand was a standard drug while the nontraceable ligand was the test compound. The last technique, kinetic binding, measures directly the decay of radioactivity of tracer ligand with time (Kenakin, 2009).

The method used by John Traynor's lab that is presented in this thesis is the displacement binding technique. The detailed method used will be discussed in Chapter 3. Principally, the cells transfected with the specific receptor are pre-incubated with a constant (fixed) concentration of a tracer ligand (radiolabelled ligand), together with a high concentration of nonlabelled ligand to measure the *nsb*, in the presence and absence of varied concentration of another nonradiolabelled ligand (the test compound) (Kenakin, 2009). Theoretically, the test compound will compete with and displace the tracer ligand which will disrupt the radioactivity of the tracer ligand in a concentration dependent manner. The remaining radioactivity of the tracer ligand bound to the receptor is measured using a scintillation counter. The percentage of receptor displacement of the tracer ligand is plotted against the

concentration of the test compound (displacing ligand) in a log scale to get the IC_{50} value (Traynor *et al.*, 1995). The IC_{50} refers to the concentration of the test compound that causes 50% decrease in the radioactivity of the tracer ligand from the original (basal) value. This value is derived from the non-linear regression graph. This IC_{50} value is then fitted into the Cheng-Prusoff equation to calculate the binding affinity (K_i) value of the displacing ligand (test compound) (Kenakin, 2009).

1.7.2 Functional assays

1.7.2.1 **[^{35}S]GTPγS binding**

[^{35}S]GTPγS refers to a non-hydrolyzable analogue of GTP that is tagged with a radioactive isotope of ^{35}S, which can be measured by a liquid scintillation counter (Harrison *et al.*, 2003; Traynor *et al.*, 1995). The [^{35}S]GTPγS binding is a functional assay, usually conducted in cell lines transfected with a homogenous (isolated) receptor type. It is commonly used nowadays as a functional bioassay alternative to the isolated tissue preparations. Although the word 'binding' is used to describe this assay, it is not similar to the receptor binding assay because this assay is not directly quantifying the receptor occupancy, as in the receptor binding assay. The [^{35}S]GTPγS is a measures of receptor activation activity by an agonist as a result of agonist-receptor interaction (Harrison *et al.*, 2003). Therefore, the 'binding' in this assay actually refers to the binding of the [^{35}S]GTPγS with the α-subunit of the activated G-proteins.

Principle and mechanism of [^{35}S]GTPγS binding assay

The [^{35}S]GTPγS assay measures the very first events of the G-protein's activation by an agonist at the receptor level (Harrison *et al.*, 2003). This event refers to the nucleotide exchange between the membrane bound α-GDP subunit of the activated

αβγ heterotrimer complex and the intracellular GTP (Figure 1.2, top (right)). In this assay system, the function of the intracellular GTP is replaced with a radiolabelled, non-hydrolyzable GTP analogue, [^{35}S]GTPγS (Harrison *et al.*, 2003). Since the amount of [^{35}S]GTPγS added in the test tube is known, the percentage of the α-[^{35}S]GTPγS complex bound to the cellular membrane during agonist occupation at the receptor can be measured (Figure 1.9) after filtering the membrane, to determine the efficacy of the agonist (expressed as % stimulation) and compared against standard agonist. The [^{35}S]GTPγS is a stable species and is not subject to hydrolysis by the intracellular GTPase activity (Traynor *et al.*, 1995). Therefore once activated, it will accumulate in the cell membranes which enables the level of this membrane-bound species to be measured (Figure 1.9).

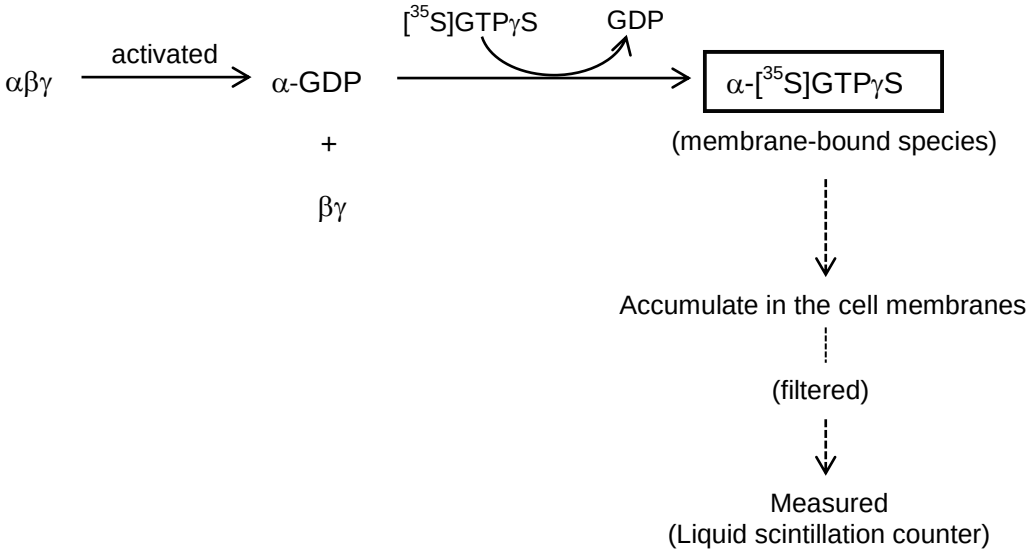

Figure 1.9: Principle of [^{35}S]GTPγS binding assay and measurements.

Since [^{35}S]GTPγS is an artificial assay system, the level of agonist expression (% stimulation) may vary between different labs, which depends on the experimental protocol. Besides the [^{35}S]GTPγS species, the important materials for this assay are the GDP, charged ions (Mg^{2+} and Na^{+}), and membranes (which contains the protein receptor) (Harrison *et al.*, 2003). The amount of these materials and the types of cell lines can be adjusted to achieve a bigger receptor stimulation, which explains why

sometimes different labs have reported huge differences of % receptor stimulation by the same agonist (Alt *et al.*, 2002; Bloms-Funke *et al.*, 2000; Spagnolo *et al.*, 2008).

1.7.2.2 **Isolated (peripheral) tissue preparations**

Peripheral tissues have been widely used to pharmacologically characterize opioid drugs at different types of opioid receptors (Leslie, 1987). Since different tissues have different opioid receptor types, the selection of tissues to be used in the bioassay is important, especially for a drug which is known to have lower efficacy (Lord *et al.*, 1977). The most commonly used tissues for the evaluation of opioid ligands are the guinea pig ileum, GPI (for μ- and κ-opioid receptors) (Leslie, 1987) and mouse vas deferens, MVD (δ-opioid receptors) (Lord *et al.*, 1977). Although the mouse vas deferens has all the three opioid receptors (μ-, κ- and δ-), they are more sensitive to the δ-opioid receptor agonist activity (Leslie, 1987). The MVD preparation however is more sensitive in detecting the antagonist activity of an opioid with a partial agonist activity (eg: cyclorphan) or an opioid that has a mixed agonist/antagonist activities, compared to the GPI preparation (Kosterlitz *et al.*, 1973; Magnan *et al.*, 1982). Due to its higher potency, cyclorphan, a partial μ-opioid agonist, shows full efficacy in the system with a higher μ-opioid receptor reserve (GPI) (Kosterlitz *et al.*, 1973).

In this project, rat vas deferens (RVD) was used to determine the binding affinity of the compounds synthesised at the μ- and ORL-1 receptors. Since RVD does not have κ-opioid receptors (Smith *et al.*, 1983), and our compounds have shown a substantial efficacy at the κ-opioid receptor during the [^{35}S]GTPγS screening (Figure 3.2), it is an advantage to conduct assays using this preparation without complications caused by the potential κ-opioid receptor activity of the compounds. Furthermore, RVD has a lower μ-opioid receptor population compared to MVD (Smith *et al.*, 1983), therefore some compounds that show efficacy (μ-opioid receptor mediated) in the MVD were antagonist in the RVD preparation (eg: buprenorphine) (Spagnolo *et al.*, 2008), which allows the potency and binding

affinity of the compound at the μ-opioid receptor to be determined using this tissue. This procedure will be discussed in greater details in Chapter 3.

The effects of receptor reserve in isolated tissue assays

Two major factors that determine the activity of drugs in each model / system are the density of receptor, which will determine the receptor reserve in the system and the efficacy of the drug (Kenakin, 2009). Receptor reserve is more common with drugs that elicit their response on smooth muscle contraction compared to other types of receptor mediated responses (Stephenson, 1956). Receptor reserve or spare receptors refers to the percentage of receptors that are not required to produce the maximal response (Kenakin, 2009). In general, the more potent the drug, there will be a greater receptor reserve available in the system. A potent and highly efficacious drug does not need to occupy a high percentage of receptors in order to produce the maximal response. The availability of the receptor reserve is a really important issue to highlight because it will determine the behaviour of the drug in the system, especially when using a drug with low efficacy. For example, [D-Ala^2,*N*-Me-Phe^4,Gly^5-ol]enkephalin acetate (DAMGO), a selective μ-opioid receptor agonist, has a different potency (IC_{50}) when measured in mouse vas deferens (311 ± 26 nM) compared to rat vas deferens (2640 ± 410 nM) (Miller *et al.*, 1986). The difference in the potency of the drug in the two systems depends on both the efficiency of the drug-receptor coupling mechanism to produce the response in the tissue and the receptor density in that particular model (Kenakin, 2009). The density or number of μ-opioid receptor is higher in the mouse vas deferens compare to rat vas deferens which explains why DAMGO was found to be more potent in mouse vas deferens compared to rat vas deferens (Smith *et al.*, 1983).

The binding affinity of a drug is system-independent but the potency of drug uniquely depends on the system (Kenakin, 2009). Although both DAMGO and morphine show high binding affinity at the μ-opioid receptor, DAMGO has a higher efficacy or intrinsic activity compared to morphine. Therefore, DAMGO acts as a full μ-opioid receptor agonist even in a system with low μ-receptor reserve. For

example, in rat vas deferens, DAMGO produced a maximal response (E_{max}) between 70-100% (Sheehan *et al.*, 1988). On the other hand, morphine behaved as a complete antagonist in rat vas deferens (Schulz *et al.*, 1979) but demonstrated full μ-opioid agonist activity in guinea pig ileum (GPI) and in mouse vas deferens (MVD) (Hutchinson *et al.*, 1975).

In order to evaluate the μ-opioid receptor activity of our buprenorphine analogues, it was important to use a highly efficacious standard agonist in our assay, especially in the rat vas deferens since this system has low μ-opioid receptor density (Smith *et al.*, 1983). This issue will be discussed throughout this thesis when the behaviour of the buprenorphine analogues is compared to the other drug in the same assay system and also between different assay systems. This problem will be more prominent when we compare the results obtained from the isolated tissue assays to the results obtained from Traynor's group in the [^{35}S]GTPγS functional assay.

Opioids agonist activity on the smooth muscle (vas deferens)

There are two main receptors that are responsible for the contraction of smooth muscle in the vas deferens which are P_{2X} receptor (purinergic) and α_1-adrenoceptor (adrenergic) (Westfall *et al.*, 2001). The purinergic receptors (for ATP) were reported to occupy mainly the prostatic end while adrenergic receptors (for noradrenaline) were mainly distributed at the epididymal end of the vas deferens (Westfall *et al.*, 2001). This is the reason why, in the present study, 20% of the vas deferens was removed at the prostatic end during tissue preparation since it was occupied by non-adrenergic receptor, to isolate noradrenergic responses (Andrews *et al.*, 2010). In the isolated vas deferens preparation, as well as the smooth muscle, there are also axons and nerve terminals of postganglionic sympathetic neurons. As such, when the isolated vas deferens is electrically stimulated, the postganglionic sympathetic axons are activated and the noradrenaline (NA) stored in the vesicles at the nerve terminals is released by exocytosis and binds to the postjunctional α_1-adrenoceptor on the smooth muscle cells (Westfall *et al.*, 2001). The α_1-adrenoceptor is a G_q-coupled GPCR, so activation of the receptor leads to activation

of the phospholipase C enzyme (effector for G_q G-protein). Inositol(1,4,5)trisphosphate (IP_3) is one of the key products of hydrolysis activity of phospholipase C which in turn acts on its specific IP_3 receptor (a ligand-gated calcium channel) located on the sarcoplasmic reticulum. Activation of the IP_3 receptor will then release the Ca^{2+} which is stored in the endoplasmic reticulum into the cytosol and activates the calcium binding protein, calmodulin. The Ca^{2+}-calmodulin will then activate myosin through the activity of myosin light-chain kinase (MLCK) and causes contraction of the vas deferens (Berridge, 2008). At the later stage, IP_3 can also be phosphorylated into inositoltetrakiphosphate (IP_4) which will induce the opening of calcium channel located at the cell membranes, and therefore cause influx of extracellular Ca^{2+} into the cells (Figure 1.10) (Vauquelin *et al.*, 2007).

In the vas deferens tissue, the opioid receptors are located at the presynaptic nerve terminals of the sympathetic nervous system (Leslie, 1987; Westfall *et al.*, 2001). Opioid drugs inhibit the electrically evoked contraction of vas deferens by inhibiting the NA release from the postganglionic sympathetic nerves in a concentration-dependent manner (Henderson *et al.*, 1976; Leslie, 1987). As mentioned earlier (Chapter 1.3.3), the opioid receptors belong to $G_{i/o}$ G-protein subtypes (Brody *et al.*, 1998; Connor *et al.*, 1999). Although the opioid receptors couple to both G_i and G_o G-protein subtypes, their effects in altering the cellular activities will depend on which effector is expressed by that particular cell (Connor *et al.*, 1999). The main effects of opioid receptor activation in the vas deferens are the inhibition of voltage-gated calcium channels and inducing the opening of potassium channels (Satoh *et al.*, 1995). These happen directly through the coupling of $\beta\gamma$ subunits of G_o G-proteins to the ion channel without the involvement of other second messenger systems (Connor *et al.*, 1999). NA is released from vesicles through exocytosis as a response to increasing intracellular Ca^{2+} during neuronal depolarisation (Cunnane, 1984). Therefore, the inhibition of Ca^{2+} influx through the inhibition of voltage-gated calcium channel by opioid agonists will cause inhibition of the NA release from the vesicles (Westfall *et al.*, 2001). Similarly, opening of potassium channels by activation of opioid receptors will lead to hyperpolarization of the nerve terminal membranes, decreasing the opening of voltage-gated calcium channels. As a result, there will be a reduction of NA in the synapse to interact with the postjunctional α_1-adrenoceptors such that activation of opioid receptors causes

inhibition of the electrically-evoked vas deferens contraction in a concentration-dependent manner (Figure 1.10).

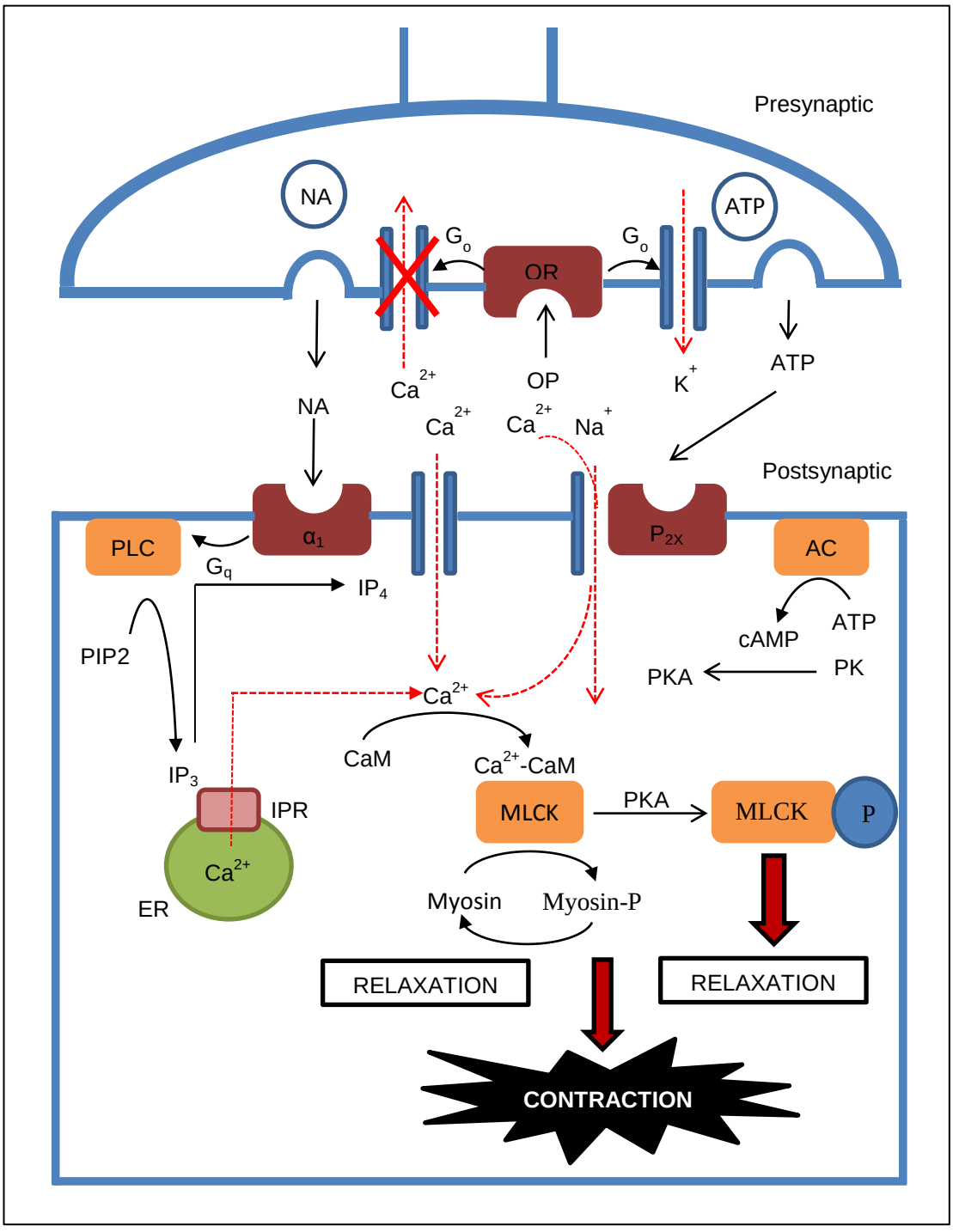

Figure 1.10: Cellular mechanism of electrically evoked and inhibition of vas deferens contractions mediated by noradrenaline and opioid agonist. AC, adenylyl cyclase; CaM, calmodulin; SR, sarcoplasmic reticulum; MLCK, myosin light-chain kinase; OP, opioid agonist; OR, opioid receptor; PK, protein kinase; PLC, phospholipase C.

1.7.3 Advantages, strengths and limitations of different assay systems

Different assay systems have their own advantages, strengths and limitations. Therefore, careful consideration needs to be made before interpreting and comparing the results, not only between different assay systems, but also between different labs. This is because the experimental protocols might be different which have impact on the values reported.

Amongst all the three *in vitro* techniques that have been discussed above, the isolated tissue preparations is at least the closest to mimic the in vivo environment. Although the environment is artificial (the organ bath), the tissues are still intact (Leslie, 1987). In our experiment, the isolated tissue preparation was used to evaluate the potency of the test compounds relative to buprenorphine and to estimate their binding affinity in a more physiological environment (Kenakin, 2009; Leslie, 1987). The end physiological response shown by the tissue (eg: inhibition of muscle contraction) is a result of a series of biochemical events starting from the receptor activation at the cell membranes and intracellular effectors response (eg: activation / inhibition of ion channels / cyclic adenosine monophosphate (cAMP)) (Lemaire *et al.*, 1978). In contrast to the [^{35}S]GTPγS, the receptor stimulation shows is not a translation of the downstream biochemical events of the cells (Harrison *et al.*, 2003).

The [^{35}S]GTPγS binding can also be used to evaluate the potency of the test compounds and offers some advantages compared to the isolated tissue preparation (Traynor *et al.*, 1995). For example, there will be less physiological obstacles (eg: drug diffusion) for the test compounds to reach the receptor binding site compare to the intact tissue and it can be performed in a cell cultures with homogenous receptor type (Leslie, 1987). The density of the receptor also can be adjusted and other materials can be quantified to achieve bigger receptor stimulation. The [^{35}S]GTPγS binding also is a sensitive assay that can be used to measure efficacy of the compound tested. Although this function also can be shown in isolated tissue preparations, the ability of a compound to show efficacy (especially

for a lower efficacy compound), will depend on the receptor reserve available in the tissue (Smith *et al.*, 1983). Therefore in some tissues a compound can be agonist, but it may be an antagonist in a different tissue. This is discussed in greater detail in the Chapter 3.

For an artificial system (eg: [^{35}S]GTPγS), not only the amount of the component added (GDP) will influence the result, but the expression levels of the receptor will also have a significant impact on the outcome of the assay. Often the cell culture itself is modified in order to achieve very high expression levels to achieve a robust result (Law *et al.*, 1982). This is proven when buprenorphine, which is known as having partial efficacy at the ORL-1 receptor at most *in vivo* and in isolated tissue assays, can show full efficacy, as efficacious as the standard full agonist, nociceptin in CHO cells with high receptor expression levels (Wnendt *et al.*, 1999). Although the isolated tissue does not fully represent the actual environment *in vivo*, the receptor expression levels, signal transduction pathways, and internal tissue environment are as they are *in vivo*.

1.8 Schild Analysis and Schild Equation

Schild analysis is a powerful tool to measure the affinity of an antagonist in a functional system (to obtain the value of K_B) (Kenakin, 2009; Leslie, 1987). After the affinity of an antagonist has been determined, the relative potency of different antagonists acting at the same receptor type can be compared. The two important criteria that are essential in order to achieve an accurate Schild analysis are that the concentration range of antagonist tested has to be wide and the slope of the regression line is equal to unity (Leslie, 1987). For Schild analysis, a series of at least three concentration ratios (CRs) of an agonist in the absence and in the presence of known concentrations of antagonist that produced equivalent responses are calculated (Kenakin, 2009). The x-intercept that derives from the linear regression line with slope equal to 1 gives the pK_B value of the antagonist. If this slope is not significantly different from unity, the antagonist can be assumed to be

competitive and reversible, and constraining the slope to 1 gives a more accurate K_B value (Kenakin, 2009).

K_B is the equilibrium dissociation constant of the antagonist-receptor complex, and also refers to the concentration of antagonist that occupies 50% of the measured receptor, and therefore in this case K_B is equal to K_i which also is a parameter to measure binding affinity of a ligand (antagonist in this case) (Kenakin, 2009). pK_B is also commonly referred to as pA_2, a concentration of antagonist that caused a twofold shift of agonist concentration-response curve (characteristic of simple competitive antagonism) (Kenakin, 2009). The K_B or pA_2 values are independent of the agonist and the system used (Leslie, 1987). The only differences between K_B and K_i is the assay used to measure this value in which K_i was obtained from a radioligand binding assay whereas K_B was measured from a functional assay. In contrast, in the case when the slope is significantly different from unity, pK_B cannot be assumed as pK_i (Motulsky, 2007).

In the cases that the Schild plot slope is not significantly different from 1, but there is a significant decrease in the maximum agonist response in the presence of higher concentrations of antagonist, this pattern may suggest noncompetitive behaviour of the antagonist. Alternatively it could be due to hemi-equilibrium conditions where the agonist and antagonist do not achieved equilibrium with the receptor (Kenakin, 2009). If this is the case, Schild analysis still can be used to estimate the antagonist potency of the test compound (Kenakin, 2009).

There are also cases where Schild analysis is no longer a valid method to estimate the potency of the antagonist. For example, in cases where either the Schild slope was found to be significantly less than unity or in the case where only a single concentration of antagonist was compared to an agonist. In either case, the single concentration method (Schild equation) can be used to empirically estimate the potency of an antagonist without defining the molecular model of antagonism of antagonist in a particular system studied (Kenakin, 2009). This equation use pA_2 as a parameter, assuming that the value measured is a prediction of antagonist

concentration that produced a twofold shift of agonist concentration-response curve. Another limitations of the Schild equation is the general assumptions that the antagonist tested is following a simple competitive antagonism model and the receptor-antagonist-agonist equilibrium is achieved, although this is sometimes not always right (Leslie, 1987). Therefore, according to Gaddum (1954), in order to ensure the prediction of pA_2 is reliable, the value of CR-1 has to be at least 5 or greater (Gaddum *et al.*, 1954). However, Kenakin (2009) suggests that log (CR-1) has to be a positive value (not specified) and Schild equation analysis should use a minimum concentration of antagonist that produced a twofold shift of agonist concentration response-curve.

Despite these disadvantages, the single concentration method offers a few advantages, as it is a faster method to estimate the antagonist affinity and potency especially if the antagonist tested has affinity to multiple opioid receptors that can present in a single tissue (eg: buprenorphine in mouse vas deferens, MVD) (Leslie, 1987; Spagnolo *et al.*, 2008). Not only related to the antagonist, the problem with agonist receptor selectivity can also be avoided with the single concentration method. Although agonists with high receptor selectivity are commercially available, it is rarely possible to maintain their selectivity at a higher concentration (Leslie, 1987). This will cause a problem especially when a high concentration of antagonist is used during the Schild analysis. Therefore, the selection of a high affinity and potent agonist as a standard drug is important, together with the selective antagonist to block the unwanted receptor present in the isolated tissue. Furthermore, if the agonist used has slow wash-out, or is such that concentration-response curves can only be constructed non-cumulatively, Schild plot analysis (requiring four or more concentration-response curves on the same tissue) is not possible.

Another example of where Schild plot analysis is not possible, and so the single concentration Schild equation approach is preferred is with competitive reversible or pseudo-irreversible antagonism.

A compound is defined as being a competitive antagonist if it competes at the same binding site on the receptor as the agonist to achieve effect (Kenakin, 2009). The ability of either the agonist or the antagonist to occupy the binding sites depends on its relative binding affinity and concentration (Kenakin, 2009). The reversibility (surmountability) of the antagonist is shown by a dextral displacement (parallel shift to the right) of the agonist concentration-response curve without causing significant diminution (suppression) of the maximal response. Or alternatively if the agonist manages to regain its baseline response after the antagonist is washed from the tissue (Kenakin, 2009; Motulsky, 2007). Ideally, the agonist, antagonist and the receptor are allowed to achieve re-equilibrium before the tissue response to agonist is measured in the presence of antagonist (Kenakin, 2009). However, there is a case where the re-equilibria is hardly achieved due to the slow offset of antagonist from the receptor during this period and therefore the pattern of the concentration-response curve shows diminution of agonist maximal response in the presence of this antagonist. If this is the case, the compound that was competing with the agonist is concluded as having a pseudo-irreversible behaviour of antagonism (Kenakin, 2009).

1.9 Objective of Studies

1.9.1 General objectives

To synthesize several single compound(s) similar in activity to buprenorphine/naltrexone combination with higher activity at the ORL-1 and κ-opioid receptor to treat psychological dependence (reduce relapse) related to drug addiction.

1.9.2 Specific objectives

1) To synthesis several new orvinols (Figure 1.11 (a)) closely related to the lead compound BU127 by introducing a small substituent group (methyl) at different positions of the C_{20}-phenyl (Figure 1.11 (b)).

2) To introduce a heterocyclic group (thiophene including substituted thiophenes) at the C_{20}-position of the orvinols (Figure 1.11 (c)) and to compare the receptor profiles of these ligands with the BU127 analogues (Figure 1.1 (b)) and buprenorphine.

3) To assess the receptor behaviour and the relative potency of the analogues against buprenorphine in the isolated tissue preparation (rat vas deferens (μ- and ORL-1 opioid receptors) and mouse vas deferens (κ-opioid receptor)).

4) To assess the receptor behaviour and the relative potency of the analogues' having methyl substituent at C_7 position of orvinol compared to the analogues without methyl at this position.

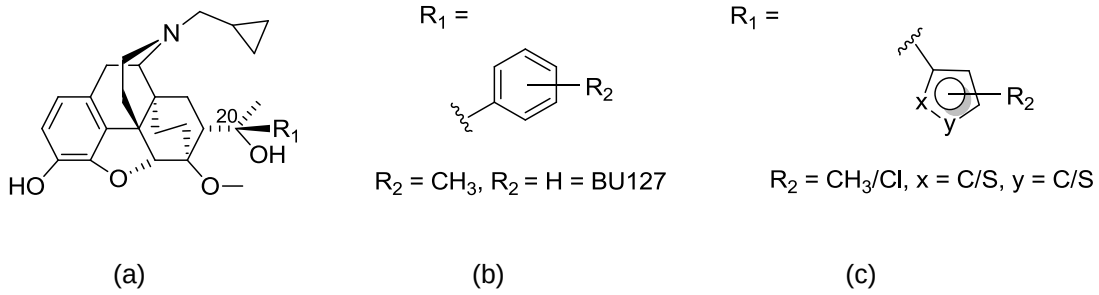

(a) (b) (c)

Figure 1.11: Structure modification of orvinols; (a) General structure of orvinols; (b) BU127 and its analogues; (c) thiophene analogues.

CHAPTER 2.0: CHEMISTRY

2.1 Introduction

2.1.1 BU127 as the lead buprenorphine/naltrexone single compound alternative

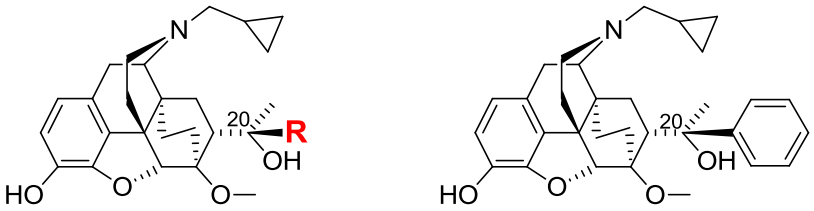

(15)

Figure 2.1: Left, parent structure of buprenorphine analogues with point of modification at C_{20}. Right, lead compound of buprenorphine/naltrexone analogues, BU127 **(15)** (R = phenyl)

Of all the orvinols synthesized within the group, varying the R-substituent (eg: branched alkyl, cycloalkyl and aryl (eg: phenyl) substituents) and the stereochemistry at C_{20}, BU127 **(15)** (Figure 2.1) is one of the only examples to have little to no efficacy at the κ-opioid receptor and substantially lower efficacy at the μ-opioid receptor than buprenorphine (Figure 2.2).

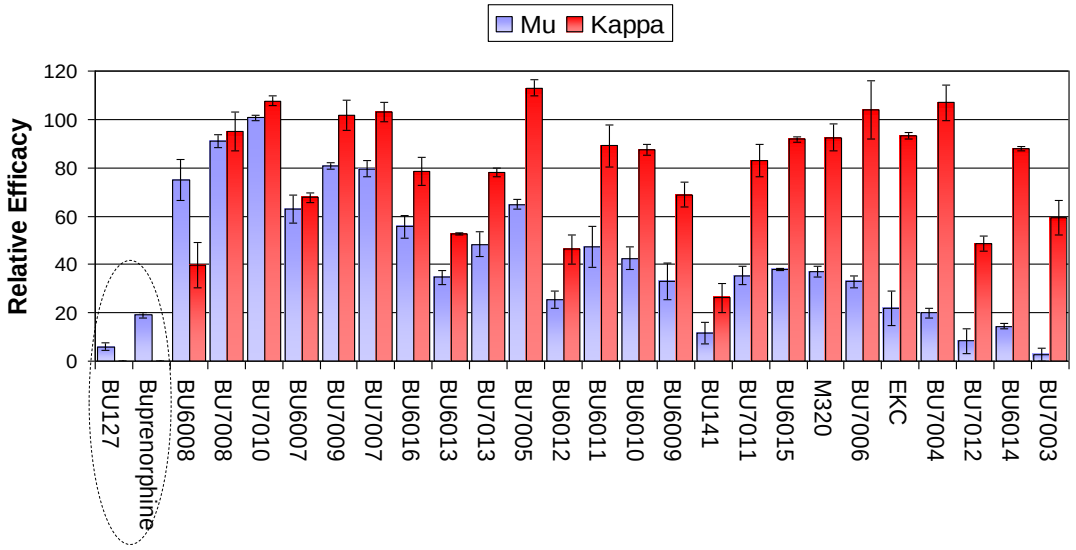

Figure 2.2: Comparison of relative efficacies ([^{35}S]GTPγS binding) of buprenorphine analogues (compared to full opioid agonists DAMGO and U69593) at μ- and κ-opioid receptors conducted in CHO transfected cells (Husbands (unpublished work)).

Due to the interesting profile of BU127 **(15)** to this project, we have targeted close analogues having a substituted phenyl ring and those having alternative aryl groups (Figure 2.3). All of the compounds were designed using compound BU127 **(15)** as a lead due to its successful profile observed at all of the targeted receptors (μ-, κ-, and ORL-1 receptor). Compound BU127 **(15)** has a phenyl substituent at R position of C_{20} (Figure 2.3). Compounds BU10101 **(16)**, BU10092 **(17)** and BU10135 **(18)** are the closest analogues to BU127 **(15)** with a methyl group attached to the phenyl (BU127 **(15)**) at ortho (o-), meta (m-) and para (p-) positions respectively (Figure 2.3). The idea of introducing and varying the methyl group on the phenyl ring was to investigate whether introducing a small amount of bulk, the pharmacological profile at the opioid receptors would improve. We aimed to investigate the effects of the methyl position on the phenyl ring compared to BU127 **(15)**. On the other hand, compounds BU08026 **(19)**, BU11001 **(22)**, BU10093 **(20)** and BU10136 **(21)** also have aromatic substitution at R position (Figure 2.3) but contain a sulphur atom in the heterocyclic system. The aim of these compounds was to study if a small heterocyclic system had any implication on the pharmacological activity of this orvinol series at the main opioid receptors. Compound BU08026 **(19)** is a 2-thiophene whereas compound BU11001 **(22)** is a 3-thiophene. Compound BU10093 **(20)** was similar to BU08026 **(19)** but with a methyl side change attached to the thiophene ring. Instead of a small alkyl group, compound BU10136 **(21)** has a

halogen atom (chloro) attached to the heterocyclic system (Figure 2.3). We aimed to observe the effects of relocation of the sulphur in the aromatic ring and the effects of introducing different substituents.

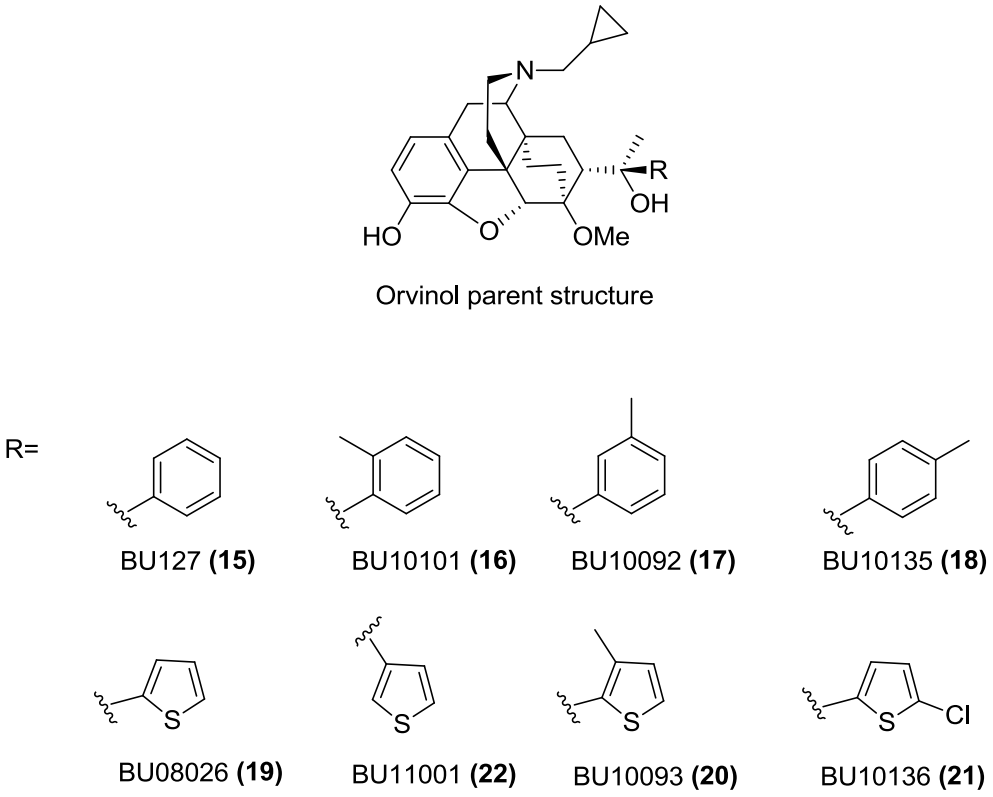

Figure 2.3: Buprenorphine analogues.

2.2 Results and Discussion

All of the compounds have been synthesised using thebaine **(1)** as the starting material, except for the first compound (phenyl orvinol **(15)**) where M5028 (dihydrothevinone, **3**) was used. Both of these starting materials were obtained from Reckitt Benkinser.

2.2.1 Diels-Alder reaction of Thebaine **(1)** to give Thevinone **(2)**

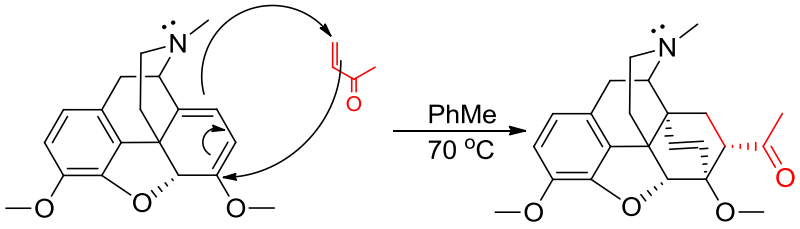

(1) **(2)**

Thevinone **(2)** was prepared from thebaine **(1)** under reflux through a Diels-Alder reaction with methyl vinyl ketone which acts as the dienophile in this reaction. The cycloaddition of the methyl vinyl ketone with the conjugated diene system is a stereospecific reaction (a *cis* addition) (Fessenden *et al.*, 1986) which produces an adduct (thevinone / 6,14-*endo*-ethenotetrahydrothebaine) **(2)** having an α-acetyl group at C_7 (regiospecific) as the major product (Casy *et al.*, 1986). The formation of the regioisomer of the adduct (acetyl at the C_8 position) is unlikely to occur, due to the polarizing electronic effects of electrons between the oxygen in the C_6-methoxy group and the diene system in the morphinan rings and also the steric effects of the morphinan skeleton (Hutchins *et al.*, 1981; Knipmeyer *et al.*, 1985). This is a high yield reaction which in our case, gave 76% total adduct of 7α-ketone and the remainder was identified as the starting material (thebaine **(1)**) which was confirmed with ^{1}H-NMR. The final percentage yield obtained from our experiment was slightly lower than previously reported which was 96.3% (7α-ketone) and 1.5% (7β-ketone) (Bentley *et al.*, 1967a). In Bentley's (1967a) study, the main adduct isolated was 93% and the remaining crops were isolated from the insoluble 7β epimer through repeated recrystallization of the mother liquors with methanol (60°C). According to Bentley (1967a), the presence of 7β epimer could be detected from both the thin layer chromatography (TLC) and ^{1}H-NMR (Bentley *et al.*, 1967a). The 7β-ketone is less polar than its epimer and the 5β-H appears in a different chemical shift for both epimers which can be easily detected using the ^{1}H-NMR (Bentley *et al.*, 1967a; Fulmor *et al.*, 1967). Bentley (1967a) has reported that the 5β-H signals for the 7α- ketone appears at the lower field (4.55) whereas at a slightly higher field for its 7β epimer (4.98). The 5β-H signal appears at the higher field for the 7β epimer due

to the anisotropy of the acetyl group (Hutchins *et al.*, 1981). In our current work, 69% of the main adduct was purified from the first crop. The 5β-H signal appears at 4.56 which was in line with Bentley's (1967a) findings. Our experiment also shows no evidence of 7β epimer detected from the remaining mother liquors, proved by both TLC and ^{1}H-NMR.

2.2.2 Catalytic hydrogenation of Diels-Alder adduct (Thevinone) **(2)** to give Dihydrothevinone **(3)**

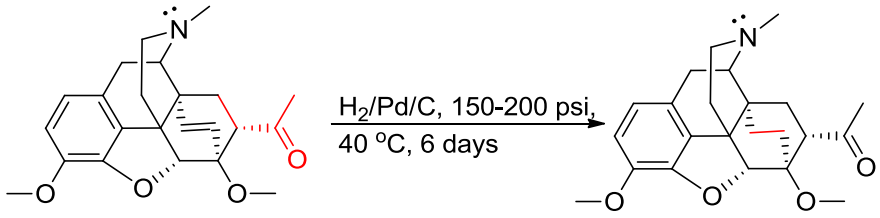

(2) **(3)**

The hydrogenation of thevinone **(2)** was conducted using a mild temperature (slightly above the room temperature) to overcome the shielding effects on the etheno bridge by the $COCH_3$ group at C_7 (Bentley *et al.*, 1967d). This catalytic hydrogenation was conducted with a slightly modified procedure by referring to Bentley's (1967b) and Grivas' (1995) previous works. The initial reaction was conducted using 0.01% wequiv. of 10% Paladium on Carbon (Pd/C) in ethanol, under 65 psi which only gave 59% yield of dihydrothevinone **(3)**, and 27% was identified as the starting material, thevinone **(2)** based on the ^{1}H-NMR (Grivas, 1995). It was later noticed that the starting material, thevinone **(2)** was not fully dissolved in the ethanol, which is thought to contribute to the low yield percentage. This procedure was modified by dissolving the thevinone **(2)** into a mixture of ethanol and ethyl acetate (1:1), increasing the amount of catalyst (0.1% wequiv.) (Bentley *et al.*, 1967d) and performed under a higher pressure (200 psi). With these modified procedures, the yield increased to 86%. The adduct **(2)** formed a suspension in ethanol even when heated at 50°C but fully dissolved into a clear orange solution after ethyl acetate was added. Although thevinone **(2)** is fully

dissolved in ethyl acetate, alcohol (eg: ethanol) is needed in order to dissolve the hydrogen gas necessary for this reaction.

2.2.3 Demethylation of Dihydrothevinone **(3)** to give Dihydronorthevinone **(4)**

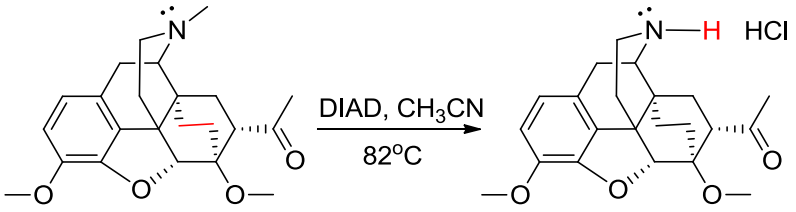

(3) **(4)**

The reagents that are commonly used for N-demethylation are cyanogen bromide (CNBr) and azodicarboxylic acid ((:N.$CO_2H)_2$) (Casy *et al.*, 1986; Kroutil *et al.*, 2000; Marton *et al.*, 1997). Azodicarboxylic acid (eg: diethyl azodicarboxylate (DEAD), diisopropyl azodicarboxylate (DIAD)) is more preferable for a lab scale productions compared to CNBr which is usually used for industrial scale. Although N-demethylation with CNBr was reported to produce a higher yield of **(4)** compared to azodicarboxylic acid (DEAD) (92% vs 71%) (Marton *et al.*, 1997), CNBr is a highly toxic reagent due to its volatility which is readily absorbed through skin upon direct contact and also during inhalation.

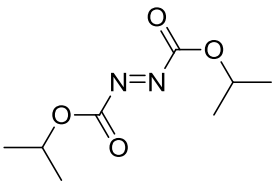

Figure 2.4: Diisopropyl azodicarboxylate (DIAD).

The N-demethylation of tertiary amines to secondary amines by DIAD (Figure 2.4) initially involves nucleophilic attack by the nitrogen atom of the tertiary amine then formation of a reactive ylide, followed by a two-step intermediate (ylide) rearrangement (3(a) and 3(b)) (Figure 2.5 (a) and Figure 2.5 (b)) (Kenner *et al.*, 1952; Smissman *et al.*, 1973). The acid hydrolysis (weak acid) of the unstable adduct (3(c)) (Kenner *et al.*, 1952) gave an intermediate hydrochloride salt, which was reported by Smissman (1973) containing an NH group and two nonequivalent carbonyl group, detected using infrared spectroscopy (IR) from the reaction between a tertiary amine (N-methyl-piperidine) and a azocarboxylic acid (dimethyl azodicarboxylate). Although IR analysis was not performed in our experiment, the ^{1}H-NMR of dihydronorthevinone **(4)** has confirmed the disappearance of N-CH_3 signals which was previously seen with dihydrothevinone **(3**) ^{1}H-NMR. The yield percentage of **(4)** obtained from our experiment with DIAD was 69.3% which is nearly similar to the yield that has been previously reported with DEAD (71%) (Marton *et al.*, 1997). The N-demethylation of tertiary amines with azodicarboxylic acids were reported to consistently gave good yields of the N-demethylated amines (> 70%) as the main adducts (Kroutil *et al.*, 2000). According to Kroutil (2000), the side products of this reaction when DIAD was used as the reagent were an aldehyde of the dealkylated group and also a diisopropyl hydrazinodicarboxylate (DIHD). However, we did not characterize the remaining side products in our current work. The suggested mechanism for the N-demethylation of **(3)** by DIAD, followed by acid hydrolysis by pyridinium chloride/ethanol is shown in Figure 2.5:

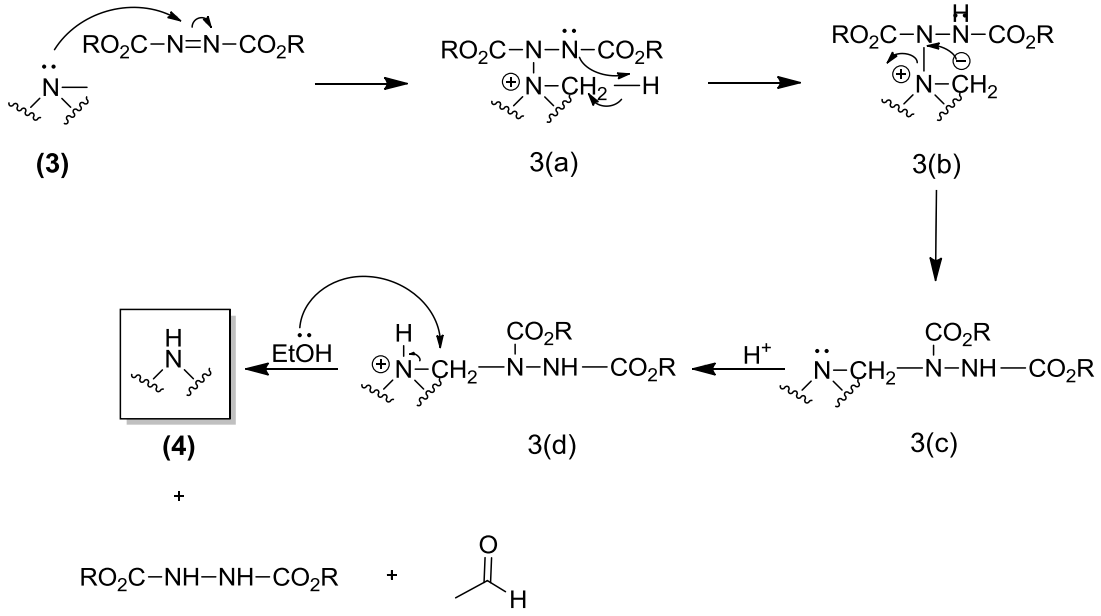

Figure 2.5 (a): N-demethylation of dihydrothevinone **(3)** by DIAD (Mechanism 1)

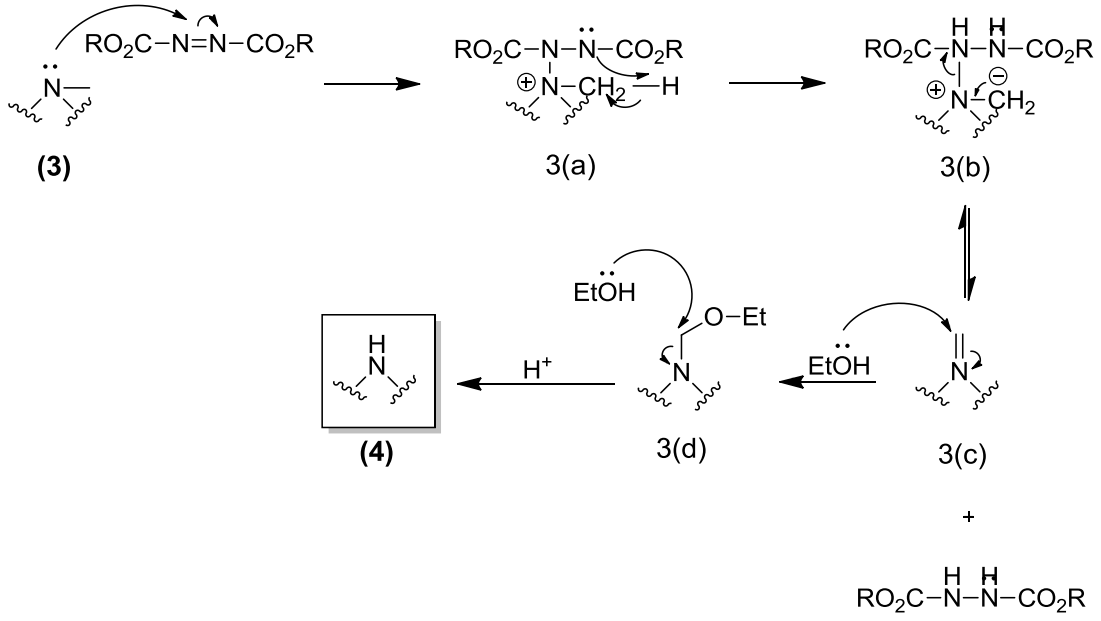

Figure 2.5 (b): N-demethylation of dihydrothevinone **(3)** by DIAD (Mechanism 2)

2.2.4 Synthesis of N-CPM dihydronorthevinone **(6)**

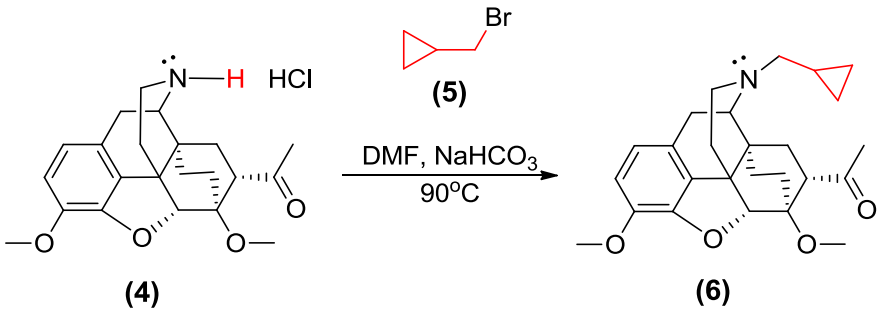

The alkylation of dihydronorthevinone **(4)** to its N-alkyl substituted derivatives is a high yield reaction which in the case of phenyl dihydronorthevinone (C_{20} = phenyl ketone) gave 72% yield with cyclopropylmethyl bromide **(5)** (Marton *et al.*, 1997). The yield percentage obtained for **(6)** from our experiment was 83% which is higher than the value reported for phenyl dihydronorthevinone. This may be due to the steric hindrance caused by the phenyl substituent around the N_{17} and C_{20} region. The alkylation involves a simple nucleophilic substitution mechanism as shown (Figure 2.6):

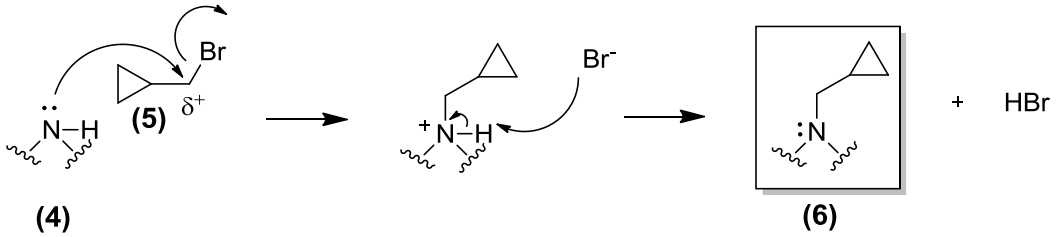

Figure 2.6: Alkylation of dihydronorthevinone **(4)** with cyclopropylmethyl bromide **(5)** to give N-CPM dihydronorthevinone **(6)**

The cyclopropylmethyl bromide **(5)** (CPMBr) reagent used in this reaction (Cowan, 1995) was prepared by bromination of the commercially available cyclopropyl methanol with phosphorus tribromide. Initial attack by oxygen to form an

intermediate with oxygen part of a better leaving group, as shown below (Figure 2.7):

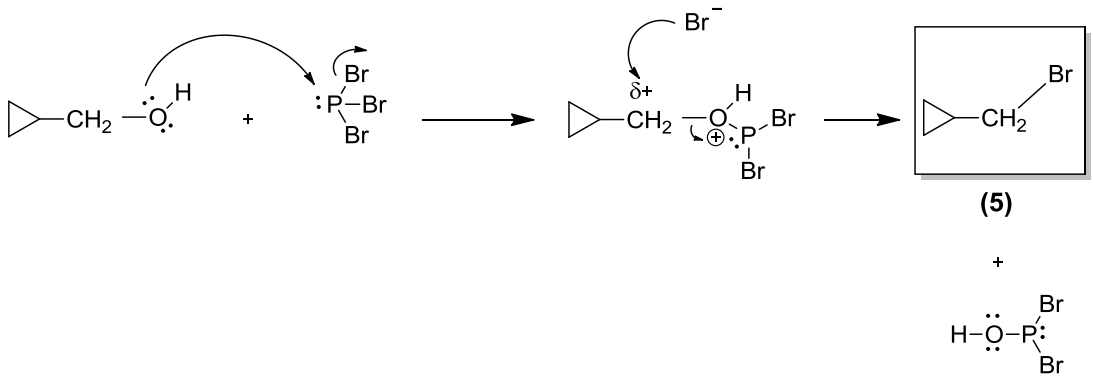

Figure 2.7: Bromination of cyclopropyl methanol with phosphorus tribromide.

2.2.5 Grignard addition to give Thevinol

All the Grignard reagents (R-MgX) used in this reaction were commercially available. However, 3-thienyl magnesium bromide was prepared in the lab due to the stability issues of the 3-thienyl magnesium iodide that was previously purchased. The synthesis route of 3-thienyl magnesium bromide is shown below (Figure 2.8) (Nyberg *et al.*, 1970); involving production of the aryl lithium species and reaction of this with $MgBr_2$, prepared from treatment of magnesium with dibromoethene.

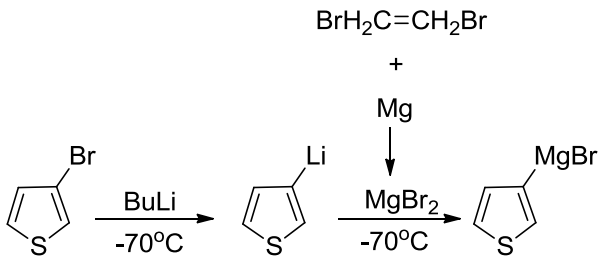

Figure 2.8: Synthesis of 3-thienyl magnesium bromide from 3-bromothiophene.

The Grignard addition to the ketone (N-CPM dihydronorthevinone, **(6)**) is a stereospecific reaction, yielding an almost pure tertiary alcohol (thevinol) with the alkyl group (R) adding from the upper face (major product of Grignard reaction) (Bentley *et al.*, 1967d).

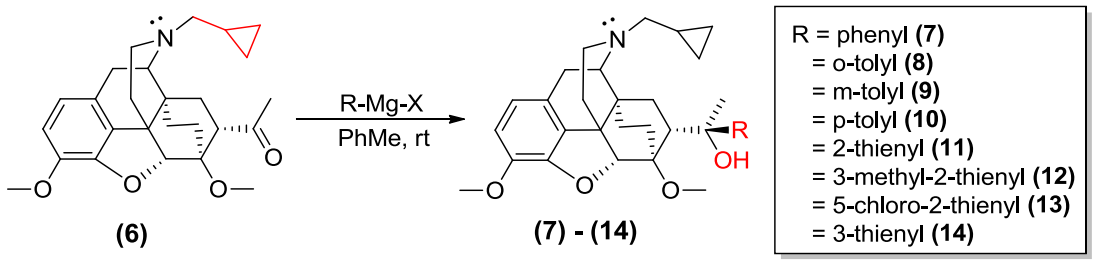

During the transition state of the Grignard addition, a six-membered intermediate is believed to have formed (Figure 2.9) (Bentley *et al.*, 1967b). The rate of addition, of the R group, during this transition state versus rate of deprotonation of C_7-H or Grignard reduction, will determine the proportion of the major product obtained from this reaction.

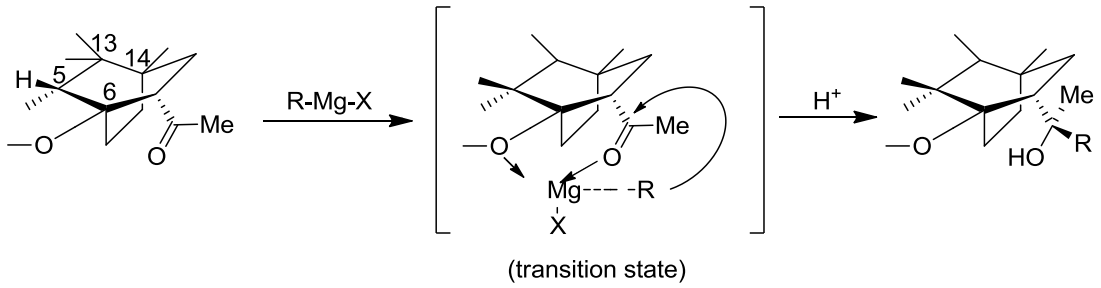

Figure 2.9: A six-membered intermediate was formed during transition state of Grignard addition.

Although; in many cases, a minor product of Grignard reduction (2° alcohol) can also be produced from Grignard reaction (can account for up to 30% of the total

product), it cannot happen in our particular series due to the absence of a reactive β-hydrogen in the aromatic Grignard reagents used in our experiments (Bentley *et al.*, 1967d). If the diastereomer of the major product (tertiary alcohol) or reduction side product is suspected, it can be initially detected by thin layer chromatography (TLC) and confirmed by infrared spectroscopy (IR) and ^{1}H-NMR (Bentley *et al.*, 1967d; Fulmor *et al.*, 1967). As expected, no evidence of secondary product was observed (after 22-44 hours). The low yield obtained in some of the reactions was due to bulkier nature of the Grignard reagent and unreacted starting material **(6)** was obtained at the end of reaction which was confirmed by TLC and ^{1}H-NMR. When the starting material **(6)** was observed during TLC, extra Grignard reagent was added to the reaction mixture and the reaction was left to go to completion for another 22 hours. In some cases, especially when the rate of reaction was suspected to be slower than usual (eg: due to the steric hindrance at C_{20} during aryl addition), no further Grignard reagent was added. This action was taken to avoid base-catalyzed rearrangement which can occur as the Grignard reagent can also act as a base (Bentley *et al.*, 1967c; Bentley *et al.*, 1967d) (Figure 2.10). This was suspected to happen during o-tolyl magnesium bromide addition that contributes to the low yield of BU10101 **(16)**. From the TLC of o-tolyl thevinol **(8)** reaction, a compound that is more polar than the starting material **(6)** was detected which was suspected to be the phenolic alcohol II (product of rearrangement) (Figure 2.10).

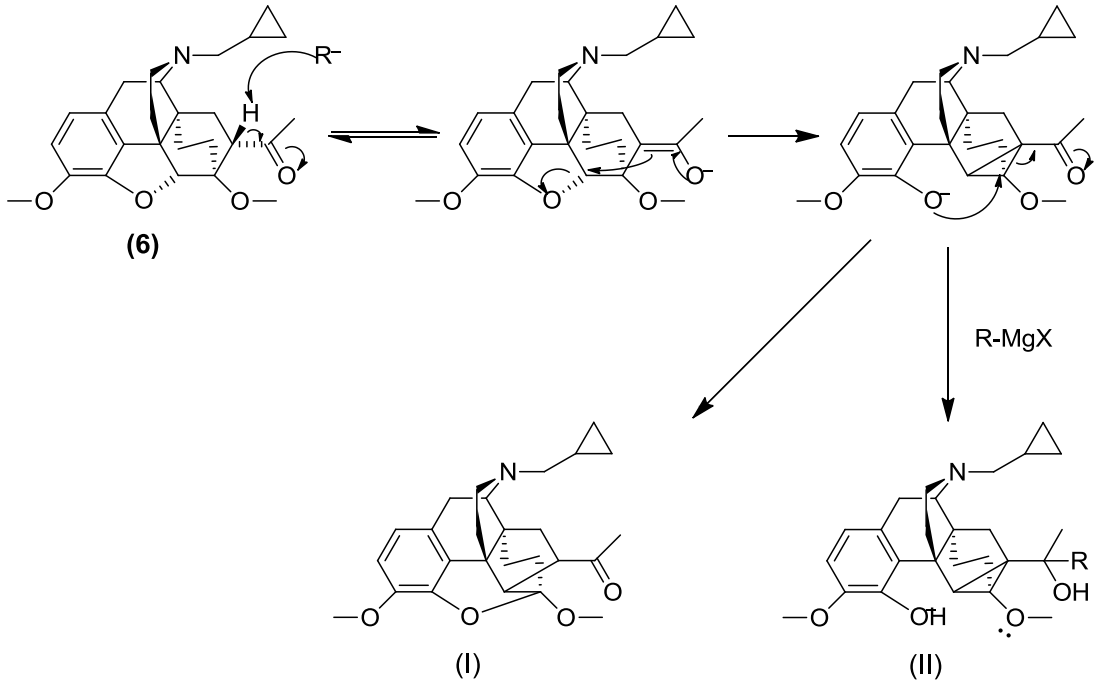

Figure 2.10: Base-catalyzed rearrangement during Grignard addition due to a slow rate Grignard addition and also in the presence of excess Grignard reagent.

Over the range of Grignard reagents used, yields after silica gel chromatography ranged from 29-83% (Table 2.1). The lowest yield was o-tolyl thevinol **(8)**, followed by 3-methyl-2-thienyl thevinol **(12)**, indicating that the steric bulk of the o-methyl group was hindering the reaction. Best yields were with the less sterically demanding and more electron rich Grignard reagents such as 2-thienyl, m-tolyl and p-tolyl. The presence of electron withdrawal group (chloro) in 5-chloro-2-thienyl did not reduce the yield of reaction. The quite low yield obtained with phenyl magnesium bromide may be because this was the first example attempted. The yield percentage obtained from the previous work carried out in the Husbands' group for phenyl magnesium bromide addition was 63% (BG1021).

Table 2.1: Percentage yields of Grignard addition to N-CPM dihydronorthevinone **(6)** from various reagents

Grignard Reagent	Product	Percentage yield (%)
Phenyl magnesium bromide	Phenyl thevinol **(7)** 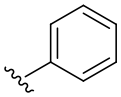	42%
o-tolyl magnesium bromide	o-tolyl thevinol **(8)** 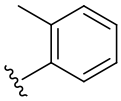	29%
m-tolyl magnesium chloride	m-tolyl thevinol **(9)** 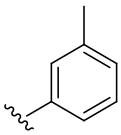	81%
p-tolyl magnesium bromide	p-tolyl thevinol **(10)** 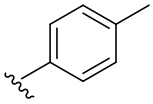	71%
2-thienyl magnesium bromide	2-thienyl thevinol **(11)** 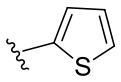	83%
3-methyl-2-thienyl magnesium bromide	3-methyl-2-thienyl thevinol **(12)** 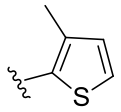	44%
5-chloro-2-thienyl magnesium bromide	5-chloro-2-thienyl thevinol **(13)** 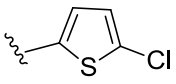	79%
3-thienyl magnesium bromide	3-thienyl thevinol **(14)** 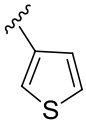	62%

2.2.6 3-O demethylation of Thevinols to Orvinols

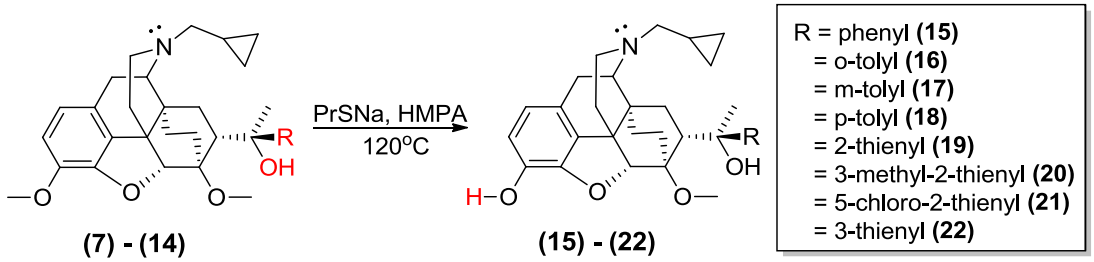

The O-demethylation with propanethiol is a selective reaction for thevinols, in which only 3-O demethylation occurs. Another alternative for a selective 3-O demethylation is by using potassium hydroxide (KOH), a strong nucleophile. However, KOH is highly corrosive and it also needs a higher temperature (200-215°C) to perform this reaction (Bentley *et al.*, 1967b; Marton *et al.*, 1997). These is in contrast to demethylation using some other reagents (eg: bromo tribromide (BBr_3) and hydrobromic acid (HBr)) (Kopcho *et al.*, 1986; Kotick *et al.*, 1983; Rice, 1977) which cause 6-O demethylation and 3-O demethylation.

The 3-O demethylation of thevinol with propanethiol is another example of S_N2 reaction where the formation of phenoxide intermediate is a rate limiting step. The 3-O demethylation of the thevinols must be conducted under base conditions to avoid acid-catalyzed rearrangement of the alcohols (Bentley *et al.*, 1967b; Casy *et al.*, 1986). A highly polar aproctic solvent, hexamethylphosphoramide (HMPA) was used in this reaction. Although liquid ammonia and dimethylformamide (DMF) also can be used as solvents for the reaction, the advantage of using HMPA is its high polarity which makes the nucleophile (eg: propanethiolate) more nucleophilic, and also eases the electron transfer reaction, and therefore helps to increase the yield of reaction (Knipmeyer *et al.*, 1985; Testaferri *et al.*, 1982). Under anhydrous condition, an excess sodium hydride (NaH) deprotonates propanethiol, creating a strong nucleophile, propanethiolate (Michne, 1978; Testaferri *et al.*, 1982). Propanethiolate is a strong nucleophile and will attack the 3-methoxy carbon which is electrophilic. Phenoxide is a leaving group in this reaction (Figure 2.11) (Testaferri *et al.*, 1982) and the aromatic group (ring A) of morphinan will delocalize the negative charge of

phenoxide around the phenyl ring to make it a stable species and therefore likely to form.

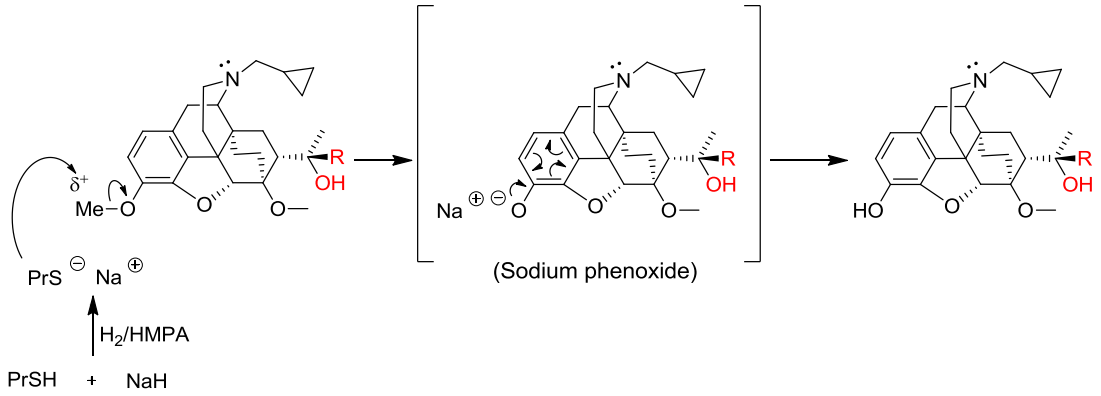

Figure 2.11: The formation of phenoxide sodium intermediate during 3-O demethylation with propanethiol.

TLC was carried out 1 and 4 hour after the reaction was set up to detect the formation of product. If reaction was not proceeding (based on TLC), more sodium hydride was added to ensure all the propanethiol was deprotonated. The yield percentage obtained for the 3-O demethylation products (orvinol) in our experiments were varied (39-82%), partly depending of the dryness of the HMPA (Grivas, 1995). HMPA is commercially available, but requires distilling after prolonged storage. A previous study has also reported freshly distilling propanethiol before the reaction was performed in order to achieve a high yield (Knipmeyer *et al.*, 1985). This was not done in the current project. It also seemed that some product was lost on the column during the purification process, especially when the purification was conducted manually. This could also explain the lower yield achieved with some of the orvinols synthesised.

In summary, eight N-CPM orvinols (end products) have been successfully prepared (including BU127 **(15)** which were used as lead). These bases were converted into

their hydrochloric salts (as described in the experimental section) for pharmacological evaluation.

2.3 Experimental

2.3.1 Experimental techniques

The NMR spectra (^{1}H, ^{1}H-COSY, ^{13}C, DEPT) were recorded on either a JEOL Delta 270 MHz or Varian Mercury 400 MHz spectrometer and referenced to external standards using the deuterium lock signal. All chemical shifts and coupling constants are given in ppm and Hz respectively.

Low and high resolution mass spectra were obtained on ESIMS:micrOTOF (BRUKER).

Elemental analysis were obtained on a Perkin-Elmer 240C analyzer.

All reactions were monitored by either thin layer chromatography (Rf) on aluminium silica sheets coated with silica gel 60 F_{254} (Merck), or by proton NMR spectroscopy in the case of catalytic hydrogenation.

All purifications were carried out by either gravity elution chromatography on Fluka silica gel 60, or flash column chromatography (Combiflash Rf) on silica RediSep Rf (12-24 g).

All reagents and solvents were used as supplied by commercial sources (Sigma-Aldrich, Fischer Scientific, Abcam) unless otherwise stated.

All solvents used were dried according to literature methods (Armarego *et al.*, 2003) whenever necessary.

2.3.2 Synthetic procedures

2.3.2.1 **General procedures**

Procedure A : Diels Alder Reaction of Thebaine (1) to give Thevinone (2)

A mixture of thebaine **1** (1 equiv.) and methyl vinyl ketone (1.2 equiv.) were heated at 70°C in anhydrous toluene (0.25 $mmolml^{-1}$) for 24 hours. The solvent and excess methyl vinyl ketone were removed under reduced pressure to yield a viscous residue which was purified by recrystallisation in methanol.

Procedure B : Catalytic Hydrogenation of Diels-Alder Adduct (Thevinone) (2) to give Dihydrothevinone (3)

A solution of thevinone **2** in mixture of ethanol (0.63 $mmolml^{-1}$) and ethyl acetate (0.63 $mmolml^{-1}$), and 10% palladium on carbon (0.1 wequiv.) was hydrogenated at 200 psi at 41°C for 6 days. The mixture was cooled to room temperature, the catalyst was removed by filtration over cellite and the solvent was evaporated under reduced pressure to yield a foam which was used without any further purification.

Procedure C : Synthesis of N-CPM dihydronorthevinone (6)

A solution of dihydrothevinone **3** (1 equiv.) in acetonitrile (anhydrous, 5.0 $mmolml^{-1}$ of **3**) and diisopropyl azodicarboxylate (DIAD, 2.8 equiv.) was heated at reflux (acetonitrile boiling point, 82°C) for 3 hours. The reaction mixture was then evaporated and the residue was dissolved in ethanol (3.3 $mmolml^{-1}$ of **3**). Pyridinium chloride (0.9 equiv.) was added and the mixture was stirred overnight at room temperature. The hydrochloride which precipitated was filtered off and washed with cold ethanol. The white isolated powder was dried under vacuum. The hydrochloride intermediate **4** obtained was dissolved in dimethylformamide, DMF (2 $mmolml^{-1}$ of **4**) and treated subsequently with anhydrous sodium hydrogen carbonate, $NaHCO_3$ (4.5 equiv.) and cyclopropylmethyl bromide **5** was added. The resultant mixture was heated at 90°C for 19 hours. The mixture was filtered to remove $NaHCO_3$ before removing DMF under vacuum and the residue was then dissolved in water. The aqueous phase was then extracted with chloroform and washed with brine. The organic layers obtained were then dried over magnesium sulphate, filtered and evaporated.

Procedure D : Synthesis of Cyclopropylmethyl bromide (5)

Cyclopropyl methanol (1 equiv.) was treated with phosphorus tribromide, PBr_3 (0.37 equiv.) in anhydrous diethyl ether at -78°C (0.3 $mmolml^{-1}$). The reaction was stirred overnight and allowed to warm to room temperature. Water (10 ml) was added and the phases were separated. The aqueous phase was extracted with diethyl ether. The organic layers obtained were then dried over magnesium sulphate and filtered. Diethyl ether was removed under vacuum and the product obtained by distillation (80-100°C).

Procedure E : Grignard Addition to give thevinols

N-CPM dihydronorthevinone **6** (1 equiv.) was dissolved in anhydrous toluene (0.1 $mmolml^{-1}$). The appropriate Grignard reagent (2 equiv.) was added and the reaction mixture was stirred at room temperature for 22 hours. Thin layer chromatography (TLC) was done after 1, 4 and 22 hour(s) to detect the product. The reaction mixture

was quenched with saturated ammonium chloride (NH_4Cl) and extracted with ethyl acetate, washed with brine and dried with magnesium sulphate ($MgSO_4$).

Procedure F : 3-O Demethylation of thevinols (3-methyl ethers) to give orvinols

To a mixture of sodium hydride, NaH (3.5 equiv.) and thevinol (1 equiv.) in hexamethylphosphoramide, HMPA (0.20 $mmolml^{-1}$) under nitrogen, 1-propanethiol (3.5 equiv.) was added drop wise. Once the addition had been completed the mixture was heated to 120°C under stirring for 5 hours before cooling to room temperature and adding a saturated aqueous solution of ammonium chloride, NH_4Cl. The mixture was extracted with diethyl ether (3x) and then was washed with water (3x) and a saturated aqueous solution of sodium chloride (2x) and finally dried with magnesium sulphate, $MgSO_4$. The extracts were evaporated to dryness under reduced pressure and the product was purified by chromatography.

Procedure G : Preparation of salts

Into a stirred solution of the freebase (1.0 equiv.) in methanol, hydrogen chloride in diethyl ether (2.0 equiv.) was added and stirred at room temperature for 30 minutes (until no further precipitation was observed). The solvent was then evaporated under reduced pressure. The salt was purified by recrystallisation from either ethanol or 2-propanol.

Procedure H : Synthesis of Grignard reagent (3-thienyl magnesiumbromide)

3-thienyllithium was prepared from 3-bromothiophene (1.0 g, 6.13 mmol) in anhydrous diethyl ether (2.26 $mmolml^{-1}$) and butyllithium (345.0 mg, 5.59 mmol) in anhydrous diethyl ether (0.67 $mmolml^{-1}$) at -70°C and was subsequently added (at -70°C) under nitrogen to a well-stirred solution of magnesium bromide in ether-toluene (anhydrous). The latter was prepared by carefully adding ethylene bromide (1.5 g, 8.0 mmol) in a mixture of anhydrous diethyl ether (2.20 $mmolml^{-1}$) and anhydrous toluene (22.1 $mmolml^{-1}$) to magnesium (300.0 mg, 12.1 mmol) in

anhydrous diethyl ether (6.74 $mmolml^{-1}$). A clear solution of 3-thienylmagnesium bromide was formed.

2.3.2.2 **Experimental data**

Thevinone (2)

Thebaine **1** (20.0 g, 64.2 mmol) and methyl vinyl ketone (6.4 ml, 77.1 mmol) in anhydrous toluene (150 ml) were treated as in general procedure A. The adduct **2** (thevinone) was purified by recrystallisation from MeOH (18.5 g, 76%). Rf (5% MeOH.DCM-0.5%NH_3) 0.38. δ_H (400M Hz; $CDCl_3$) 6.62 (1H, d, *J* 8.12, 2-H), 6.52 (1H, d, *J* 8.12, 1-H), 5.89 (1H, d, *J* 8.88, 18-H), 5.56 (1H, d, *J* 8.84, 19-H), 4.56 (1H, s, 5β-H), 3.81 (3H, s, 3-OCH_3), 3.59 (3H, s, 6-OCH_3), 3.21 (1H, d, *J* 19.12, 10β-H), 3.18 (1H, d, *J* 6.88, 9α-H), 2.88-2.95 (2H, m, 7β-H, 8β-H), 2.49-2.53 (1H, m, 15/16-NCH_2CH_2-), 2.40-2.44 (1H, m, 15/16-NCH_2CH_2-), 2.37-2.38 (1H, m, 10α-H), 2.36 (3H, s, 17-NCH_3), 2.13 (3H, s, 20-OCH_3), 1.93-1.97 (1H, m, 15/16-NCH_2,CH_2-), 1.82-1.86 (1H, m, 15/16-NCH_2,CH_2-), 1.32-1.39 (1H, dd, *J* 10.84, *J* 6.08, 8α-H); δ_C (100.56 MHz; $CDCl_3$) 209.12 (C_{20}), 141.88, 135.99, 134.08, 126.10, 119.48, 113.54, 95.23, 81.30, 81.29, 60.02, 56.66, 53.54, 50.70, 50.69, 47.55, 45.54 (CH_2), 43.27, 33.54 (CH_2), 30.59, 30.02 (CH_2), 22.47 (CH_2); m/z 382 (M^+ + 1, 100%), (Found: M^+ + 1, 382.2011. $C_{23}H_{28}NO_4$ requires 382.2018).

Dihydrothevinone (3)

Adduct **2** (16.9 g, 44.3 mmol) and 10% palladium on carbon (1.7 g) was treated as in general procedure **B** (reaction time: 6 days) to yield **3** (14.7 g, 87%). δ_H (400 MHz; $CDCl_3$) 6.70 (1H, d, *J* 8.12, 2-H), 6.57 (1H, d, *J* 8.08, 1-H), 4.46 (1H, s, 5β-H), 3.87 (3H, s, 3-OCH_3), 3.43 (3H, s, 6-OCH_3), 3.09 (1H, d, *J* 18.44, 10β-H), 3.00-3.04 (1H, dd, *J* 10.04, *J* 5.20, 9α-H), 2.62-2.71 (2H, m, 7β-H, 8β-H), 2.41-2.45 (1H, m, 15/16-NCH_2CH_2-), 2.27-2.30 (1H, m, 15/16-NCH_2CH_2-), 2.27 (3H, s, 17-NCH_3), 2.25-2.27 (1H, m, 10α-H), 2.25 (3H, s, 20-CH_3), 1.98-2.06 (1H, td, *J* 12.6, *J* 5.8, 15/16-NCH_2CH_2-), 1.70-1.75 (1H, dd, *J* 13.08, *J* 6.20, 8α-H), 1.64-1.68 (1H, m, 15/16-

NCH_2CH_2-), 1.51-1.56 (2H, m, 2 x 18/19-H), 1.23-1.33 (1H, m, 18/19-H), 0.69-0.76 (1H, m, 18/19-H).); δ_C (100.56 MHz; $CDCl_3$) 210.68 (C_{20}), 146.84, 141.82, 132.52, 128.77, 119.21, 114.17, 94.71, 61.37, 56.84, 52.24, 49.65, 45.79, 45.24 (CH_2), 43.51, 35.61, 35.21 (CH_2), 33.70, 30.40 (CH_2), 28.60 (CH_2), 22.02 (CH_2), 17.46 (CH_2); m/z 384 (M^+ + 1, 100%), (Found: M^+ + 1, 384.2171. $C_{23}H_{30}NO_4$ requires 384.2175).

Dihydronorthevinone (4)

Dihydrothevinone **3** (14.0 g, 36.5 mmol), DIAD (20.7 g, 102.2 mmol) and pyridinium chloride (3.8 g, 32.9 mmol) was treated as in general procedure **C** to yield **4** (10.2 g, 69%). Rf (40% EtOAc.Pet.Ether-0.5% NH_3) 0.30. δ_H (400 MHz; $CDCl_3$) 6.78 (1H, d, *J* 8.24, 2-H), 6.67 (1H, d, *J* 8.24, 1-H), 4.52 (1H, s, 5β-H), 3.88 (3H, s, 3-OCH_3), 3.61-3.65 (1H, m), 3.42 (3H, s, 6-OCH_3), 3.29-3.41 (2H, m), 3.05-3.13 (2H, m), 2.27 (3H, s, 20-CH_3), 1.98-2.03 (1H, m, 15/16-NCH_2,CH_2-), 1.85-1.90 (1H, m, 15/16-NCH_2,CH_2-), 0.68-0.76 (1H, m)); δ_C (100.56 MHz; $CDCl_3$) 210.60 (C_{20}), 146.94, 145.78, 142.75, 130.00, 124.58, 120.36, 115.20, 106.56, 93.83, 93.81, 81.35, 56.78, 54.00, 52.51, 52.50, 48.64, 45.17 (CH_2), 35.71, 34.06 (CH_2), 34.02 (CH_2), 30.98 (CH_2), 16.97 (CH_2); m/z 370 (M^+ + 1, 100%), (Found: M^+ + 1, 370.2011. $C_{22}H_{28}NO_4$ requires 370.2018).

Cyclopropylmethyl bromide (5)

δ_H (400 MHz; $CDCl_3$) 3.31 (2H, d, *J* 8.00, CH_2), 1.26-1.30 (1H, m, cyclopropyl-CH), 0.73-0.75 (2H, m, cyclopropyl-CH_2), 0.33-0.35 (2H, m, cyclopropyl-CH_2)

N-CPM dihydronorthevinone (6)

Dihydronorthevinone **4** (2.2 g, 5.4 mmol), anhydrous $NaHCO_3$ (2.1 g, 24.4 mmol) and cyclopropylmethyl bromide **5** (1.1 g, 8.1 mmol) was treated as in general procedure **C** to yield **6** (2.0 g, 83%). Rf (5% MeOH.DCM-0.5% NH_3) 0.70. δ_H (400 MHz; $CDCl_3$) 6.70 (1H, d, *J* 8.08, 2-H), 6.55 (1H, d, *J* 8.12, 1-H), 4.47 (1H, s, 5β-H), 3.87 (3H, s, 3-OCH_3), 3.43 (3H, s, 6-OCH_3), 3.02-3.06 (2H, m, includes 9α-H), 2.95-

3.00 (1H, d, *J* 18.32, 10β-H), 2.70-2.77 (1H, m, 7β-H), 2.60-2.64 (1H, dd, *J* 11.92, *J* 5.24, 8β-H), 2.28-2.34 (4H, m, includes 10α-H), 2.26 (3H, s, 20-CH_3), 1.99-2.07 (1H, m, 15/16-NCH_2,CH_2-), 1.70-1.75 (1H, dd, *J* 13.16, *J* 6.28, 8α-H), 1.64-1.68 (1H, m, 15/16-NCH_2,CH_2-), 1.52-1.56 (2H, m, 18/19-H), 1.26-1.33 (2H, m, 18/19-H), 0.68-0.79 (1H, m, N-$CH_2CH(CH_2$-$CH_2)$), 0.44-0.49 (2H, m, N-$CH_2CH(CH_2$-$CH_2)$), 0.08-0.09 (2H, m, N-$CH_2CH(CH_2$-$CH_2)$); δ_C (100.56 MHz; $CDCl_3$) 211.08 (C_{20}), 146.81, 141.81, 137.11, 132.74, 128.85, 119.23, 113.92, 94.81, 59.88 ($NCH_2CH(CH_2)_2$), 58.43, 56.79, 52.34, 49.73, 46.53, 43.83 (CH_2), 35.50 (CH_2), 35.38, 33.88, 30.44 (CH_2), 28.74 (CH_2), 22.82 (CH_2), 17.55 (CH_2), 9.55, 4.17 (CH_2), 3.43 (CH_2), ; m/z 424 (M^+ + 1, 100%), (Found: M^+ + 1, 424.2468. $C_{26}H_{34}NO_4$ requires 424.2488).

Phenyl thevinol (7)

N-CPM dihydronorthevinone **6** (220.0 mg, 0.52 mmol) in anhydrous toluene (5.2 ml) was treated as in procedure **E** with phenyl magnesium bromide (1.5 ml, 1.04 mmol). Purification using column chromatography (30% EtOAc-Pet.Ether-0.5%NH_3) (110.0 mg, 42%). Rf (30% EtOAc.Pet.Ether-0.5%NH_3) 0.7. δ_H (270 MHz; $CDCl_3$) 7.50 (2H, d, *J* 7.16, 2 x aryl.CH), 7.33 (2H, t, *J* 7.16, *J* 7.72, 2 x aryl.CH), 7.18-7.26 (1H, m, 1 x aryl.CH). 6.69 (1H, d, *J* 8.24, 2-H), 6.52 (1H, d, *J* 7.97, 1-H), 5.50 (1H, s, 20-OH), 4.42 (1H, s, 5β-H), 3.87 (3H, s, 3-OCH_3), 3.61 (3H, s, 6-OCH_3), 2.91 (1H, d, *J* 19.28, 10β-H), 2.86 (1H, d, *J* 7.16, 9α-H), 2.39-2.44 (1H, m, 15/16-NCH_2,CH_2-), 2.11-2.55 (5H, m, includes 10α-H), 1.87-1.99 (1H, m, 15/16-NCH_2,CH_2-), 1.79-1.86 (2H, m, includes 15/16-NCH_2,CH_2-), 1.79 (3H, s, 20-CH_3), 1.54-1.58 (1H, m), 0.77-1.07 (3H, m, includes 2 x 18/19-H, 8α-H), 0.55-0.73 (1H, m, N-$CH_2CH(CH_2$-CH_2-)), 0.33-0.39 (2H, m, N- $CH_2CH(CH_2$-CH_2-)), -0.10-(-0.03) (2H, m, N- $CH_2CH(CH_2$-CH_2-)). δ_C (100.56 MHz; $CDCl_3$) 147.46, 146.94, 141.66, 132.76, 128.98, 127.92, 126.79, 126.17, 119.18, 113.97, 97.14, 80.87, 59.54 ($NCH_2CH(CH_2)_2$), 57.97, 56.90, 53.00, 48.57, 46.95, 43.52 (CH_2), 36.03, 35.70 (CH_2), 32.65, 30.06 (CH_2), 23.58, 22.72 (CH_2), 17.97 (CH_2), 9.35, 4.18 (CH_2), 3.32(CH_2); m/z 502 (M^+ + 1, 100%), (Found: M^+ + 1, 502.2958. $C_{32}H_{40}NO_4$ requires 502.2957).

o-Tolyl thevinol (8)

N-CPM dihydronorthevinone **6** (500.0 mg, 1.18 mmol) in anhydrous toluene (11.8 ml) was treated as in procedure **E** with o-tolyl magnesiumbromide (2.95 ml, 2.95 mmol). Purification using column chromatography (30% EtOAc-Pet.Ether-0.5%NH_3) (120.0 mg, 29%). Rf (40% EtOAc.Pet.Ether-0.5%NH_3) 0.85. δ_H (400 MHz; $CDCl_3$) 7.21-7.24 (1H, m, 1 x aryl.CH), 7.08-7.15 (3H, m, 3 x aryl.CH), 6.69 (1H, d, *J* 8.12, 2-H), 6.52 (1H, d, *J* 8.08, 1-H), 5.17 (1H, s, 20-OH), 4.42 (1H, s, 5β-H), 3.88 (3H, s, 3-OCH_3), 3.59 (3H, s, 6-OCH_3), 2.91 (1H, d, *J* 18.44, 10β-H), 2.86 (1H, d, *J* 6.36, 9α-H), 2.76 (3H, s, 1 x aryl.CH_3), 2.61-2.66 (1H, t, *J* 10.28, 7β-H), 2.43-2.47 (1H, m, 15/16-NCH_2,CH_2-), 2.10-2.20 (4H, m, includes 10α-H, 1 x 15/16-NCH_2,CH_2-), 1.96-2.04 (1H, m, 8β-H), 1.83-1.88 (2H, m, 2 x 18/19-H), 1.84 (3H, s, 20-CH_3), 1.78-1.81 (1H, m, 15/16-NCH_2,CH_2-), 1.56-1.61 (1H, m, 15/16-NCH_2,CH_2-), 1.02-1.10 (1H, m, 18/19-H), 0.80-0.86 (1H, dd, *J* 13.68, *J* 9.48, 8α-H), 0.71-0.77 (1H, m, 18/19-H), 0.56-0.59 (1H, m, N-CH_2CH(CH_2-CH_2-)), 0.29-0.41 (2H, m, N-CH_2CH(CH_2-CH_2-)), -0.10-(-0.04) (2H, m, N- CH_2CH(CH_2-CH_2-)); δ_C (100.56 MHz; $CDCl_3$) 145.52, 132.82, 127.49, 126.85, 124.84, 119.54, 97.76, 79.69, 59.45 ($NCH_2CH(CH_2)_2$), 57.91, 52.69, 43.69, 36.11, 32.64, 31.93, 29.88 (CH_2), 29.70, 29.36, 25.95, 22.86, 22.69 (CH_2), 18.25 (CH_2), 14.11, 9.19, 4.09 (CH_2), 3.17 (CH_2); m/z 516 (M^+ + 1, 100%), (Found: M^+ + 1, 516.3119. $C_{33}H_{42}NO_4$ requires 516.3114).

m-Tolyl thevinol (9)

N-CPM dihydronorthevinone **6** (560.0 mg, 1.32 mmol) in anhydrous toluene (13.2 ml) was treated as in procedure **E** with m-tolyl magnesiumchloride (2.64 ml, 2.64 mmol) to yield **9**. Purification using column chromatography (30% EtOAc-Pet.Ether-0.5%NH_3) (551.0 mg, 81%). Rf (30% EtOAc-Pet.Ether-0.5%NH_3) 0.59. δ_H (400 MHz; $CDCl_3$) 7.39 (1H, s, 2 x aryl.CH), 7.31 (1H, d, *J* 7.96, 1 x aryl.CH), 7.25 (1H, t, *J* 7.44, 1 x aryl.CH), 7.09 (1H, d, *J* 7.32, 1 x aryl.CH), 6.74 (1H, d, *J* 8.12, 2-H), 6.57 (1H, d, *J* 8.12, 1-H), 5.59 (1H, s, 20-OH), 4.47 (1H, s, 5β-H), 3.93 (3H, s, 3-OCH_3), 3.64 (3H, s, 6-OCH_3), 2.89 (1H, d, *J* 19.24, 10β-H), 2.87 (1H, d, *J* 7.28, 9α-H), 2.43-2.45 (1H, m, 15/16-NCH_2,CH_2-), 2.42 (3H, s, 1 x aryl.CH_3), 2.09-2.22 (5H, m, includes 7β-H, 10α-H, 1 x 15/16-NCH_2,CH_2-), 2.00-2.09 (1H, m, 15/16-NCH_2,CH_2-), 1.84-1.92 (3H, m, includes 8β-H, 1 x 15/16-NCH_2,CH_2-), 1.82 (3H, s, 20-CH_3), 1.08-1.17 (1H, m, 18/19-H), 0.90-0.98 (1H, dd, *J* 13.2, *J* 8.96, 8α-H), 0.74-0.84 (1H, m,

18/19-H), 0.61-0.70 (1H, m, N-$CH_2CH(CH_2$-CH_2-)), 0.35-0.46 (2H, m, N-$CH_2CH(CH_2$-CH_2-)), -0.02-0.00 (2H, m, N- $CH_2CH(CH_2$-CH_2-)). δ_C (100.56 MHz; $CDCl_3$) 147.41, 146.92, 141.62, 137.20, 132.77, 128.96, 127.58, 127.43, 126.77, 123.23, 119.07, 113.98, 97.02, 80.81, 59.38 ($NCH_2CH(CH_2)_2$), 57.81, 56.88, 52.88, 48.36, 46.85, 43.55 (CH_2), 35.96, 35.61, 32.57, 29.99 (CH_2), 23.62, 22.65 (CH_2), 21.77, 18.00 (CH_2), 9.24, 4.19 (CH_2), 3.09 (CH_2); m/z 516 (M^+ + 1, 100%), (Found: M^+ + 1, 516.3113. $C_{33}H_{42}NO_4$ requires 516.3114).

p-Tolyl thevinol (10)

N-CPM dihydronorthevinone **6** (220.0 mg, 0.52 mmol) in anhydrous toluene (5.2 ml) was treated as in procedure **E** with p-tolyl magnesiumbromide (1.04 ml, 1.04 mmol). Purification using column chromatography (30% EtOAc-Pet.Ether-0.5%NH_3) (190.0 mg, 71%). Rf (30% EtOAc.Pet.Ether-0.5%NH_3) 0.56. δ_H (400 MHz; $CDCl_3$) 7.39 (2H, d, *J* 8.16, 1 x aryl.CH), 7.14 (2H, d, *J* 8.04, 2 x aryl.CH), 6.70 (1H, d, *J* 8.08, 2-H), 6.53 (1H, d, *J* 8.08, 1-H), 5.51 (1H, s, 20-OH), 4.25 (1H, s, 5β-H), 3.88 (3H, s, 3-OCH_3), 3.60 (3H, s, 6-OCH_3), 2.92 (1H, d, *J* 18.32, 10β-H), 2.87 (1H, d, *J* 6.32, 9α-H), 2.42-2.46 (1H, m, 15/16-NCH_2,CH_2-), 2.34 (3H, s, 1 x aryl.CH_3), 2.12-2.22 (4H, m, includes 7β-H, 10α-H), 2.08-2.11 (1H, m, 15/16-NCH_2,CH_2-), 1.95-2.02 (1H, m, 15/16-NCH_2,CH_2-), 1.80-1.86 (3H, m, includes 8β-H, 1 x 15/16-NCH_2,CH_2-), 1.76 (3H, s, 20-CH_3), 1.02-1.10 (1H, m, 18/19-H), 0.87-0.92 (1H, dd, *J* 13.24, *J* 5.2, 8α-H), 0.72-0.78 (1H, m, 18/19-H), 0.57-0.61 (1H, m, N-$CH_2CH(CH_2$-CH_2-)), 0.35-0.41 (2H, m, N-$CH_2CH(CH_2$-CH_2-)), -0.05-0 (2H, m, N-$CH_2CH(CH_2$-CH_2-)); δ_C (100.56 MHz; $CDCl_3$) 146.95, 144.54, 141.57, 135.95, 132.76, 128.94, 128.38, 125.88, 118.98, 114.21, 96.96, 80.70, 59.43 ($NCH_2CH(CH_2)_2$), 58.03, 56.90, 52.72, 48.44, 46.78, 43.40 (CH_2), 35.95, 35.58, 32.55, 29.93 (CH_2), 23.49, 22.68 (CH_2), 20.91, 17.90 (CH_2), 9.18, 3.91 (CH_2), 3.12 (CH_2). m/z 516 (M^+ + 1, 100%), (Found: M^+ + 1, 516.3182. $C_{33}H_{41}NO_4$ requires 516.3114).

2-Thienyl thevinol (11)

N-CPM dihydronorthevinone **6** (800.0 mg, 1.89 mmol) was treated in anhydrous toluene (18.9 ml) as in procedure **E** with 2-thienyl magnesiumbromide (3.78 ml, 3.78 mmol). Purification using column chromatography (30% EtOAc-Pet.Ether-0.5%NH_3)

(800.0 mg, 83%). Rf (30% EtOAc.Pet.Ether-0.5%NH_3) 0.52. δ_H (400 MHz; $CDCl_3$) 7.28 (1H, d, *J* 1.16, 1 x thienyl.CH), 6.94 (1H, t, *J* 5.04, 1 x thienyl.CH), 6.90 (1H, d, *J* 3.52, 1 x thienyl.CH), 6.72 (1H, d, *J* 8.12, 2-H), 6.56 (1H, d, *J* 8.08, 1-H), 5.78 (1H, s, 20-OH), 4.51 (1H, s, 5β-H), 3.90 (3H, s, 3-OCH_3), 3.62 (3H, s, 6-OCH_3), 2.96 (1H, d, *J* 18.32, 10β-H), 2.90 (1H, d, *J* 6.24, 9α-H), 2.50-2.55 (1H, m, 15/16-NCH_2,CH_2-), 2.18-2.25 (6H, m, includes 7β-H, 10α-H, 15/16-NCH_2,CH_2-), 1.85-1.89 (3H, m, includes 8β-H, 1 x 15/16-NCH_2,CH_2-), 1.85 (3H, s, 20-CH_3), 1.60-1.64 (1H, m, 15/16-NCH_2,CH_2-), 1.05-1.13 (1H, m, 18/19-H), 0.95-1.01 (1H, dd, *J* 12.68, *J* 8.68, 8α-H), 0.75-0.81 (1H, m, 18/19-H), 0.66-0.69 (1H, m, N-CH_2CH(CH_2-CH_2-)), 0.40-0.43 (2H, m, N-CH_2CH(CH_2-CH_2-)), -0.05-0.02 (2H, m, N-CH_2CH(CH_2-CH_2-)); δ_C (100.56 MHz; $CDCl_3$) 153.12, 146.99, 141.67, 132.72, 128.97, 125.84, 124.55, 123.05, 119.14, 114.25, 98.99, 80.78, 59.58 ($NCH_2CH(CH_2)_2$), 58.18, 56.95, 52.94, 49.72, 47.06, 43.42 (CH_2), 36.05, 35.67 (CH_2), 32.67 (CH_2), 29.93 (CH_2), 24.12, 22.80 (CH_2), 17.86 (CH_2), 9.35, 3.96 (CH_2), 3.37 (CH_2). m/z 508 (M^+ + 1, 100%), (Found: M^+ + 1, 508.2559. $C_{30}H_{38}NO_4S$ requires 508.2522).

3-Methyl-2-Thienyl thevinol (12)

N-CPM dihydronorthevinone **6** (600.0 mg, 1.42 mmol) in anhydrous toluene (14.2 ml) was treated as in procedure **E** with 3-methyl-2-thienyl magnesiumbromide (5.68 ml, 2.84 mmol). Purification using column chromatography (30% EtOAc.Pet.Ether-0.5%NH_3) (325.0 mg, 44%). Rf (30% EtOAc-Pet.Ether-0.5%NH_3) 0.54. δ_H (400 MHz; $CDCl_3$) 7.04 (1H, d, *J* 5.08, 1 x thienyl.CH), 6.77 (1H, d, *J* 5.12, 1 x thienyl.CH), 6.71 (1H, d, *J* 8.12, 2-H), 6.54 (1H, d, *J* 8.08, 1-H), 5.39 (1H, s, 20-OH), 4.43 (1H, s, 5β-H), 3.89 (3H, s, 3-OCH_3), 3.59 (3H, s, 6-OCH_3), 2.93-2.97 (1H, m, 10β-H), 2.88-2.90 (1H, m, 9α-H), 2.50-2.52 (1H, m, 15/16-NCH_2,CH_2-), 2.49 (3H, s, 1 x thienyl.CH_3), 2.17-2.32 (5H, m, includes 7β-H, 10α-H, 15/16-NCH_2,CH_2-), 1.82-1.88 (3H, m, 15/16-NCH_2,CH_2-, 2 x 18/19-H), 1.88 (3H, s, 20-CH_3), 1.61-1.64 (1H, m, 15/16-NCH_2,CH_2-), 1.23-1.28 (1H, m), 1.05-1.13 (1H, m, 8α-H), 0.74-0.79 (1H, m, 18/19-H), 0.63-0.69 (1H, m, N-CH_2CH(CH_2-CH_2-)), 0.35-0.45 (2H, m, N-CH_2CH(CH_2-CH_2-)), 0.00-0.01 (2H, m, N-CH_2CH(CH_2-CH_2-)); δ_C (100.56 MHz; $CDCl_3$) 147.00, 144.14, 141.65, 133.14, 132.74, 131.74, 129.01, 121.18, 119.15, 114.25, 97.18, 80.49, 59.46 ($NCH_2CH(CH_2)_2$), 57.93, 56.95, 52.85, 47.43, 47.00, 43.54 (CH_2), 36.02, 35.74 (CH_2), 32.23 (CH_2), 29.95 (CH_2), 25.59, 22.75 (CH_2), 18.00 (CH_2),

16.03, 9.32, 4.13 (CH_2), 3.12 (CH_2). m/z 522 (M^+ + 1, 100%), (Found: M^+ + 1, 522.2760. $C_{31}H_{40}NO_4S$ requires 522.7186).

5-Chloro-2-Thienyl thevinol (13)

N-CPM dihydronorthevinone **6** (250.0 mg, 0.59 mmol) in anhydrous toluene (5.9 ml) was treated as in procedure **E** with 5-chloro-2-thienyl magnesiumbromide (2.36 ml, 1.18 mmol). Purification using column chromatography (30% EtOAc-Pet.Ether-0.5%NH_3) (254.0 mg, 79%). Rf (30% EtOAc.Pet.Ether-0.5%NH_3) 0.56. δ_H (400 MHz; $CDCl_3$) 6.72 (1H, d, *J* 3.80, 1 x thienyl.CH), 6.70 (1H, d, *J* 8.12, 2-H), 6.61 (1H, d, *J* 3.84, 1 x thienyl.CH), 6.54 (1H, d, *J* 8.12, 1-H), 5.82 (1H, s, 20-OH), 4.40 (1H, s, 5β-H), 3.88 (3H, s, 3-OCH_3), 3.59 (3H, s, 6-OCH_3), 2.95 (1H, d, *J* 17.56, 10β-H), 2.92 (1H, d, *J* 5.88, 9α-H), 2.52-2.56 (1H, m, 15/16-NCH_2,CH_2-), 2.16-2.34 (5H, m, includes 7β-H, 10α-H, 15/16-NCH_2,CH_2-), 1.83-1.90 (3H, m, 15/16-NCH_2,CH_2-, 2 x 18/19-H), 1.76 (3H, s, 20-CH_3), 1.58-1.64 (1H, m, 15/16-NCH_2,CH_2-), 1.02-1.09 (1H, m, 18/19-H), 0.87-0.96 (1H, m, 8α-H), 0.71-0.81 (1H, m, 18/19-H), 0.67-0.70 (1H, m, N-CH_2CH(CH_2-CH_2-)), 0.40-0.45 (2H, m, N-CH_2CH(CH_2-CH_2-)), -0.03-0.05 (2H, m, N-CH_2CH(CH_2-CH_2-)); δ_C (100.56 MHz; $CDCl_3$) 151.81, 146.75, 141.55, 132.47, 129.06, 128.80, 124.93, 122.13, 119.10, 113.84, 96.91, 80.65, 59.52 ($NCH_2CH(CH_2)_2$), 57.84, 56.76, 52.99, 49.40, 47.00, 43.37 (CH_2), 35.90, 35.53 (CH_2), 32.59 (CH_2), 29.81 (CH_2), 23.41, 22.55 (CH_2), 17.69 (CH_2), 14.16, 9.27, 4.07 (CH_2), 3.25 (CH_2). m/z 542 (M^+ + 1, 100%), (Found: M^+ + 1, 542.2161. $C_{30}H_{37}ClNO_4S$ requires 542.2132).

3-Thienyl thevinol (14)

N-CPM dihydronorthevinone **6** (288.0 mg, 0.68 mmol) in anhydrous toluene (6.8 ml) was treated as in procedure **E** with 3-thienyl magnesiumbromide (4.80 ml, 1.36 mmol). Purification using column chromatography (30% EtOAc-Pet.Ether-0.5%NH_3) (215.0 mg, 62%). Rf (30% EtOAc.Pet.Ether-0.5%NH_3) 0.58. δ_H (400 MHz; $CDCl_3$) 7.27 (1H, d, *J* 3.00, 1 x thienyl.CH), 7.20 (1H, d, *J* 5.00, 1 x thienyl.CH), 7.16 (1H, d, *J* 1.80, 1 x thienyl.CH), 6.70 (1H, d, *J* 8.08, 2-H), 6.53 (1H, d, *J* 8.12, 1-H), 5.39 (1H, s, 20-OH), 4.43 (1H, s, 5β-H), 3.89 (3H, s, 3-OCH_3), 3.60 (3H, s, 6-OCH_3), 2.94 (1H, d, *J* 18.28, 10β-H), 2.85 (1H, d, *J* 6.44, 9α-H), 2.48-2.52 (1H, m, 15/16-NCH_2,CH_2-),

2.12-2.26 (6H, m, 7β-H, 8β-H, 10α-H, 15/16-NCH_2,CH_2-), 1.80-1.90 (3H, m, 15/16-NCH_2,CH_2-, 2 x 18/19-H), 1.78 (3H, s, 20-CH_3), 1.57-1.63 (1H, m, 15/16-NCH_2,CH_2-), 1.01-1.09 (1H, m, 18/19-H), 0.87-0.95 (1H, dd, *J* 18.44, *J* 14.36, 8α-H), 0.70-0.80 (1H, m, 18/19-H), 0.60-0.70 (1H, m, N-$CH_2CH(CH_2$-CH_2-)), 0.34-0.44 (2H, m, N-$CH_2CH(CH_2$-CH_2-)), -0.06-0.03 (2H, m, N-$CH_2CH(CH_2$-CH_2-)); δ_C (100.56 MHz; $CDCl_3$) 149.44, 146.97, 141.63, 126.42, 124.93, 120.42, 119.05, 114.32, 96.95, 80.52, 59.46 ($NCH_2CH(CH_2)_2$), 58.20, 56.91, 52.75, 48.21, 46.84, 43.39 (CH_2), 35.97, 35.58 (CH_2), 32.45 (CH_2), 29.89 (CH_2), 22.84 (CH_2), 17.81 (CH_2), 9.16, 3.87 (CH_2), 3.28 (CH_2). m/z 508 (M^+ + 1, 100%), (Found: M^+ + 1, 508.2604. $C_{30}H_{37}NNaO_4S$ requires 530.2341).

Phenyl orvinol (15)

The thevinol **7** (103.0 mg, 0.21 mmol) was treated as in procedure **F** to yield orvinol **15** after purification using column chromatography (30% EtOAcPet.Ether-0.5%NH_3) (40.0 mg, 39%). Rf (30% EtOAc.Pet.Ether-0.5%NH_3) 0.2. δ_H (270 MHz; $CDCl_3$) 7.50 (2H, d, *J* 7.16, 2 x aryl.CH), 7.32 (2H, t, *J* 6.86, 7.97, 2 x aryl.CH), 7.18-7.26 (1H, m, 1 x aryl.CH). 6.62 (1H, d, *J* 7.99, 2-H), 6.45 (1H, d, *J* 7.97, 1-H), 5.58 (1H, s, 20-OH), 4.60 (1H, s, 3-OH), 4.42 (1H, s, 5β-H), 3.56 (3H, s, 6-OCH_3), 2.89 (1H, d, *J* 17.87, 10β-H), 2.84 (1H, d, *J* 4.43, 9α-H), 2.40-2.42 (1H, m, 15/16-NCH_2,CH_2-), 2.10-2.19 (5H, m, includes 10α-H, 15/16-NCH_2,CH_2-), 1.90-2.08 (1H, m, 15/16-NCH_2,CH_2-), 1.72-1.84 (3H, m, includes 15/16-NCH_2,CH_2-), 1.80 (3H, s, 20-CH_3), 1.54-1.58 (1H, m, 15/16-NCH_2,CH_2-), 1.02-1.10 (1H, m, 18/19-H), 0.89-0.94 (1H, dd, *J* 12.2, *J* 9.48, 8α-H), 0.69-0.76 (1H, m, 18/19-H), 0.56-0.65 (1H, m, N-$CH_2CH(CH_2$-CH_2-)), 0.30-0.40 (2H, m, N-$CH_2CH(CH_2$-CH_2-)), -0.1-0 (2H, m, N-$CH_2CH(CH_2$-CH_2-)); δ_C (100.56 MHz; $CDCl_3$) 147.27, 132.44, 127.93, 126.83, 126.14, 119.56, 116.51, 97.39, 80.92, 59.52 ($NCH_2CH(CH_2)_2$), 58.01, 52.91, 48.48, 47.24, 43.53 (CH_2), 36.10, 35.60 (CH_2), 32.60, 29.95 (CH_2), 23.59, 22.80 (CH_2), 17.97 (CH_2), 9.32, 4.15 (CH_2), 3.31(CH_2) ; m/z 488 (M^+ + 1, 100%), (Found M^+ + 1, 488.2778. $C_{31}H_{38}NO_4$ requires 488.2801).

Phenol was converted to the corresponding hydrochloride salt as in general procedure **G** and assigned **BU127 (15)**.

o-Tolyl orvinol (16)

The thevinol **8** (200.0 mg, 0.39 mmol) was treated as in procedure **F** to yield orvinol **16** after purification using column chromatography (30% EtOAc-Pet.Ether-0.5%NH_3) (159.0 mg, 81%). Rf (30% EtOAc-Pet.Ether-0.5%NH_3) 0.30. δ_H (400 MHz; $CDCl_3$) 7.16-7.23 (1H, m, 1 x aryl.CH), 7.10-7.16 (3H, m, 3 x aryl.CH), 6.68 (1H, d, *J* 8.04, 2-H). 6.49 (1H, d, *J* 8.04, 1-H), 5.12 (1H, s, 20-OH), 4.64 (1H, s, 3-OH) 4.46 (1H, s, 5β-H), 3.58 (3H, s, 6-OCH_3), 2.91 (1H, d, *J* 18.52, 10β-H), 2.87 (1H, d, *J* 6.56, 9α-H), 2.76 (3H, s, 1 x aryl.CH_3), 2.62-2.67 (1H, t, *J* 9.88, 7β-H), 2.45-2.49 (1H, m, 15/16-NCH_2,CH_2-), 2.13-2.21 (4H, m, includes 10α-H, 1 x 15/16-NCH_2,CH_2-), 1.97-2.02 (1H, m, 8β-H), 1.86-1.90 (2H, m, 2 x 18/19-H), 1.85 (3H, s, 20-CH_3), 1.79-1.83 (1H, m, 15/16-NCH_2,CH_2-), 1.59-1.63 (1H, m, 15/16-NCH_2,CH_2-), 1.02-1.10 (1H, m, 15/16-NCH_2,CH_2-), 0.83-0.88 (1H, dd, *J* 13.56, *J* 9.36, 8α-H), 0.70-0.76 (1H, m, 18/19-H), 0.56-0.60 (1H, m, N-CH_2CH(CH_2-CH_2-)), 0.32-0.40 (2H, m, N-CH_2CH(CH_2-CH_2-)), -0.08-(-0.03) (2H, m, N-CH_2CH(CH_2-CH_2-)); δ_C (100.56 MHz; $CDCl_3$) 145.55, 137.28, 136.92, 132.90, 128.43, 127.60, 126.95, 124.91, 119.57, 116.42, 97.77, 80.90, 79.85, 59.51 ($NCH_2CH(CH_2)_2$), 57.85, 52.84, 47.25, 43.70, 43.61 (CH_2), 36.12, 35.66 (CH_2), 29.93 (CH_2), 29.80, 25.99, 22.96, 22.72 (CH_2), 18.27 (CH_2), 9.28, 4.11 (CH_2) , 3.23 (CH_2); m/z 502 (M^+ + 1, 100%), (Found M^+ + 1, 502.3052. $C_{32}H_{40}NO_4$ requires 502.2957).

Phenol was converted to the corresponding hydrochloride salt as in general procedure **G** and assigned **BU10101**.

Found: C, 69.70; H, 7.38; N, 2.46. $C_{32}H_{40}ClNO_4.0.75H_2O$ requires C, 69.67; H, 7.58; N, 2.54%.

m-tolyl orvinol (17)

The thevinol **9** (530.0 mg, 1.03 mmol) was treated as in procedure **F** to yield orvinol **17** after purification using column chromatography (30% EtOAc.Pet.Ether-0.5%NH_3) (349.5 mg, 68%). Rf (30% EtOAc-Pet.Ether-0.5%NH_3) 0.21. δ_H (400 MHz; $CDCl_3$) 7.34 (1H, s, 1 x aryl.CH), 7.25 (1H, d, *J* 7.96, 1 x aryl.CH), 7.21 (1H, t, *J* 7.48, 1 x aryl.CH), 7.05 (1H, d, *J* 7.36, 1 x aryl.CH), 6.67 (1H, d, *J* 8.04, 2-H), 6.48 (1H, d, *J* 8.04, 1-H), 5.41 (1H, s, 20-OH), 4.67 (1H, s, 3-OH), 4.45 (1H, s, 5β-H), 3.56 (3H, s, 6-OCH_3), 2.91 (1H, d, *J* 19.24, 10β-H), 2.88 (1H, d, *J* 7.28, 9α-H), 2.43-2.46 (1H, m,

15/16-NCH_2,CH_2-), 2.38 (3H, s, 1 x aryl.CH_3), 2.08-2.23 (5H, m, includes 7β-H, 10α-H, 15/16-NCH_2,CH_2-), 2.00-2.09 (1H, m, 15/16-NCH_2,CH_2-), 1.79-1.91 (3H, m, includes 8β-H, 15/16-NCH_2,CH_2-), 1.76 (3H, s, 20-CH_3), 1.02-1.11 (1H, m, 18/19-H), 0.91-0.97 (1H, dd, *J* 13.2, *J* 8.96, 8α-H), 0.68-0.77 (1H, m, 18/19-H), 0.57-0.65 (1H, m, N-CH_2CH(CH_2-CH_2-)), 0.31-0.43 (2H, m, N-CH_2CH(CH_2-CH_2-)), -0.09-0.01 (2H, m, N-CH_2CH(CH_2-CH_2-)); δ_C (100.56 MHz; CD_3OD) 150.81. 145.39, 145.14, 137.56, 132.37, 127.94, 127.66, 127.58, 127.42, 124.03, 123.12, 119.60, 116.77, 91.62, 64.49, 59.75 ($NCH_2CH(CH_2)_2$), 58.47, 50.49, 45.85, 40.82, 36.19, 35.94, 29.33 (CH_2), 25.20, 22.81, 21.47, 18.98 (CH_2), 9.19, 4.16, 3.35 (CH_2). m/z 502 (M^+ + 1), (Found M^+ + 1, 502.2968. $C_{32}H_{40}NO_4$ requires 502.2957).

Phenol was converted to the corresponding hydrochloride salt as in general procedure G and assigned **BU10092**.

Found: C, 71.10; H, 7.64; N, 2.49. $C_{32}H_{40}ClNO_4$ requires C, 71.42; H, 7.49; N, 2.60%.

p-Tolyl orvinol (18)

The thevinol **10** (155.0 mg, 0.30 mmol) was treated as in procedure **F** to yield orvinol **18** after purification using column chromatography (30% EtOAc-Pet.Ether-0.5%NH_3) (87.0 mg, 58%). Rf (30% EtOAc.Pet.Ether-0.5%NH_3) 0.23. δ_H (400 MHz; $CDCl_3$) 7.39 (2H, d, *J* 8.20, 2 x aryl.CH), 7.14 (2H, d, *J* 7.92, 2 x aryl.CH), 6.68 (1H, d, *J* 8.04, 2-H), 6.49 (1H, d, *J* 8.08, 1-H), 5.42 (1H, s, 20-OH), 4.62 (1H, s, 3-OH), 4.51 (1H, s, 5β-H), 3.57 (3H, s, 6-OCH_3), 2.91 (1H, d, *J* 18.88, 10β-H), 2.87 (1H, d, *J* 6.80, 9α-H), 2.43-2.47 (1H, m, 15/16-NCH_2,CH_2-), 2.35 (3H, s, 1 x aryl.CH_3), 2.12-2.21 (4H, m, includes 7β-H, 10α-H), 2.07-2.12 (1H, m, 15/16-NCH_2,CH_2-), 1.95-2.02 (1H, m, 15/16-NCH_2,CH_2-), 1.82-1.88 (1H, m, 15/16-NCH_2,CH_2-), 1.79-1.83 (1H, m, 8β-H), 1.77 (3H, s, 20-CH_3), 1.00-1.09 (1H, m, 18/19-H), 0.87-0.93 (1H, m, 8α-H), 0.69-0.76 (1H, m, 18/19-H), 0.56-0.64 (1H, m, N-CH_2CH(CH_2-CH_2-)), 0.32-0.43 (2H, m, N-CH_2CH(CH_2-CH_2-)), -0.09-0.00 (2H, m, N-CH_2CH(CH_2-CH_2-)); δ_C (100.56 MHz; $CDCl_3$) 145.34, 137.00, 136.03, 132.38, 128.45, 125.86, 119.45, 116.13, 80.71, 59.41 ($NCH_2CH(CH_2)_2$), 57.88, 52.72, 48.30, 47.14, 43.42 (CH_2), 35.97 (CH_2), 32.49, 22.64 (CH_2), 20.98, 17.86 (CH_2), 9.17, 4.00 (CH_2), 3.13 (CH_2). m/z 502 (M^+ + 1), (Found M^+ + 1, 502.3048. $C_{32}H_{40}NaO_4$ requires 502.2957).

Phenol was converted to the corresponding hydrochloride salt as in general procedure G and assigned **BU10135**.

Found: C, 68.80; H, 7.16; N, 2.57. $C_{32}H_{40}ClNO_4.H_2O$ requires C, 69.11; H, 7.61; N, 2.52%.

2-Thienyl orvinol (19)

The thevinol **11** (800.0 mg, 1.58 mmol) was treated as in procedure **F** to yield orvinol **19** after purification using column chromatography (30% EtOAc-Pet.Ether-0.5%NH_3) (324.0 mg, 42%). Rf (30% EtOAc.Pet.Ether-0.5%NH_3) 0.19. δ_H (400 MHz; $CDCl_3$) 7.25 (1H, d, *J* 1.12, 1 x thienyl.CH), 6.91 (1H, t, *J* 5.00, 1 x thienyl.CH), 6.88 (1H, d, *J* 3.52, 1 x thienyl.CH), 6.68 (1H, d, *J* 8.00, 2-H), 6.49 (1H, d, *J* 8.04, 1-H), 5.73 (1H, s, 20-OH), 4.61 (1H, s, 3-OH), 4.46 (1H, s, 5β-H), 3.58 (3H, s, 6-OCH_3), 2.92 (1H, d, *J* 18.64, 10β-H), 2.88 (1H, d, *J* 6.48, 9α-H), 2.48-2.53 (1H, m, 15/16-NCH_2,CH_2-), 2.12-2.25 (6H, m, includes 7β-H, 8β-H, 10α-H, 15/16-NCH_2,CH_2-), 1.80-1.89 (3H, m, includes, 1 x 15/16-NCH_2,CH_2-, 2 x 18/19-H), 1.83 (3H, s, 20-CH_3), 1.59-1.62 (1H, m, 15/16-NCH_2,CH_2-), 1.02-1.10 (1H, m, 18/19-H), 0.92-0.97 (1H, m, 8α-H), 0.70-0.77 (1H, m, 18/19-H), 0.61-0.67 (1H, m, N-$CH_2CH(CH_2$-CH_2-)), 0.38-0.42 (2H, m, N-$CH_2CH(CH_2$-CH_2-)), -0.21-0.00 (2H, m, N-$CH_2CH(CH_2$-CH_2-)); δ_C (100.56 MHz; $CDCl_3$) 153.03, 145.45, 137.10, 132.40, 128.54, 125.85, 124.58, 123.08, 119.60, 116.27, 97.51, 80.83, 59.57 ($NCH_2CH(CH_2)_2$), 58.19, 52.87, 49.68, 47.45, 43.41 (CH_2), 36.13, 35.57 (CH_2), 32.64 (CH_2), 29.81 (CH_2), 24.13, 22.85 (CH_2), 17.82 (CH_2), 9.35, 3.93 (CH_2), 3.37 (CH_2). m/z 494 (M^+ + 1), (Found M^+ + 1, 494.2344. $C_{29}H_{36}NO_4S$ requires 494.2365).

Phenol was converted to the corresponding hydrochloride salt as in general procedure **G** and assigned **BU08026**.

Found: C, 63.30; H, 6.96; N, 2.42. $C_{29}H_{36}ClNO_4S.H_2O$ requires C, 63.54; H, 6.99; N, 2.56%.

3-Methyl-2-Thienyl orvinol (20)

The thevinol **12** (262.0 mg, 0.50 mmol) was treated as in procedure **F** to yield orvinol **20** after purification using column chromatography (30% EtOAc-Pet.Ether-0.5%NH_3)

(135.0 mg, 53%). Rf (30% EtOAc.Pet.Ether-0.5%NH_3) 0.17. δ_H (400 MHz; $CDCl_3$) 7.03 (1H, d, *J* 5.04, 1 x thienyl.CH), 6.76 (1H, d, *J* 5.12, 1 x thienyl.CH), 6.68 (1H, d, *J* 8.04, 2-H), 6.50 (1H, d, *J* 8.08, 1-H), 5.30 (1H, s, 20-OH), 4.51 (1H, s, 3-OH), 4.46 (1H, s, 5β-H), 3.56 (3H, s, 6-OCH_3), 2.93 (1H, d, *J* 18.04, 10β-H), 2.90 (1H, d, *J* 6.36, 9α-H), 2.46-2.51 (2H, m, includes 15/16-NCH_2,CH_2-), 2.48 (3H, s, 1 x thienyl.CH_3), 2.15-2.31 (5H, m, includes 7β-H, 10α-H, 15/16-NCH_2,CH_2-), 1.79-1.89 (3H, m, 15/16-NCH_2,CH_2-, 2 x 18/19-H), 1.87 (3H, s, 20-CH_3), 1.60-1.64 (1H, m, 15/16-NCH_2,CH_2-), 1.04-1.10 (1H, m, 8α-H), 0.68-0.78 (1H, m, 18/19-H), 0.62-0.68 (1H, m, N-CH_2CH(CH_2-CH_2-)), 0.34-0.45 (2H, m, N-CH_2CH(CH_2-CH_2-)), -0.02-0.01 (2H, m, N-CH_2CH(CH_2-CH_2-)); δ_C (100.56 MHz; $CDCl_3$) 145.49, 144.06, 137.18, 133.14, 132.40, 131.75, 128.47, 121.22, 119.59, 116.35, 97.60, 80.53, 59.45 ($NCH_2CH(CH_2)_2$), 57.94, 52.78, 47.35, 43.54 (CH_2), 36.09, 35.63 (CH_2), 32.20 (CH_2), 29.84 (CH_2), 25.61, 22.80 (CH_2), 21.03, 18.00 (CH_2), 16.02, 14.20, 9.30, 4.10 (CH_2), 3.22 (CH_2). m/z 508 (M^+ + 1), (Found M^+ + 1, 508.2572. $C_{30}H_{38}NO_4S$ requires 508.2522).

Phenol was converted to the corresponding hydrochloride salt as in general procedure G and assigned **BU10093**.

Found: C, 65.30; H, 7.06; N, 2.55. $C_{30}H_{38}ClNO_4S.0.5H_2O$ requires C, 65.14; H, 7.11; N, 2.53%.

5-Chloro-2-Thienyl orvinol (21)

The thevinol **13** (215.0 mg, 0.40 mmol) was treated as in procedure **F** to yield orvinol **21** after purification using column chromatography (30% EtOAc.Pet.Ether-0.5%NH_3) (149.0 mg, 71%). Rf (30% EtOAc.Pet.Ether-0.5%NH_3) 0.12. δ_H (400 MHz; $CDCl_3$) 6.72 (1H, d, *J* 3.80, 1 x thienyl.CH), 6.68 (1H, d, *J* 8.04, 2-H), 6.61 (1H, d, *J* 3.84, 1 x thienyl.CH), 6.50 (1H, d, *J* 8.08, 1-H), 5.69 (1H, s, 20-OH), 4.56 (1H, s, 3-OH), 4.42 (1H, s, 5β-H), 3.57 (3H, s, 6-OCH_3), 2.94 (1H, d, *J* 18.56, 10β-H), 2.90 (1H, d, *J* 6.52, 9α-H), 2.52-2.57 (1H, m, 15/16-NCH_2,CH_2-), 2.15-2.35 (5H, m, includes 7β-H, 10α-H, 15/16-NCH_2,CH_2-), 1.77-1.88 (3H, m, 15/16-NCH_2,CH_2-, 2 x 18/19-H), 1.76 (3H, s, 20-CH_3), 1.59-1.63 (1H, m, 15/16-NCH_2,CH_2-), 1.00-1.10 (1H, m, 18/19-H), 0.86-0.95 (1H, m, 8α-H), 0.67-0.77 (2H, m, 18/19-H, N-CH_2CH(CH_2-CH_2-)), 0.36-0.47 (2H, m, N-CH_2CH(CH_2-CH_2-)), -0.04-0.06 (2H, m, N-CH_2CH(CH_2-CH_2-)); δ_C (100.56 MHz; $CDCl_3$) 151.81, 146.75, 141.55, 132.47, 129.06, 128.80, 124.93,

122.13, 119.10, 113.84, 96.91, 80.65, 59.52 ($NCH_2CH(CH_2)_2$), 57.84, 56.76, 52.99, 49.40, 47.00, 43.37 (CH_2), 35.90, 35.53 (CH_2), 32.59 (CH_2), 29.81 (CH_2), 23.41, 22.55 (CH_2), 17.69 (CH_2), 9.27, 4.07 (CH_2), 3.25 (CH_2). m/z 550 (M^+ + Na), (Found M^+ + Na, 550.1774. $C_{29}H_{34}ClNNaO_4S$ requires 550.1795).

Phenol was converted to the corresponding hydrochloride salt as in general procedure **G** and assigned **BU10136**.

Found: C, 58.30; H, 6.40; N, 2.28. $C_{29}H_{35}ClNO_4S.2H_2O$ requires C, 57.99; H, 6.55; N, 2.33%.

3-Thienyl orvinol (22)

The thevinol **14** (324.0 mg, 0.64 mmol) was treated as in procedure **F** to yield orvinol **22** after purification using column chromatography (30% EtOAc-Pet.Ether-0.5%NH_3) (236.0 mg, 75%). Rf (30% EtOAc.Pet.Ether-0.5%NH_3) 0.11. δ_H (400 MHz; $CDCl_3$) 7.26 (1H, d, *J* 2.96, 1 x thienyl.CH), 7.20 (1H, d, *J* 5.00, 1 x thienyl.CH), 7.16 (1H, d, *J* 2.88, 1 x thienyl.CH), 6.68 (1H, d, *J* 8.04, 2-H), 6.50 (1H, d, *J* 8.00, 1-H), 5.32 (1H, s, 20-OH), 4.59 (1H, s, 3-OH), 4.46 (1H, s, 5β-H), 3.58 (3H, s, 6-OCH_3), 2.93 (1H, d, *J* 18.40, 10β-H), 2.86 (1H, d, *J* 6.16, 9α-H), 2.49-2.53 (1H, m, 15/16-NCH_2,CH_2-), 2.12-2.28 (6H, m, 7β-H, 8β-H, 10α-H, 15/16-NCH_2,CH_2-), 1.81-1.92 (3H, m, 15/16-NCH_2,CH_2-, 2 x 18/19-H), 1.79 (3H, s, 20-CH_3), 1.58-1.63 (1H, m, 15/16-NCH_2,CH_2-), 1.04-1.07 (1H, m, 18/19-H), 0.89-0.97 (1H, m, 8α-H), 0.70-0.80 (1H, m, 18/19-H), 0.60-0.70 (1H, m, N-$CH_2CH(CH_2$-CH_2-)), 0.34-0.45 (2H, m, N-$CH_2CH(CH_2$-CH_2-)), -0.06-0.03 (2H, m, N-$CH_2CH(CH_2$-CH_2-)); δ_C (100.56 MHz; $CDCl_3$) 149.44, 137.04, 126.37, 124.94, 120.41, 119.48, 116.18, 97.52, 80.63, 59.47 ($NCH_2CH(CH_2)_2$), 58.22, 52.67, 48.22, 47.29, 43.33 (CH_2), 36.05, 35.57 (CH_2), 32.47 (CH_2), 29.76 (CH_2), 23.90, 22.85 (CH_2), 17.79 (CH_2), 9.27, 3.79 (CH_2), 3.28 (CH_2). m/z 494 (M^+ + 1), (Found M^+ + 1, 494.2411. $C_{29}H_{36}NO_4S$ requires 494.2365).

Phenol was converted to the corresponding hydrochloride salt as in general procedure **G** and assigned **BU11001**.

Found: C, 65.90; H, 6.77; N, 2.58. $C_{29}H_{36}ClNO_4S$ requires C, 65.70; H, 6.84; N, 2.64%.

CHAPTER 3.0: PHARMACOLOGY

3.1 Introduction

The aim of the experiments presented in this chapter is to assess the affinity and efficacy of novel, newly-synthesised compounds on the mu (μ-), kappa (κ-) and ORL-1 receptors. Following an initial screen of compounds in cell-based radioligand binding and GTPγS studies, we conducted a series of isolated tissue experiments.

To study μ- and ORL-1 receptors, the rat vas deferens tissue was used, to study κ-opioid receptors; the mouse vas deferens was used.

3.2 Materials

3.2.1 Animals

Adult male albino Sprague Dawley rats weighing 300-350 g were purchased from Charles River UK Ltd, whereas adult male CD-1 albino mice weighing 25-30 g were bred in-house and obtained from Animal Facilities, University of Bath, United Kingdom. They were housed in colony cages and maintained under a 12 hours light/dark cycle (lights on 7 am) and temperature (21 ± 1°C) controlled environment and given free access to rodent chow and water. Experiments were carried out in accordance with the ethical guidelines set by Animal (Scientific Procedures) Act 1986.

3.2.2 Physiological salt / buffer solution

Modified Krebs solution was used as a physiological salt solution in isolated tissue assays. The composition of Krebs solution for rat vas deferens (RVD) was as follows (mM): NaCl 118, KCl 4.74, $CaCl_2$ 2.50 (1.25 for mouse vas deferens (MVD)), KH_2PO_4 1.19, $MgSO_4$ 1.20 (Mg^{2+}-free for mouse vas deferens), $NaHCO_3$ 25, glucose 11. Krebs solution was maintained at 36.9°C (30.9°C for mouse vas deferens) and aerated with 95% O_2 and 5% CO_2. 20 µM bestatin and 2 µM thiorphan (peptidase inhibitors) were added to Krebs solution in the organ bath reservoir 15 minutes prior to nociceptin addition with / without the presence of antagonist / test compound.

3.2.3 Drugs

Drugs were obtained from the following sources: bestatin (N-[(2S,3R)-3-Amino-2-hydroxy-1-oxo-4-phenylbutyl]-L-leucine) from Tocris Biosciences, UK; buprenorphine hydrochloride from NIDA; CTAP (H-D-Phe-Cys-Tyr-D-Trp-Arg-Thr-Pen-Thr-NH_2) from Tocris, Biosciences, UK; DAMGO ([D-Ala^2,*N*-Me-Phe^4,Gly^5-ol]enkephalin acetate) from Bachem; U-69593 ((+)-5α,7α,8β)-*N*-methyl-*N*-[7-(1-pyrrolidinyl)-1-oxaspiro[4.5]dec-8-yl]-benzeneacetamide) from Enzo Life Sciences, UK, Ltd; DL-Thiorphan ((±)-N-(3-Mercapto-2-benzylpropionyl)glycine,DL-3-Mercapto-2-benzylpropanoylglycine) from Sigma Aldrich, UK; naltrexone hydrochloride; Nociceptin (Phe-Gly^2-Phe-Thr-Ala-Arg-Lys-Ser-Ala-Arg-Lys-Leu-Ala-Asn-Gln) from Tocris Biosciences, UK; [Arg^{14},Lys^{15}]nociceptin (Phe-Gly^2-Phe-Thr-Gly-Ala-Arg-Lys-Ser-Ala-Arg-Lys-Arg-Lys-Asn-Gln) from Tocris Biosciences, UK; nor-BNI (*nor*-binaltorphimine dihydrochloride) (17,17'-(Diclopropylmethyl)-6,6',7,7'-6,6'-imino-7,7'-binorphinan-3,4',14,14'-tetrol dihydrochloride) from Tocris Biosciences, UK; SB 612111 hydrochloride (7-[[4-(2,6-Dichlorophenyl)-1-piperidinyl]methyl]-6,7,8,9-tetrahydro-1-methyl-5H-benzocyclohepten-5-ol hydrochloride) from Tocris Biosciences; SCH 221510 (3-Endo-8-[bis(2-methylphenyl)methyl]-3-phenyl-8-azabicyclo[3.2.1]octan-3-ol) from Tocris Biosciences; U-69593 ((+)-5α,7α,8β)-*N*-methyl-*N*-[7-(1-pyrrolidinyl)-1-oxaspiro[4.5]dec-8-yl]-benzeneacetamide) from Enzo Life Sciences, UK, Ltd.

BU127, BU10101, BU10136, BU10119, BU10112 were synthesised in the laboratory using methods as previously described.

CTAP, DAMGO, nociceptin, [Arg^{14},Lys^{15}]nociceptin, nor-BNI and naltrexone were prepared as a 10 mM stock solution in distilled water and stored at -20°C, while bestatin was prepared in 1 eq NaOH as a 50 mM stock in distilled water and also stored at -20°C. On the day of experiment, more dilute stock solutions were made using distilled water for these drugs. All other compounds (test compounds) were solubilized in dimethylsulfoxide (DMSO) at the final concentration of 10 mM, and stored at -20°C. Further dilutions on the day of experiment were also made in DMSO for the test compounds. The total amount of DMSO in the bath did not exceed 0.2 %.

3.3 Methods

All studies presented in this thesis were conducted *in vitro*. Three assays were used to pharmacologically characterize the compounds synthesised. The first two assays, referring to receptor binding and the [^{35}S]GTPγS binding were performed by John Traynor's group at Department of Pharmacology, University of Michigan, United States. The methods used by Traynor's group and the corresponding data are presented in this thesis. Meanwhile, the electrically evoked isolated tissue assay in both rat and mouse vas deferens was conducted at the University of Bath premises as a part of this PhD project and will be discussed in detail.

3.3.1 Experimental methods

3.3.1.1 **Binding assay**

Radioligand receptor binding

The receptor binding assays were performed by Traynor's group in C6 glioma cells stably expressing the rat μ-opioid receptor and in chinese hamster ovarian (CHO) cells stably expressing the human κ-opioid or ORL-1 receptor. For the μ-opioid receptor cell cultures, the cells were grown in Dulbecco's modified eagle medium (DMEM) supplemented with 10% fetal bovine serum (FBS), 90 units/ml penicillin, 90 μg/ml streptomycin and 0.5 mg/ml geneticin; CHO transfected cells were maintained in DMEM-F12 medium. All cells were grown under 5% CO_2 at 37°C. Cells were washed in phosphate buffered saline (PBS), centrifuged and the cell pellet was resuspended in 50mM Tris-HCl at pH 7.4 and re-homogenized with Tissue Tearor (Biospec Products, Inc). The final pellet was frozen at -80°C. Protein concentration was determined using the Bicinchoninic acid (BCA) protein assay. Cell membranes (20 μg) were incubated in 50 mM Tris-HCl at pH 7.4 with [3H]diprenorphine (for μ- or κ-opioid receptor transfected cells) or [3H]nociceptin (for ORL-1 receptor transfected cells) in the presence of varying concentrations of test compounds for 60 minutes in a shaking water bath at 25°C. Nonspecific binding was measured using 10 μM naloxone (for μ- and κ-opioid receptors) or nociceptin (for ORL-1 receptor). Samples were filtered through filtermats mounted on a Brandel cell harvester and rinsed four times with 50 mM Tris-HCl at 4°C (pH 7.4). 0.1 ml EcoLume scintillation cocktail was added to each sample area to soak the filter. Each filtermat (in a heat-sealed bag) was counted in a Wallac 1450 MicroBeta Liquid Scintillation and Luminescence Counter. IC_{50} values for test compounds were determined from concentration effect curves and converted to K_i values using GraphPad Prism Software.

3.3.1.2 **Functional assays**

[^{35}S]GTPγS binding

Membranes (20 µg) from cells expressing μ-, κ- or ORL-1 receptors (same methods were used to prepare the cell cultures as in the previously receptor binding assays) are incubated in 20 mM Tris-HCl, pH 7.4, 5 mM $MgCl_2$, 100 mM NaCl, 2.2 mM dithiothreitol (freshly prepared), 30 µM GDP, 0.1 nM [^{35}S]GTPγS, with or without 10 µM of test compound or the standard agonists (10 µM DAMGO (μ), 10 µM U-69593 (κ) or 1 µM nociceptin (ORL-1) as appropriate) or H_2O for 60 min at 25°C. Samples were filtered through GF/C glass-fiber filtermats mounted on a Brandel cell harvester and rinsed four times with ice-cold 50 mM Tris-HCl, pH 7.4 containing 5 mM $MgCl_2$, and 100 mM NaCl. Filtermats were processed as described for receptor binding above. The non-hydrolyzable GTP analogue, [^{35}S]GTPγS was measured using a liquid scintillation and lumination counter. The ability of buprenorphine and its analogues (10 µM) to stimulate [^{35}S]GTPγS binding was measured and is represented as a percentage of the maximal stimulation produced by the standard full agonists.

Isolated tissue preparations (vas deferens assay)

Tissue preparations

Rats / mice were euthanized in a closed-contained CO_2 environment. Both vasa deferentia connecting the prostate gland and testes (Figure 3.1) were dissected out as a single unit. The adhering fat, connective tissue and blood vessels were carefully removed and the tissue was gently pressed to expel the seminal contents (Hughes *et al.*, 1975). About 20% of the dissected tissue connecting to the prostate gland was excised (Andrews *et al.*, 2010). This part of vas deferens was removed

because it is believed to have a non-adrenergic component while the adrenergic component of the tissue predominantly sits near to the epididymal half (Kitchen, 1984; Westfall *et al.*, 2001). The extracted tissues were then mounted in Krebs solution, aerated with 95% O_2 and 5% CO_2 and maintained at 36.9°C for rat vas deferens or 30.9°C for mouse vas deferens. The tissues were then transferred into a 3 ml organ bath.

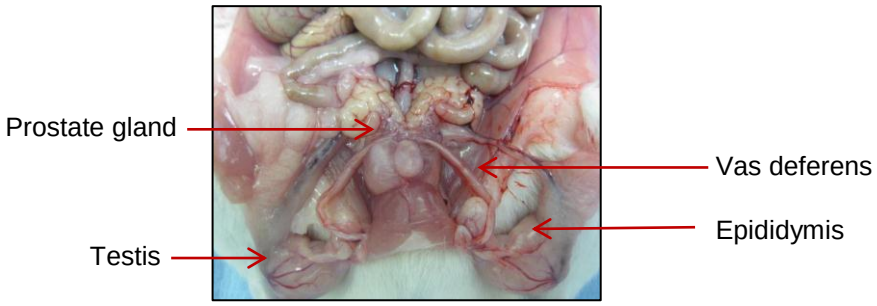

Figure 3.1: Dissection of the rat vas deferens.

3.3.1.3 **Experimental protocols (general)**

A single vas deferens was mounted in a 3 ml organ bath containing appropriate Krebs solution at 36.9°C for rat vas deferens or 30.9°C for mouse vas deferens and aerated with 95% O_2 and 5% CO_2. For electrical field stimulation, a platinum ring anode was placed on the top of the bath and a platinum hook cathode at the bottom. One end of the vas deferens was tied to the hook and the other end to the force transducer (Biegestab K30, Hugo Sachs Elektronik, Germany). Tissues were continuously stimulated (Grass S88 stimulator, Grass Medical Instruments, Quincy, USA) through two platinum ring electrodes and the electrically evoked contractions were measured isometrically and recorded with the computer-based acquisition system MacLab/4e (ADInstruments Pty Ltd., Castle Hill, Australia). Rat vas deferens: 1.0 g initial tension was applied to the tissue. Electrically evoked muscle contractions were induced with supramaximal voltage single square pulses, 0.1 ms duration and 0.1 Hz frequency. The experiments started after 60 minutes equilibration under direct stimulation for the ORL-1 receptor assay and after 90

minutes for the μ-opioid receptor assay (including 30 minutes of initial equilibrium under resting tension). Mouse vas deferens: 0.5 g initial tension was applied to the tissue. Electrically evoked muscle contractions were induced with supramaximal voltage with trains of 3 square pulses, 0.1 ms duration and 100 Hz frequency. Trains were repeated at a frequency of 0.05 Hz. Tissues were allowed to equilibrate for 60 minutes under electrical field stimulation before beginning the experiment.

3.3.2 Analytical methods

3.3.2.1 **Nonlinear regression**

A cumulative concentration-response curve for the standard receptor agonist was constructed using GraphPad Prism v5.0 software (GraphPad Software Inc, CA, USA) in the absence and in the presence of increasing concentrations of a selected standard receptor antagonist (or test compound). Data were fitted into nonlinear regression equation and analysed with sigmoidal dose-response (variable slope) model. The response of the tissue which referred to the percentage inhibition of smooth muscle contraction at each concentration was calculated using the equation as shown below:

$$\% \text{ Twitch Inhibition} = \frac{\text{Height of twitch (a-b)}}{\text{Height of twitch (a)}} \times 100$$

where a = baseline (prior to agonist treatment or baseline)
b = in the presence of antagonist

The cumulative concentration-response curve for each tissue was individually fitted and the analysis was calculated by the four parameter nonlinear regression equation using GraphPad Prism v5.0 software (Kenakin, 2009; Motulsky, 2007). The

minimum response parameter was constrained to 0%. The equation used as stated below:

$$Y = \text{Bottom} + \frac{(\text{Top-Bottom})}{1 + 10^{(\text{Log EC}_{50}\text{-X})\cdot\text{Hill Slope}}}$$

However, the graphs presented in this thesis were an average from multiple experiments unless stated otherwise as written in the legend.

3.3.2.2 **Schild analysis**

For most of the cases, we used the EC_{50} value to calculate the concentration ratio (CR). This series of CRs (at least three CR values) was plotted as log (CR-1) against log [B] where [B] referred to antagonist concentration. The Schild equation used as follows:

$$\text{Log (CR-1)} = \log [B] - \text{Log } K_B$$

The slope of the plot was analysed using linear regression. If the slope of the line of best-fit was not significantly different from 1, and if there was no significant suppression of the maximum agonist response (in the presence of antagonist, exceptional case when hemi-equlibria is strongly suspected), the line of best-fit was then recalculated, constraining the slope to 1.

The x-intercept of the Schild plot is the pA_2 value of the antagonist tested.

3.3.2.3 **Schild equation (single concentration method)**

For the case where Schild analysis is not a valid method to estimate the antagonist potency (eg: slope significantly different than unity or only one concentration of antagonist tested per tissue), the Schild equation was used to estimate the antagonist potency and K_B, assuming that the antagonist is following simple competitive behaviour and the ideal experiment condition is met (Kenakin, 2009; Leslie, 1987):

$$pA_2 \text{ (or } \log [K_B]) = \log (CR-1) - \log [B]$$

All data are expressed as means ± S.E.M of *n* experiments. For potency and maximum response values (E_{max}) the 95% confident limits are given. Some data have been analysed statistically using one-way ANOVA (analysis of variance), as specified in Table and Figure legends; P values less than 0.05 were considered to be significant.

3.4 Results and Discussion

3.4.1 Radioligand receptor binding

Based on the results presented in Table 3.1, the binding affinities of the selected buprenorphine analogues were similar to buprenorphine at the μ- and κ-opioid receptors. This suggests that introducing an aromatic substituent at the C_{20} of orvinols (Figure 3.3) did not influence the binding affinity of these compounds at both receptors. However, there is a slight increase (3-fold) in the binding affinity of buprenorphine analogues compared to buprenorphine at the ORL-1 receptor (Table

3.1) which suggests that introducing an aromatic substituent at C_{20} of orvinol (Figure 3.3) improves the binding affinity of this series at the ORL-1 receptor.

Table 3.1: Binding affinities (K_i) for buprenorphine and its selected analogues derived from receptor binding assays using transfected C6 glioma cells (μ-opioid receptor) and transfected CHO cells (κ- and ORL-1 receptors). Value represents mean ± S.E.M of triplicates. *n.d* (not determined / not measured).

Compound	Binding affinity (K_i) nM		
	mu (μ)	kappa (κ)	ORL-1
Buprenorphine	0.19 ± 0.02	0.067 ± 0.02	212 ± 7
BU127	*n.d*	0.04	*n.d*
BU10101	0.19 ± 0.08	0.16 ± 0.09	*n.d*
BU10119	0.10 ± 0.02	0.04 ± 0.01	80.0 ± 10.0
BU10112	0.17 ± 0.11	*n.d*	79.0 ± 8.0

3.4.2 [^{35}S]GTPγS binding

[^{35}S]GTPγS binding was used to measure the activity of buprenorphine and its analogues at μ-, κ-, and ORL-1 receptors. All buprenorphine analogues synthesised were initially screened by Traynor's group to determine their efficacy at a single high concentration (10 μM) compared to standard full agonists at the individual receptors. Data are shown as the percentage of the maximal stimulation produced by the standard full agonists. The efficacy screening was conducted in triplicate and the results are shown (Figure 3.2 and Table 3.2).

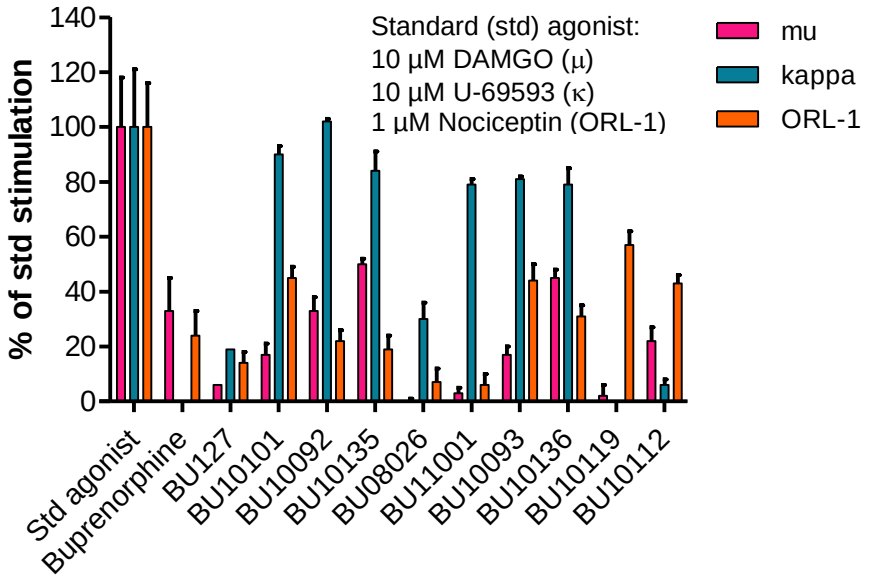

Figure 3.2: [^{35}S]GTPγS efficacy screening of buprenorphine and its analogues performed in either C6 glioma or cultured Chinese Hamster Ovarian (CHO) transfected cells. Efficacies of buprenorphine and its analogues at 10 µM were compared against standard receptor agonists (DAMGO, U-69593 and nociceptin) in triplicate (Traynor (unpublished work)).

Table 3.2: Percentage receptor stimulation of buprenorphine and its analogues at 10 µM against standard agonists (10 µM DAMGO, 10 µM U-69593 and 1 µM nociceptin) at µ-, κ- and ORL-1 receptors in [^{35}S]GTPγS efficacy screening. Value represents mean (%) ± S.E.M of triplicates (Traynor (unpublished work)).

	Receptor stimulation (%)		
	mu (µ-)	kappa (κ-)	ORL-1
Standard agonist	100 ± 18	100 ± 21	100 ± 16
Buprenorphine	33 ± 12	-12 ± 9	24 ± 9
BU127	6 ± 0	19 ± 0	14 ± 4
BU10101	17 ± 4	90 ± 3	45 ± 4
BU10092	33 ± 5	102 ± 1	22 ± 4
BU10135	50 ± 2	84 ± 7	19 ± 5
BU08026	0 ± 1	30 ± 6	7 ± 5
BU11001	3 ± 2	79 ± 2	6 ± 4
BU10093	17 ± 3	81 ± 1	44 ± 6
BU10136	45 ± 3	79 ± 6	31 ± 4
BU10119	2 ± 4	-2 ± 1	57 ± 5
BU10112	22 ± 5	6 ± 2	43 ± 3

Based on the results presented in Table 3.2 above, the presence of either methyl or chloro on the aromatic substituent at the C_{20} position of the orvinol for BU127 analogues (BU10101, BU10092, BU10135) and BU08026 analogues (BU10093, BU10136) appeared to change the analogues' efficacy at κ-opioid receptor from low partial agonist to full agonist. Although there was an increase in the efficacy of the analogues at μ- and ORL-1 receptors, they still remained partial agonists at both receptors. The presence of a methyl group on the aromatic substituent at the position 2 (BU10101, BU10093) increased the analogues efficacy at ORL-1 receptor compared to other BU127 and BU08026 analogues in this series. This may suggest that introducing bulk near to the C_{20} position of orvinols (Figure 3.3) has the effects of increasing the analogue's efficacy at the ORL-1 receptor. It appears that the presence of a methyl group on position 4 or 5 of the aromatic substituent has increased efficacy at the μ-opioid receptor, as can be seen in compound BU10135 and BU10136. Moving sulphur from 2-thiophene (BU08026) to 3-thiophene (BU11001) also increases the efficacy of the compound at κ-opioid receptor to that of a full agonist.

Compounds BU10119 and BU10112, having a methyl group at the C_7 position (Figure 3.3), met the desired pharmacological profile at μ-, κ- and ORL-1 receptors. In contrast to the series discussed in the previous paragraph, these two compounds were antagonists at the κ-opioid receptor.

Since the [^{35}S]GTPγS efficacy screenings were conducted only at a single high concentration (10 μM), the functional evaluation of buprenorphine and the new analogues were further evaluated in isolated vas deferens system.

3.4.3 Selection of compounds to be evaluated in isolated tissue preparation

All of the test compounds were synthesised in the laboratory as part of this PhD project, except for compounds BU10119 and BU10112 which were synthesised by

another member of the Husbands' group. These two compounds still belong to the orvinol series but contain a methyl group at C_7 (Figure 3.3).

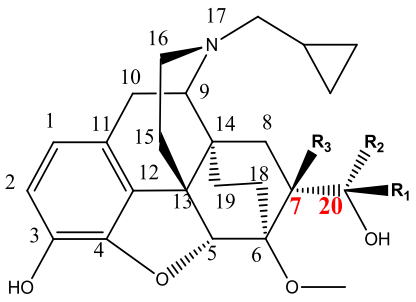

Figure 3.3: Orvinol structure with the point of manipulation at C_7 and/or C_{20} (**R_1** = aryl substitution with/without alkyl/small group side chain, **R_2** = CH_3 / H, **R_3** = H / CH_3.

Some of the compounds were further tested to confirm their receptor efficacy profiles in isolated tissues preparation. Not all of the compounds synthesised in the chemistry part of this project were evaluated in this functional assay. The selection of compounds to be investigated in the isolated tissue preparation ensured that compounds representing the full range of structures were evaluated.

3.4.4 Optimisation of experimental conditions for vas deferens assay

Previously published studies were used as guidelines to develop our own experimental protocol (Hughes *et al.*, 1975; Riba *et al.*, 2010; Spagnolo *et al.*, 2008; Spagnolo *et al.*, 2007). Besides selection of species / strain that will be further explained throughout the thesis, the other issues that needed to be addressed were the standard agonist to be used, the concentration range needed, the optimal electrolyte concentration to measure agonist responses, the length of drug exposure especially for the standard agonist, and its washout time from the tissue which was determined by the baseline of control twitches (dose cycle).

3.4.4.1 **ORL-1 receptor (rat vas deferens)**

Various concentrations of Ca^{2+} were tested in the Krebs solution to ensure that nociceptin exerted its optimum inhibition. To date, there are no studies conducted to evaluate the effect of varying calcium concentrations in the physiological buffer solution on nociceptin potency. However, it was believed that the effect might be the same as observed for classical opioid agonists since nociceptin also acts through GPCRs by inhibiting adenylyl cyclase and Ca^{2+} channels, and inducing K^+ channel opening, similar to agonists at the opioid receptors (Bignan *et al.*, 2005; Bloms-Funke *et al.*, 2000; Largent-Milnes *et al.*, 2010). A previous study has shown that the potency of opioid agonists (eg: DAMGO (μ-), [D-Ala^2, D-Leu^5]-Enkephalin (DADLE) (δ-)) was higher in a lower extracellular Ca^{2+} concentration media due to the reduction of Ca^{2+} influx into the nerve terminals during depolarization (Sheehan *et al.*, 1988). As a result, the effectiveness of the opioid agonist to block the Ca^{2+} entrance into the nerve terminals is potentiated which is caused by an increased in agonist-receptor coupling efficiency.

Therefore, a test concentration of nociceptin at 3 µM was used to determine the calcium concentration that will produce the optimal nociceptin response (Table 3.3). Between 1 and 3 mM Ca^{2+} in the Krebs, there was no noticeable difference in inhibition of twitch produced by 3 µM nociceptin. We therefore decided to use 2.5 mM Ca^{2+}-Krebs as at concentrations lower than this, the height of the baseline twitch started to decrease and become more difficult to measure. Previous studies had used calcium concentrations of between 1.2 mM-2.5 mM in their Krebs formula (Fischetti *et al.*, 2009; Riba *et al.*, 2010).

Table 3.3: The effects of 3 µM nociceptin in inhibiting electrically evoked contraction of the rat vas deferens in media of varying calcium concentration. Nociceptin was tested in Krebs medium containing 0.5 mM to 3.0 mM Ca^{2+}.

	Calcium concentration (mM)				
	0.5	1.0	1.8	2.5	3.0
% inhibition to control	36%	50%	51%	49%	46%

In our preliminary experiments to determine the onset and optimal length of time to apply at each concentration of nociceptin, nociceptin initially produced an inhibition of the electrically evoked contraction of the tissue. However, this response rapidly began to reverse after 2 minutes of nociceptin exposure (Figure 3.4). This pattern suggests that nociceptin is not stable. For this preliminary experiment, nociceptin was exposed for 10 minutes at each concentration.

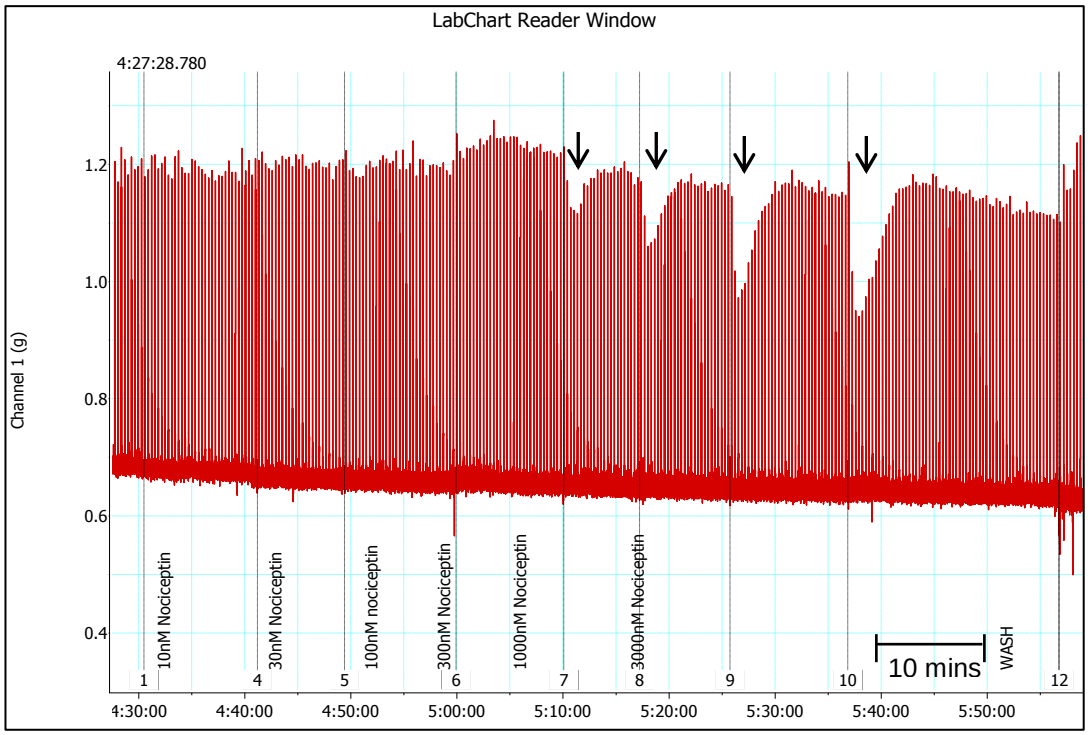

Figure 3.4: Effects of nociceptin (1 nM-3000 nM) on electrically evoked contractions of rat vas deferens.

Therefore, we decided to minimize the nociceptin contact time to 3 minutes to solve this problem, since nociceptin shows rapid onset (1.5-2 minutes). The nociceptin induced inhibition of the smooth muscle twitch was much more stable when the contact time was reduced from 10 minutes to 3 minutes (Figure 3.5).

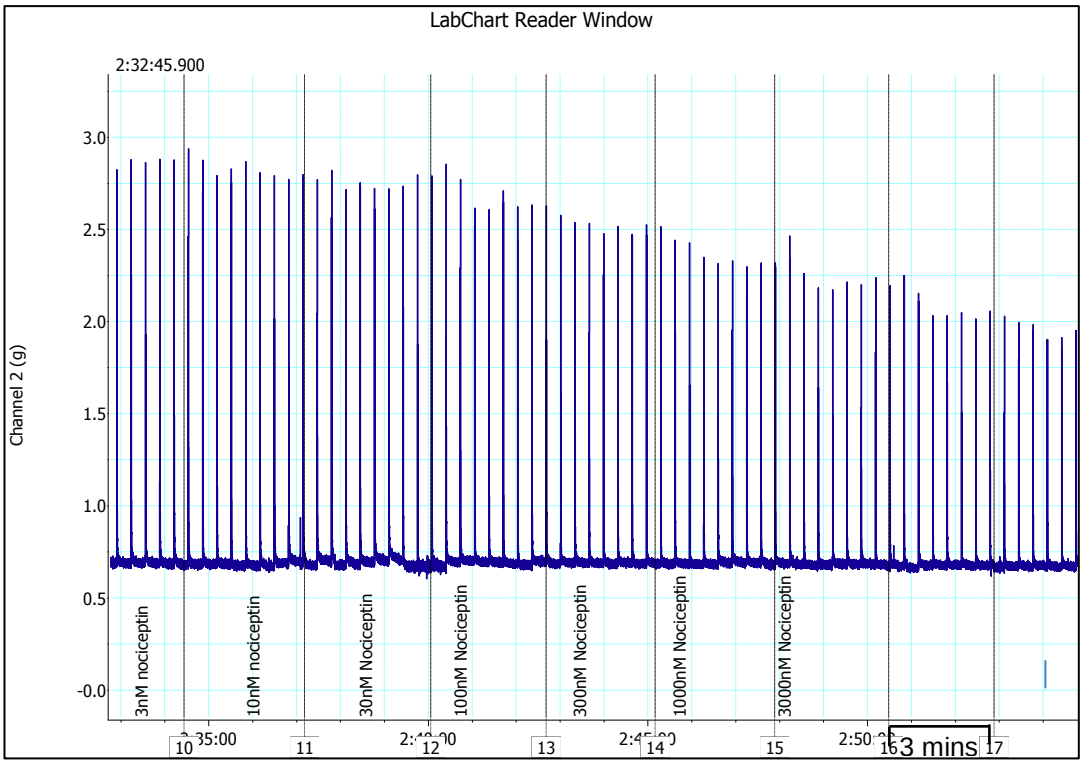

Figure 3.5: Effects of nociceptin (1 nM-3000 nM) on electrically evoked contractions of rat vas deferens.

The concentration range for nociceptin was initially set to 1 nM-3 µM (Rizzi *et al.*, 2011; Spagnolo *et al.*, 2007), although some studies have also used nociceptin up to 10 µM (Fischetti *et al.*, 2009). The average (n = 4) Log EC_{50} derived was 6.67 (5.65-7.65) and the average maximum response (E_{max}) calculated was 55.1% (28.8-81.4%) (Figure 3.6 (right)). The mean value for maximum response, E_{max} (n = 4) was found to be lower than previously reported (75-85%) (Fischetti *et al.*, 2009; Rizzi *et al.*, 2011; Spagnolo *et al.*, 2007). The 95% confidence interval for the maximum response was also found to be very wide (28.2-81.4%) which could lead to the wide error of nociceptin EC_{50} estimation (22.4-2238.7 nM). The individual concentration-response curve is shown in Figure 3.6 (left)).

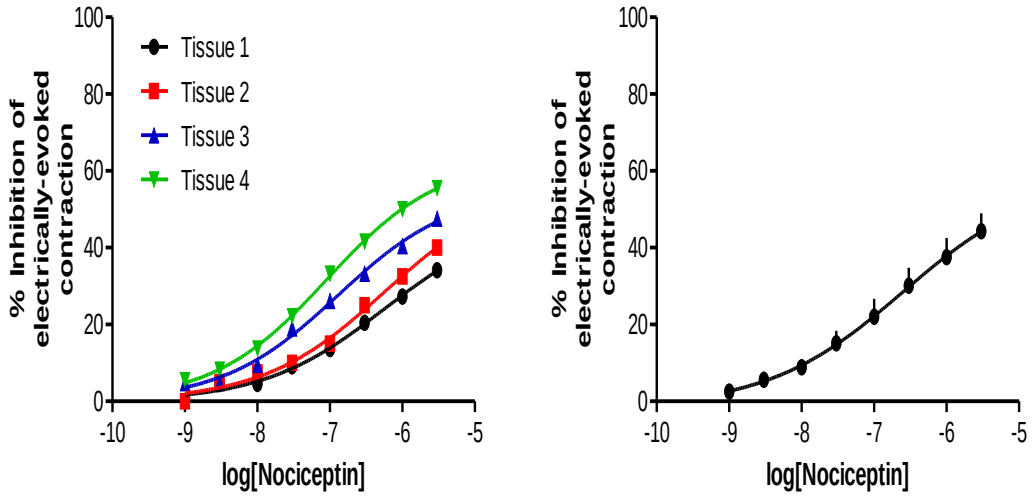

Figure 3.6: Inhibition of electrically evoked contractions of rat vas deferens by nociceptin (1 nM-3 µM). Left, individual concentration-response curve. Right, average concentration-response curve. Points represent means, and vertical lines represent S.E.M of four experiments (Right).

There are a few possibilities that might explain this situation. Initially, it was suspected that nociceptin was sticking to the glass of the organ bath, and therefore, the intended concentration of the agonist may not have been delivered to the tissue. Therefore, we decided to siliconize the organ bath to prevent nociceptin sticking to the glass. Additionally, the tissue was also sensitized using a low dose of nociceptin until consistent inhibition was established before the nociceptin response curve was constructed. The tissue sensitizing procedure was carried out to stimulate the muscles until constant twitches were established (Kitchen, 1984; McKnight *et al.*, 1983; Menzies *et al.*, 1999; Sheehan *et al.*, 1988). McKnight *et al.* (1983) reported an increase of met-enkephalin potency (IC_{50}) when the second dose-response curve was constructed compare to the first curve. The IC_{50} for the second curve was 52.1 ± 6.43 µM compared to the first control curve which was reported to be more than 100 µM. It was not necessary to sensitize the tissue with the same agonist since tissue was also reported to be sensitized with DAMGO until stable inhibition was obtained before a nociceptin concentration response curve was constructed (Menzies *et al.*, 1999). Thus, we decided to sensitize the tissue with 30 nM nociceptin instead of DAMGO due to the shorter drug washout time. Since the previous study also reported that no increase of tissue sensitivity was observed when the concentration-response curve of peptide (met-enkephalin) was repeated

for a third time in rat vas deferens, we decided to sensitize the tissue twice before proceeding with the actual experiment (McKnight *et al.*, 1983). The comparison for the dose response curve (n = 4) is shown in Figure 3.7. The maximum response (E_{max}) to nociceptin increased from 55.1% (28.8-81.4%) to 64.2% (59.5-68.6%) and the potency (EC_{50}) of nociceptin was increased 3-fold from 213.8 nM (22.4-2238.7 nM) to 74.8 nM (53.4-104.7 nM). Although these values were not statistically different, the standard error was smaller in all parameters (E_{max} and EC_{50}) in the sensitized tissues conducted in the siliconized organ bath compared to the non-sensitized tissues conducted in non-siliconized organ bath. Furthermore, when comparing the % twitch inhibition at individual concentrations, significantly increased responses were observed in tissue that had undergone the sensitizing procedure in the siliconized organ bath compared to the non-sensitized tissues at ≥ 100 nM nociceptin.

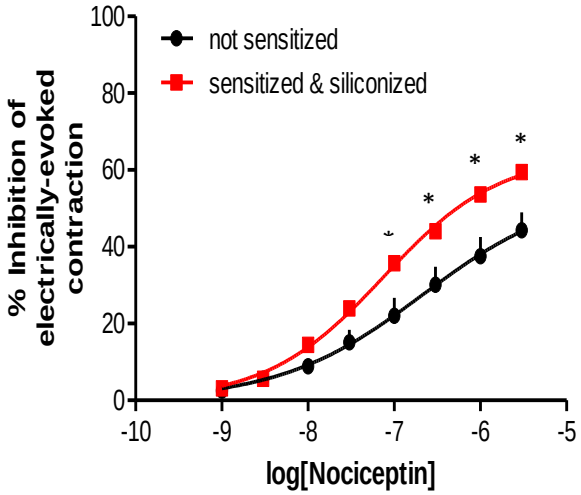

Figure 3.7: Electrically evoked contractions in rat vas deferens. Nociceptin response was compared between tissues that had undergone sensitizing procedure in siliconized organ bath to non-sensitized tissues without siliconized organ bath. Points represent means, and vertical lines represent S.E.M of four experiments. Statistical significance of the differences between mean values were determined using one-way ANOVA. *P < 0.01 compared to non-sensitized tissue.

Although the tissue response to nociceptin was increased, we still failed to achieve the maximum inhibition of twitches that had been previously reported (75-85%)

(Fischetti *et al.*, 2009; Rizzi *et al.*, 2011; Spagnolo *et al.*, 2007). Another possibility was that nociceptin quickly degraded once it started to produce an effect. Nociceptin is hydrolyzed *in vivo* into a few peptide fragments by aminopeptidase and endopeptidase, however the exact points of cleavage in the peptide varies between tissues (Sakurada *et al.*, 2002; Terenius *et al.*, 2000). According to Sakurada et al (2002), endopeptidase-24.11 was the enzyme responsible for the cleavage of the nociceptin Lys^{13}-Leu^{14} bond in the mice spinal cord membranes and its activity was inhibited by the specific endopeptidase-24.11 inhibitors (eg: thiorphan, phosphoramidon). Aminopeptidase also hydrolyses nociceptin *in vivo* and could be minimized by using aminopeptidase inhibitor, bestatin. (Sakurada *et al.*, 2002). Nociceptin metabolism in the plasma was also believed to be mediated mainly by aminopeptidase (Terenius *et al.*, 2000). Although there have been many studies conducted to investigate nociceptin metabolism *in vivo* and *in vitro* in different tissues, to date there have been no studies performed to determine nociceptin metabolism in isolated vas deferens tissues. Since enkephalins were proven to be metabolized by enzymes in isolated vas deferens tissues, there is a strong possibility that nociceptin will also be greatly metabolized in this isolated tissue preparation *in vitro*. Studies performed in rat and mouse vas deferens reported that the potencies of [Met^5]enkephalin (opioid peptides) and related peptides were significantly increased in the presence of enzyme inhibitors (McKnight *et al.*, 1983). In rat vas deferens, [Met^5]enkephalin had a roughly 178-fold higher potency in the presence of a cocktail of enzyme inhibitors (bestatin, thiorphan and captopril) (IC_{50} of 330 ± 30 nM compared to 59 ± 14 μM (McKnight *et al.*, 1983).

In order to test this hypothesis, we added endopeptidase and aminopeptidase inhibitors (peptidase inhibitors) into the organ bath before nociceptin addition. 20 μM bestatin and 2 μM thiorphan were added into the organ bath 15 minutes before the first concentration of nociceptin was applied to the tissue (Figure 3.8).

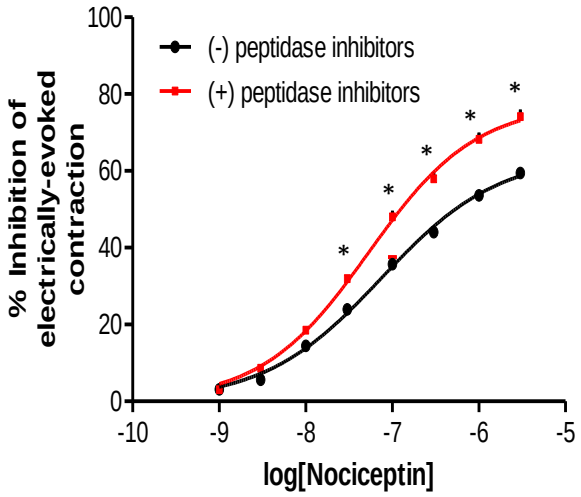

Figure 3.8: Comparison of nociceptin response between tissues treated with peptidase inhibitors (20 µM bestatin and 2 µM thiorphan) and non-treated tissues. Points represent means, and vertical lines represent S.E.M of at least four experiments. Statistical significance of the differences between mean values was determined using one-way ANOVA. *P < 0.001 compared to (-) peptidase inhibitors treated tissue.

There was a significant increase in the maximum response of nociceptin in tissues treated with peptidase inhibitors compared to non-treated tissues from 64.2% (59.5-68.8%) to 77.4% (74.5-80.4%) (n = 4-8). The mean responses from individual concentrations were significantly increased at ≥ 30 nM nociceptin. Nociceptin was also found to be more potent in the peptidase inhibitors pre-treated tissue with an EC_{50} value of 53.2 nM (44.6-63.3 nM) compared to the EC_{50} of the non-peptidase inhibitors pre-treated tissue, 74.8 nM (53.4-104.7 nM). However, the difference in the potency between these two groups was not statistically different. Although a higher maximum response was achieved, the response still did not reach a plateau and therefore, it was decided to increase the final concentration of nociceptin to 30 µM (n = 8). The result obtained is shown in Figure 3.9.

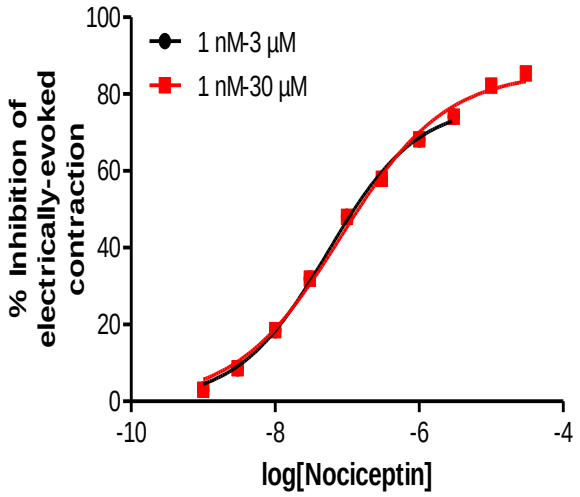

Figure 3.9: Comparison of the effects of nociceptin range on the maximum inhibition response of tissue inhibition in electrically evoked contractions in rat vas deferens. Points represent means, and vertical lines represent S.E.M of eight experiments.

With the new range of nociceptin (1 nM-30 µM), there was now a more clearly defined maximum response that reached a plateau. Furthermore, the maximum response (E_{max}) was found to be significantly higher in the tissue treated with nociceptin up to 30 µM compared to tissue treated only up to 3 µM with the E_{max} of 85.7% (83.2-88.2%) and 77.4% (74.5-80.4%) respectively. Based on these findings, we decided to use the nociceptin range of 1 nM-30 µM for the ORL-1 assays.

In order to validate the dose cycle for nociceptin (washout time), four sets of nociceptin (n = 1) concentration-response control curves were conducted on the same tissue each separated by a 15 minutes wash out period (Figure 3.10).

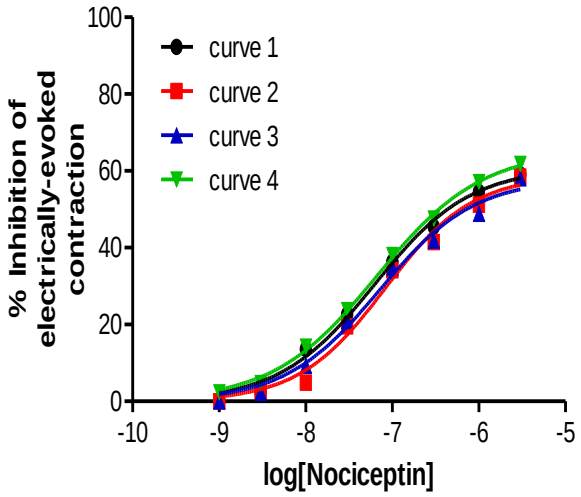

Figure 3.10: Comparison of tissue response of four nociceptin control curves in electrically evoked contractions of rat vas deferens. Experiments were conducted in a single tissue with dose-cycle of 15 minutes.

The EC_{50} of nociceptin for each curve was compared in order to ensure nociceptin was completely washed out at each dose cycle (Table 3.4). No significant differences of nociceptin potency (EC_{50}) were detected which established that nociceptin had completely washed out with the 15 minutes dose cycle protocol, and that no apparent sensitization or desensitization of the tissue occurred over this time-period.

Table 3.4: Potency comparisons of nociceptin from a single tissue in order to evaluate the suitability of nociceptin washout time for each dose-cycle.

Nociceptin	Curve 1	Curve 2	Curve 3	Curve 4
EC_{50} (nM)	62.6	82.9	71.4	66.4

As these initial experiments showed that nociceptin needed to be applied at concentrations as high as 30 µM in order to obtain a full concentration-response curve, we considered using alternative ORL-1 agonists which have been suggested to be more potent than nociceptin. The main reason for this was to try and reduce

the overall cost of these experiments. These include the peptide, [Arg^{14},Lys^{15}]nociceptin, and a synthetic non-peptide ORL-1 ligand, SCH 221510. The comparison of their binding affinities, K_i (receptor binding assay) and their relative potencies ([^{35}S]GTPγS) compared to nociceptin for the ORL-1 receptor are presented in Table 3.5.

Table 3.5: Comparison of ORL-1 receptor agonists profiles.

	Nociceptin	[Arg^{14},Lys^{15}]nociceptin	SCH 221510
Binding affinity, K_i (nM)	0.93 ± 0.50 (Okada *et al.*, 2000)	0.32 ± 0.13 (Okada *et al.*, 2000)	0.3 ± 0.05 (Varty *et al.*, 2008)
Type	Peptide	Peptide	Non-peptide
Molecular weight	1809.06	1909.18	397.55
Relative potency	1	17	0.6

Based on our preliminary experiments, [Arg^{14},Lys^{15}]nociceptin appears to have only marginally greater potency than nociceptin (Figure 3.11). Although these studies were only performed with an n of 2, the EC_{50} values of nociceptin and [Arg^{14},Lys^{15}]nociceptin were 971.2 nM (185.9-5075.0 nM) and 547.5 nM (339.4-883.2 nM). Although previous studies (Okada *et al.*, 2000) conducted using [^{35}S]GTPγS binding assay in human embryonic kidney 293 transfected cells have shown the former to be 17-fold more potent than nociceptin, we did not see such a profound effect. Moreover, the new candidate took a slightly longer time to wash out of the tissue.

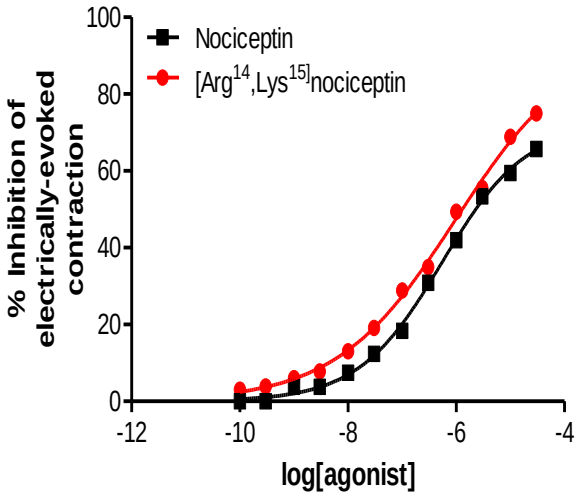

Figure 3.11: Comparison of tissue response between Nociceptin and [Arg^{14},Lys^{15}]nociceptin in electrically evoked contractions of rat vas deferens. Points represent means of two experiments.

The other candidate, SCH 221510 was not efficiently washed out of the tissue even after 1 hour (Figure 3.12) and also had a very slow onset of action with a loading concentration of 3 µM SCH 221510 taking nearly 20 minutes to reach maximum effect (Figure 3.13). Furthermore, 3 µM SCH 221510 only achieved 26.6% inhibition of control twitches. Therefore, SCH 221510 was not a suitable ligand for this assay.

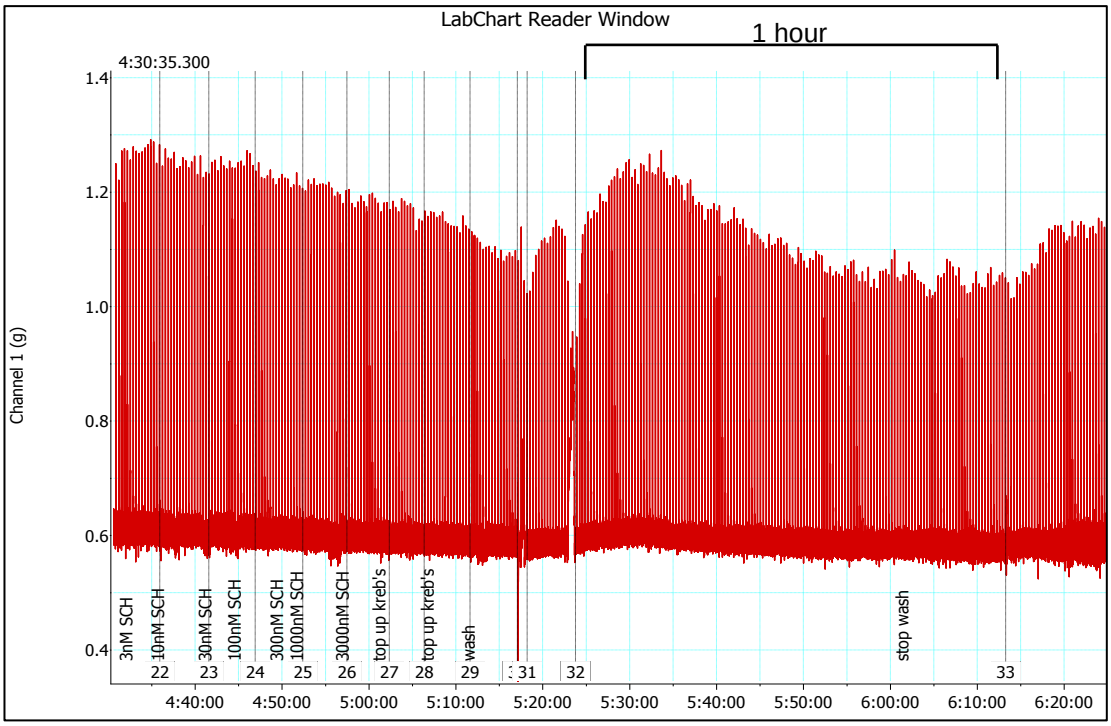

Figure 3.12: Effects of SCH 221510 (1 nM-3000 nM) on electrically evoked contractions of rat vas deferens.

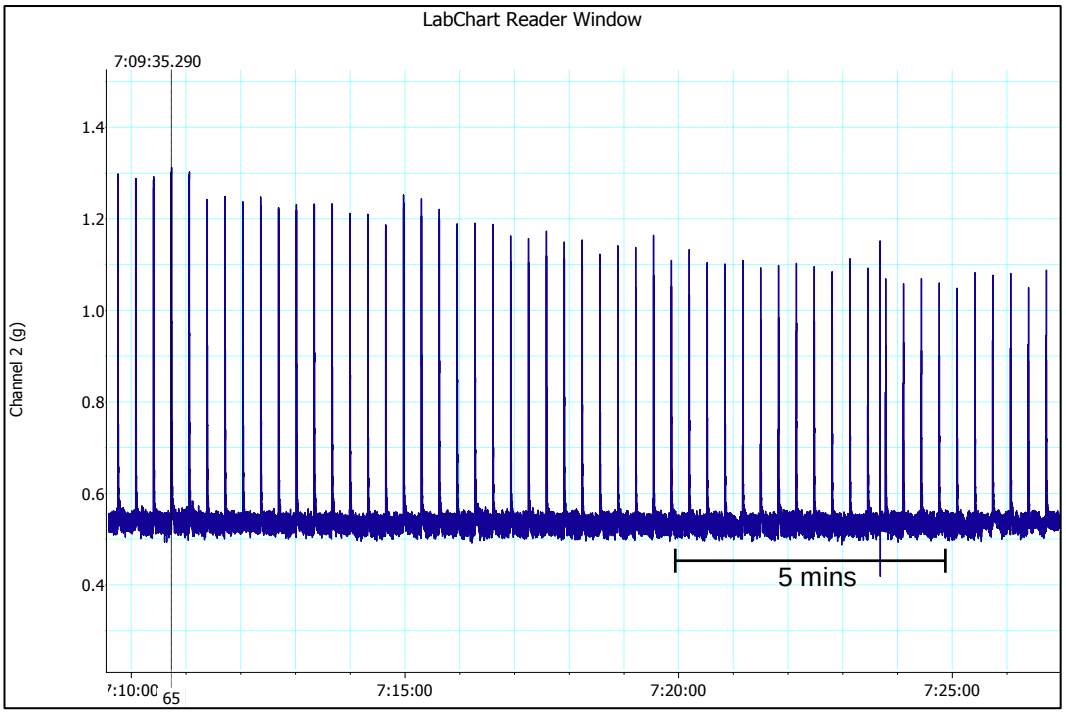

Figure 3.13: Effects of SCH 221510 (3 μM) on electrically evoked contractions of rat vas deferens.

Despite testing these alternative ligands, nociceptin was still the best option. However, because this ligand was so expensive, it was almost impossible to screen all the novel compound synthesised in this project at this receptor. Therefore, we selected a few compounds that represent the orvinol series synthesised.

Another interesting finding that was discovered during these pilot experiments was the strain difference in nociceptin response found between Sprague Dawley and Wistar rats (n = 4). Although strain-related differences in the effects of opioids in rodents have been widely documented (Bustamante *et al.*, 1991; Shoaib *et al.*, 1995), to date there have been no studies conducted to investigate the strain differences of nociceptin responses in rats. In our hands, nociceptin was found to be significantly less potent in Wistar rats compared with Sprague Dawley rats with EC_{50} values of 163.4 nM (122.4-218.1 nM) and 64.7 nM (48.8-85.8 nM) respectively (Figure 3.14).

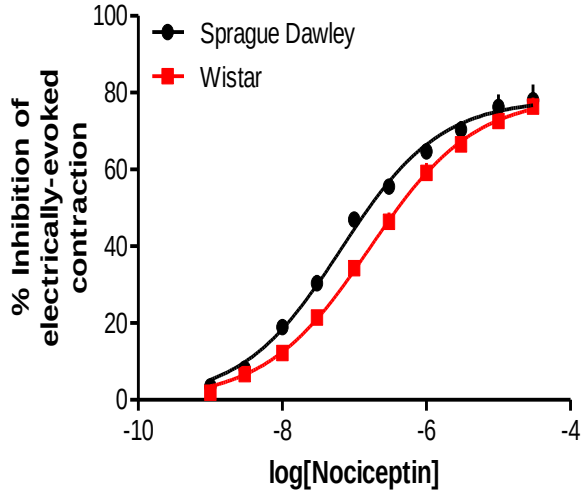

Figure 3.14: Comparison of nociceptin response in different strain of rats, Sprague Dawley and Wistar. Points represent means, and vertical lines represent S.E.M of four experiments per strain.

Such a difference in sensitivity to drug response is not uncommon, since previous studies have also discovered this phenomenon when the same tissue was used in

different strains of animals. For example, morphine was found to be significantly more potent in Sprague Dawley rats compared to Wistar rats in electrically evoked contraction of vas deferens tissue with an EC_{50} of 1895 μM and 3666 μM respectively (Bustamante *et al.*, 1991). Although the evidence was pronounced, no detailed investigations were conducted by Bustamante et al (1991) to explore the cause. Another study conducted by Shoaib et al (1995) also found Sprague Dawley rats were more sensitive to morphine than Wistar rats. This study was conducted *in vivo* to determine the difference in the response to morphine in the conditioned-place preference (CPP) model between the two strains of rat and relate it to dopamine release in nucleus accumbens. Morphine induced CPP was found to be significant at ≥ 3 mg/kg morphine in Sprague Dawley rats, but required higher doses in Wistar rats, where the significant effects in CPP were only seen at ≥ 5.0 mg/kg morphine (Shoaib *et al.*, 1995). Morphine induced dopamine release also was found to be significant at ≥ 3.0 mg/kg in Sprague Dawley rats with 221 ± 16% increase in dopamine release compared to ≥ 10.0 mg/kg morphine required in Wistar rats to produce only 158 ± 16% elevation in dopamine release after 80 minutes of morphine administration (Shoaib *et al.*, 1995). Overall, there is good evidence that μ-opioid agonists are more potent in Sprague Dawley rats compared with Wistar rats. Although the mechanism is unclear, it is likely to be due to different receptor density or, different effectiveness of receptor-drug coupling mechanism between the two strains (Bustamante *et al.*, 1991; Shoaib *et al.*, 1995). Although to date, no studies have investigated the strain differences of nociceptin responses either *in vivo* or *in vitro*, we provide evidence of a similar strain-dependent effect whereby nociceptin is more potent in Sprague Dawley rather than Wistar rats (Figure 3.14). For this reason all future experiments were conducted in Sprague Dawley rats.

3.4.4.2 μ-opioid receptor (rat vas deferens)

[D-Ala^2,*N*-Me-Phe^4,Gly^5-ol]enkephalin acetate (DAMGO), a selective μ-opioid receptor agonist, was used as the standard μ-opioid receptor agonist (control) in this isolated rat vas deferens assay. DAMGO has higher affinity at the μ-opioid receptor compared to the κ- and δ-opioid receptors with about 200 and 1200-fold differences in the binding affinities respectively (Table 3.6) (Zhao *et al.*, 2003). Moreover, a

recent study measuring the operational efficacies of 22 μ-opioid agonists has shown that DAMGO is the most efficacious μ-opioid agonist available to date (McPherson *et al.*, 2010). Operational efficacy is a parameter used to measure the relative intrinsic efficacy of a series of agonists using the concentration-effects data.

Table 3.6: Binding affinity (K_i) of DAMGO over classical opioid receptor, μ-, κ- and δ- opioid receptor (Zhao *et al.*, 2003).

	Binding Affinity, Ki (nM)		
	μ	κ	δ
DAMGO	1.18 ± 0.12	213 ± 28	1430 ± 20

The vas deferens assay using DAMGO is widely published, however we initially struggled to get an optimal response with this μ-agonist in rat tissue. The underlying issue is still unclear. Although a preliminary experiment had shown a robust effect of 10 μM DAMGO to inhibit the muscle twitch by 70% (Figure 3.15 (left)), we were unable to reproduce this effect later. Instead, a greater concentration of 30 μM DAMGO produced only a 28% inhibition of the muscle twitch (Figure 3.15 (right)).

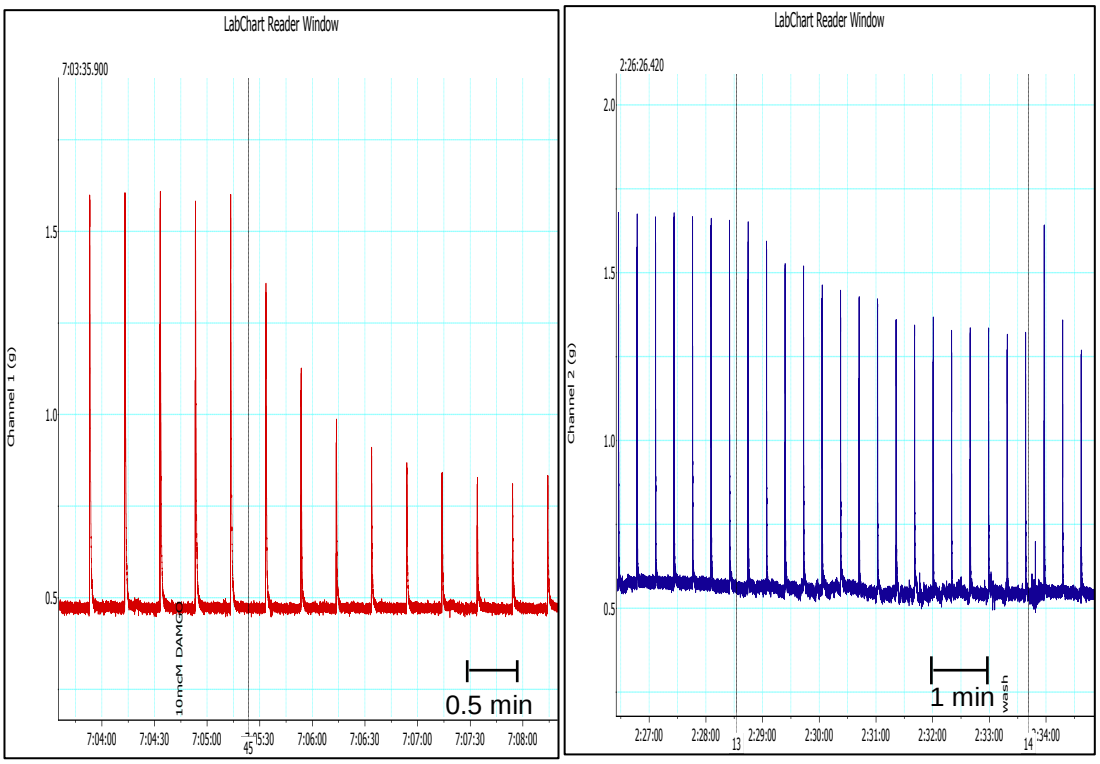

Figure 3.15: Electrically evoked contraction in rat vas deferens. (Left), tissue inhibition after a concentration of 10 µM DAMGO was given. (Right), tissue inhibition after a concentration of 30 µM DAMGO was given. Experiments were conducted in a different tissue at different time period.

Several attempts were made in order to get a more robust DAMGO effect including using newly purchased DAMGO, reducing the tension applied to the tissue, switching rat strain to Wistar and also adjusting the stimulator settings, however the result was still not reproducible. The final attempt taken was by reducing the Ca^{2+} concentration in Krebs solution since DAMGO was reported to be more potent in rat vas deferens when the Ca^{2+} concentration in the Krebs formula was reduced to half the normal concentration (Sheehan *et al.*, 1988). The cumulative concentration-response curve was constructed with 1.25 mM Ca^{2+}-Krebs concentration (Figure 3.16). DAMGO potency (EC_{50}) derived from this experiment was 280.5 nM (218.5-360.1 nM) with the maximal response (E_{max}) of 92.5% (88.1-96.8%). The mean inhibition obtained at 30 µM DAMGO from our experiment using 1.25 mM Ca^{2+}-Krebs formula was 91% compared to the 28% inhibition achieved using 30 µM DAMGO loading concentration in 2.5 mM Ca^{2+}-Krebs (Figure 3.15 (right)). These results were in line with Sheehan et al (1988) when 1.25 mM Ca^{2+}-Krebs was used, where the DAMGO potency (IC_{50}) reported was 366 ± 32 nM with 100% maximal

response. Although we did not perform a full concentration-response curve for DAMGO in 2.5 mM Ca^{2+}-Krebs to compare DAMGO potency between two different calcium concentrations, Sheehan et al (1988) reported a 10-fold increase in DAMGO potency after the calcium concentration was reduced to 1.25 mM which was 366 ± 32 nM compared to 3780 ± 610 nM.

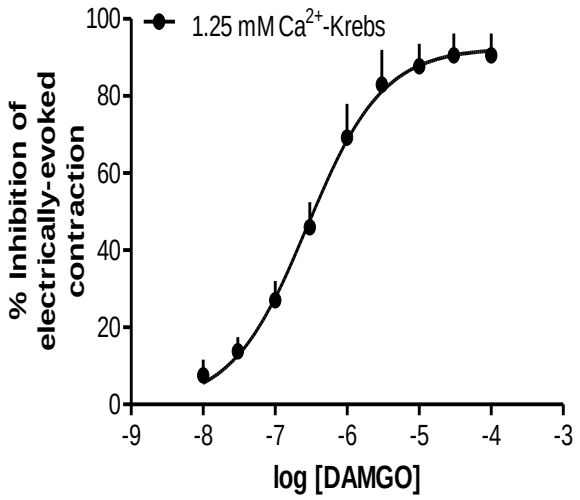

Figure 3.16: Electrically evoked contractions of rat vas deferens for DAMGO (10 nM-100 µM) in 1.25 mM Ca^{2+}-Krebs. Points represent means, and vertical lines represent S.E.M of four experiments.

It is believed that the increase of opioid agonists potency (eg: DAMGO) in lower calcium is due to the increased efficiency of receptor-effector coupling in a lower extracellular calcium media (Sheehan *et al.*, 1988). The influx of calcium into the nerve terminals during depolarisation is reduced in a lower extracellular calcium environment and therefore the effectiveness of the opioid agonist to block calcium from entering the nerve terminals is potentiated compared to in a higher extracellular calcium environment (Sheehan *et al.*, 1988).

The cycle for DAMGO was determined using the same method as used for nociceptin, by comparing the EC_{50} of four DAMGO concentration-response curve conducted on the same tissue with a 30 minute wash between curves (n = 1). The

result is shown in Figure 3.17 and the EC_{50} derived from each curves are presented in Table 3.7.

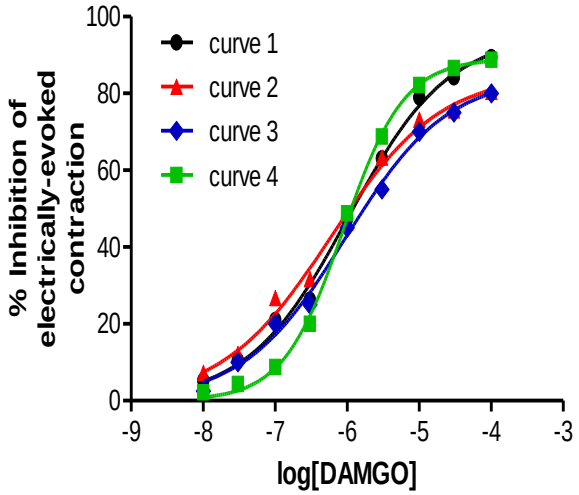

Figure 3.17: DAMGO concentration-response curve conducted in the same tissue to determine the suitability of DAMGO dose-cycle in electrically evoked contraction of rat vas deferens.

Table 3.7: Potency comparisons of DAMGO from a single tissue in order evaluate the suitability of DAMGO washout time for each dose-cycle.

DAMGO	Curve 1	Curve 2	Curve 3	Curve 4
EC_{50} (nM)	1031.0	592.8	945.3	890.8

Although there is some variability between each of the four concentration response curves, the effect is not statistically significant, and there is no consistent pattern to suggest either that DAMGO does not wash-out fully between cycles (which would appear as an apparent increase in DAMGO potency over time) or that DAMGO induces desensitization of the response (which would appear as an apparent decrease in DAMGO potency over time). For future experiments we therefore used this protocol: a dose cycle of 30 minutes and contact time of 5 minutes at each concentration.

Similar to when using the rat vas deferens to study ORL-1 receptors, the vas deferens was sensitized with nociceptin for the same reason as previously discussed (Chapter 3.4.4.1). No peptidase inhibitors were used in the μ-opioid receptor assay since DAMGO was found to be stable peptide (Van Dorpe *et al.*, 2010) compared to nociceptin in this tissue even though each concentration was applied for 5 minutes (Figure 3.15).

3.4.4.3 κ-opioid receptor (mouse vas deferens)

κ-opioid receptors are not present in the rat vas deferens (Sheehan *et al.*, 1988; Smith *et al.*, 1983), but are present in the mouse vas deferens (Miller *et al.*, 1983; Ward *et al.*, 1982).

Out of the few candidates tested (U-69593, (±)U-50488, (-)U-50488)), compound U-69593, a selective κ-opioid receptor agonist was finally selected to be used as a standard agonist in these assays. In rat brain membranes, U-69593 was found to have 300 and 800-fold higher affinity at the κ-opioid receptor (K_i = 10.40-18.46 nM) compared to the μ-opioid receptor (3191 ± 661 nM), and δ-opioid receptor (8534 ± 1577 nM) respectively (La Regina *et al.*, 1988).

Although they have comparable binding affinities and selectivities for the κ-opioid receptors, the reason both compounds (±)U-50488 and its single enantiomer, (-)U-50488 were not selected was because of very slow washout (incomplete after 2 hours). U-69593 had faster washout, but still took 90-120 minutes. For this reason, and because the electrically-evoked twitch response in the mouse vas deferens tends to deteriorate over time (Enna *et al.*, 1998), it was not feasible to conduct these experiments in the same manner as the ORL-1 and μ-opioid receptor assays. So, affinity constants for each compound tested at the κ-opioid receptor were determined using the single concentration of antagonist method, rather than Schild plot analysis.

Our pilot experiment demonstrated that the washout time used was sufficient based on the similar EC_{50} of the four U-69593 control curves (Table 3.8) obtained from the same tissue (n = 1) suggesting U-69593 had completely washed out after each dose cycle (Figure 3.18).

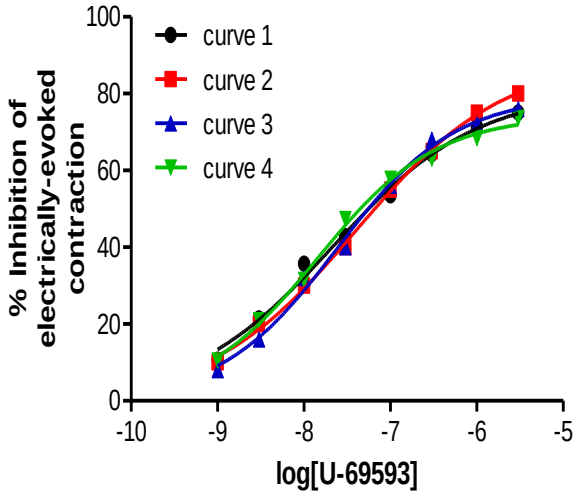

Figure 3.18: U-69593 concentration-response curve conducted in the same tissue to determine the suitability of U-69593 dose-cycle in electrically evoked contractions of mouse vas deferens.

Table 3.8: Potency comparisons of U-69593 from a single tissue in order to evaluate the suitability of U-69593 washout time for each dose-cycle.

U-69593	Curve 1	Curve 2	Curve 3	Curve 4
EC_{50} (nM)	21.6	40.7	24.4	14.4

There were no significant differences in potencies between the four U-69593 control curves except for the last curve (curve 4) which suggested U-69593 was completely removed after a 90-120 minutes washout interval.

For the κ-opioid receptor assays conducted in mouse vas deferens, all tissues were pre-treated with 1 μM CTAP (a selective μ-opioid receptor antagonist) 15 minutes

before the administration of U-69593 (for control curves) and test compound (for antagonist curves). Since mouse vas deferens has significantly larger μ-opioid receptor population compared to rat vas deferens (Smith *et al.*, 1983), CTAP was administered to the tissue to block any μ-opioid receptor mediated response induced by test compounds. For example, a previous study has shown the ability of buprenorphine to inhibit the electrically evoked contraction of mouse vas deferens with EC_{50} of 21.4 nM (20.4-22.9 nM) and achieved 63 ± 4% maximal response (E_{max}) (Spagnolo *et al.*, 2008). Based on Spagnolo et al (2008) studies, this inhibition was proven to be mediated by μ-opioid receptor activity of buprenorphine. In the results section as will be discussed later, 1 μM CTAP was proven to successfully block any μ-opioid receptor efficacy mediated by buprenorphine on mouse vas deferens tissue. Therefore, in order to standardize the experimental protocol for κ-opioid receptor assays, all tissues were pre-treated with 1 μM CTAP.

3.4.5 Isolated tissue preparation (vas deferens assay)

Functional assays were carried out in either rat vas deferens to evaluate the ORL-1 and μ-opioid receptor activity of the compounds or in mouse vas deferens to evaluate the κ-opioid receptor activity. Initially, a single high concentration (10 μM) of buprenorphine and its analogues was tested to determine if the compounds had any efficacy at the different receptors in either the rat or mouse vas deferens system.

3.4.5.1 **ORL-1 receptor rat vas deferens assays**

Buprenorphine and five of its analogues (BU127, BU10101, BU10136, BU10112 and BU10119) showed no agonist response in this tissue and so were evaluated at the ORL-1 receptor against nociceptin, a selective ORL-1 receptor agonist. A synthetic non-peptide compound, SB 612111 was used as a standard ORL-1 receptor antagonist in these assays. SB 612111 is > 1000-fold more selective for

the ORL-1 receptor compared to the μ- and κ-opioid receptors (Spagnolo *et al.*, 2007).

Using Sprague Dawley rats, the average potency (EC_{50}) for nociceptin derived from our experiments (n = 45) was 138.0 nM (109.6-166.0 nM), slightly less potent compared to the value previously reported, 56.2 nM (38.1-83.2 nM) (Fischetti *et al.*, 2009). Fischetti et al (2009) also found that nociceptin was slightly more potent in mouse vas deferens compared to rat vas deferens as shown in Table 3.9. Although nociceptin was less potent in our experiment, this was not a critical issue since the compound's potency was calculated based on individual tissue responses and was analyzed using individual concentration-ratio values to determine the antagonist potency values (pA_2) and binding affinities (K_B).

Table 3.9: Potency, EC_{50} (nM) of nociceptin in rats and mouse vas deferens (Fischetti *et al.*, 2009). Data marked * derived from our experiments.

	Potency, EC_{50} (nM)			
	Mouse vas deferens		Rat vas deferens	
	Swiss	CD1	Sprague Dawley	Sprague Dawley*
	(n = 5)	(n = 5)	(n = 5)	(n = 45)
Nociceptin	42.7 nM	24.0 nM	56.2 nM	138.0 nM
	(33.9-53.7 nM)	(20.9-27.5 nM)	(38.1-83.2 nM)	(109.6-166.0 nM)

Results

SB 612111

SB 612111, the standard ORL-1 receptor antagonist used in this assay, caused a parallel rightward shift of the nociceptin control curves (n = 4-8) (Figure 3.19 (left)).

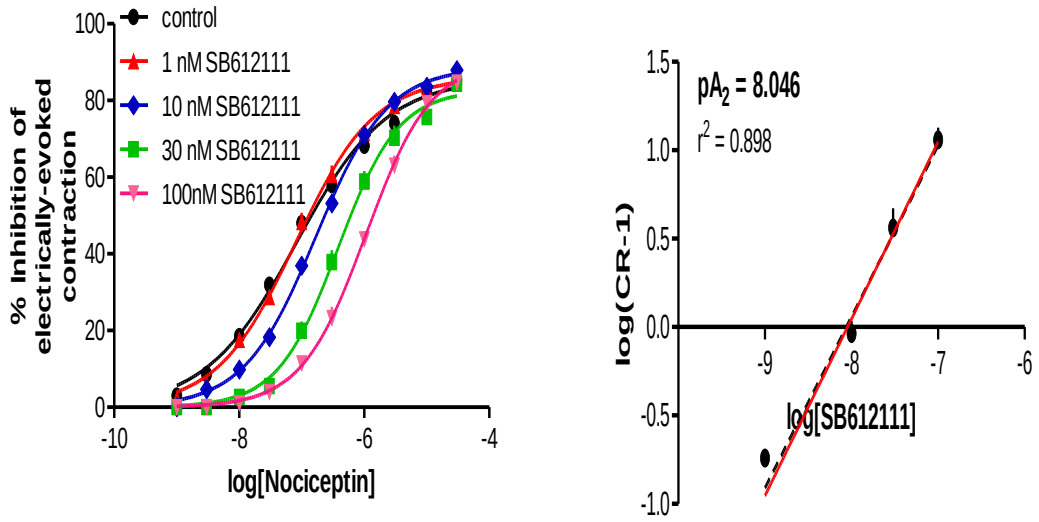

Figure 3.19: Electrically evoked contractions of rat vas deferens. Left, concentration-response curve to nociceptin obtained in the absence and in the presence of increasing concentrations of SB 612111 (1-100 nM); the corresponding Schild plot is shown on the right. The straight line (red) is after the slope was constrained to 1 and the dotted line (black) is the best fit line. Points represent means, and vertical lines represent S.E.M. of at least four experiments.

No significant diminution of the maximum inhibition to the control curve was observed by SB 612111, even at the highest concentration used. A Schild plot was constructed (n = 4-8) (Figure 3.19 (right)) to evaluate the antagonist pattern of SB 612111 and gave a straight line with a slope of 0.967 ± 0.0724 (95% confidence interval of 0.816-1.118) that was not significantly different to unity. As discussed earlier (Chapter 3.3.3.2), this situation permitted the straight line to be constrained to 1. The x-intercept of the Schild plot (when the slope was constrained to 1) gave the pA_2 value of 8.046 (7.957-8.136) for SB 612111. Therefore, SB 612111 was shown to be a competitive reversible antagonist in this system. The pA_2 value derived from this assay is in line with the value that has been previously reported (8.20-9.70) (Spagnolo *et al.*, 2008; Zaratin *et al.*, 2004).

Buprenorphine

A 10 µM concentration of buprenorphine did not inhibit the electrically evoked contractions of rat vas deferens, demonstrating that buprenorphine had no efficacy in this system (Kajiwara *et al.*, 1986) up to 10 µM (Figure 3.20).

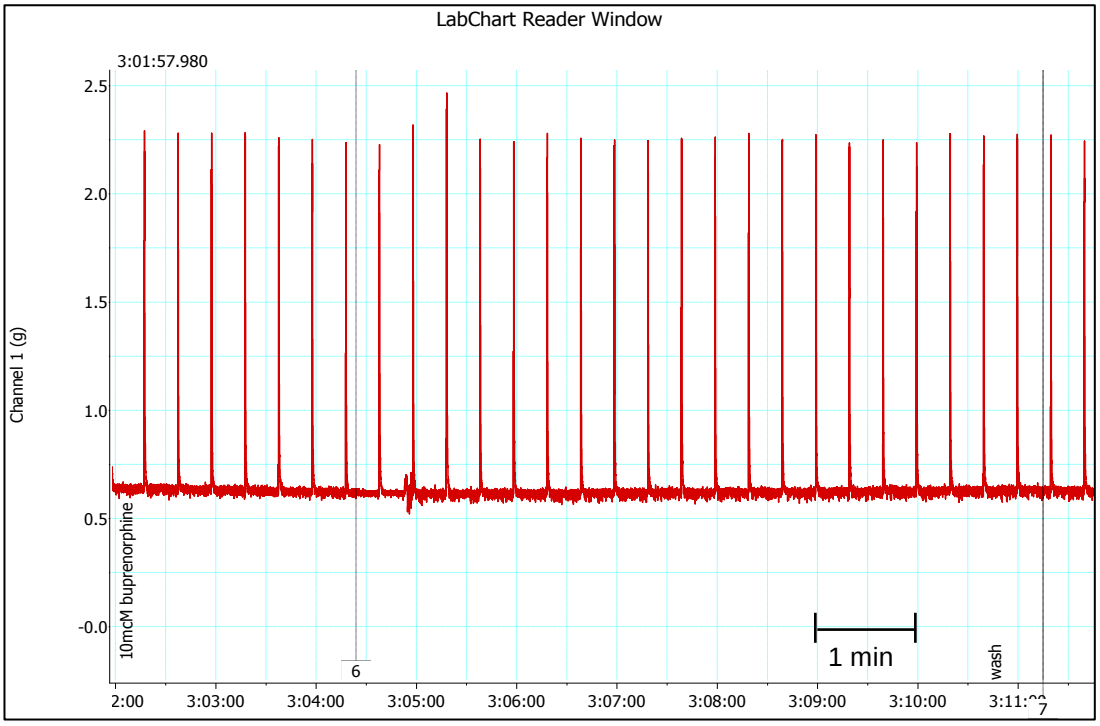

Figure 3.20: Effects of buprenorphine (10 µM) on electrically evoked contractions of rat vas deferens.

Increasing concentrations of buprenorphine (1 µM, 3 µM and 10 µM) were used and a Schild plot (n = 4) was constructed to evaluate the ORL-1 receptor antagonist characteristics of buprenorphine in this system (Figure 3.21).

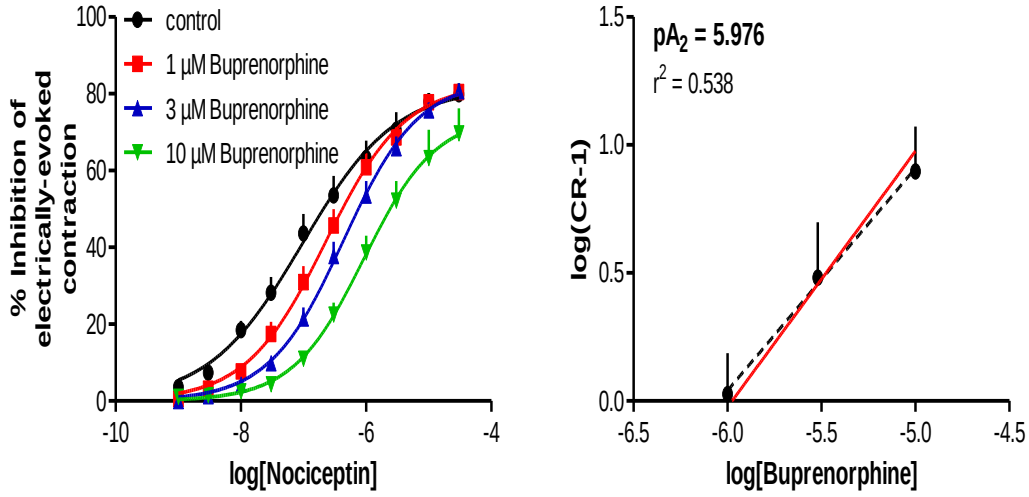

Figure 3.21: Electrically evoked contractions of rat vas deferens. Left, concentration-response curve to nociceptin obtained in the absence and in the presence of increasing concentrations of buprenorphine (1-10 µM); the corresponding Schild plot is shown on the right. The straight line (red) is after the slope was constrained to 1 and the dotted line (black) is the best fit line. Points represent means, and vertical lines represent S.E.M. of four experiments.

The best fit slope obtained from the straight line was 0.869 ± 0.248 (0.316-1.421) and was not significantly different to unity. The pA_2 value derived from the Schild plot for buprenorphine was 5.976 (5.760-6.191) with the slope constrained to 1. Therefore, in this case, pA_2 was equal to pK_B. Similar to SB 612111, buprenorphine was also shown to be a competitive reversible antagonist in this system with no significant difference in the maximum response (E_{max}) compared to the control even in the presence of 10 µM buprenorphine. In this experiment, buprenorphine was 100-fold less potent at the ORL-1 receptor compared to the standard ORL-1 antagonist used in this assay, SB 612111, with a binding affinities of 1056.8 nM (644.2-1737.8 nM) and 9.0 nM (7.3-11.0 nM) respectively. The inability of 10 µM buprenorphine to inhibit the electrically evoked contraction of the rat vas deferens and also the parallel rightward shift of the nociceptin concentration-response curves in the presence of buprenorphine (Figure 3.21) demonstrates that buprenorphine acts as an ORL-1 antagonist in rat vas deferens.

BU127

A 30 µM concentration of BU127 did not inhibit electrically evoked contractions of rat vas deferens, indicating that BU127 has no efficacy in this system up to 30 µM (Figure 3.22).

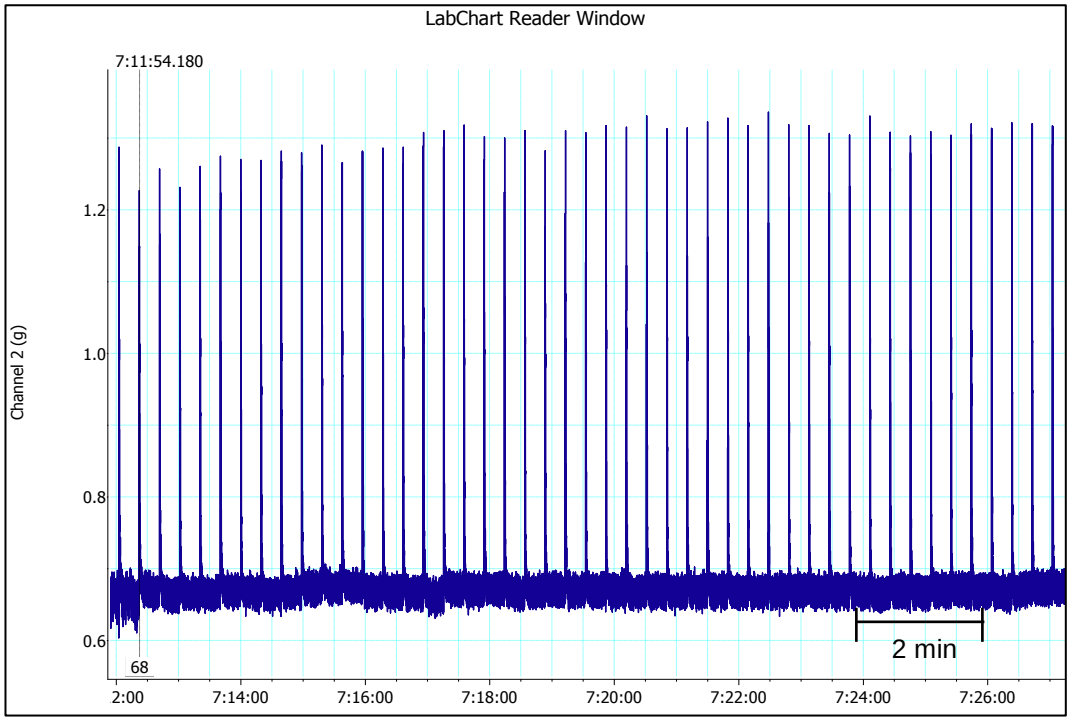

Figure 3.22: Effects of BU127 (30 µM) on electrically evoked contractions of rat vas deferens.

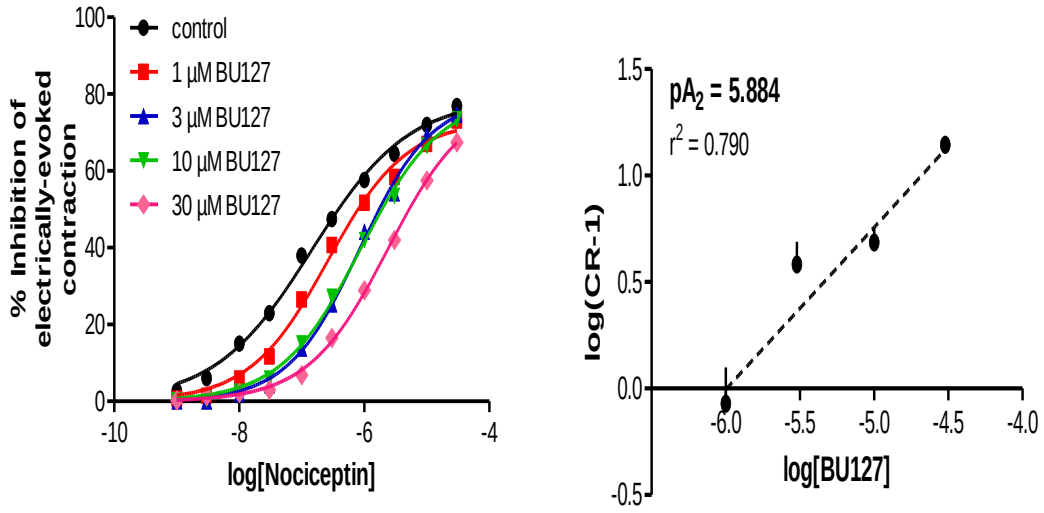

Figure 3.23: Electrically evoked contractions of rat vas deferens. Left, concentration-response curve to nociceptin obtained in the absence and in the presence of increasing concentrations of BU127 (1-30 µM); the corresponding Schild plot is shown on the right. The dotted line (black) is the best fit line. Points represent means, and vertical lines represent S.E.M. of at least three experiments.

Although there is no diminution of the maximal response to the control nociceptin curves observed, the Schild analysis (n = 3-8) gave a slope value of 0.761 ± 0.0877 with 95% CI significantly less than 1 (0.578-0.944). Therefore, a different approach was used to empirically estimate the pA_2 value of this compound since the x-intercept of the Schild plot is no longer valid to obtain this value (Kenakin, 2009). From the Schild equation (single concentration method), the pA_2 value calculated based on the procedure described in the methods section was 5.884 ± 0.108 (5.594-6.104). Based on the parallel rightward shift of the concentration-response curves and the fact that the maximum agonist response did not decrease (Figure 3.23 (left)), BU127 seems to behave as a competitive reversible antagonist. Both the lack of activity of 30 µM BU127 on its own and also the parallel rightward shift of nociceptin concentration-response curves in the presence of BU127 (Figure 3.23) demonstrate that BU127 acts as an ORL-1 antagonist in rat vas deferens.

BU10101

A 10 µM concentration of BU10101 did not inhibit electrically evoked contraction of rat vas deferens, which means that BU10101 had no efficacy in this system up to 10 µM (Figure 3.24).

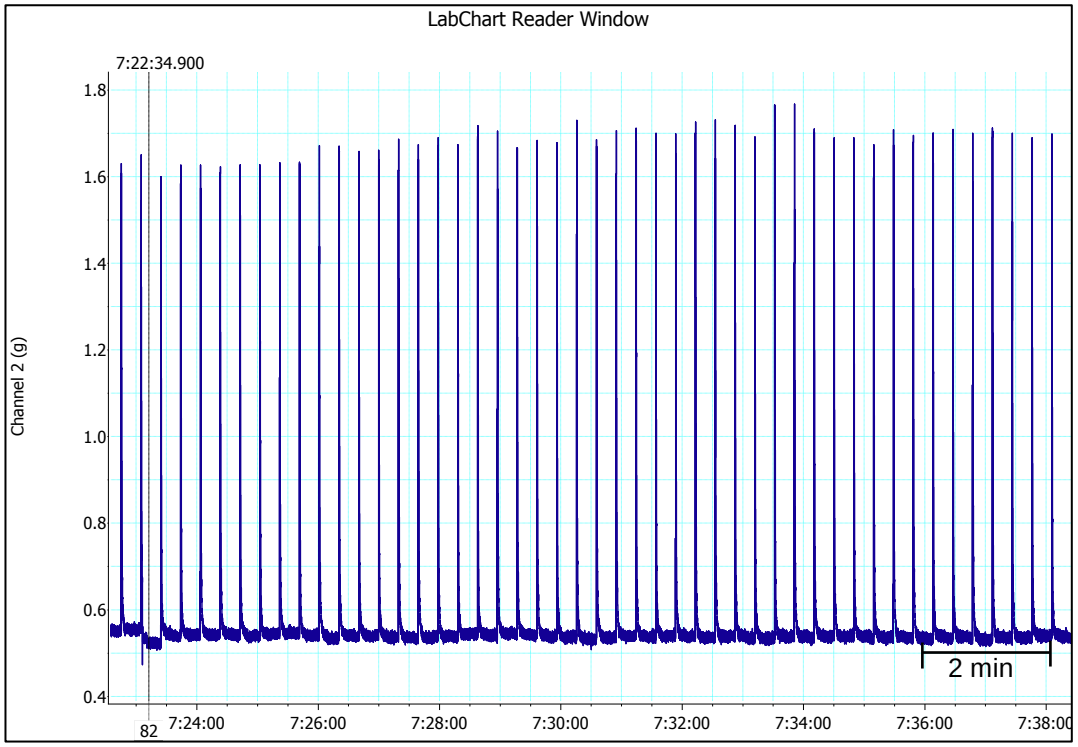

Figure 3.24: Effects of BU10101 (10 µM) on electrically evoked contractions of rat vas deferens.

Compound BU10101 was evaluated at the ORL-1 receptor to determine if the presence of a methyl group on the phenyl substituent at the C_{20} position improves the potency of BU127 analogue (BU10101) at this receptor. Based on Figure 3.25 (left), the concentration-response curves showed a significant suppression of the maximal response compared to the control at 30 µM BU10101 (n = 4-8) with an E_{max} value of 42.4% (37.8-46.9%) and 77.2% (72.2-82.2%) respectively. This suggests either a pseudo-irreversible action of BU10101 or hemi-equilibrium.

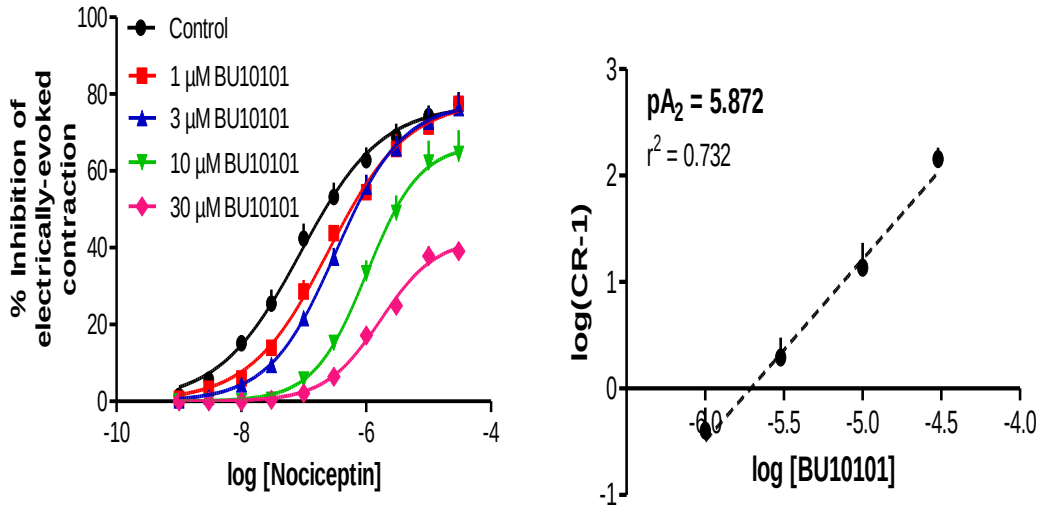

Figure 3.25: Electrically evoked contractions of rat vas deferens. Left, concentration-response curve to nociceptin obtained in the absence and in the presence of increasing concentrations of BU10101 (1-10 µM); the corresponding Schild plot is shown on the right. The dotted line (black) is the best fit line. Points represent means, and vertical lines represent S.E.M. of at least four experiments.

From the Schild analysis, the slope derived from the regression line was 1.703 (1.248-2.159), which was significantly greater than 1. This Schild analysis has further proved that either BU10101 is a pseudo-irreversible ORL-1 antagonist (based on the fact that the presence of antagonist cause a parallel shift of the dose-response curve, but the maximal response was significantly suppressed) or that equilibrium of agonist and antagonist with the receptors was not achieved (based on the fact that the slope was significantly greater than 1) (Kenakin, 2009). As the regression line on the Schild plot was significantly different from unity, we used the single concentration method in order to empirically estimate the potency (pA_2) value of compound BU10101 in this system. The nociceptin concentration-response curve in the presence of the lowest concentration of antagonist that caused the shift at each individual experiment was used to estimate the pA_2 value of compound BU10101. The estimated pA_2 value calculated using the Schild equation (single concentration method) for compound BU10101 was 5.872 ± 0.180 (5.446-6.297). Compound BU10101 was found to be a pseudo-irreversible antagonist in this system or the assay is in hemi-equilibrium as demonstrated by the reduction of the maximal response in the presence of 10 µM BU10101 (Figure 3.25 (left)), and the fact that the slope was significantly greater than 1 (Figure 3.25 (right)). Both the lack

of activity of 10 µM BU10101 on its own and also the rightward shift of nociceptin concentration-response curves in the presence of BU10101 (Figure 3.25 (left)) demonstrate that BU10101 acts as an ORL-1 antagonist in rat vas deferens.

BU10136

A 10 µM concentration of BU10136 did not inhibit electrically evoked contraction of rat vas deferens, suggesting BU10136 has no efficacy in this system up to 10 µM (Figure 3.26).

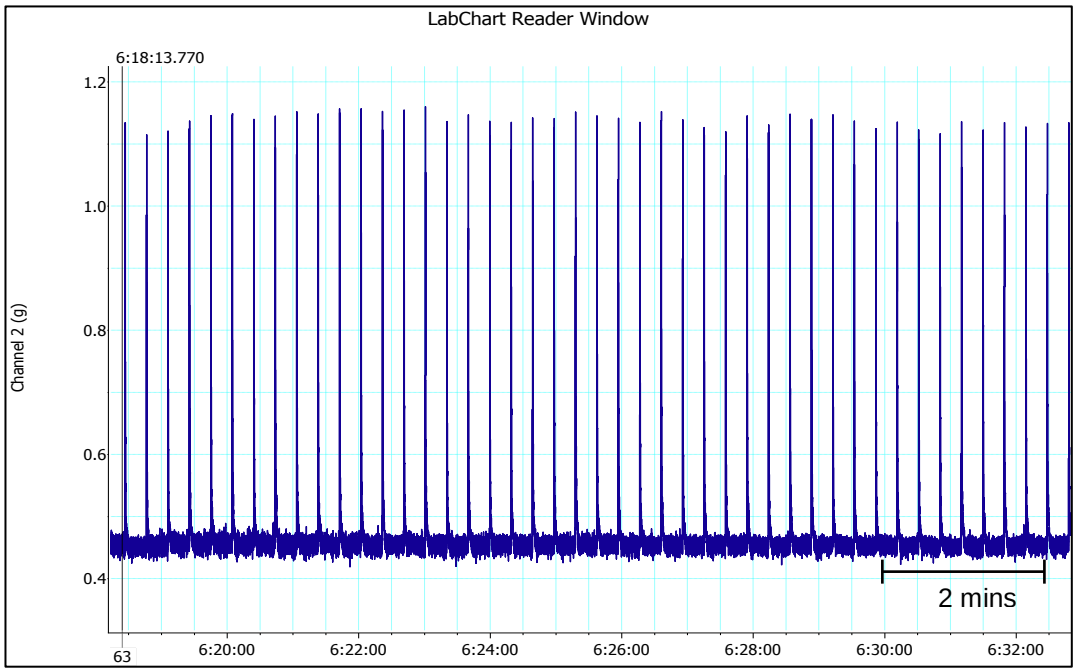

Figure 3.26: Effects of BU10136 (10 µM) on electrically evoked contractions of rat vas deferens.

Compound BU10136 has a 5-chlorothiophene at the C_{20} position of the orvinol. This compound was selected to see if it would retain its functional activity with the presence of a heteroatom rather than carbon in the aromatic system. Based on structure, thiophene is smaller compared to phenyl, which may be an advantage

during synthesis, however its pharmacological implications still needed to be investigated.

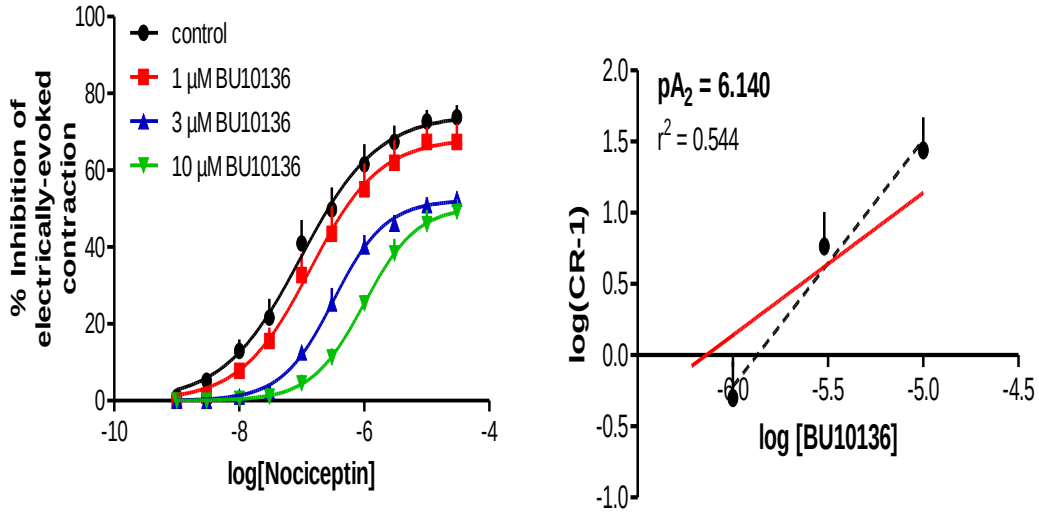

Figure 3.27: Electrically evoked contractions of rat vas deferens. Left, concentration-response curve to nociceptin obtained in the absence and in the presence of increasing concentrations of BU10136 (1-10 µM); the corresponding Schild plot is shown on the right. The straight line (red) is after the slope was constrained to 1 and the dotted line (black) is the best fit line. Points represent means, and vertical lines represent S.E.M. of four experiments.

From the concentration-response curves shown in Figure 3.27 (left) (n = 4), the maximal response of nociceptin in the presence of 3 µM and 10 µM of BU10136 was suppressed compared to the control with the E_{max} value of 74.5% (68.0-80.9%) for the control, and 52.3% (49.2-55.3%) and 50.6% (45.7-55.4%) in the presence of 3 µM BU10136 and in the presence of 10 µM BU10136,respectively. The decrease in the maximal response was statistically significant which indicates that compound BU10136 is a pseudo-irreversible ORL-1 receptor antagonist in this system, possibly due to the slow offset of BU10136 from the receptor during pre-equilibria period. The Schild slope derived from the Schild analysis for this compound was 1.732 (0.978-2.486) which was not significantly different to unity. Therefore hemi-equilibria rather than a true non-competitive nature of the antagonist is suspected. In this case, where a hemi-equilibria condition was suspected, Schild analysis still can be used to estimate the pK_B (= pA_2) of compound BU10136 (Kenakin, 2009). The pA_2 value

derived from the Schild plot for this compound was 6.140 (5.789-6.491) after the slope was constrained to 1. Both the lack of activity of 10 µM BU10136 on its own and also the parallel rightward shift of nociceptin concentration-response curves in the presence of BU10136 (Figure 3.27 (left)) demonstrates that BU10136 acts as an ORL-1 antagonist in rat vas deferens.

BU10119

A concentration of 10 µM of BU10119 did not inhibit electrically evoked contraction of rat vas deferens, which means BU10119 has no efficacy in this system up to 10 µM (Figure 3.28).

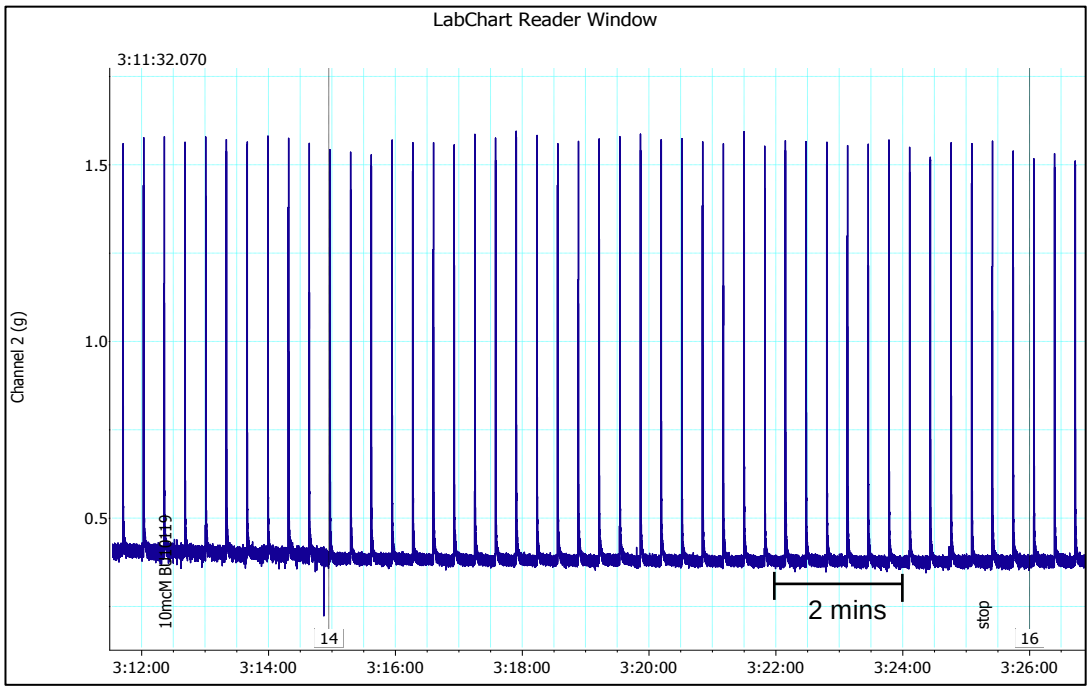

Figure 3.28: Effects of BU10119 (10 µM) on electrically evoked contractions of rat vas deferens.

Compound BU10119 has a similarity in the chemical structure with compound BU127, except the presence of a methyl group at the C_7 position and a proton at the C_{20} position of orvinol.

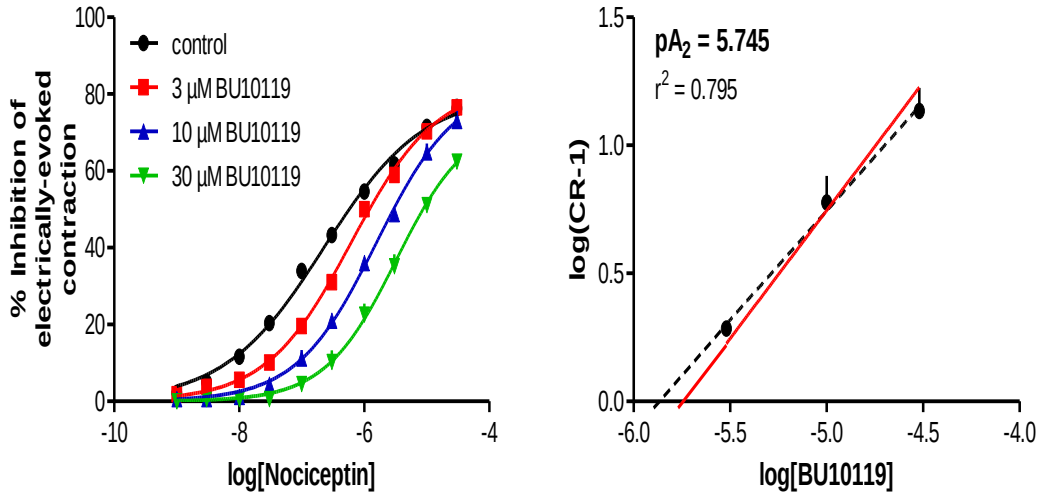

Figure 3.29: Electrically evoked contractions of rat vas deferens. Left, concentration-response curve to nociceptin obtained in the absence and in the presence of increasing concentrations of BU10119 (3-30 µM); the corresponding Schild plot is shown on the right. The straight line (red) is after the slope was constrained to 1 and the dotted line (black) is the best fit line. Points represent means, and vertical lines represent S.E.M. of five experiments.

The pA_2 value derived for compound BU10119 was based on the value obtained from Schild plot (n = 5) since the concentration-response curve for this compound showed no significant decrease in the maximal response at all of the concentration of BU10119 tested and the slope for the best fit line was not significantly different to 1 (0.851 ± 0.111 (0.612-1.089)) which allowed the slope to be constrained to 1. Both the lack of activity of 10 µM BU10119 on its own and also the parallel rightward shift of nociceptin concentration-response curves in the presence of BU10119 (Figure 3.29 (left)) demonstrate that BU10119 acts as an ORL-1 antagonist in rat vas deferens with the pA_2 value of 5.745 (5.646-5.845) after the slope was constrained to 1.

BU10112

A 30 µM concentration of BU10112 did not inhibit electrically evoked contraction of rat vas deferens, which means BU10112 had no efficacy in this system up to 30 µM (Figure 3.30). A single concentration of 30 µM BU10112 was tested since this was the highest dose range used in the actual assay (Figure 3.31 (left)).

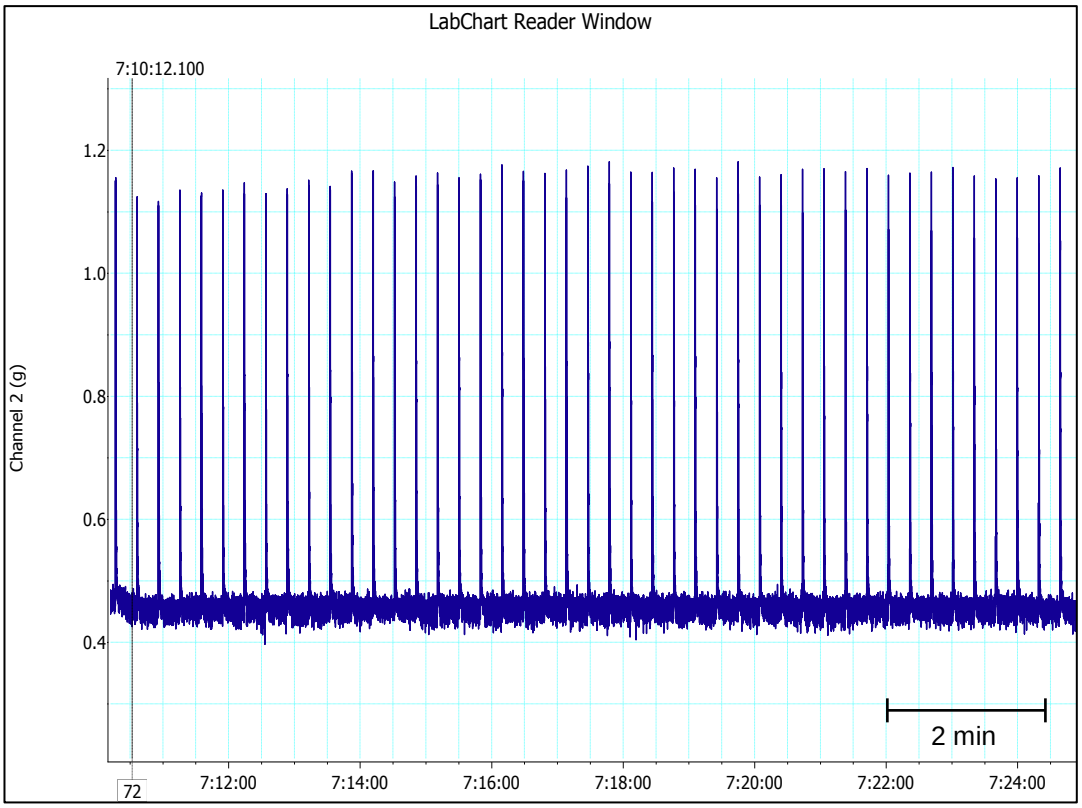

Figure 3.30: Effects of BU10112 (30 μM) on electrically evoked contractions of rat vas deferens.

Compound BU10112 has a similarity in structure to BU10101. Compound BU10112 also has a modification at the C_7 and C_{20} position of the orvinol as seen in BU101119.

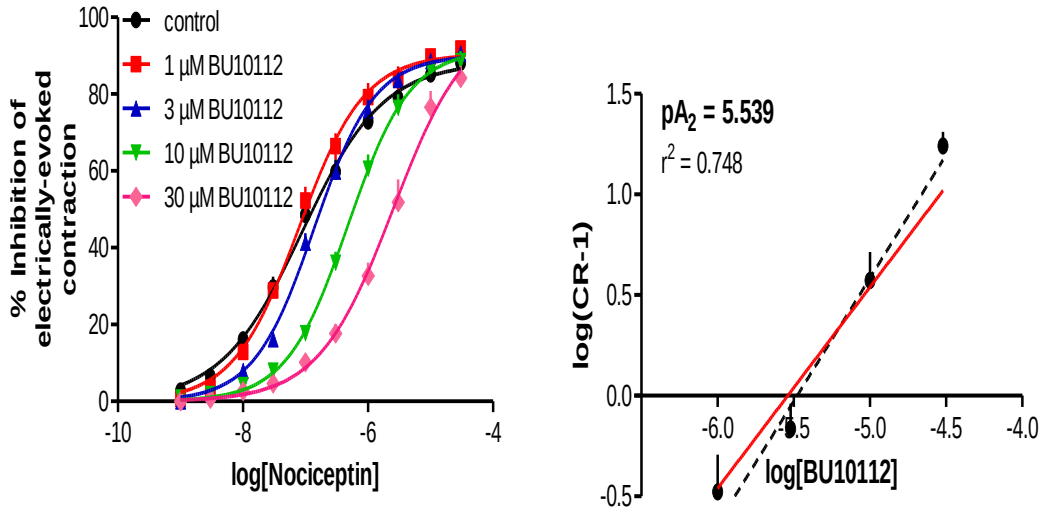

Figure 3.31: Electrically evoked contractions of rat vas deferens. Left, concentration-response curve to nociceptin obtained in the absence and in the presence of increasing concentrations of BU10112 (1-30 µM); the corresponding Schild plot is shown on the right. The straight line (red) is after the slope constraint to 1 and the dotted line (black) is the best fit line. Points represent means, and vertical lines represent S.E.M. of at least three experiments.

Unlike BU10101, compound BU10112 (n = 4-8) did not decrease the maximal nociceptin response even at 30 µM BU10112 (Figure 3.31 (left)). This was different to compound BU10101, where the decrease of the maximal response was detected at 10 µM (Figure 3.25 (left)). The pA_2 value derived from the Schild plot for BU10112 (n = 3-8) was 5.539 (5.385-5.693) after the slope was constrained to 1. The slope obtained from the best fit line was 1.223 ± 0.152 (0.906-1.540). Although there was not a significant difference the potency of compounds BU10112 and BU10101, 5.539 (5.385-5.693) and 5.872 ± 0.180 (5.446-6.297) respectively, these two compounds showed different antagonistic behaviour in this system. Compound BU10112 showed a competitive reversible antagonist pattern based on both concentration-response curves and Schild analysis, whereas compound BU10101 acted as a pseudo-irreversible antagonist at the ORL-1 receptor. Both the lack of activity of 30 µM BU10112 on its own and also the parallel rightward shift of nociceptin concentration-response curves in the presence of BU10112 (Figure 3.31 (left)) demonstrate that BU10112 acts as an ORL-1 antagonist in rat vas deferens.

Discussion

Are buprenorphine and its analogs ORL-1 agonists or antagonists ?

Although the [^{35}S]GTPγS initial screening (Figure 3.2 and Table 3.2) has shown all buprenorphine analogues evaluated have partial efficacy at the ORL-1 receptor (14-57%), none of them show any efficacy when tested in rat vas deferens. This was not surprising since a number of previous studies have also reported similar trends (Butour *et al.*, 1998). For example, [F/G]N/OFQ(1-13)NH_2, a nociceptin peptide fragment was previously reported to be an ORL-1 receptor antagonist due to its failure to inhibit the electrically evoked contraction of mouse vas deferens and guinea pig ileum. However it was found to show partial efficacy at the ORL-1 receptor in [^{35}S]GTPγS assay system (Burnside *et al.*, 2000; Guerrini *et al.*, 1998). Moreover, in cAMP accumulation assay, this same peptide was found to exert a full efficacy at the ORL-1 receptor (Butour *et al.*, 1998). These inconsistencies were believed to happen due to the different capacity of receptor reserve available between different assay systems (Spagnolo *et al.*, 2008).

Spagnolo et al (2008) has compared the profile of two different compounds with mixed ORL-1/μ-opioid receptor agonist activities (SR14150 and SR16476) and has found the relevance of this hypothesis. These studies suggest both compounds have similar affinity for ORL-1 receptor with K_i value of 1.39 ± 0.42 nM and 3.96 ± 1.55 nM respectively. Compound SR14150 however has 20-fold receptor selectivity for ORL-1 receptor over the μ-opioid receptor, significantly higher than SR16476 which only has 2-fold receptor selectivity. Surprisingly, only compound SR16476 which has slightly lower binding affinity and much lower selectivity for ORL-1 receptor, managed to maintain its agonist activity at this receptor in mouse vas deferens in the presence of naloxone while the efficacy of SR14150 at ORL-1 receptor was completely abolished by naloxone which shows that the inhibition of the mouse vas deferens contraction by compound SR14150 was mainly μ-opioid receptor mediated (Spagnolo *et al.*, 2008). When traced backward, it was found that although both compounds were equipotent at the ORL-1 receptor in [^{35}S]GTPγS

functional assay with EC_{50} of 20.8 ± 3.1 nM (SR14150) and 26.5 ± 4.3 nM (SR16476), only SR16476 managed to 100% stimulate ORL-1 receptor in this assay system compared to SR14150 which only partially stimulated the receptor (54.2% ORL-1 receptor stimulation) (Spagnolo *et al.*, 2008). Therefore, it is suggested that the GTPγS assay system which was conducted using CHO cells transfected with ORL-1 receptor might have a significantly higher ORL-1 receptor reserve compared to the vas deferens system (Spagnolo *et al.*, 2008). Therefore, a compound with low efficacy has an increased capability to stimulate the ORL-1 receptor in GTPγS assay might be due to the saturated number of ORL-1 receptors.

Thus, in order for a compound to show efficacy at ORL-1 receptor, especially in a system with a lower receptor reserve, a compound must possess a full agonist efficacy in a system with higher receptor density, such as in [^{35}S]GTPγS assay. In our case, since buprenorphine and all of its analogues only managed to partially stimulate the ORL-1 receptor in the [^{35}S]GTPγS assay, it was predicted that they would also be ORL-1 antagonists in mouse vas deferens. Any efficacy that may appear in the mouse vas deferens is believed to be mediated by the μ-opioid receptor. In conclusion, only compounds that show full ORL-1 efficacy in the [^{35}S]GTPγS assay can potentially show efficacy in a system with a lower receptor reserve, such as vas deferens (Spagnolo *et al.*, 2008).

In the current work, all of the compounds evaluated at the ORL-1 receptor in the rat vas deferens assay were compared against the standard ORL-1 receptor antagonist, SB 612111. SB 612111 was found to be 100-300-fold more potent antagonist at ORL-1 receptor compared to buprenorphine and its analogues, with pA_2 value of 8.046 (7.957-8.136). In previous studies SB 612111 was shown to be a pure ORL-1 receptor antagonist and inactive as an agonist at this receptor across a wide range of assay systems including the cAMP accumulation assay, [^{3}H]Leucyl-N/OFQ and [^{35}S]GTPγS binding assays, CRE-luciferase gene reporter assay and in electrically evoked isolated tissues assays (mouse / rat vas deferens and guinea pig ileum) (Spagnolo *et al.*, 2007; Zaratin *et al.*, 2004). pA_2 values ranged between 8.20-9.70 and therefore agreed with the value obtained in the current work. SB 612111 was confirmed to be a competitive reversible ORL-1 antagonist in rat vas deferens system (Figure 3.19).

Although we were unable to detect any existence of ORL-1 receptor efficacy of either buprenorphine or its analogues in rat vas deferens assays, previous studies have suggested that the activation of ORL-1 receptor by buprenorphine has potential as a new target in relapse prevention associated with drug addiction (McCann, 2008). The potential role of ORL-1 receptor in relapse prevention due to opioid, cocaine and alcohol consumption has been discussed in an earlier chapter. Thus, we aimed to design buprenorphine analogues that have certain profiles at targeted opioid receptors, which includes having high efficacy and potency at ORL-1 receptor.

One aspect of buprenorphine's profile that is believed to be beneficial in the treatment of drug addiction is its ability to activate ORL-1 receptors (McCann, 2008). From Traynor's finding, buprenorphine acted as a partial ORL-1 agonist in the [^{35}S]GTPγS assay with 24 ± 9% receptor stimulation at 10 μM. Previous studies show that buprenorphine displays inconsistent efficacy at the ORL-1 receptor at the cellular level, believed to highly rely on the sensitivity of the assay system which will influence the capacity of receptor reserve. For example, in one case buprenorphine was totally inactive as an agonist at the ORL-1 receptor in [^{35}S]GTPγS binding assay which was in contrast to Traynor's findings (Spagnolo *et al.*, 2008). In another study, buprenorphine shows higher partial ORL-1 receptor efficacy with 50 ± 4% receptor stimulation in [^{35}S]GTPγS assay conducted using ORL-1 transfected CHO-K1 cell lines (Bloms-Funke *et al.*, 2000). The higher ORL-1 receptor stimulation by buprenorphine obtained by Blooms-Funke (2000) compare to Traynor's results is suspected to be due to the different sensitivity of the GTPγS assay system used. Besides varying the amount of GDP added during their preliminary assay in order to optimize the measurement of the [^{35}S]GTPγS binding, Blooms-Funke's lab also has added the SPA-beads into their assay kit. SPA-bead (Scintillation proximity assay beads) is a sensitive microscopic size bead containing scintillant used to detect radioactivity signal (Park *et al.*, 1999) (eg: ^{35}S from the GTPγS species). This component is not present in Traynor's assay which is believed to contribute to the different extent of receptor stimulation seen in buprenorphine between these two lab. The most extreme case was reported from the reporter gene assay system where buprenorphine exerts its full and potent ORL-1 agonist efficacy with an IC_{50} value of 8.4 ± 2.8 nM and an E_{max} of 82.9 ± 2.1%, which was as efficacious as nociceptin. The IC_{50} value for nociceptin was 0.81 ± 0.5 nM with E_{max} of 81.9 ± 8.6%

at 10 μM in the same assay (Wnendt *et al.*, 1999). This assay that used reporter gene system has incorporated a cAMP-sensitive luciferase gene into the CHO-K1 transfected cells under the control of a promoter. Since the receptor activation by nociceptin inhibits the cAMP, this biochemical event can be detected and measured by the gene-reporter that was incorporated into the cell lines (inhibition of fosrskolin-induced luciferase expression). Therefore, sensitivity is not only different within similar assay system but with different receptor reserve, but the sensitivity of the cell lines and the variability in the experimental protocols is also believed to have a significant impact on the results (Harrison *et al.*, 2003; Kenakin, 2002; Leslie, 1987).

Synthetic chemistry approaches to increasing efficacy at ORL-1 receptor

Among all the buprenorphine analogues evaluated by Traynor's [^{35}S]GTPγS functional screening, the aromatic analogues of buprenorphine that have extra bulk near to the C_{20} position show significantly higher efficacy at the ORL-1 receptor compared to others in the series (Figure 3.32). This includes compounds BU10101, BU10093, BU10119 and BU10112 with ORL-1 receptor stimulation between 43-57%.

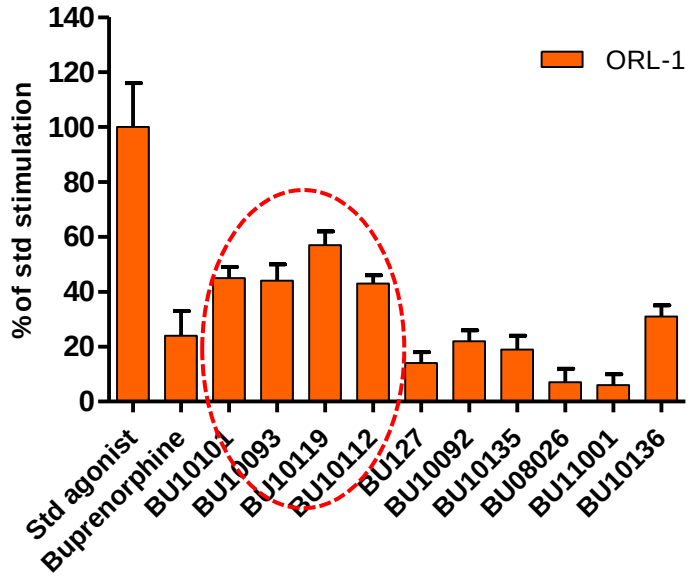

Figure 3.32: [^{35}S]GTPγS efficacy screening of buprenorphine and its analogues performed in cultured Chinese Hamster Ovarian (CHO) transfected cells. Efficacies of buprenorphine and its analogues at 10 µM were compared against standard ORL-1 receptor agonist (nociceptin) in triplicate. BU10101, BU10093, BU10119 and BU10119 (marked in red) shows significantly higher efficacy at ORL-1 receptor compared to the rest of the orvinol series (Traynor (unpubished work).

Compounds BU10101, BU10093 and BU10112 have a methyl group attached to the ortho position of the aromatic substituent (phenyl / thiophene) at the C_{20} position. Although compound BU10119 did not have such a methyl group, it is believed that the efficacy of this compound at the ORL-1 receptor is high due to the presence of a methyl group at the C_7 position of the orvinol. The presence of a methyl group at C_7 increases the steric bulk of this orvinol series near to C_{20}. BU10112 has both a methyl group at the ortho position of phenyl ring and at C_7 but does not have even higher efficacy for BU10119 suggesting that the effect of adding methyl groups is not additive, or that the C_{18}-C_{19} bridge (double bond in BU10112 and single bond in BU10119) also affects efficacy. Of all the analogues, compounds BU08026 and BU11001 have the lowest efficacies at the ORL-1 receptor. Both compounds have a thiophene substituent at the C_{20} position of the orvinol but have no alkyl or small groups attached to the thiophene ring compared to BU10093 (3-methyl-2-thienyl) and BU10135 (5-chloro-2-thienyl). In terms of the aromatic system, thiophene (5 membered ring) is smaller compared to phenyl (6 membered ring). Therefore, these

2 compounds (BU08026 and BU11001) have slightly lower efficacy compared to BU127 (phenyl). In terms of the efficacy at the ORL-1 receptor, there were no differences seen by relocating sulphur from 2-thiophene to 3-thiophene (Figure 3.32).

In conclusion, neither buprenorphine nor the newly synthesised buprenorphine analogues display agonist activity at ORL-1 receptors in a functional *in vitro* assay, although cell-based assays show that they may be agonists with very low intrinsic efficacy (Figure 3.32). Although these compounds appear to act functionally as ORL-1 antagonists, there is still evidence that a component of buprenorphine's action *in vivo* are caused by activation of ORL-1 receptors. This level of efficacy is not likely to play a major role in their actions *in vivo*, and so they would act as ORL-1 antagonists. This is based on buprenorphine *in vivo* effects seen in mice, where the bell-shaped dose response curve for buprenorphine induced antinociception (using high light intensity) was converted to a sigmoidal dose-response curve when the ORL-1 antagonist, J-113397 was administered (Lutfy *et al.*, 2003b). J-113397 is 600 times more selective at the ORL-1 receptor compared to the μ-opioid receptor, 1000 times compared to κ-opioid receptor and inactive at δ-opioid receptor (Kawamoto *et al.*, 1999).

Antagonist potency of compounds at the ORL-1 receptor

In terms of antagonist potency, buprenorphine was found to be 117-fold less potent at the ORL-1 receptor compared to SB 612111 with pA_2 value of 5.976 (5.760-6.191). The affinity (K_B) of buprenorphine in rat vas deferens was found to be about 5-fold lower than the binding affinity (K_i) at the ORL-1 receptor reported by Traynor's group using radioligand binding in transfected CHO_{ORL-1} cells (212 ± 7 nM) (Table 3.1). Similar to SB 612111, buprenorphine also behaved as a competitive reversible antagonist at the ORL-1 receptor in the rat vas deferens system.

The effect on antagonist potency of increasing the steric bulk near to the C_{20} position of the orvinol series was the opposite to the effect on efficacy. Introducing bulk near to C_{20} slightly reduces the antagonist potency of analogues for the ORL-1 receptor compared to buprenorphine, although the differences were not statistically significant except for compound BU10112 (Table 3.10). Compound BU10112 has about 3-fold less affinity for the ORL-1 receptor than buprenorphine with a K_B value ($\approx K_i$) of 2890.7 nM (2027.7-4121.0 nM) and 1056.8 nM (644.2-1737.8 nM) respectively (Table 3.10).

As mentioned, although introducing phenyl at C_{20} (BU127) slightly reduces the analogue potency at ORL-1 receptors compared to buprenorphine, the differences were not statistically proven, which suggests that the presence of a methyl on the phenyl substituent at the C_{20} position of orvinol has little effect on this parameter. However the slight difference in chemical structure causes BU10101 to be pseudo-irreversible as can be seen in the concentration-response curve in Figure 3.25 (left). One possible explanation is the difference in lipophilicity between these compounds which is calculated by measuring log P. High lipophilicity ensures the compounds are able to diffuse through the tissue, however it can also cause the compounds to have slow receptor kinetics, making it difficult to remove from the active site. Log P is a quantitative descriptor of compound lipophilicity and it helps to understand pharmacological behaviour of compounds in a biological system (Riba *et al.*, 2010). It measures the partition coefficient of a compound in octanol-water. Higher values indicate higher lipophilic properties of the compound (Riba *et al.*, 2010). The log P calculated using Chemdraw software for compound BU10101 was 4.45, higher than compound BU127 which was 3.96. This means that BU10101 is more lipophilic than BU127 which might explain the pseudo-irreversible behaviour of this compound. In addition, BU10136 (5-chloro-2-thienyl orvinol) (log P = 4.32) was also found to be more lipophilic than BU127 and also displayed a pseudo-irreversible behaviour of antagonism at the ORL-1 receptor. Unfortunately, compound BU08026 (2-thienyl orvinol) was not tested in this assay as a comparison. Log P calculations show that compound BU10136 was slightly more lipophilic than BU08026 with calculated log P to be 4.32 and 3.95 respectively, suggesting that BU08026 would be reversible.

All findings at the ORL-1 receptor in rat vas deferens are summarized in Table 3.10.

Compound	pA_2	K_B (nM)	Log P	Potency vs. Buprenorphine	Antagonist Behaviour
SB 612111 (Standard ORL-1 antagonist) 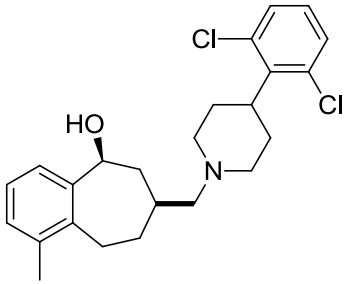	8.046 (7.957-8.136)	9.0 (7.3-11.0)	6.24	117	Competitive reversible
Buprenorphine 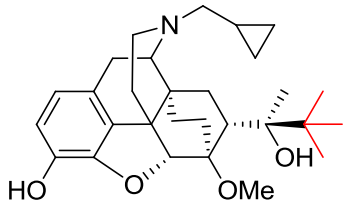	5.976 (5.760-6.191)	1056.8 (644.2-1737.8)	3.99	1	Competitive reversible

BU127 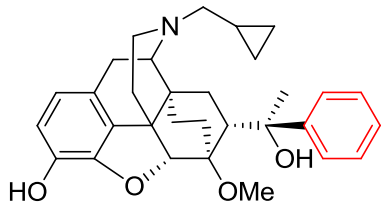	5.884 ± 0.108 (5.594-6.104)	1305.9 (787.0-2546.8)	3.96	0.8	Competitive reversible
BU10101 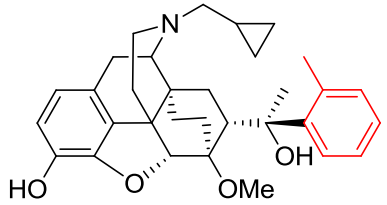	5.872 ± 0.180 (5.446-6.297)	1342.8 (504.7-3581.0)	4.45	0.8	Pseudo-irreversible
BU10136 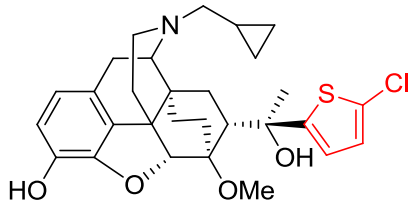	6.140 (5.789-6.491)	724.4 (322.8-1625.5)	4.32	1.5	Pseudo-irreversible

BU10119 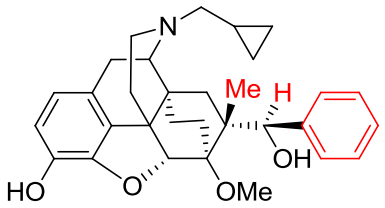	5.745 (5.645-5.845)	1762.0 (1429.0-2259.4)	4.37	0.6	Competitive reversible
BU10112 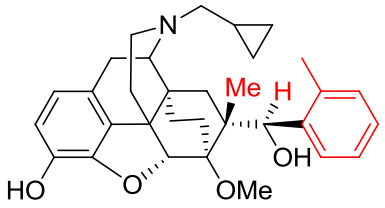	5.539 (5.385-5.693)	2890.7 (2027.7-4121.0)	4.86	0.4	Competitive reversible

Table 3.10: Summary of ORL-1 receptor assays conducted in rat vas deferens.

3.4.5.2 μ-opioid receptor rat vas deferens assays

Based on the initial [^{35}S]GTPγS efficacy screening done by Traynor's lab (Figure 3.2), only three buprenorphine analogues (BU127, BU10101 and BU10119), in addition to buprenorphine, were selected to be evaluated at the μ-opioid receptor against DAMGO, a selective μ-opioid receptor agonist in the rat vas deferens system. BU127 and BU10119 were selected because these two analogues have shown successful profile at all the targeted receptors. Compound BU10101 was selected as the representative of the analogues having small substituent group at the C_{20} aromatic ring, and also due to the high partial efficacy shown at the ORL-1 receptors (Figure 3.2).

Cumulative DAMGO concentration-response curves (10 nM-100 μM) were constructed in the presence and in the absence of increasing concentrations of the test compounds. Instead of naloxone, we used naltrexone as the standard μ-opioid receptor antagonist in this assay. Both naloxone and naltrexone are universal opioid receptor antagonists. Naloxone is relatively more selective than naltrexone for the μ-opioid receptor compared to δ- and κ-opioid receptors (Table 3.11) (Magnan *et al.*, 1982). However, since the compounds synthesised are δ-antagonists and rat vas deferens (which does not have κ-opioid receptor population) (Smith *et al.*, 1983) was used to evaluate their μ-opioid receptor activity, this will not cause a problem.

Table 3.11: The opioid receptor selectivity of naltrexone and naloxone.

Compound	Binding affinity, Ki (nM)		
	μ	δ	κ
Naltrexone	1.08 ± 0.17	6.6 ± 0.08	8.5 ± 0.82
Naloxone	1.78 ± 0.25	27.0 ± 6.1	17.2 ± 3.5

Results

In the current studies, naltrexone showed no efficacy in rat vas deferens at 10 µM as expected (Figure 3.33).

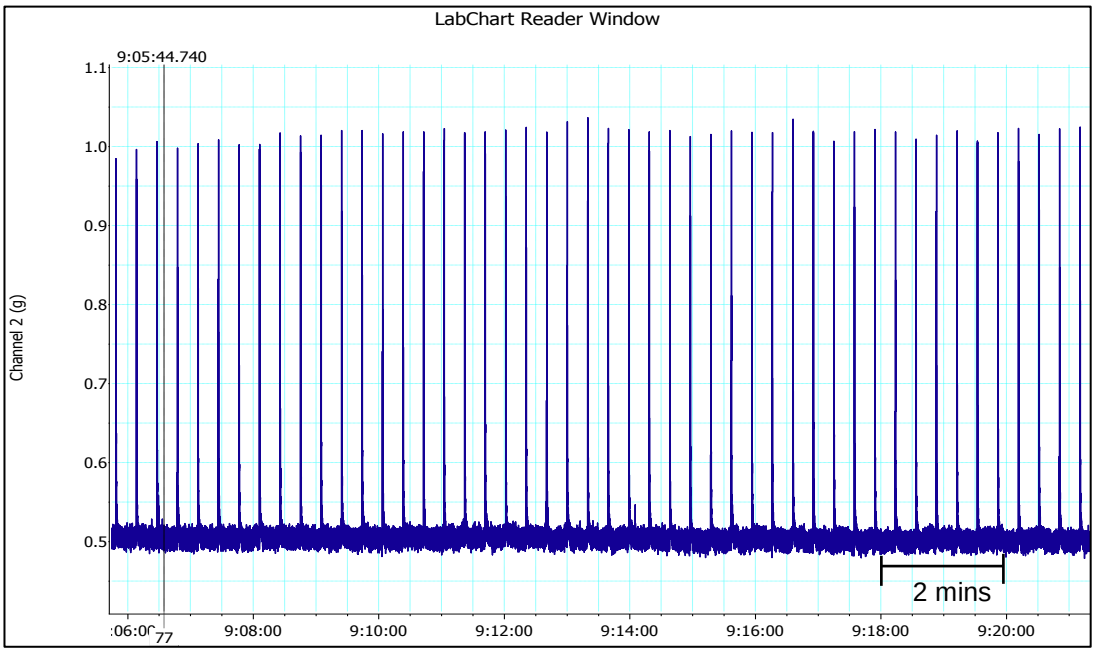

Figure 3.33: Effects of naltrexone (10 µM) on electrically evoked contractions of rat vas deferens.

Naltrexone caused a parallel rightward shift to the control DAMGO curves (n = 5) with no suppression of the maximal response at all concentrations used (1 nM, 10 nM, 30 nM) (Figure 3.34 (left)). The slope for the best fit line was not significantly different to 1 (0.869 ± 0.179 (0.482-1.255) (Figure 3.34 (right)). The Schild plot was constructed with the slope constrained to 1 and gave the pA_2 value of 8.898 (8.665-9.131) for naltrexone. This was similar with the previous pK_B value reported (9.04) for naltrexone (single concentration method) in rat vas deferens (Riba *et al.*, 2010).

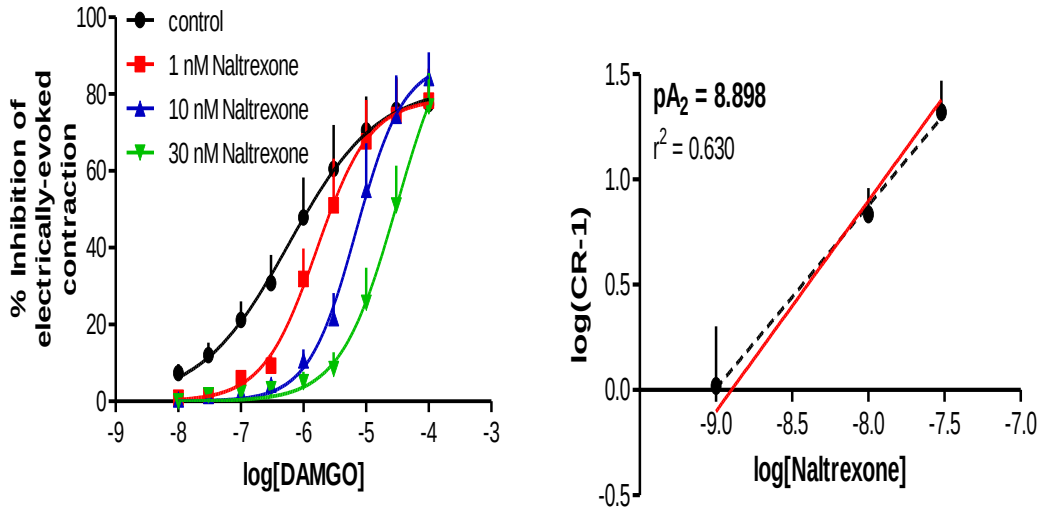

Figure 3.34: Electrically evoked contractions of rat vas deferens. Left, concentration-response curve to DAMGO obtained in the absence and in the presence of increasing concentrations of naltrexone (1-30 nM); the corresponding Schild plot is shown on the right. The straight line (red) is after the slope was constrained to 1 and the dotted line (black) is the best fit line. Points represent means, and vertical lines represent S.E.M. of five experiments.

From both graphs, naltrexone was shown to be a competitive reversible μ-opioid receptor antagonist in this system.

Buprenorphine

As shown in the previous ORL-1 receptor assay, buprenorphine does not show any agonist activity in the rat vas deferens tissue at ≤ 10 μM (Figure 3.20). Although buprenorphine is a partial μ-opioid agonist, the inability of this drug to inhibit the twitches is due to the low μ-receptor reserve in the rat vas deferens system (Liao *et al.*, 1981; Smith *et al.*, 1983) compare to the mouse vas deferens (Huidobro-Toro *et al.*, 1981; Maldonado *et al.*, 2001), where the agonist activity of buprenorphine was seen (Spagnolo *et al.*, 2008). The concept of receptor reserve has already been introduced in the first chapter (Chapter 1.7.2.2) and been discussed extensively in the previous ORL-1 discussion's section.

To investigate buprenorphine's activity in this system, DAMGO concentration-response curves were performed in the presence of increasing buprenorphine concentrations (1 nM, 3 nM and 10 nM) (n = 3-4). The results are presented in Figure 3.35.

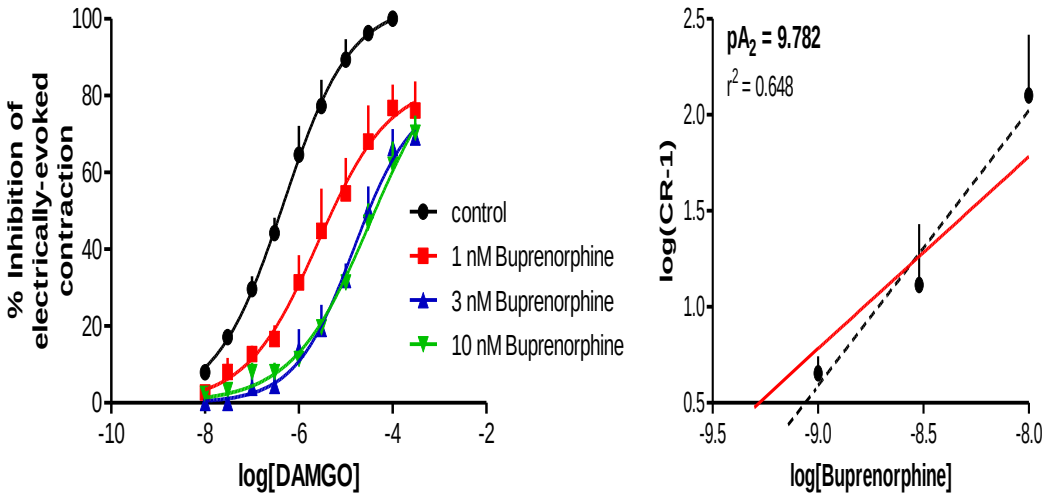

Figure 3.35: Electrically evoked contractions of rat vas deferens. Left, concentration-response curve to DAMGO obtained in the absence and in the presence of increasing concentrations of buprenorphine (1-10 nM); the corresponding Schild plot is shown on the right. The straight line (red) is after the slope was constrained to 1 and the dotted line (black) is the best fit line. Points represent means, and vertical lines represent S.E.M. of at least three experiments.

Although DAMGO shows a parallel rightward shift of the concentration-response curves in the presence of increasing concentration of buprenorphine (1-10 nM) (Figure 3.35 (left)), the graph pattern clearly suggesting buprenorphine is a pseudo-irreversible antagonist in this system. This is based on the decreasing pattern of the maximal response of DAMGO when buprenorphine is presence. This suppression is however is not significantly different from the control curve, except at 3 nM buprenorphine (E_{max}; control 100.0%, 1 nM (83.6% (65.7-100.0%), 3 nM (80.2% (62.8-97.6%), 10 nM (95.0% (64.7-100.0%)) (calculated E_{max}), which technically allows Schild analysis to be used to get the pA_2 value of buprenorphine. The slope of the linear regression line derived from the Schild plot for buprenorphine (Figure

3.35 (right)) was 1.432 ± 0.321 (0.691-2.172) which was not significantly different to unity. This has permitted the slope to be constrained to 1 to estimate the pA_2 value (= pK_B) of buprenorphine which was 9.665 (9.468-10.100). The pA_2 value of buprenorphine has also been estimated using the Schild equation. Although the slope of the linear regression is not significantly different from unity, the confidence interval is wide. Using the Schild equation, the estimated pA_2 value for buprenorphine was 9.837 ± 0.057. These two values have shown to be not statistically different. Based on the graph pattern seen in Figure 3.39(left), buprenorphine appears to behave as a pseudo-irreversible antagonist at the μ-opioid receptor in this system. This could be explained by the slow dissociation kinetics of buprenorphine, which will be discussed in further detail in the discussion section. The parallel rightward shift of DAMGO concentration-response curves in the presence of buprenorphine (Figure 3.35 (left)) and the previously shown lack of activity of 10 μM buprenorphine on its own (Figure 3.20) demonstrate that buprenorphine acts as a μ-opioid receptor antagonist in rat vas deferens.

BU127

Up to 10 experiments were performed to evaluate the activity of compound BU127 at the μ-opioid receptor in rat vas deferens. Unfortunately, on some days, the tissue was less responsive to DAMGO than usual as evidenced by the wide range in the EC_{50} of the DAMGO control curves (219.7-4705.0 nM). When the tissue was less responsive, a higher concentration of DAMGO (300 μM) was needed to define the maximal response (E_{max}). Because such high concentrations of DAMGO were required, theoretically more μ-opioid receptors needed to be activated in order to produce the response. This situation is likely to be due to lower receptor reserve in the tissues where DAMGO was seen as less potent. Indeed, there is good evidence that the rat vas deferens has a lower μ-opioid receptor density compared to mouse vas deferens and guinea pig ileum as discussed earlier (Smith *et al.*, 1983). This problem becomes more prominent when the control curve in the presence of 1 nM BU127 was constructed where the maximal response cannot be defined even when 300 μM DAMGO was used. Figure 3.36 represents traces from a single tissue where the EC_{50} for DAMGO was 4705.0 nM.

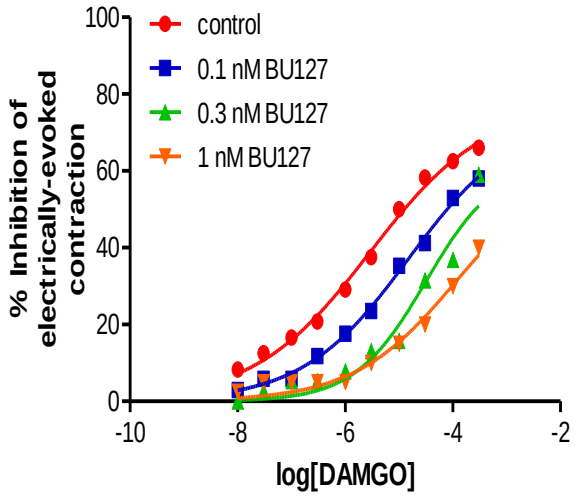

Figure 3.36: Electrically evoked contractions of rat vas deferens. Concentration-response curve to DAMGO obtained in the absence and in the presence of increasing concentrations of BU127 (0.1-1 nM) conducted from a single experiment.

Based on the results obtained (Figure 3.36), it was not possible to determine the maximal response to DAMGO, and so it was not possible to derive accurate EC_{50} values required to construct the Schild plot. Therefore, we decided to exclude data from tissues where the DAMGO maximal response could not be empirically determined (Figure 3.37 (left)). This excluding criteria is only applied for BU127, since no similar problem (Figure 3.36) was observed on days when other compounds were tested in the rat vas deferens assay.

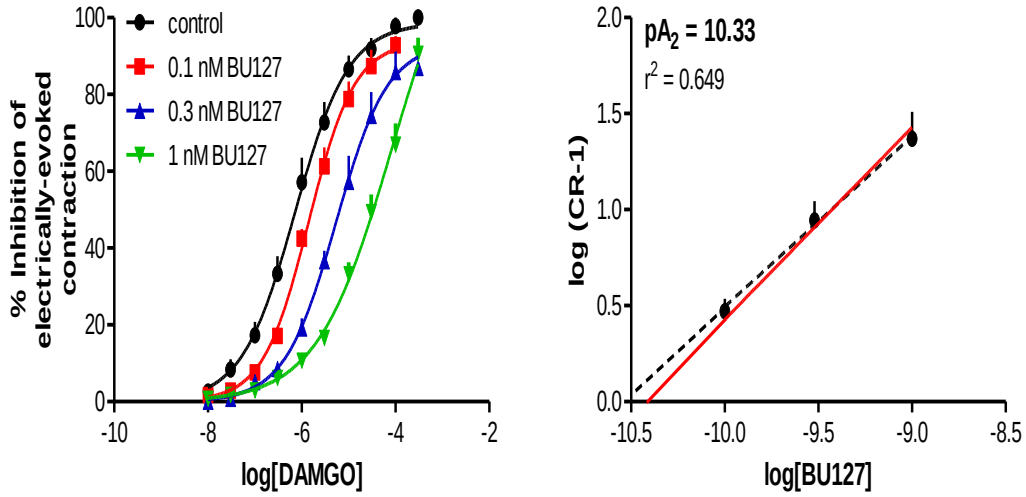

Figure 3.37: Electrically evoked contractions of rat vas deferens. Left, concentration-response curve to DAMGO obtained in the absence and in the presence of increasing concentrations of BU127 (0.1-1 nM); the corresponding Schild plot is shown on the right. The straight line (red) is after the slope was constrained to 1 and the dotted line (black) is the best fit line. Points represent means, and vertical lines represent S.E.M. of at least seven experiments.

Based on the results presented in Figure 3.37 (left), no decrease in the maximal response was detected in the presence of compound BU127 at all concentrations used (n = 7-10). This suggests that BU127 acts as a competitive reversible antagonist. This was supported by the findings revealed from the Schild plot (n = 7-10, Figure 3.37 (right)) where the slope from the best fit line was found to be not significantly different to unity (1.217 ± 0.196 (0.810-1.624)). The pA_2 value for compound BU127 was 10.33 (10.17-10.50) when the slope was constrained to 1.

<u>BU10101</u>

Similar to compound BU127, BU10101 was also found to be a competitive reversible antagonist at this receptor with the pA_2 value of 9.846 (9.644-10.050) derived from the Schild plot (n = 3-4). The slope obtained from the best fit line was 1.014 ± 0.240 (0.471-1.558) which was not significantly different to unity. No decrease in the maximal response was detected in the presence of increasing

concentrations of BU10101 compared to control. The results are presented in Figure 3.38.

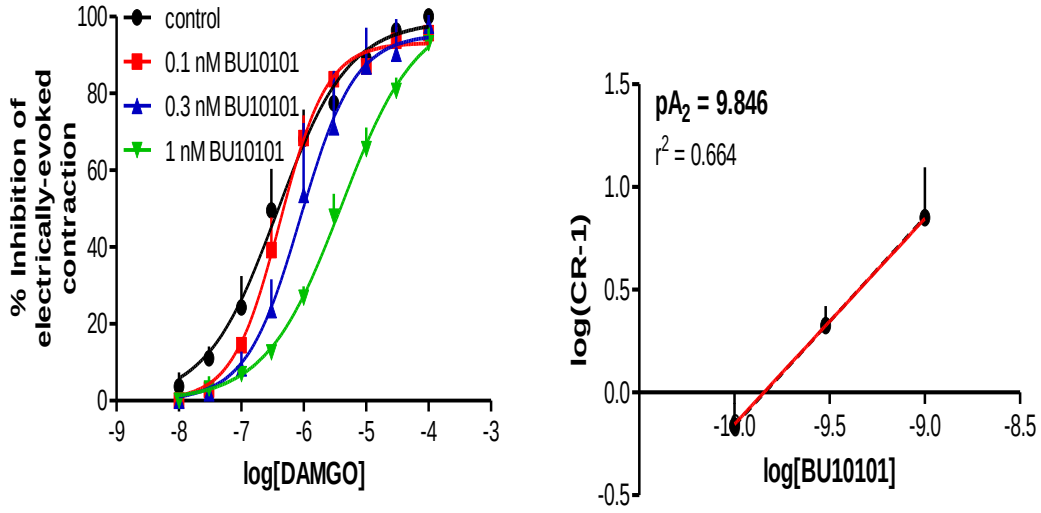

Figure 3.38: Electrically evoked contractions of rat vas deferens. Left, concentration-response curve to DAMGO obtained in the absence and in the presence of increasing concentrations of BU10101 (0.1-1 nM); the corresponding Schild plot is shown on the right. The straight line (red) is after the slope was constrained to 1 and the dotted line (black) is the best fit line. Points represent means, and vertical lines represent S.E.M. of at least three experiments.

BU10119

Compound BU10119 was slightly different in structure compared to its closest analogue (BU127). As presented in Figure 3.39, compound BU10119 was also found to be a competitive reversible antagonist in nature with no suppression of the maximal DAMGO response compared to control (n = 6) in the presence of increasing concentrations of BU10119 (0.1-1 nM).

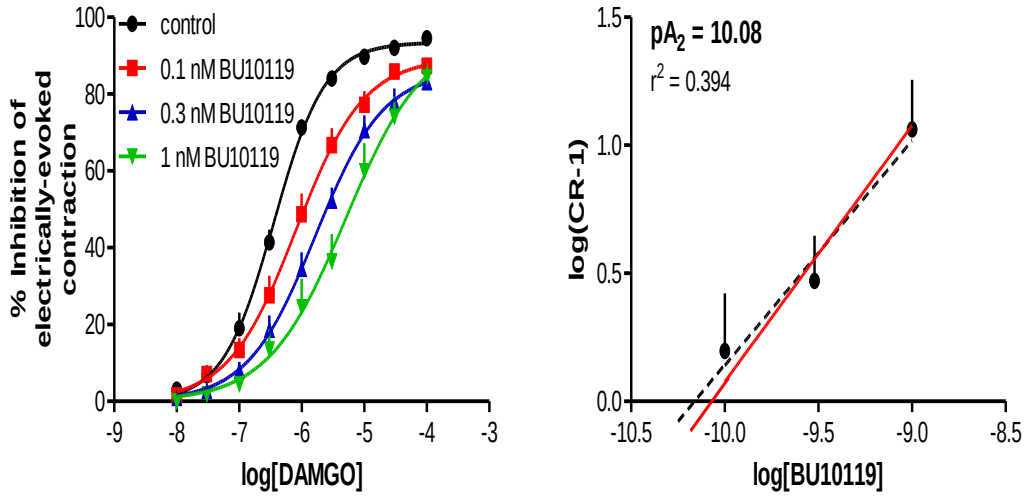

Figure 3.39: Electrically evoked contractions of rat vas deferens. Left, concentration-response curve to DAMGO obtained in the absence and in the presence of increasing concentrations of BU101119 (0.1-1 nM); the corresponding Shild plot is shown on the right. The straight line (red) is after the slope was constrained to 1 and the dotted line (black) is the best fit line. Points represent means, and vertical lines represent S.E.M. of six experiments.

The best fit line gave a slope of 0.878 ± 0.277 (0.288-1.468) which was not significantly different to unity. The pA_2 value for compound BU10119 was 10.08 (9.847-10.310) when determined from the correspondence Schild plot (n = 5-6) after the slope was constrained to 1.

Discussion

Are buprenorphine and its analogs μ-opioid receptor agonists or antagonists ?

Buprenorphine has a high affinity at the μ-opioid receptor (subnanomolar to nanomolar concentrations) and has a wide range of efficacy from a complete antagonist to a partial μ-opioid receptor agonist (0-65% receptor stimulation) *in vitro* across various assay systems (Huang *et al.*, 2001; Kajiwara *et al.*, 1986; Lee *et al.*,

2011; Lutfy *et al.*, 2003b; Spagnolo *et al.*, 2008). This was in line with our findings where in both [^{35}S]GTPγS and rat vas deferens assays, buprenorphine shows high affinity for the μ-opioid receptors, with the binding affinity values of 0.195 ± 0.02 nM and 0.15 nM (0.10-0.23 nM) respectively. In term of efficacy, buprenorphine shows partial efficacy in the [^{35}S]GTPγS assay at the μ-opioid receptor with 33 ± 12% receptor stimulation, obtained from Traynor's lab (Figure 3.2 and Table 3.2). A similar [^{35}S]GTPγS experiment conducted in CHO transfected cells also found buprenorphine to be a potent partial μ-opioid receptor agonist with an EC_{50} of 24.9 ± 14 nM and an E_{max} of 17.7 ± 0.4% (Spagnolo *et al.*, 2008). Further functional experiments conducted in mouse vas deferens have shown that buprenorphine was as potent as nociceptin in inhibiting the electrically evoked contraction, but produced different maximal response, with E_{max} of 63 ± 4% and 92 ± 1% respectively. Although buprenorphine has partial efficacy at both the ORL-1 and μ-opioid receptors, the inhibition seen in mouse vas deferens was believed to be mediated by the μ-opioid receptor (Spagnolo *et al.*, 2008). A different assay system which measures opioid activity through the activation of mitogen-activated protein kinase (MAP kinase) *in vitro* also showed that buprenorphine is a partial agonist, with low efficacy but high affinity at the μ-opioid receptor with an E_{max} of 42.97 ± 4.65% (Lutfy *et al.*, 2003b). However in our assay, conducted in rat vas deferens, buprenorphine did not show any efficacy even at 10 μM (Figure 3.20). This was supported by a previous study where buprenorphine also failed to show any efficacy in the rat vas deferens system when tested at doses ranging from 10 nM-10 μM (Kajiwara *et al.*, 1986). The failure of buprenorphine and its analogues to show any efficacy in rat vas deferens system is related to the lower μ-opioid receptor population in rat vas deferens and therefore a lower capacity of receptor reserve as compared to the other systems. Despite this limitation, in that it is not possible to determine agonist potency of lower efficacy agonists in the rat vas deferens, it can actually be considered as an advantage in our assays since it allows the affinity of buprenorphine at the μ-opioid receptor to be easily measured.

In our assay, buprenorphine was an antagonist at the μ-opioid receptor and caused a parallel rightward shift of the DAMGO control curves (Figure 3.35 (left)) with pA_2 value of 9.782 (9.468-10.100) derived from Schild plot and estimated pA_2 value of 9.837 ± 0.057 calculated using Schild equation. Based on the concentration-response curve constructed in the presence of increasing concentration of

buprenorphine (Figure 3.35 (left)), buprenorphine appeared to behave as a pseudo-irreversible antagonist. Although there is no significant suppression of the maximal response of DAMGO in the presence of buprenorphine, the decreasing pattern visibly observed from the concentration-response curve of DAMGO and the maximum parallel shift at ≥ 3 nM buprenorphine suggest that buprenorphine is not a competitive reversible antagonist at this receptor (Kenakin, 2009). Previous studies conducted in mouse vas deferens have proven buprenorphine to have a slow onset and also difficult removal from the tissue (slow receptor off-set) even after repeated prolonged washing (Kajiwara *et al.*, 1986; Kosterlitz *et al.*, 1975). As a result, there will be fewer μ-opioid receptor site left for the agonist to occupy, which could explain the decreasing in the maximal response of agonist, especially after the tissue was pre-treated with a high concentration of buprenorphine (≥ 3 nM) (Englberger *et al.*, 2006). Kajiwara et al (1986) believed that the difficulties to wash off buprenorphine from the tissues were due to the high lipophilicity of buprenorphine, where buprenorphine was believed to be trapped in the tissue membranes. As reported by Kajiwara (1986), buprenorphine took 2 hours to be completely removed from the mouse vas deferens tissue while it failed to be removed from the guinea pig ileum even after 2 hours washing. Although Kajiwara (1986) has postulated that this incidence was due to the high lipophilicity of buprenorphine, our recent findings with the buprenorphine analogues suggest that besides lipophilicity, there could be other factors that also contribute to the pseudo-irreversibility behaviour of buprenorphine. From our assay, compounds BU10101 (log P = 4.45) and BU10119 (log P = 4.37) were more lipophilic than buprenorphine (log P = 3.99), as shown with the calculated log P value, however were proven to be competitive reversible antagonists in this system (Table 3.12). Moreover, compound BU127 which has similar lipophilicity value with buprenorphine (3.96 and 3.99 respectively), has shown a competitive reversible behaviour in this assay system. It is not surprising that buprenorphine has different antagonist behaviour than its analogue, BU127, since buprenorphine and fentanyl which have similar physicochemical properties (lipophilicity), also were proven to have different receptor kinetics (pharmacodynamics) profiles *in vivo* (Yassen *et al.*, 2005). This suggests that there are other factors that could explain the pseudo-irreversibility behaviour of buprenorphine compared to the rest of the analogues tested at this receptor in this assay system. Based on their chemical structures, buprenorphine has a t-butyl group attached at the C_{20} position of orvinol (Figure 1.3(c)), while BU127 and other analogues tested (BU10101 and BU101119) has a phenyl ring with only one small group attach to the phenyl at most (Figure 2.3 and Figure 3.3). Buprenorphine has

been shown to have a restricted rotation ability about the C_7 and the C_{20} position due to the t-butyl moeity (Loew *et al.*, 1979), compared to other analogues tested. This could theoretically suggest that the chemical structures at this region (C_7,C_{20}) could contribute to the different antagonist behaviour of buprenorphine compared to its analogues, for example by tightly locking buprenorphine to the μ-opioid receptor binding sites once it was bound to the receptors compared to others.

Furthermore, it is interesting to note that although buprenorphine appears to be pseudo-irreversible at the μ-opioid receptor, it is fully reversible at the ORL-1 receptor, in the same tissue. Again, suggesting that the mechanism for its pseudo-irreversible effects at the μ-opioid receptor are by a mechanism other than high lipophilicity.

Similar to the results seen previously in the ORL-1 receptor assays, none of the compounds evaluated (including buprenorphine) show efficacies at the μ-opioid receptors in the rat vas deferens whereas these compounds manage to stimulate the ORL-1 receptor in the [^{35}S]GTPγS as reported by Traynor's lab (2-33% receptor stimulation) (Table 3.2). Again, this is likely to be due to the different receptor reserve in these two assay system.

Structure modification and effects on μ-opioid receptor efficacy

In the current work, our aim was to synthesise buprenorphine analogues with very low partial efficacy or antagonism at the μ-opioid receptor. Based on Traynor's results, replacing the aliphatic alkyl group (as in buprenorphine) with a simple aromatic substituent at the C_{20} position of the orvinol has decreased the efficacy of analogues at the μ-opioid receptor compared to the parent drug, buprenorphine. This can be seen in compound BU127, BU08026, BU11001 and BU10119 (Figure 3.40).

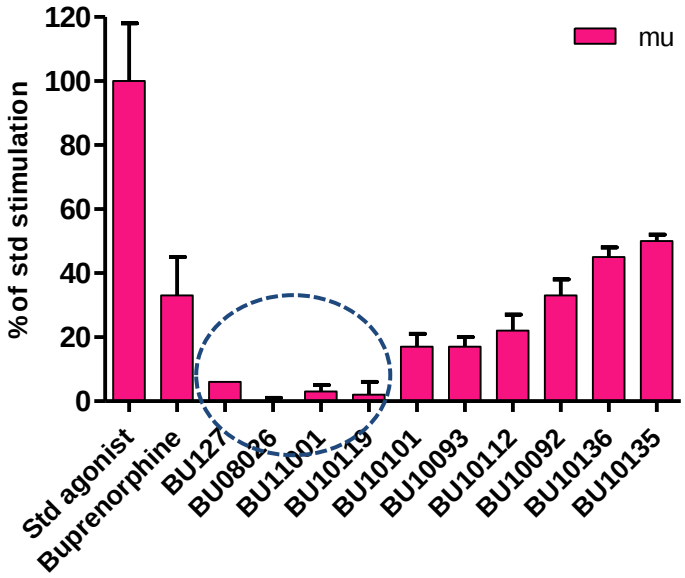

Figure 3.40: [^{35}S]GTPγS efficacy screening of buprenorphine and its analogues performed in C6 glioma transfected cells. Efficacies of buprenorphine and its analogues at 10 μM were compared against the standard μ-opioid receptor agonist (DAMGO) in triplicate. BU127, BU08026, BU11001 and BU10119 (marked in blue) shows significantly lower efficacy at the μ-opioid receptor compared to the rest of the orvinol series (Traynor (unpublished work)).

However, unlike the ORL-1 receptor, introducing a small group on the aromatic substituent appears to increase the efficacy of analogues at the μ-opioid receptor (BU10101, BU10093, BU10112, BU10092 and BU10136 and BU10135). These effects in increasing the μ-opioid receptor efficacy were most obviously seen when a small group was attached at the furthest position on the aromatic substituent as can be seen in compounds BU10136 and BU10135. Compound BU10136 has a chloro attached to the 5-position of the thiophene substituent, while compound BU10135 has a methyl group attached at para position of the phenyl substituent. The smallest effects were seen in compounds BU10101, BU10093 and BU10112 when a small group was attached at the 2-position of the thiophene (BU10093) or at the ortho position of the phenyl substituent (BU10101 and BU10112). The size of the aromatic system (5/6 members ring) does not influence the analogues efficacy at the μ-opioid receptor as was seen previously at the ORL-1 receptor.

Affecting antagonist potency of compounds at the μ-opioid receptor

The binding affinity (K_B) obtained for naltrexone was 1.26 nM (0.74-2.16 nM) which was similar to the value previously reported using the same assay system in Wistar rats (0.91 ± 0.10 nM) (Al-Khrasani *et al.*, 2007). The K_B value for naltrexone at the μ-opioid receptor derived from this functional assay was also close to the binding affinity (K_i) obtained from the receptor binding assays performed in mouse brain which were 1.26 nM (0.74-2.16 nM) and 2.57 ± 0.48 nM respectively (Uwai *et al.*, 2004).

All of the compounds evaluated were found to be at least 2 times more potent than naltrexone, the standard μ-opioid receptor antagonist used in this assay. Out of all the buprenorphine analogues analyzed at this receptor, only compound BU127 showed a significantly higher potency compared to buprenorphine with pA_2 value of 10.33 (10.17-10.50) and 9.814 (9.631-9.995) respectively. Compared to BU127, the introduction of a methyl group at the ortho position of the phenyl substituent (BU10101) has decreased the potency towards the μ-opioid receptor almost 3-fold, with the comparative pA_2 value of 10.33 (10.17-10.50) and 9.846 (9.664-10.050) respectively (Table 3.12). From the rat vas deferens assay, it was also found that the presence of a methyl at C_7 position of the orvinol did not affect the potency of this orvinol series towards the μ-opioid receptor as was seen at the ORL-1 receptor. There was no evidence to suggest any relation between the lipophilicity of the compound and their antagonistic behaviour at the μ-opioid receptor in rat vas deferens (Table 3.12). All analogues evaluated at the μ-opioid receptor in this system displayed competitive reversible behaviour, except for the parent drug buprenorphine.

The summary of the results are presented in Table 3.12.

Compound	pA_2	K_B (nM)	Log P	Potency vs. Buprenorphine	Antagonist Behaviour
Naltrexone 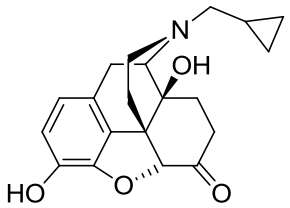	8.898 (8.665-9.131)	1.26 (0.74-2.16)	0.82	0.1	Competitive reversible
Buprenorphine 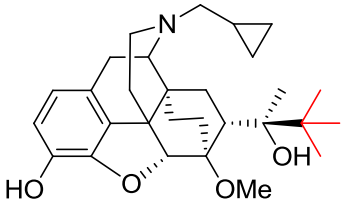	9.782 (9.468-10.100) or 9.837 ± 0.057	0.15 (0.10-0.23) or 0.15 (0.13-0.17)	3.99	1	Pseudo-irreversible
BU127 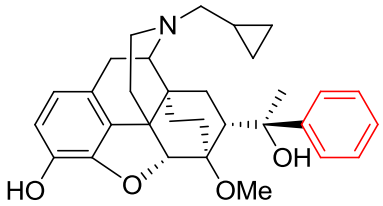	10.33 (10.17-10.50)	0.047 (0.032-0.068)	3.96	3.3	Competitive reversible

BU10101 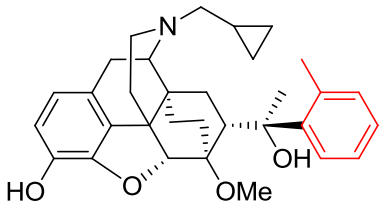	9.846 (9.644-10.050)	0.14 (0.089-0.23)	4.45	1.1	Competitive reversible
BU10119 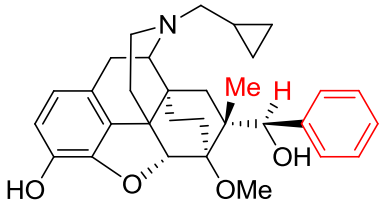	10.08 (9.847-10.310)	0.083 (0.049-0.14)	4.37	1.8	Competitive reversible

Table 3.12: Summary of μ-opioid receptor assays conducted in rat vas deferens.

3.4.5.3 κ-opioid receptor mouse vas deferens assays

While the previous two assays were performed in rat vas deferens, mouse vas deferens was used to evaluate the compounds functional activity at the κ-opioid receptors. Buprenorphine and two of its analogues (BU127 and BU10119) were evaluated against U-69593, a selective κ-opioid receptor agonist. Since this was the final assay used, the selection of buprenorphine analogues to be evaluated were based on their successful profile at all opioid receptors shown during the [^{35}S]GTPγS initial efficacy screening (Figure 3.2), especially at the κ-opioid receptors. BU127 was included since this compound is the lead in this project.

The potency of buprenorphine and its analogues at the κ-opioid receptor were compared against norbinaltorphimine (nor-BNI), a selective κ-opioid receptor antagonist. In guinea pig brain membranes, nor-BNI is about 150-fold more selective at κ-opioid receptor compared to μ- and δ-opioid receptors with binding affinities (K_i) of 0.28 ± 0.07 nM, 47.2 ± 3.3 nM and 42.9 ± 11.0 nM respectively (Takemori *et al.*, 1988).

Due to the reasons mentioned previously in the methods section, we decided to use just one antagonist concentration per tissue. The Schild equation (single concentration method) was used to determine the pA_2 value of the test compounds. The disadvantage of performing assays using only one single concentration of antagonist was that it only gave an empirical estimation of the potency (pA_2) and affinity constant (K_B). The antagonist behaviour of the test compounds (eg: whether the antagonist is competitive or pseudo-irreversible) also cannot be determined. Therefore, we only aimed to compare the potency of the analogues to buprenorphine through this assay.

As previously mentioned, all tissues were pre-incubated with 1 μM CTAP (a selective μ-opioid receptor antagonist) 15 minutes before U-69593 or test compounds were administered in order to standardize the experimental protocol.

Results

nor-BNI

Nor-BNI at 1 μM concentration has been previously reported to cause a slight inhibition of the electrically evoked contraction in mouse vas deferens with E_{max} of 16 ± 6% (Portoghese *et al.*, 1987). The receptor mediating the agonist response observed in the mouse vas deferens tissue was not discussed in this paper. However, in our experiment, nor-BNI did not show any efficacy in the mouse vas deferens even at 10 μM (Figure 3.41).

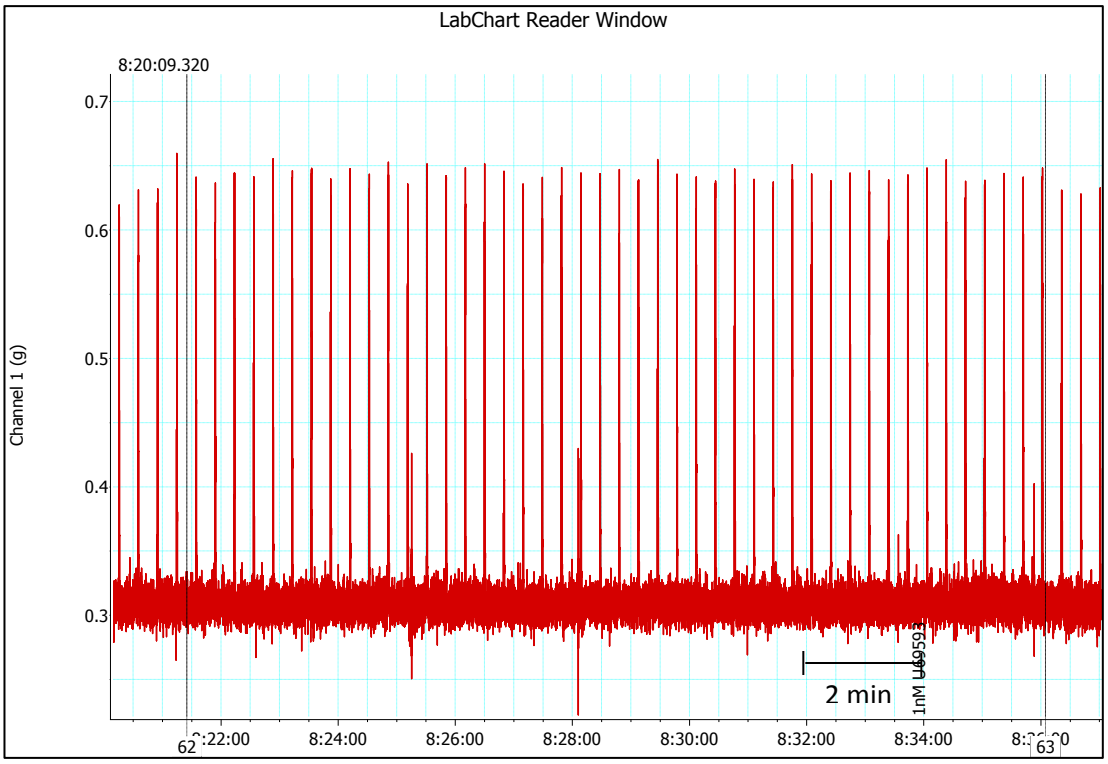

Figure 3.41: Effects of nor-BNI (10 μM) on electrically evoked contractions of mouse vas deferens.

.

1 μM CTAP was used to block any μ-opioid agonist mediated activity of the compounds evaluated. A previous study has shown that although CTAP is a μ-opioid selective antagonist, at 10 μM concentration it has ability to significantly block the κ-opioid agonist activity (κ_2-opioid receptor subtype) of U-69593 at 10 μM concentration (Heyliger *et al.*, 1999). However this study, conducted using [^{35}S]GTPγS binding technique performed in guinea pig caudate membranes, also proved that at a 1 μM concentration CTAP did not reduce the efficacy of U-69593 at the κ-opioid receptor.

The trace obtained with 10 μM nor-BNI in the presence of 1 μM CTAP is shown in Figure 3.42.

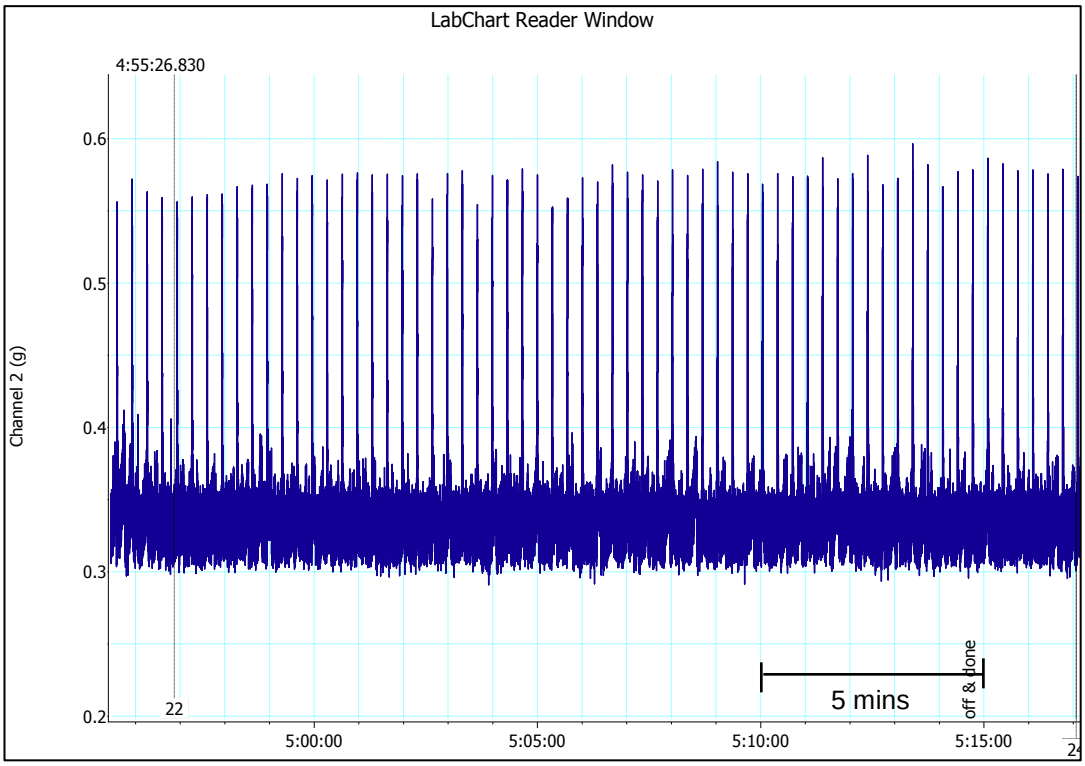

Figure 3.42: Effects of nor-BNI (10 μM) in the presence of CTAP (1 μM) on electrically evoked contractions of mouse vas deferens.

Concentration-response curves of U-69593 (1 nM-3 μM) were constructed in the absence and in the presence of single concentrations of nor-BNI (Figure 3.43).

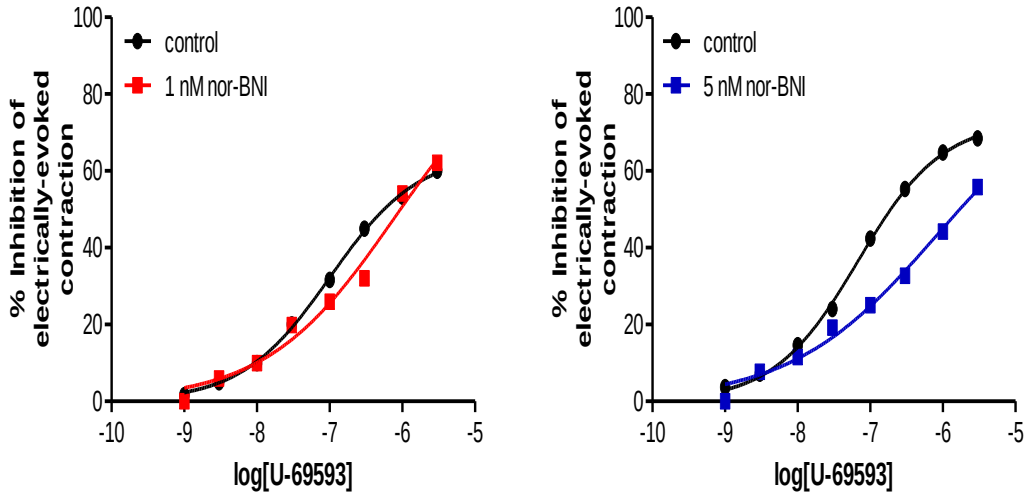

Figure 3.43: Electrically evoked contractions of mouse vas deferens. Concentration-response curve to U-69593 obtained in the absence and in the presence of 1 nM nor-BNI (left) and 5 nM nor-BNI (right). Points represent means from two separate experiments.

An individual pA_2 was calculated for each set of experiments (n = 4) and gave the average value of 9.545 ± 0.123 (9.155-9.935).

Buprenorphine

A previous study has shown that buprenorphine inhibits the electrically evoked contraction of mouse vas deferens at a concentration ≥ 1 µM, which is shown to be µ-opioid receptor mediated (Spagnolo *et al.*, 2008). Therefore, instead of testing the effects of buprenorphine alone in this tissue, we decided to directly block any µ-opioid receptor mediated efficacy of buprenorphine in this assay by pre-incubating the tissue with the selective µ-opioid receptor antagonist, CTAP (Heyliger *et al.*, 1999), in order to more accurately determine the affinity of buprenorphine at the κ-opioid receptor.

A 10 µM concentration of buprenorphine (in the presence of 1 µM CTAP) does not inhibit electrically evoked contraction of the mouse vas deferens, which confirmed buprenorphine has no efficacy at the κ-opioid receptors in this system up to 10 µM.

1 μM CTAP sufficiently blocked any μ-opioid agonist mediated response induced by buprenorphine (Figure 3.44).

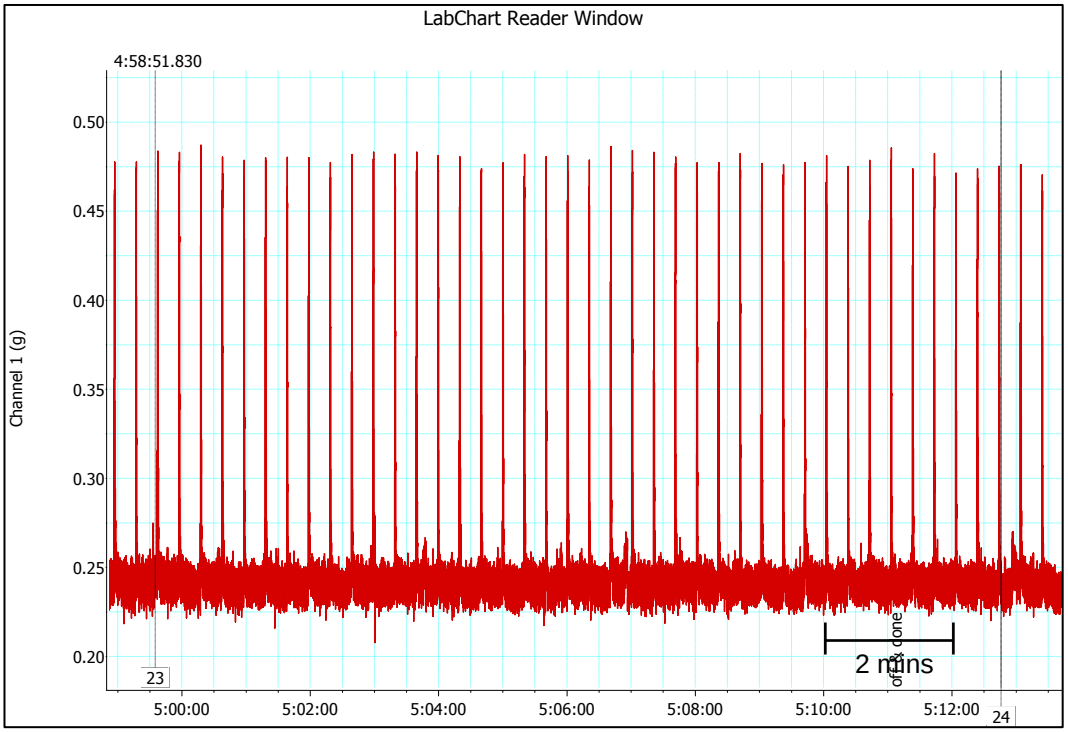

Figure 3.44: Effects of buprenorphine (10 μM) in the presence of CTAP (1 μM) on electrically evoked contractions of mouse vas deferens.

The functional assays conducted for buprenorphine (n = 6) gave the average pA_2 value of 9.245 ± 0.105 (8.975-9.515). The concentration-response curves in the presence and in the absence of buprenorphine are presented in Figure 3.45 as follows:

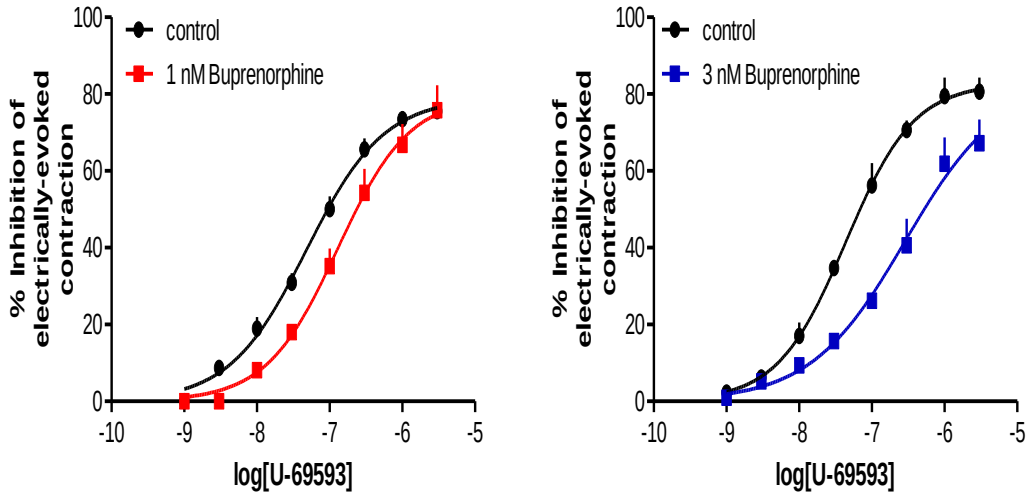

Figure 3.45: Electrically evoked contractions of mouse vas deferens. Concentration-response curve to U-69593 obtained in the absence and in the presence of 1 nM buprenorphine (left) and 3 nM buprenorphine (right). Points represent means, and vertical lines represent S.E.M. of three experiments.

There is no significant decrease in the maximal response and hill slope of the agonist concentration-response curve in the presence of buprenorphine at both concentrations, which at this point suggests that buprenorphine might be a competitive antagonist. However, it is important to highlight that the single concentration method cannot be used to estimate the antagonist behaviour of the compound (Kenakin, 2009). In addition, the single concentration method assumes that the antagonist is competitive and the equilibrium between the agonist, antagonist and the receptors has been achieved (Leslie, 1987).

Both the lack of activity of 10 μM buprenorphine (in the presence of 1 μM CTAP) and also the parallel rightward shift of U-69593 concentration-response curves in the presence of buprenorphine (pre-incubated with 1 μM CTAP) (Figure 3.45) demonstrated that buprenorphine acts as a κ-opioid receptor antagonist in mouse vas deferens.

BU127

Similar to buprenorphine, in order to standardize the assay protocol, the tissue was directly pre-incubated with CTAP without testing the effects of BU127 alone in the tissue. A 10 μM loading concentration of BU127 (in the presence of 1 μM CTAP) did not inhibit the electrically evoked contraction of mouse vas deferens, which confirmed BU127 has no κ-opioid receptor efficacy in this system up to 10 μM (Figure 3.46). However a slight increase in the amplitude of baseline twitches (33%) was detected after 2 minutes of BU127 administration. The reason for this elevation was still unclear. There is the possibility that BU127 might be an inverse agonist, but in order to ensure this possibility, an extensive investigation needs to be done (Cruz *et al.*, 1996). An 'inverse agonist' refer to a compound that is able to spontaneously formed a new receptor active sites once it is bound to the receptors (Kenakin, 2009). An inverse agonist compound will have a higher binding affinity towards an inactive receptor site compared to the active receptor sites, thus cause opposite response of the agonist (de Ligt *et al.*, 2000). Since the baseline twitch was unaffected in the presence of lower concentration of BU127 (1 nM) that was used in this assay (Figure 3.47), no further investigation is done for compound BU127 to establish its inverse agonism activity.

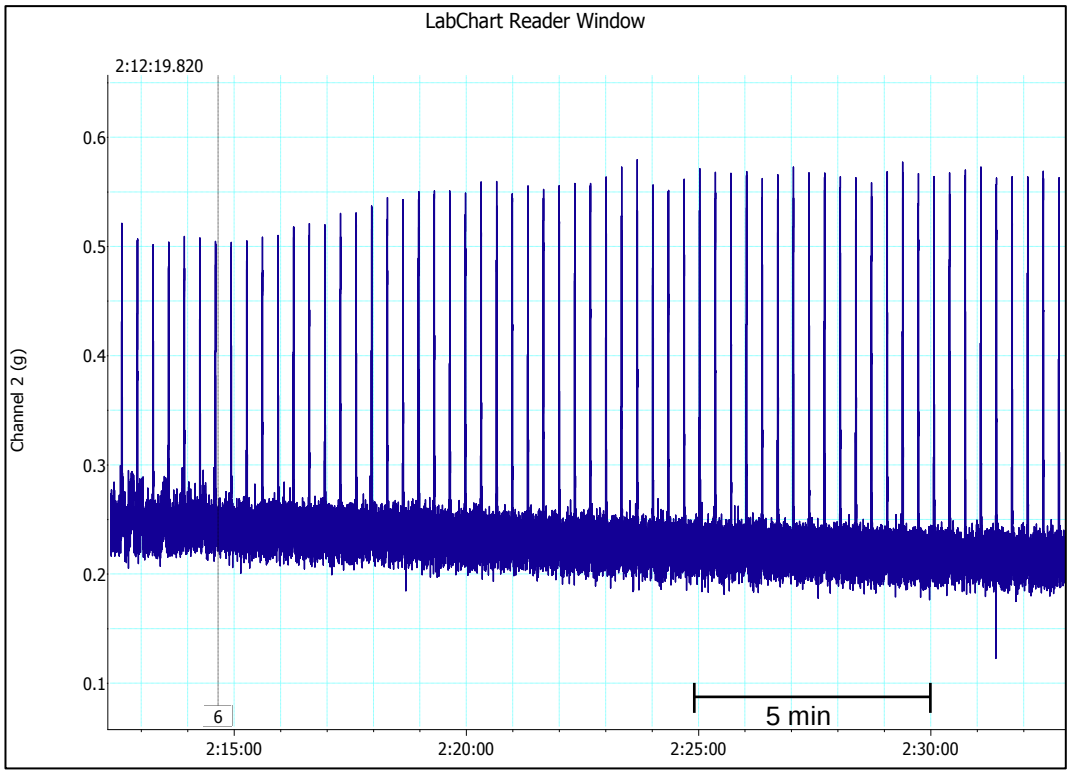

Figure 3.46: Effects of BU127 (10 μM) in the presence of CTAP (1 μM) on electrically evoked contractions of mouse vas deferens.

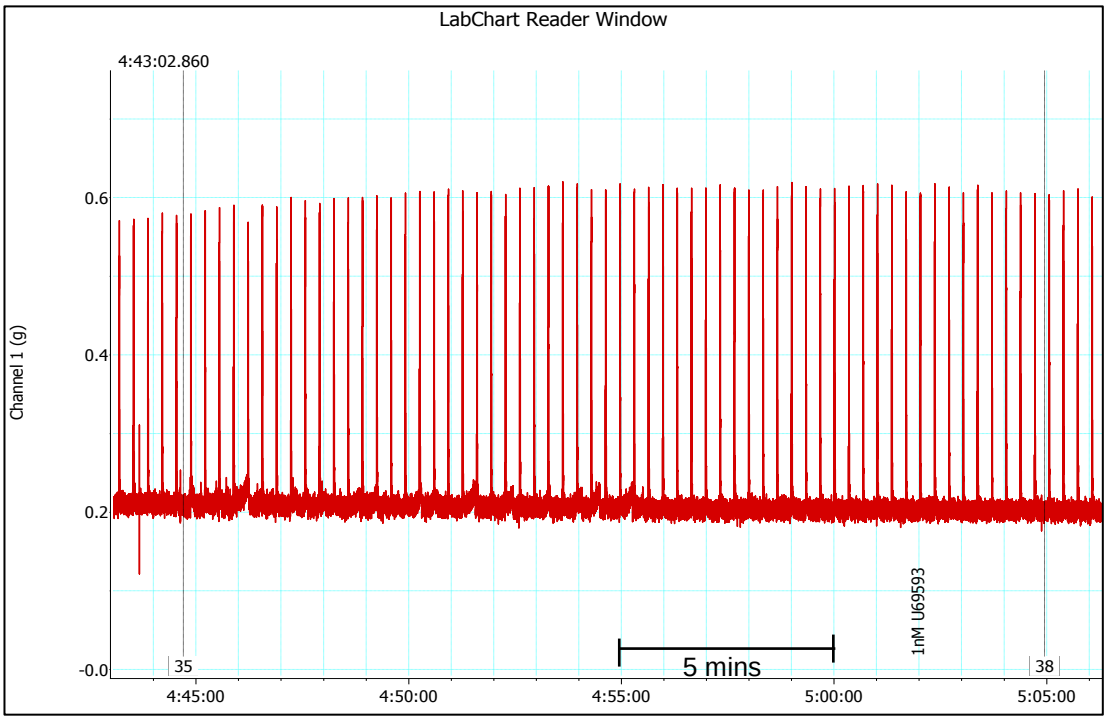

Figure 3.47: Effects of BU127 (1 nM) in the presence of CTAP (1 μM) on electrically evoked contractions of mouse vas deferens.

An individual concentration-response curve of U-69593 in the presence of various concentrations of compound BU127 (n = 5) caused a parallel rightward shift of the control curve as low as at 0.5nM BU127. The graphs as shown in Figure 3.48:

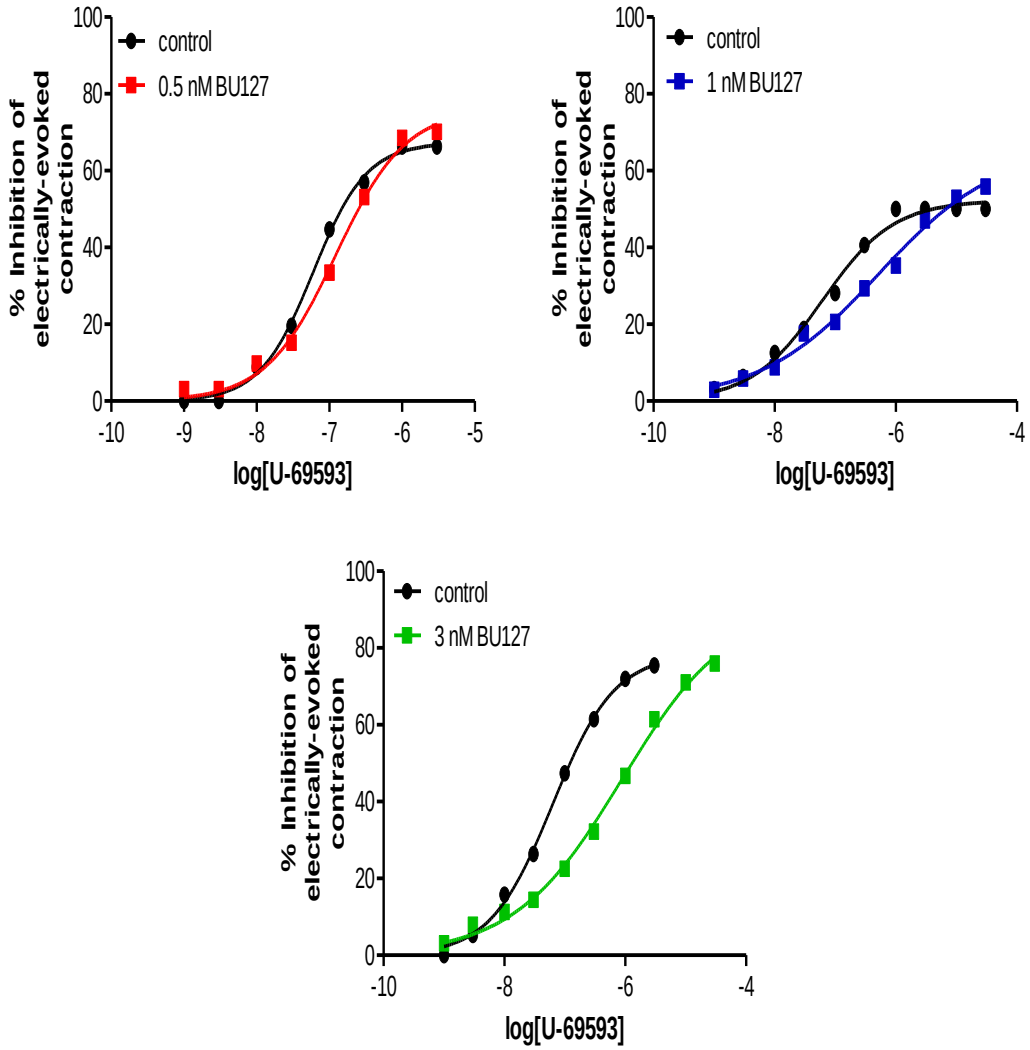

Figure 3.48: Electrically evoked contractions of mouse vas deferens. Concentration-response curve to U-69593 obtained in the absence and in the presence of 0.5 nM BU127 (top, left), 1 nM BU127 (top, right) and 3nM BU127 (bottom). Points represent means from two separate experiments (except only one experiment at 1 nM BU127).

Using the Schild equation (single concentration method), the average pA_2 value calculated for compound BU127 was 9.591 ± 0.086 (9.317-9.865). Both the lack of apparent agonist activity of 10 µM BU127 (in the presence of 1 µM CTAP) and also

the parallel rightward shift of U-69593 concentration-response curves in the presence of BU127 (pre-incubated with 1 µM CTAP) (Figure 3.48) demonstrated that BU127 acts as a κ-opioid receptor antagonist in mouse vas deferens.

BU10119

A 10 µM concentration of BU10119 (in the presence of 1 µM CTAP) did not inhibit the electrically evoked contraction of mouse vas deferens, which confirmed BU10119 has no efficacy in this system at least up to 10 µM (Figure 3.49). Similar to compound BU127, a slight increase (13%) of baseline twitches was also detected after 2 minutes of BU10119 administration. However, no baseline elevation was detected when lower concentration of BU10119 (0.5 nM) was used (Figure 3.50).

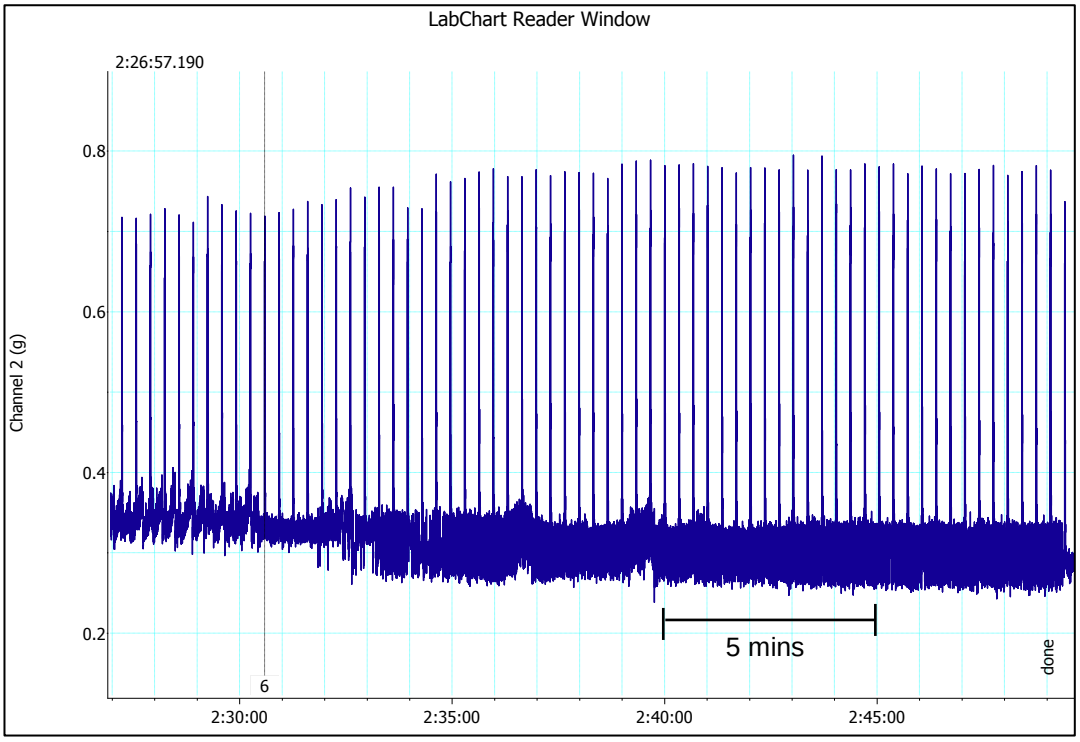

Figure 3.49: Effects of BU10119 (10 µM) in the presence of CTAP (1 µM) on electrically evoked contractions of mouse vas deferens.

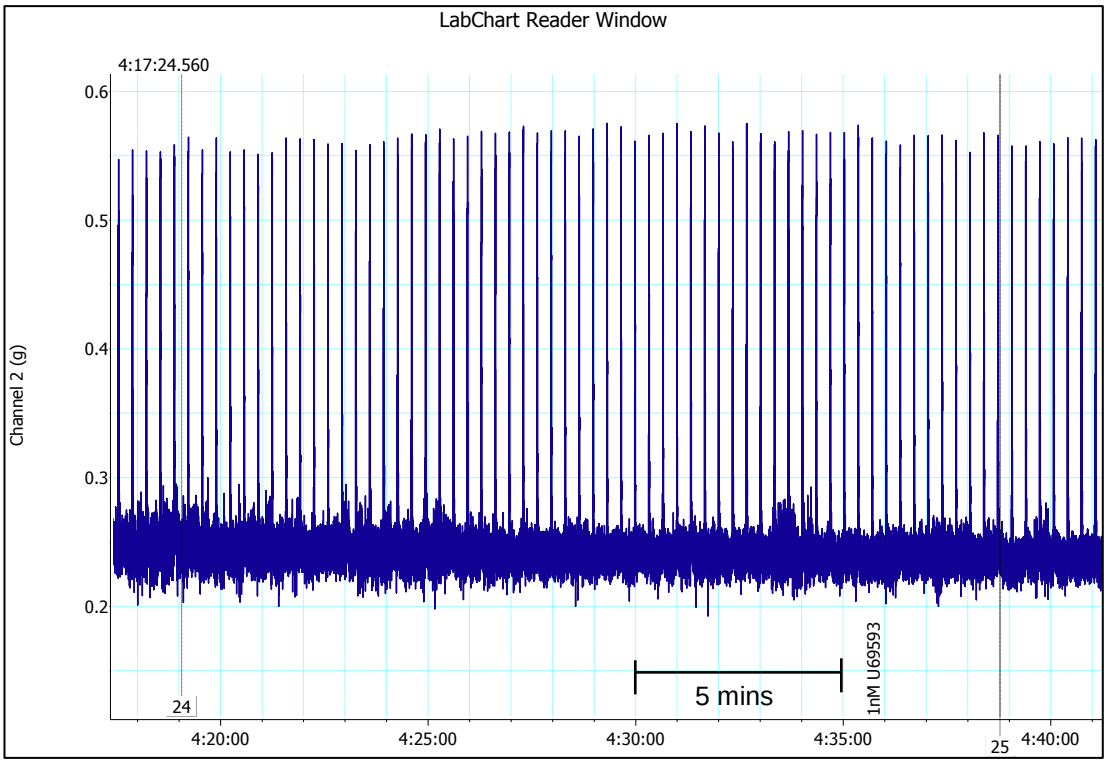

Figure 3.50: Effects of BU10119 (0.5 nM) in the presence of CTAP (1 μM) on electrically evoked contractions of mouse vas deferens.

Five individual experiments using the various concentrations of compound BU10119 between 0.1-3 nM were conducted in order to estimate the pA_2 value of this compound (Figure 3.51).

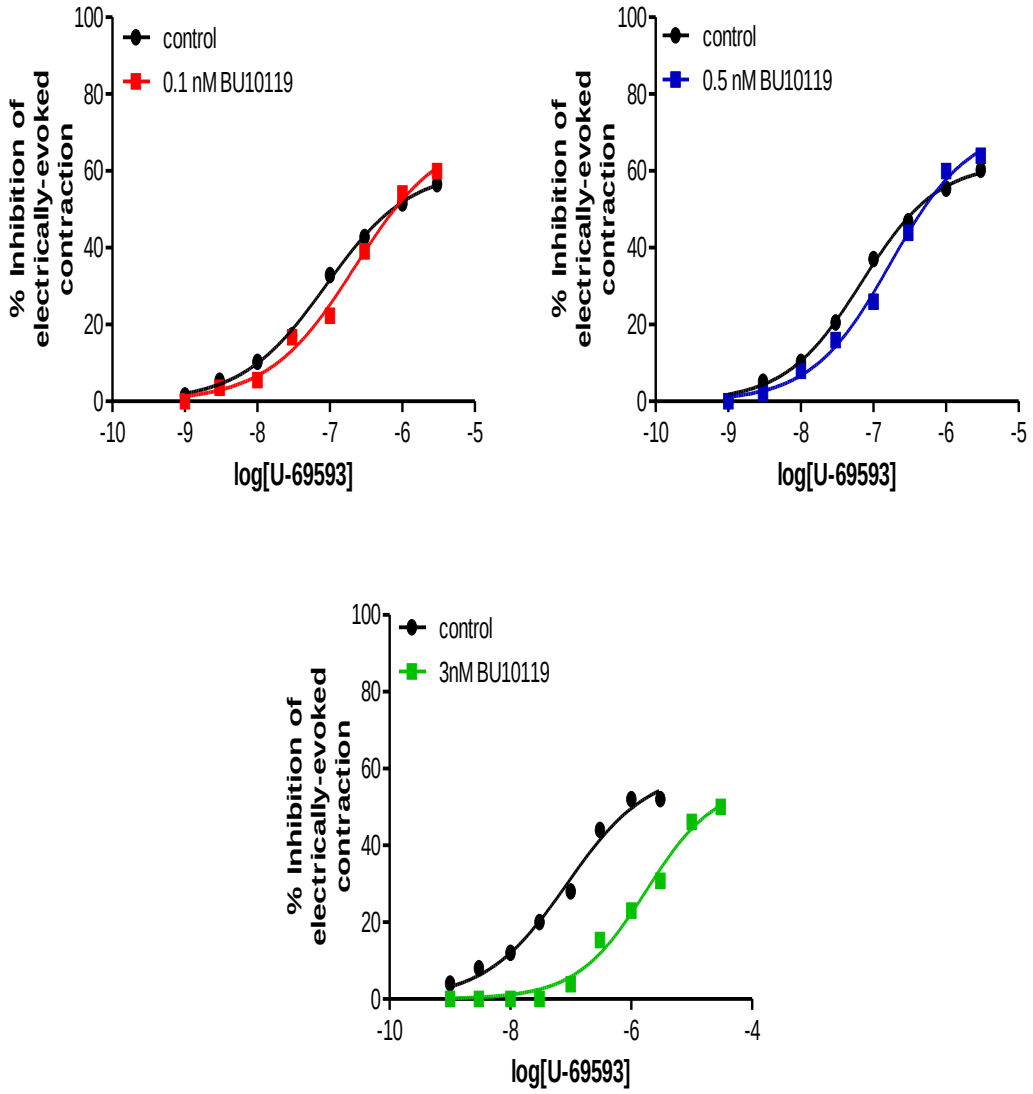

Figure 3.51: Electrically evoked contractions of mouse vas deferens. Concentration-response curve to U-69593 obtained in the absence and in the presence of 0.1 nM BU10119 (top, left), 0.5 nM BU10119 (top, right) and 3 nM BU10119 (bottom). Points represent means from two separate experiments (except only one experiment at 3 nM BU10119).

From these assays, compound BU10119 was found to have an average pA_2 value of 9.831 ± 0.235 (9.084-10.58), calculated using the Schild equation (single concentration method). Both the lack of activity of 10 µM BU10119 (in the presence of 1 µM CTAP) and also the parallel rightward shift of U-69593 concentration-response curves in the presence of BU10119 (pre-incubated with 1 µM CTAP) (Figure 3.51) demonstrated that BU10119 acts as a κ-opioid receptor antagonist in mouse vas deferens.

Discussion

An individual pA_2 value for nor-BNI was calculated from each set of experiments giving the average pA_2 value of 9.545 ± 0.123 (9.155-9.935). The potency of nor-BNI at the κ-opioid receptor estimated from our mouse vas deferens assay using the Schild equation (single concentration method) (0.29 nM (0.12-0.70 nM)) was similar to the value reported from a radioligand binding assay conducted using guinea pig brain membranes (0.28 ± 0.07 nM) (Takemori *et al.*, 1988). Other studies have reported a slightly higher binding affinity of nor-BNI in their assay systems. For example, a previous study conducted in the [^{35}S]GTPγS binding assay using guinea pig caudate membranes has reported a higher binding affinity of nor-BNI (K_i = 0.03 nM) (Heyliger *et al.*, 1999). This was similar to the value reported by the other study performed in the mouse vas deferens using a single antagonist concentration per tissue, which estimates the potency of nor-BNI to be 0.06 ± 0.02 nM (Bell *et al.*, 1998). However, the differences were only about 5-fold compared to the values obtained from our experiments and the study conducted by Takemori (1998) which were in the subnanomolar range.

Buprenorphine was proven to be a κ-opioid receptor antagonist in the mouse vas deferens assay with an estimated potency (pA_2) of 9.245 ± 0.105 (8.975-9.515) (Figure 3.45). From Traynor's [^{35}S]GTPγS initial efficacy screening, 10 μM buprenorphine totally failed to stimulate the κ-opioid receptor in this system (% stimulation = -12 ± 9%). Traynor's result was in line with the previous published data, where buprenorphine also failed to stimulate the κ-opioid receptor at < 10 μM (Spagnolo *et al.*, 2008). A subnanomolar to nanomolar potency of the buprenorphine at the κ-opioid receptor predicted from our assay (0.57 nM (0.31-1.06 nM)) was not much different from buprenorphine binding affinity (K_i) that has been previously reported which (between 0.11-1.5 nM), conducted in CHO transfected cells stably expressing the κ-opioid receptor (Huang *et al.*, 2001; Spagnolo *et al.*, 2008; Toll *et al.*, 1998). While most of the studies have confirmed the non-existence of κ-opioid receptor efficacy mediated by buprenorphine, Huang et al (2001) have reported otherwise. Through [^{35}S]GTPγS binding assays using similar cell lines, (-)-buprenorphine was reported to produce 10 ± 4% maximal response with an EC_{50}

value of 0.04 ± 0.01 nM, while no stimulation was reported when (+)-buprenorphine was tested (Huang *et al.*, 2001). From this study, Huang et al (2001) concluded buprenorphine behaves as a pure antagonist to low partial agonist at the κ-opioid receptor.

Structure modification and effects on κ-opioid receptor efficacy

For this receptor, our aim was to synthesise buprenorphine analogues that have no efficacy (antagonist) at the κ-opioid receptor. Together, with having efficacy at ORL-1 receptor, κ-opioid receptor antagonism may hold the major key in preventing relapse to drug addiction as mentioned earlier in this thesis as evidenced through buprenorphine/naltrexone combination therapy (Spagnolo *et al.*, 2008). Unfortunately, as can be seen from Traynor's initial screening, the majority of the buprenorphine analogues show full efficacy at κ-opioid receptor with > 80% receptor stimulation (Figure 3.52).

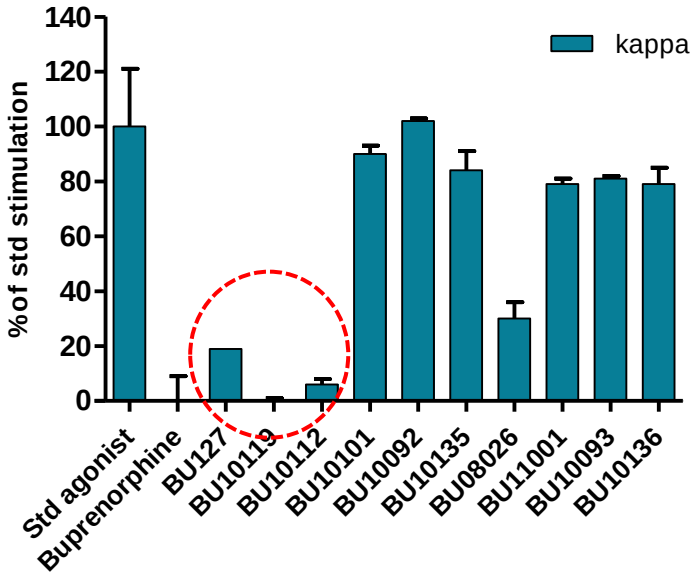

Figure 3.52: [^{35}S]GTPγS efficacy screening of buprenorphine and its analogues performed in chinese hamster ovarian (CHO) transfected cells. Efficacies of buprenorphine and its analogues at 10 μM were compared against a standard κ-opioid receptor agonist (U-69593) in triplicate. BU127, BU10119, and BU10112 (marked in red) shows significantly lower efficacy at the κ-opioid receptor compared to the rest of the orvinol series (Traynor (unpublished work)).

Only compounds BU10119 and BU10112 have met the desired profile at the κ-opioid receptor with almost no receptor stimulation for BU10119 (0 ± 1% stimulation) and 6 ± 2% stimulation (BU10119). Compound BU127 can also be considered as having a potential profile at the κ-opioid receptor with a comparatively low receptor stimulation (19 ± 0 %) in the [^{35}S]GTPγS assay compared to the majority of the analogues synthesised. From this initial efficacy screening, few modifications seem to efficiently sustain buprenorphine analogues profile at the κ-opioid receptor as seen in the parent drug, buprenorphine. The presence of a methyl group at the C_7 position of orvinol has maintained the κ-opioid antagonistic profile of compounds BU10119 and BU10112. For example, compound BU10119 which is an analogue of BU127; both have a simple phenyl substituent group attach to the C_{20} position of the orvinol. However, it is suggested that compound BU10119 has zero efficacy at the κ-opioid receptor due to the presence of a methyl group at the C_7 position, as compared to a proton at this position in BU127. Another example is compound BU10112 which is an analogue of BU10101. Both have a methyl group

attached at the ortho position of the phenyl substituent at the C_{20} position of the orvinol. Based on Figure 3.52, compound BU10112 only shows 6 ± 2% stimulation at the κ-opioid receptor compared to compound BU10101 which highly stimulates the κ-opioid receptor in this system (90 ± 3%). Although compound BU10112 has an unsaturated bridge at C_{18}-C_{19} in the morphinan ring, the ability of this compound to display antagonistic properties at the κ-opioid receptor is believed to be due to the presence of a methyl group at the C_7 position. On the other hand, introducing a small aromatic system seems to be unhelpful in optimizing the analogue's profile at the κ-opioid receptor as can be seen with compound BU08026 (2-thiophene). Moreover, relocating sulphur from 2-thiophene to 3-thiophene seems to drastically increase the efficacy from a partial to a full κ-opioid receptor agonist. Therefore the thiophene substituent was not ideal at this receptor. Since only a few analogues were evaluated at this receptor, the structure activity relationships being developed are only preliminary.

Affecting antagonist potency of compounds at the κ-opioid receptor

In terms of potency, there is little difference between buprenorphine and the analogues evaluated at the κ-opioid receptor in mouse vas deferens, suggesting that neither the modification at C_7 nor C_{20} of orvinols had significant impact on buprenorphine's potency at the κ-opioid receptor.

The summary of the findings are shown in Table 3.13.

Compound	pA_2	K_B (nM)	Log P	Potency vs. Buprenorphine
nor-BNI 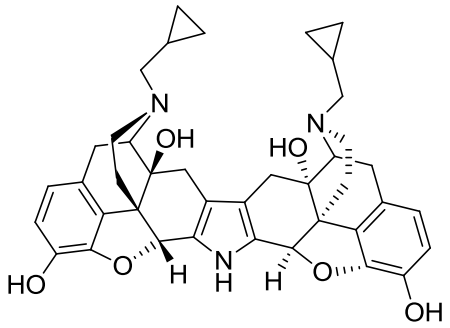	9.545 ± 0.123 (9.155-9.935)	0.29 (0.21-0.38)	N.D	2
Buprenorphine 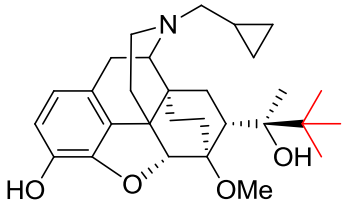	9.245 ± 0.105 (8.975-9.515)	0.57 (0.31-1.06)	3.99	1
BU127 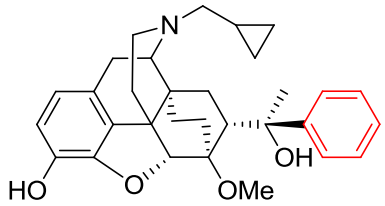	9.591 ± 0.086 (9.317-9.865)	0.26 (0.14-0.48)	3.96	2.2

BU10119 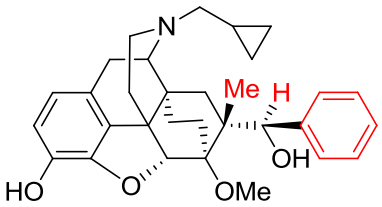	9.831 ± 0.235 (9.084-10.58)	0.15 (0.026-0.82)	4.37	3.9

Table 3.13: Summary of κ-opioid receptor assays conducted in mouse vas deferens.

CHAPTER 4.0: CONCLUSION

Compounds	Profiles	Opioid receptors			Relative potency to buprenorphine			Antagonist behaviour (Reversibility)	
		ORL-1	μ	κ	ORL-1	μ	κ	ORL-1	μ
Buprenorphine	[^{35}S]GTPγS efficacy	24 ± 9*	33 ± 12*	-12 ± 9*					
	pA_2	5.976	9.782 or 9.837 ± 0.057	9.245 ± 0.105	1	1	1	*C*	*P*
	Binding affinity, K_B (nM)	1056.8	0.15	0.57					
BU127	[^{35}S]GTPγS efficacy	14 ± 4*	6 ± 0*	19 ± 0*					
	pA_2	5.884 ± 0.108	10.33	9.591 ± 0.086	0.8	3.3	2.2	*C*	*C*
	Binding affinity, K_B (nM)	1305.9	0.047	0.26					
BU10101	[^{35}S]GTPγS efficacy	45 ± 4*	17 ± 4*	90 ± 3*					
	pA_2	5.872 ± 0.180	9.846	*n.d*	0.8	1.1	*n.d*	*P*	*C*
	Binding affinity, K_B (nM)	1342.8	0.14	*n.d*					
BU10119	[^{35}S]GTPγS efficacy	57 ± 5*	2 ± 4*	-2 ± 1*					
	pA_2	5.745	10.08	9.831 ± 0.235	0.6	1.8	3.9	*C*	*C*
	Binding affinity, K_B (nM)	1762.0	0.083	0.15					
BU10136	[^{35}S]GTPγS efficacy	31 ± 4*	45 ± 3*	79 ± 6*					
	pA_2	6.140	*n.d*	*n.d*	1.5	*n.d*	*n.d*	*P*	*n.d*
	Binding affinity, K_B (nM)	724.4	*n.d*	*n.d*					
BU10112	[^{35}S]GTPγS efficacy	43 ± 3*	22 ± 5*	6 ± 2*					
	pA_2	5.539	*n.d*	*n.d*	0.4	*n.d*	*n.d*	*C*	*n.d*
	Binding affinity, K_B (nM)	2890.7	*n.d*	*n.d*					

Table 4.1: Pharmacological profiles ([^{35}S]GTPγS binding (Traynor (unpublished work))*, potency (pA_2) and binding affinity (K_B) of all compounds evaluated in the vas deferens tissues (RVD (ORL-1 and μ) and MVD (κ)); *n.d*, not determined; *C*, Competitive reversible; *P* = Pseudo-irreversible.

The difference in kinetics observed with buprenorphine at different opioid receptor types (ORL-1 and μ-opioid receptors) within the same strain was an interesting finding. Unfortunately, buprenorphine antagonist behaviour at the κ-opioid receptor cannot be determined since the assay on this tissue was based on the single concentration method. However, it has recently been shown that buprenorphine's activity at the κ-opioid receptors *in vivo* is of much shorter duration than at the μ-opioid receptors (Paronis *et al.*, 2011). In the rat vas deferens assays, buprenorphine was a competitive reversible antagonist at the ORL-1 receptor, but a pseudo-irreversible antagonist at the μ-opioid receptors. The pseudo-irreversibility of buprenorphine *in vitro* and *in vivo* has been widely published, and is related to its slow receptor off-rate (slow receptor dissociation) once it is bound to the receptors (Boas *et al.*, 1985; Kajiwara *et al.*, 1986; Kosterlitz *et al.*, 1975). However in previous work, the focus was towards the μ-opioid receptor kinetics, whereas no work has been done to determine its ORL-1 receptor reversibility.

It is not unusual for a compound to have different receptor kinetics at different receptor types. Previous studies have shown that an analogue of buprenorphine, BU74 (a full κ-opioid receptor agonist, partial δ–opioid receptor agonist and μ-opioid receptor antagonist), has different receptor kinetics at the κ- and δ-opioid receptors in isolated tissues (Husbands *et al.*, 2005). The κ-agonist activity of BU74 could not be reversed by nor-BNI (a selective κ-opioid receptor antagonist) or with a repeated prolonged washing in GPI, but was reversible by naltrindole (δ-opioid receptor antagonist) in the mouse vas deferens, suggesting the different receptor kinetics of BU74 at different opioid receptors. It is, however, still debatable since these assays were conducted in different species whether variability of the tissue environment could be a contributing factor (Kajiwara *et al.*, 1986).

In this project, seven orvinols related to the lead BU127 had been successfully synthesised by using the standard techniques for orvinol synthesis with one significant improvement being the use of ethyl acetate as a solvent in the catalytic hydrogenation. The aim of this project is to find a single compound (buprenorphine analogue), having a similar profile as seen with the buprenorphine/naltrexone combination (Gerra *et al.*, 2006; Rothman *et al.*, 2000). This profile has been

suggested to be an ideal pharmacological profile for relapse prevention to drug taking, including as a potential intervention for polydrug abuse (McCann, 2008). The intended profiles for these analogues are antagonist / very low efficacy for the μ-opioid receptor, partial efficacy at the ORL-1 receptor and antagonist at the κ-opioid receptor.

Although only the analogues with the general structure A (Figure 4.1) were synthesised in this project, a few analogues from Husbands' group with the general structure B (Figure 4.1) were also selected for evaluation in this project due to their interesting profiles seen during an initial [^{35}S]GTPγS efficacy screen (Figure 4.2). Particularly interesting was their κ-efficacy (relatively lower κ-efficacy compared to analogues with general structure A).

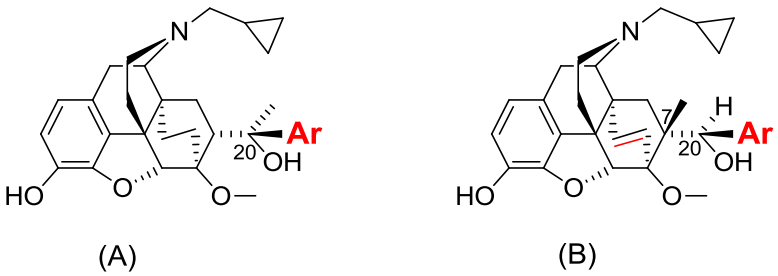

Figure 4.1: Orvinol series with general structure (A) and (B) (Ar = aromatic substituent).

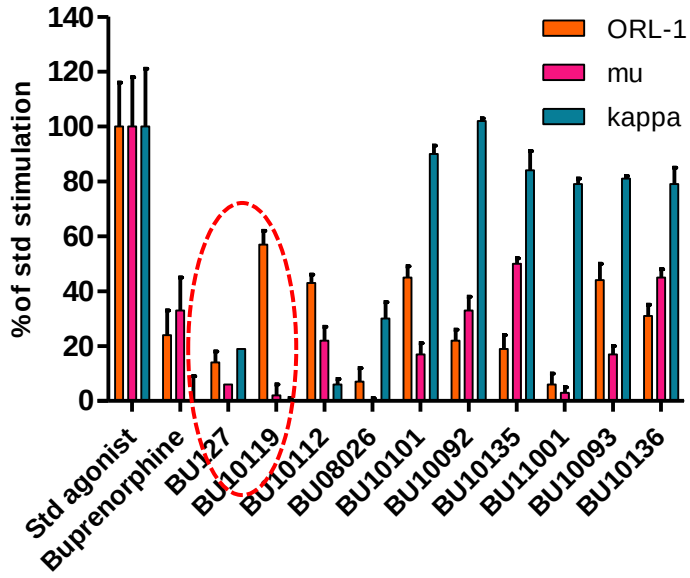

Figure 4.2: [^{35}S]GTPγS efficacy screening of buprenorphine and its analogues performed in either C6 glioma or cultured chinese hamster ovarian (CHO) transfected cells. Efficacies of buprenorphine and its analogues at 10 μM were compared against the standard receptor agonists (DAMGO, U-69593 and nociceptin) in triplicate. BU127 and BU10119 (marked in red) shows optimum profiles at targeted opioid receptors compared to the rest of the orvinol series (Traynor (unpublished work)).

For the series of compounds that was synthesised in this project (Figure 4.1 (A)), the aim was to introduce bulk around C_7 and C_{20}, by introducing a small group to the aromatic system in the hope of increasing the efficacy of the analogues at the ORL-1 receptors, while retaining the κ-opioid antagonist activity (Husbands (personal communication)) and very low μ- efficacy as seen with the lead compound (BU127) (Figure 4.2). Although the relative efficacy of the analogues at the ORL-1 receptors did increase (compared to the unsubstituted aromatic analogues, BU127, BU08026), unfortunately all the analogues with a small group attached to the aromatic substituents also showed sudden increase in their κ-opioid receptor efficacy (> 75% receptor stimulation relative to U-69593) (Figure 4.2). Also a surprise was that BU11001, an analogue of BU08026, with no group attached to the thiophene ring, showed completely different efficacy at the κ-opioid receptors. BU11001 (3-thiophene orvinol) has shown nearly full efficacy at the κ-opioid receptors (79 ± 2%) compared to BU08026 (2-thiophene) which had relatively lower κ-opioid receptor stimulation (30 ± 6%). Although increasing bulk by introducing a

small group on the aromatic substituent (C_{20}) has had the desired effect in increasing the efficacy of the analogues at the ORL-1 receptors, overall this modification has had a negative impact due to the increase in efficacy at the κ-opioid receptor. Related to the ORL-1 activity, only the efficacy of the analogues was increased with this modification, while the binding affinity was not greatly affected compared to buprenorphine and the lead compound (BU127). Although the binding affinity at ORL-1 of buprenorphine and its analogues was 1000-times lower than their binding affinity at the μ- and κ-opioid receptors, the *in vivo* effects on buprenorphine profile of ORL-1 stimulation are believed to be significant. For example, the bell-shaped-buprenorphine dose-response curve for buprenorphine-induced antinociception in the wild type mice was eliminated in the presence of ORL-1 antagonist (Lutfy *et al.*, 2003b). At the μ-opioid receptor, in general the binding affinity of the analogues with aromatic substituent increased compared to buprenorphine, but only to minimal extent (1-3 fold). The efficacy of the analogues towards the μ-opioid receptors has also decreased relative to buprenorphine with the aromatic substituent without the small group attached to their aromatic ring (BU127, BU08026, BU11001). Introducing a small group into the aromatic substituent has increased the efficacy of this series towards the μ-opioid receptors (lower efficacy to partial agonist). From these findings, it shows that in order to achieve the optimum opioid pharmacological profiles as mentioned before, at this point, the moiety needed with the analogues with general structure A is having at least 6-membered aromatic ring without any small group attach to the aromatic substituent.

For the orvinol with the general structure B (Figure 4.1), the important structure modification is the introduction of methyl at the C_7 position. From the [^{35}S]GTPγS efficacy screenings (Figure 4.2), compound BU10119 has shown the highest efficacy at the ORL-1 receptor among the rest of the analogues tested. This suggests that it is not necessary to have a group attached to the aromatic substituent in order to improve the efficacy of the analogues at the ORL-1 receptor. As shown by compound BU10119 (phenyl substituent), the methyl at C_7 also can act as bulk in place of the small group (eg: BU10101). Although it is hard to make definitive conclusions based on only a small number of compounds, BU10112 also provides evidence that the C_7-methyl group is beneficial in increasing ORL-1 efficacy and minimising stimulation of κ-opioid receptors. There is no big difference

in terms of binding affinity of this series compared to the series with general structure A (Figure 4.1). Therefore, it is suggested that for the orvinol with general structure B, essential features is having a small group at C_7 (eg: methyl).

Of all the analogues synthesised and evaluated, only compounds BU127 and BU10119 (Figure 4.3) have technically met the desired pharmacological profile at all targeted opioid receptors (Table 4.2) (Gerra *et al.*, 2006; McCann, 2008; Rothman *et al.*, 2000). The combined opioid profiles for the optimum buprenorphine analogues are partial efficacy at ORL-1 receptor, low efficacy or antagonism at the μ-opioid receptor and antagonism at the κ-opioid receptor (Figure 4.1). Although compound BU127 displayed some efficacy at the κ-opioid receptor in a [^{35}S]GTPγS assay, further *in vivo* studies (unpublished) conducted by Traynor's group has confirmed the lack of agonist activity of this compound. The assay (mouse tail withdrawal) was conducted in warmed water at 48°C, a very low stimulus intensity that would have allowed even a low efficacy κ-agonist to be found (Husbands (personal communication)).

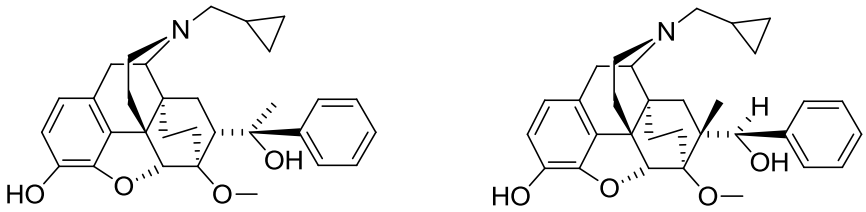

BU127 **(15)** BU10119

Figure 4.3: Compound BU127 **(15)** and BU10119.

Table 4.2: Pharmacological profile of compound BU127 **(15)** and BU10119 at μ-, κ- and ORL-1 receptors. The [^{35}S]GTPγS data were obtained from Traynor's group (unpublished work).

	BU127 (15)			BU10119		
	μ-	κ-	ORL-1	μ-	κ-	ORL-1
[^{35}S]GTPγS efficacy	6 ± 0%*	19 ± 0%*	14 ± 4%*	2 ± 4%*	-2 ± 1% *	57 ± 5% *
Binding affinity, K_B (nM)	0.05	0.3	1306	0.08	0.2	1762
Relative potency to standard antagonist	3.3	2.2	0.8	1.8	3.9	0.6

In this project, we rely on the shift in the agonist concentration-response curve in the presence of increasing concentration of antagonists, followed by Schild analysis to predict the reversibility of the compound synthesised (Kenakin, 2009). Schild analysis is a powerful tool to determine the affinity constant of an antagonist, while it indirectly evaluates the pharmacological behaviours of the compound such as the competitive / non-competitive receptor interaction and also the reversibility (dissociation) of the compound from the receptor. However, the evaluation of the pharmacological behaviours of the compound can also be misleading. The outcome of this assay system is highly reliant on the receptor reserve available in the tissue used. For example, a high affinity, potent antagonist does not need high receptor occupancy to exert its effects. In this case, this antagonist could actually be a non-competitive antagonist, however it can appear to show competitive reversible behaviour if there is sufficient unoccupied receptor left for the agonist. As a result, the parallel shift of the agonist concentration-response curve with no suppression of the maximal response still can be observed, unless a high dose of antagonist is used. Therefore, in future work another method that can be used to validate the competitive reversible antagonist behaviour of buprenorphine analogues evaluated from this project is by comparing the EC_{50} value of the standard agonist after repeated washing (Spagnolo *et al.*, 2007).

Due to time constraints and limited resources, only limited work was done at the κ-opioid receptor. From the [^{35}S]GTPγS result, most of the compounds synthesised in this project had substantial efficacy at the κ-opioid receptor. Although in general this could be related to the small group attached to the aromatic system, the different κ-opioid receptor efficacy shown by both BU08026 (2-thiophene) and BU11001 (3-thiophene) suggests further investigation. Therefore, the GPI preparation is suggested in order to evaluate the κ-opioid receptor efficacy in the isolated tissue preparation. GPI is a more sensitive tissue and commonly used to evaluate the compounds with κ-opioid receptor efficacy. Although the mouse vas deferens also has κ-opioid receptor, the receptor population is lower than in the GPI (Leslie, 1987).

Finally, since the introduction of C_7-methyl (orvinol with general structure B, Figure 4.1) has shown a promising overall pharmacological profile, further exploration of this series should be done to further our knowledge of the SAR, especially related to κ-opioid receptor efficacy.

References

Ahmed SH, Koob GF (1997). Cocaine- but not food-seeking behavior is reinstated by stress after extinction. *Psychopharmacology (Berl)* **132**(3)**:** 289-295.

Al-Khrasani M, Spetea M, Friedmann T, Riba P, Kiraly K, Schmidhammer H*, et al.* (2007). DAMGO and 6 beta-glycine substituted 14-O-methyloxymorphone but not morphine show peripheral, preemptive antinociception after systemic administration in a mouse visceral pain model and high intrinsic efficacy in the isolated rat vas deferens. *Brain Research Bulletin* **74**(5)**:** 369-375.

Alt A, Clark MJ, Woods JH, Traynor JR (2002). Mu and Delta opioid receptors activate the same G proteins in human neuroblastoma SH-SY5Y cells. *British Journal of Pharmacology* **135**(1)**:** 217-225.

Amass L, Kamien JB, Mikulich SK (2000). Efficacy of daily and alternate-day dosing regimens with the combination buprenorphine-naloxone tablet. *Drug and Alcohol Dependence* **58**(1-2)**:** 143-152.

(2010). Agonist-induced μ-opioid receptor desensitization in peripheral neurones. *BPS Winter Meeting 2010*; Queen Elizabeth II Conference Centre, London. British Pharmacological Society.

Armarego WLF, Chai CLL, Christina LL (2003). Purification of laboratory chemicals, 5th edn. Cornwall: Elsevier.

Atcheson R, Lambert DG (1994). Update on opioid receptors. *British Journal of Anaesthesia* **73**(2)**:** 132-134.

Beardsley PM, Howard JL, Shelton KL, Carroll FI (2005). Differential effects of the novel kappa opioid receptor antagonist, JDTic, on reinstatement of cocaine-seeking induced by footshock stressors vs cocaine primes and its antidepressant-like effects in rats. *Psychopharmacology* **183**(1)**:** 118-126.

Bell KM, Traynor JR (1998). Dynorphin A(1-8): stability and implications for in vitro opioid activity. *Canadian Journal of Physiology and Pharmacology* **76**(3)**:** 325-333.

Bentley KW, Hardy DG (1967a). Novel analgesics and molecular rearrangements in the morphine-thebaine group. I. Ketones derived from 6,14-endo-ethenotetrahydrothebaine *Journal of the American Chemical Society* **89**(13)**:** 3267-3273.

Bentley KW, Hardy DG (1967b). Novel analgesics and molecular rearrangements in the morphine-thebaine group. III. Alcohols of the 6,14-endo-ethenotetrahydrooripavine series and derived analogs of N-allylnormorphine and -norcodeine. *Journal of the American Chemical Society* **89**(13)**:** 3281-3292.

Bentley KW, Hardy DG, Crocker HP, Haddlese.Di, Mayor PA (1967c). Novel analgesics and molecular rearrangements in morphine-thebaine group .VI. Base-catalyzed rearrangements in 6,14-endo-ethenotetrahydrothebaine series. *Journal of the American Chemical Society* **89**(13)**:** 3312-3321.

Bentley KW, Hardy DG, Meek B (1967d). Novel analgesics and molecular rearrangements in the morphine-thebaine group. II. Alcohols derived from 6,14-endo-etheno- and 6,14-endo-ethanotetrahydrothebaine. *Journal of the American Chemical Society* **89**(13)**:** 3273-3280.

Bentley KW, Lewis JW (eds) (1972). *Agonist and antagonist actions of narcotic analgesic drugs*. University Park Press: London.

Berridge MJ (2008). Smooth muscle cell calcium activation mechanisms. *The Journal of Physiology* **586**(21)**:** 5047-5061.

Bidlack JM (2000). Detection and function of opioid receptors on cells from the immune system. *Clinical and Vaccine Immunology* **7**(5)**:** 719-723.

Bignan GC, Connolly PJ, Middleton SA (2005). Recent advances towards the discovery of ORL-1 receptor agonists and antagonists. *Expert Opinion on Therapeutic Patents* **15**(4)**:** 357-388.

Blakemore PR, White JD (2002). Morphine, the proteus of organic molecules. *Chemical Communications***:** 1159-1168.

Bloms-Funke P, Gillen C, Schuettler AJ, Wnendt S (2000). Agonistic effects of the opioid buprenorphine on the nociceptin/OFQ receptor. *Peptides* **21**(7)**:** 1141-1146.

Boas RA, Villiger JW (1985). Clinical actions of fentanyl and buprenorphine. The significance of receptor binding. *British Journal of Anaesthesia* **57**(2)**:** 192-196.

Boyle AE, Stewart RB, Macenski MJ, Spiga R, Johnson BA, Meisch RA (1998). Effects of acute and chronic doses of naltrexone on ethanol self-administration in rhesus monkeys. *Alcoholism: Clinical and Experimental Research* **22**(2)**:** 359-366.

Briand LA, Blendy JA (2010). Molecular and genetic substrates linking stress and addiction. *Brain Research* **1314:** 219-234.

Brody TM, Larner J, Minneman KP (1998). *Human pharmacology : molecular to clinical*. 3rd edn. Mosby: St. Louis, London.

Broom DC, Guo L, Coop A, Husbands SM, Lewis JW, Woods JH*, et al.* (2000). BU48: a novel buprenorphine analog that exhibits δ-opioid-mediated convulsions but not δ-opioid-mediated antinociception in mice. *The Journal of Pharmacology and Experimental Therapeutics* **294**(3)**:** 1195-1200.

Brown RM, Lawrence AJ (2009). Neurochemistry underlying relapse to opiate seeking behaviour. *Neurochemical Research* **34**(10)**:** 1876-1887.

Burnside JL, Rodriguez L, Toll L (2000). Species differences in the efficacy of compounds at the nociceptin receptor (ORL1). *Peptides* **21**(7)**:** 1147-1154.

Bustamante D, Miranda HF (1991). Differences in the bimodal effects of morphine in the vas deferens of two strains of rats. *Comparative Biochemistry and Physiology. C: Comparative Pharmacology* **100**(3)**:** 349-352.

Butour JL, Moisand C, Mollereau C, Meunier JC (1998). [Phe^{1}ψ(CH$_2$-NH)Gly^2]nociceptin-(1-13)-NH$_2$ is an agonist of the nociceptin (ORL1) receptor. *European Journal of Pharmacology* **349**(1)**:** R5-R6.

Calo G, Guerrini R, Rizzi A, Salvadori S, Regoli D (2000). Pharmacology of nociceptin and its receptor: a novel therapeutic target. *British Journal of Pharmacology* **129**(7)**:** 1261-1283.

Casy AF, Parfitt RT (1986). *Opioid analgesics : chemistry and receptors*. 1st edn. Plenum: New York ; London.

Chartoff EH, Papadopoulou M, Konradi C, Carlezon WA, Jr. (2003). Dopamine-dependent increases in phosphorylation of cAMP response element binding protein (CREB) during precipitated morphine withdrawal in primary cultures of rat striatum. *Journal of Neurochemistry* **87**(1)**:** 107-118.

Christie MJ (2008). Cellular neuroadaptations to chronic opioids: tolerance, withdrawal and addiction. *British Journal of Pharmacology* **154**(2)**:** 384-396.

Christoph T, Kogel B, Schiene K, Meen M, De Vry J, Friderichs E (2005). Broad analgesic profile of buprenorphine in rodent models of acute and chronic pain. *European Journal of Pharmacology* **507**(1-3)**:** 87-98.

Ciccocioppo R, Economidou D, Rimondini R, Sommer W, Massi M, Heilig M (2007). Buprenorphine reduces alcohol drinking through activation of the nociceptin/orphanin FQ-NOP receptor system. *Biological Psychiatry* **61**(1)**:** 4-12.

Connor M, Christie MD (1999). Opioid receptor signalling mechanisms. *Clinical and Experimental Pharmacology and Physiology* **26**(7)**:** 493-499.

Corbett AD, Paterson SJ, McKnight AT, Magnan J, Kosterlitz HW (1982). Dynorphin$_{1-8}$ and dynorphin$_{1-9}$ are ligands for the κ-subtype of opiate receptor. *Nature* **299**(5878)**:** 79-81.

Cowan A (2007). Buprenorphine: The basic pharmacology revisited. *Journal of Addiction Medicine* **1**(2)**:** 68-72.

Cowan A (1995). *Update on the general pharmacology of buprenorphine*. edn.

Cowan A, Doxey JC, Harry EJ (1977a). The animal pharmacology of buprenorphine, an oripavine analgesic agent. *British Journal of Pharmacology* **60**(4)**:** 547-554.

Cowan A, Lewis JW (eds) (1995). *Buprenorphine: combatting drug abuse with a unique opioid*. Wiley-Liss, Inc: New York.

Cowan A, Lewis JW, Macfarlane IR (1977b). Agonist and antagonist properties of buprenorphine, a new antinociceptive agent. *British Journal of Pharmacology* **60**(4)**:** 537-545.

Cowan A, Lewis JW, Macfarlane IR, Whittle BA (1971). Analgesic and dependence studies with oripavine partial agonists. *British Journal of Pharmacology* **43**(2)**:** 461P-462P.

Crabtree BL (1984). Review of naltrexone, a long-acting opiate antagonist. *Clinical Pharmacy* **3**(3)**:** 273-280.

Cruz SL, Villarreal JE, Volkow ND (1996). Further evidence that naloxone acts as an inverse opiate agonist: implications for drug dependence and withdrawal. *Life Sciences* **58**(26)**:** PL381-389.

Cunnane TC (1984). The mechanism of neurotransmitter release from sympathetic nerves *Trends in Neurosciencea* **7**(7).

Dahan A, Yassen A, Romberg R, Sarton E, Teppema L, Olofsen E*, et al.* (2006). Buprenorphine induces ceiling in respiratory depression but not in analgesia. *British Journal of Anaesthesia* **96**(5)**:** 627-632.

de Ligt RA, Kourounakis AP, AP IJ (2000). Inverse agonism at G protein-coupled receptors: (patho)physiological relevance and implications for drug discovery. *British Journal of Pharmacology* **130**(1)**:** 1-12.

Dean RL, Bilsky EJ, Negus SS (eds) (2009). *Opiate receptors and antagonist: from bench to clinic*. Humana Press: New York.

DePaoli AM, Hurley KM, Yasada K, Reisine T, Bell G (1994). Distribution of κ opioid receptor mRNA in adult mouse brain: an in situ hybridization histochemistry study. *Molecular and Cellular Neurosciences* **5**(4)**:** 327-335.

Dhaher R, Toalston JE, Hauser SR, Bell RL, McKinzie DL, McBride WJ*, et al.* (2012). Effects of naltrexone and LY255582 on ethanol maintenance, seeking, and relapse responding by alcohol-preferring (P) rats. *Alcohol* **46**(1)**:** 17-27.

Dole VP (1988). Implications of methadone maintenance for theories of narcotic addiction. *The Journal of the American Medical Association* **260**(20)**:** 3025-3029.

Downey KK, Helmus TC, Schuster CR (2000). Treatment of heroin-dependent poly-drug abusers with contingency management and buprenorphine maintenance. *Experimental and Clinical Psychopharmacology* **8**(2)**:** 176-184.

Downing JW, Leary WP, White ES (1977). Buprenorphine: a new potent long-acting synthetic analgesic. Comparison with morphine. *British Journal of Anaesthesia* **49**(3)**:** 251-255.

Dum J, Blasig J, Herz A (1981). Buprenorphrine: demonstration of physical dependence liability. *European Journal of Pharmacology* **70**(3)**:** 293-300.

Duvauchelle CL, Ikegami A, Castaneda E (2000). Conditioned increases in behavioral activity and accumbens dopamine levels produced by intravenous cocaine. *Behavioral Neuroscience* **114**(6)**:** 1156-1166.

Duvauchelle CL, Sapoznik T, Kornetsky C (1998). The synergistic effects of combining cocaine and heroin ("speedball") using a progressive-ratio schedule of drug reinforcement. *Pharmacology, Biochemistry and Behavior* **61**(3)**:** 297-302.

Edwards S, Graham DL, Bachtell RK, Self DW (2007). Region-specific tolerance to cocaine-regulated cAMP-dependent protein phosphorylation following chronic self-administration. *European Journal of Neuroscience* **25**(7)**:** 2201-2213.

Englberger W, Kogel B, Friderichs E, Strassburger W, Germann T (2006). Reversibility of opioid receptor occupancy of buprenorphine in vivo. *European Journal of Pharmacology* **534**(1-3)**:** 95-102.

Enna SJ, Nichael W, Ferkany JW, Kenakin T, Porsolt RD, Sullivan JP (eds) (1998). *Current protocols in pharmacology*. Wiley: New York.

Feltenstein MW, See RE (2008). The neurocircuitry of addiction: an overview. *British Journal of Pharmacology* **154**(2)**:** 261-274.

Fessenden RJ, Fessenden JS (1986). *Organic chemistry*. 3rd edn. Brooks/Cole Publishing Company: California.

Fischetti C, Rizzi A, Gavioli EC, Marzola G, Trapella C, Guerrini R*, et al.* (2009). Further studies on the pharmacological features of the nociceptin/orphanin FQ receptor ligand ZP120. *Peptides* **30**(2)**:** 248-255.

Fulmor W, Lancaster JE, Morton GO, Brown JJ, Howell CF, Nora CT*, et al.* (1967). Nuclear magnetic resonance studies in the 6,14-endo-ethenotetrahydrothebaine series. *Journal of the American Chemical Society* **89**(13)**:** 3322-3330.

Gaddum JH, Hameed KA, Hathway DE, Stephens FF (1954). Quantitative studies of antagonists for 5-hydroxytryptamine. *Quarterly Journal of Experimental Physiology and Cognate Medical Sciences* **40**(1)**:** 49-74.

Gerra G, Fantoma A, Zaimovic A (2006). Naltrexone and buprenorphine combination in the treatment of opioid dependence. *Journal of Psychopharmacology* **20**(6)**:** 806-814.

Gold MS, Pottash AL, Extein I, Martin DA, Finn LB, Sweeney DR*, et al.* (1981). Evidence for an endorphin dysfunction in methadone addicts: lack of ACTH response to naloxone. *Drug and Alcohol Dependence* **8**(3)**:** 257-262.

Gossop M (1988). Clonidine and the treatment of the opiate withdrawal syndrome. *Drug and Alcohol Dependence* **21**(3)**:** 253-259.

Grivas K Analogues of buprenorphine as treatments for opioid dependence. Doctor of Philosophy (PhD thesis), University of Bristol, Bristol, 1995.

Guerrini R, Calo G, Rizzi A, Bigoni R, Bianchi C, Salvadori S*, et al.* (1998). A new selective antagonist of the nociceptin receptor. *British Journal of Pharmacology* **123**(2)**:** 163-165.

Harrison C, Traynor JR (2003). The [^{35}S]GTPγS binding assay: approaches and applications in pharmacology. *Life Sciences* **74**(4)**:** 489-508.

Henderson G, Hughes J (1976). The effects of morphine on the release of noradrenaline from the mouse vas deferens. *British Journal of Pharmacology* **57**(4)**:** 551-557.

Heyliger SO, Jackson C, Rice KC, Rothman RB (1999). Opioid peptide receptor studies. 10. Nor-BNI differentially inhibits kappa receptor agonist-induced G-protein activation in the guinea pig caudate: further evidence of kappa receptor heterogeneity. *Synapse* **34**(4)**:** 256-265.

Hollinger MA (2008). *Introduction to pharmacology*. 3rd edn. CRC Press Boca Raton.

Huang P, Kehner GB, Cowan A, Liu-Chen LY (2001). Comparison of pharmacological activities of buprenorphine and norbuprenorphine: norbuprenorphine is a potent opioid agonist. *The Journal of Pharmacology and Experimental Therapeutics* **297**(2)**:** 688-695.

Hughes J, Kosterlitz HW, Leslie FM (1975). Effect of morphine on adrenergic transmission in the mouse vas deferens. Assessment of agonist and antogonist potencies of narcotic analgesics. *British Journal of Pharmacology* **53**(3)**:** 371-381.

Huidobro-Toro JP, Way EL (1981). Comparative study on the effect of morphine and the opioid-like peptides in the vas deferens of rodents: species and strain differences, evidence for multiple opiate receptors. *Life Sciences* **28**(12)**:** 1331-1336.

Husbands SM, Lewis JW (2000). Structural determinants of efficacy for κ opioid receptors in the orvinol series: 7,7-spiro analogues of buprenorphine. *Journal of Medicinal Chemistry* **43**(2)**:** 139-141.

Husbands SM, Neilan CL, Broadbear J, Grundt P, Breeden S, Aceto MD*, et al.* (2005). BU74, a complex oripavine derivative with potent kappa opioid receptor agonism and delayed opioid antagonism. *European Journal of Pharmacology* **509**(2-3)**:** 117-125.

Hutchins CW, Cooper GK, Purro S, Rapoport H (1981). 6-Demethoxythebaine and its conversion to analgesics of the 6,14-ethenomorphinan type. *Journal of Medicinal Chemistry* **24**(7)**:** 773-777.

Hutchins CW, Rapoport H (1984). Analgesics of the orvinol type. 19-Deoxy and 6,20-epoxy derivatives. *Journal of Medicinal Chemistry* **27**(4)**:** 521-527.

Hutchinson M, Kosterlitz HW, Leslie FM, Waterfield AA (1975). Assessment in the guinea-pig ileum and mouse vas deferens of benzomorphans which have strong antinociceptive activity but do not substitute for morphine in the dependent monkey. *British Journal of Pharmacology* **55**(4)**:** 541-546.

Johnson RE, Fudala PJ, Payne R (2005). Buprenorphine: considerations for pain management. *Journal of Pain and Symptom Management* **29**(3)**:** 297-326.

Johnson SW, North RA (1992). Opioids excite dopamine neurons by hyperpolarization of local interneurons. *The Journal of Neuroscience* **12**(2)**:** 483-488.

June HL, Cason CR, Chen SH, Lewis MJ (1998). Buprenorphine alters ethanol self-administration in rats: dose-response and time-dependent effects. *Psychopharmacology (Berl)* **140**(1)**:** 29-37.

Kajiwara M, Aoki K, Ishii K, Numata H, Matsumiya T, Oka T (1986). Agonist and antagonist actions of buprenorphine on three types of opioid receptor in isolated preparations. *Japan Journal of Pharmacology* **40**(1)**:** 95-101.

Kamei J, Saitoh A, Suzuki T, Misawa M, Nagase H, Kasuya Y (1995). Buprenorphine exerts its antinociceptive activity via μ_1-opioid receptors. *Life Sciences* **56**(15)**:** PL285-290.

Kamei J, Sodeyama M, Tsuda M, Suzuki T, Nagase H (1997). Antinociceptive effect of buprenorphine in μ_1-opioid receptor deficient CXBK mice. *Life Sciences* **60**(22)**:** PL 333-337.

Katz JL, Woods JH, Winger GD, Jacobson AE (1982). Compounds of novel structure having kappa-agonist behavioral effects in rhesus monkeys. *Life Sciences* **31**(20-21)**:** 2375-2378.

Kawamoto H, Ozaki S, Itoh Y, Miyaji M, Arai S, Nakashima H*, et al.* (1999). Discovery of the first potent and selective small molecule opioid receptor-like (ORL1) antagonist: 1-[(3R,4R)-1-cyclooctylmethyl-3- hydroxymethyl-4-piperidyl]-3-ethyl-1, 3-dihydro-2H-benzimidazol-2-one (J-113397). *Journal of Medicinal Chemistry* **42**(25)**:** 5061-5063.

Kenakin T (2002). Drug efficacy at G protein-coupled receptors. *Annual Review of Pharmacology and Toxicology* **42:** 349-379.

Kenakin TP (2009). *A pharmacological primer: theory, application, and methods*. 3rd edn. Academic Press: London.

Kenner GW, Stedman RJ (1952). The compounds of alkylamines with esters of azodicarboxylic acid. *Journal of the Chemical Society***:** 2089-2093.

Kirchmayer U, Davoli M, Verster AD, Amato L, Ferri A, Perucci CA (2002). A systematic review on the efficacy of naltrexone maintenance treatment in opioid dependence. *Addiction* **97**(10)**:** 1241-1249.

Kishioka S, Paronis CA, Lewis JW, Woods JH (2000). Buprenorphine and methoclocinnamox: agonist and antagonist effects on respiratory function in rhesus monkeys. *European Journal of Pharmacology* **391**(3)**:** 289-297.

Kitchen I (1984). *Textbook of in vitro practical pharmacology*. 1st edn. Blackwell Scientific: Oxford.

Knipmeyer LL, Rapoport H (1985). Analgesics of the 6,14-ethenomorphinan type. 6-deoxy-7α-orvinols and 6-deoxy-8α-orvinols. *Journal of Medicinal Chemistry* **28**(4)**:** 461-466.

Ko MC, Divin MF, Lee H, Woods JH, Traynor JR (2006). Differential in vivo potencies of naltrexone and 6β-naltrexol in the monkey. *The Journal of Pharmacology and Experimental Therapeutics* **316**(2)**:** 772-779.

Kopcho JJ, Schaeffer JC (1986). Selective O-demethylation of 7-α-(aminomethyl)-6,14-endo-ethenotetrahydrothebaine. *Journal of Organic Chemistry* **51**(9)**:** 1620-1622.

Kosten TR, Kleber HD, Morgan C (1989). Treatment of cocaine abuse with buprenorphine. *Biological Psychiatry* **26**(6)**:** 637-639.

Kosterlitz HW, Leslie FM, Waterfield AA (1975). Rates of onset and offset of action of narcotic analgesics in isolated preparations. *European Journal of Pharmacology* **32**(1)**:** 10-16.

Kosterlitz HW, Waterfield AA, Berthoud V (1973). Assessment of the agonist and antagonist properties of narcotic analgesic drugs by their actions on the morphine receptor in the guinea pig ileum. *Advances in Biochemical Psychopharmacology* **8**(0)**:** 319-334.

Kotick MP, Leland DL, Polazzi JO, Howes JF, Bousquet A (1983). Analgesic narcotic antagonists. 15. Potent narcotic agonist 7β-(arylalkyl)-4,5α-epoxymorphinans. *Journal of Medicinal Chemistry* **26**(7)**:** 1050-1056.

Kroutil J, Trnka T, Cerny M (2000). Selective N-debenzylation of benzylamino derivatives of 1,6-anhydro-beta-D-hexopyranoses. *Organic Letters* **2**(12)**:** 1681-1683.

La Regina A, Petrillo P, Sbacchi M, Tavani A (1988). Interaction of U-69,593 with μ-,δ- and κ-opioid binding sites and its analgesic and intestinal effects in rats. *Life Sciences* **42**(3)**:** 293-301.

Lacy CF, Armstrong LL, Goldman LP (2005). *Drug information handbook*. 7th edn. Ed.Lexi-Comp.

Largent-Milnes TM, Vanderah TW (2010). Recently patented and promising ORL-1 ligands: where have we been and where are we going? *Expert Opinion on Therapeutic Patents* **20**(3)**:** 291-305.

Law PY, Koehler JE, Loh HH (1982). Comparison of opiate inhibition of adenylate cyclase activity in neuroblastoma N18tG2 and neuroblastoma x glioma NG108-15 hybrid cell lines. *Molecular Pharmacology* **21**(2)**:** 483-491.

Le AD, Quan B, Juzytch W, Fletcher PJ, Joharchi N, Shaham Y (1998). Reinstatement of alcohol-seeking by priming injections of alcohol and exposure to stress in rats. *Psychopharmacology (Berl)* **135**(2)**:** 169-174.

Leander JD (1988). Buprenorphine is a potent κ-opioid receptor antagonist in pigeons and mice. *European Journal of Pharmacology* **151**(3)**:** 457-461.

Lee CWS, Yan JY, Chiang YC, Hung TW, Wang HL, Chiou LC*, et al.* (2011). Differential pharmacological actions of methadone and buprenorphine in human embryonic kidney 293 cells coexpressing human μ-opioid and opioid receptor-like 1 receptors. *Neurochemical Research* **36**(11)**:** 2008-2021.

Lemaire S, Magnan J, Regoli D (1978). Rat vas deferens: specific bioassay for endogenous opioid peptides. *British Journal of Pharmacology* **64**(3)**:** 327-329.

Leri F, Bruneau J, Stewart J (2003). Understanding polydrug use: review of heroin and cocaine co-use. *Addiction* **98**(1)**:** 7-22.

Leslie FM (1987). Methods used for the study of opioid receptors. *Pharmacological Reviews* **39**(3)**:** 197-249.

Lewis JW (1985). Buprenorphine. *Drug and Alcohol Dependence* **14**(3-4)**:** 363-372.

Lewis JW (1974). Ring C-bridged derivatives of thebaine and oripavine. *Advances in Biochemical Psychopharmacology* **8:** 123-136.

Lewis JW, Bentley KW, Cowan A (1971). Narcotic analgesics and antagonists. *Annual Review of Pharmacology* **11:** 241-270.

Lewis JW, Husbands SM (2004). The orvinols and related opioids: high affinity ligands with diverse efficacy profiles. *Current Pharmaceutical Design* **10**(7)**:** 717-732.

Liao CS, Day AR, Freer RJ (1981). Evidence for a single opioid receptor type on the field stimulated rat vas deferens. *Life Sciences* **29**(25)**:** 2617-2622.

Lizasoain I, Leza JC, Lorenzo P (1991). Buprenorphine: bell-shaped dose-response curve for its antagonist effects. *General Pharmacology* **22**(2)**:** 297-300.

Lobmaier P, Kornor H, Kunoe N, Bjorndal A (2008). Sustained-release naltrexone for opioid dependence. *Cochrane Database Systematic Review*(2)**:** CD006140.

Loew GH, Berkowitz DS (1979). Intramolecular hydrogen bonding and conformational studies of bridged thebaine and oripavine opiate narcotic agonists and antagonists. *Journal of Medicinal Chemistry* **22**(6)**:** 603-607.

Lord JA, Waterfield AA, Hughes J, Kosterlitz HW (1977). Endogenous opioid peptides: multiple agonists and receptors. *Nature* **267**(5611)**:** 495-499.

Lutfy K, Cowan A (2004). Buprenorphine: a unique drug with complex pharmacology. *Current Neuropharmacology* **2**(4)**:** 395-402.

Lutfy K, Do T, Maidment NT (2001). Orphanin FQ/nociceptin attenuates motor stimulation and changes in nucleus accumbens extracellular dopamine induced by cocaine in rats. *Psychopharmacology (Berl)* **154**(1)**:** 1-7.

Lutfy K, Eitan S, Bryant CD, Yang YC, Saliminejad N, Walwyn W*, et al.* (2003a). Buprenorphine-induced antinociception is mediated by μ-opioid receptors and compromised by concomitant activation of opioid receptor-like receptors. *The Journal of Neuroscience* **23**(32)**:** 10331-10337.

Lutfy K, Eitan S, Bryant CD, Yang YC, Saliminejad N, Walwyn W*, et al.* (2003b). Buprenorphine-induced antinociception is mediated by mu-opioid receptors and compromised by concomitant activation of opioid receptor-like receptors. *The Journal of Neuroscience* **23**(32)**:** 10331-10337.

Magnan J, Paterson SJ, Tavani A, Kosterlitz HW (1982). The binding spectrum of narcotic analgesic drugs with different agonist and antagonist properties. *Naunyn Schmiedeberg's Archives of Pharmacology* **319**(3)**:** 197-205.

Maldonado R, Severini C, Matthes HW, Kieffer BL, Melchiorri P, Negri L (2001). Activity of mu- and delta-opioid agonists in vas deferens from mice deficient in MOR gene. *British Journal of Pharmacology* **132**(7)**:** 1485-1492.

Mannelli P, Peindl K, Wu LT, Patkar AA, Gorelick DA (2012). The combination very low-dose naltrexone-clonidine in the management of opioid withdrawal. *The American Journal of Drug and Alcohol Abuse* **38**(3)**:** 200-205.

Marquez P, Nguyen AT, Hamid A, Lutfy K (2008). The endogenous OFQ/N/ORL-1 receptor system regulates the rewarding effects of acute cocaine. *Neuropharmacology* **54**(3)**:** 564-568.

Martin WR (1967). Opioid agonists. *Pharmacological Reviews* **19**(4)**:** 463-521.

Martin WR, Eades CG, Thompson JA, Huppler RE, Gilbert PE (1976). The effects of morphine- and nalorphine- like drugs in the nondependent and morphine-dependent chronic spinal dog. *The Journal of Pharmacology and Experimental Therapeutics* **197**(3)**:** 517-532.

Martin WR, Eades CG, Thompson WO, Thompson JA, Flanary HG (1974). Morphine physical dependence in the dog. *The Journal of Pharmacology and Experimental Therapeutics* **189**(3)**:** 759-771.

Marton J, Simon C, Hosztafi S, Szabo Z, Marki A, Borsodi A*, et al.* (1997). New nepenthone and thevinone derivatives. *Bioorganic and Medicinal Chemistry* **5**(2)**:** 369-382.

Mattick RP, Kimber J, Breen C, Davoli M (2008). Buprenorphine maintenance versus placebo or methadone maintenance for opioid dependence. *Cochrane Database Systematic Review*(2)**:** CD002207.

McCann DJ (2008). Potential of buprenorphine/naltrexone in treating polydrug addiction and co-occurring psychiatric disorders. *Clinical Pharmacology and Therapeutics* **83**(4)**:** 627-630.

McKnight AT, Corbett AD, Kosterlitz HW (1983). Increase in potencies of opioid peptides after peptidase inhibition. *European Journal of Pharmacology* **86**(3-4)**:** 393-402.

McLaughlin JP, Marton-Popovici M, Chavkin C (2003). κ opioid receptor antagonism and prodynorphin gene disruption block stress-induced behavioral responses. *The Journal of Neuroscience* **23**(13)**:** 5674-5683.

McLellan AT, Lewis DC, O'Brien CP, Kleber HD (2000). Drug dependence, a chronic medical illness: implications for treatment, insurance, and outcomes evaluation. *The Journal of the American Medical Association* **284**(13)**:** 1689-1695.

McPherson J, Rivero G, Baptist M, Llorente J, Al-Sabah S, Krasel C*, et al.* (2010). μ-opioid receptors: correlation of agonist efficacy for signalling with ability to activate internalization. *Molecular Pharmacology* **78**(4)**:** 756-766.

Mello NK, Lukas SE, Mendelson JH, Drieze J (1993). Naltrexone-buprenorphine interactions: effects on cocaine self-administration. *Neuropsychopharmacology* **9**(3)**:** 211-224.

Mello NK, Mendelson JH, Bree MP, Lukas SE (1989). Buprenorphine suppresses cocaine self-administration by rhesus monkeys. *Science* **245**(4920)**:** 859-862.

Menzies JR, Glen T, Davies MR, Paterson SJ, Corbett AD (1999). In vitro agonist effects of nociceptin and [$Phe^1\psi(CH_2\text{-}NH)Gly^2$]nociceptin(1-13)$NH_2$ in the mouse and rat colon and the mouse vas deferens. *European Journal of Pharmacology* **385**(2-3)**:** 217-223.

Meunier JC, Mollereau C, Toll L, Suaudeau C, Moisand C, Alvinerie P*, et al.* (1995). Isolation and structure of the endogenous agonist of opioid receptor-like ORL1 receptor. *Nature* **377**(6549)**:** 532-535.

Michne WF (1978). 2,6-Methano-3-benzazocine-11-propanols. Lack of antagonism between optical antipodes and observation of potent narcotic antagonism by two n-methyl derivatives. *Journal of Medicinal Chemistry* **21**(12)**:** 1322-1324.

Middaugh LD, Lee AM, Bandy AL (2000). Ethanol reinforcement in nondeprived mice: effects of abstinence and naltrexone. *Alcoholism: Clinical and Experimental Research* **24**(8)**:** 1172-1179.

Miller L, Shaw JS (1983). Multiple opiate receptors in the mouse vas deferens. *European Journal of Pharmacology* **90**(2-3)**:** 257-261.

Miller L, Shaw JS, Whiting EM (1986). The contribution of intrinsic activity to the action of opioids in vitro. *British Journal of Pharmacology* **87**(3)**:** 595-601.

Minozzi S, Amato L, Vecchi S, Davoli M, Kirchmayer U, Verster A (2011). Oral naltrexone maintenance treatment for opioid dependence. *Cochrane Database of Systematic Reviews*(2)**:** CD001333.

Mogil JS, Pasternak GW (2001). The molecular and behavioral pharmacology of the orphanin FQ/nociceptin peptide and receptor family. *Pharmacological Reviews* **53**(3)**:** 381-415.

MOH (2005). MMT guidelines: national methadone maintenance therapy guidelines. Putrajaya: Ministry of Health Malaysia.

Montoya ID, Gorelick DA, Preston KL, Schroeder JR, Umbricht A, Cheskin LJ*, et al.* (2004). Randomized trial of buprenorphine for treatment of concurrent opiate and cocaine dependence. *Clinical Pharmacology and Therapeutics* **75**(1)**:** 34-48.

Motulsky H (2007). The regression guide. San Diego, California: GraphPad Prism, Inc.

Mucha RF (1990). High-dose oral naltrexone: aversive response in drug-naive rat. *Biological Psychiatry* **27**(5)**:** 543-545.

Mucha RF, Millan MJ, Herz A (1985). Aversive properties of naloxone in non-dependent (naive) rats may involve blockade of central β-endorphin. *Psychopharmacology (Berl)* **86**(3)**:** 281-285.

Nicholson JR, Paterson SJ, Menzies JR, Corbett AD, McKnight AT (1998). Pharmacological studies on the "orphan" opioid receptor in central and peripheral sites. *Canadian Journal of Physiology and Pharmacology* **76**(3)**:** 304-313.

NIDA (2010). Commonly abused drugs. United States: National Institute on Drug Abuse (https://www.drugabuse.gov/sites/default/files/cadchart.pdf).

Noda J, Umeda S, Arai T, Harima A, Mori K (1989). Continuous subcutaneous infusion of buprenorphine for cancer pain control. *The Clinical Journal of Pain* **5**(2)**:** 147-152.

Nutt D, Lingford-Hughes A (2008). Addiction: the clinical interface. *British Journal of Pharmacology* **154**(2)**:** 397-405.

Nyberg K, Ostman B, Wallerbe.G (1970). Investigations of dithienylglycolic esters .1. Preparation of methyl dithienylglycolates - magnetically nonequivalent protons in dithienylglycolates. *Acta Chemica Scandinavica* **24**(5)**:** 1590-1596.

Okada K, Sujaku T, Chuman Y, Nakashima R, Nose T, Costa T*, et al.* (2000). Highly potent nociceptin analog containing the Arg-Lys triple repeat. *Biochemical and Biophysical Research Communications* **278**(2)**:** 493-498.

Park YW, Cummings RT, Wu L, Zheng S, Cameron PM, Woods A*, et al.* (1999). Homogeneous proximity tyrosine kinase assays: scintillation proximity assay versus homogeneous time-resolved fluorescence. *Analytical Biochemistry* **269**(1)**:** 94-104.

Paronis CA, Bergman J (2011). Buprenorphine and opioid antagonism, tolerance, and naltrexone-precipitated withdrawal. *The Journal of Pharmacology and Experimental Therapeutics* **336**(2)**:** 488-495.

Pfeiffer A, Brantl V, Herz A, Emrich HM (1986). Psychotomimesis mediated by κ opiate receptors. *Science* **233**(4765)**:** 774-776.

Ponizovsky AM, Grinshpoon A, Margolis A, Cohen R, Rosca P (2006). Well-being, psychosocial factors, and side-effects among heroin-dependent inpatients after detoxification using buprenorphine versus clonidine. *Addictive Behaviors* **31**(11)**:** 2002-2013.

Pontieri FE, Tanda G, Di Chiara G (1995). Intravenous cocaine, morphine, and amphetamine preferentially increase extracellular dopamine in the "shell" as compared with the "core" of the rat nucleus accumbens. *Proceedings of the National Academy of Sciences of the United States of America* **92**(26)**:** 12304-12308.

Portoghese PS, Lipkowski AW, Takemori AE (1987). Binaltorphimine and nor-binaltorphimine, potent and selective κ-opioid receptor antagonists. *Life Sciences* **40**(13)**:** 1287-1292.

Rang HP, Dale MM, RItter JM, Flower RJ (2007). *Pharmacology*. 6 edn. Churchill Livingstone: Philadelphia.

Redila VA, Chavkin C (2008). Stress-induced reinstatement of cocaine seeking is mediated by the kappa opioid system. *Psychopharmacology (Berl)* **200**(1)**:** 59-70.

Reinscheid RK, Ardati A, Monsma FJ, Jr., Civelli O (1996). Structure-activity relationship studies on the novel neuropeptide orphanin FQ. *The Journal of Biological Chemistry* **271**(24)**:** 14163-14168.

Riba P, Friedmann T, Kiraly KP, Al-Khrasani M, Sobor M, Asim MF*, et al.* (2010). Novel approach to demonstrate high efficacy of μ opioids in the rat vas deferens: a simple model of predictive value. *Brain Research Bulletin* **81**(1)**:** 178-184.

Rice KC (1977). A rapid, high-yield conversion of codeine to morphine. *Journal of Medicinal Chemistry* **20**(1)**:** 164-165.

Rizzi A, Molinari S, Marti M, Marzola G, Calo G (2011). Nociceptin/orphanin FQ receptor knockout rats: in vitro and in vivo studies. *Neuropharmacology* **60**(4)**:** 572-579.

Rothman RB, Gorelick DA, Heishman SJ, Eichmiller PR, Hill BH, Norbeck J*, et al.* (2000). An open-label study of a functional opioid κ antagonist in the treatment of opioid dependence. *Journal of Substance Abuse Treatment* **18**(3)**:** 277-281.

Rutten K, De Vry J, Bruckmann W, Tzschentke TM (2010). Effects of the NOP receptor agonist Ro65-6570 on the acquisition of opiate- and psychostimulant-induced conditioned place preference in rats. *European Journal of Pharmacology* **645**(1-3)**:** 119-126.

Rutten K, De Vry J, Bruckmann W, Tzschentke TM (2011). Pharmacological blockade or genetic knockout of the NOP receptor potentiates the rewarding effect of morphine in rats. *Drug and Alcohol Dependence* **114**(2-3)**:** 253-256.

Sakurada C, Sakurada S, Orito T, Tan-No K, Sakurada T (2002). Degradation of nociceptin (orphanin FQ) by mouse spinal cord synaptic membranes triggered by endopeptidase-24.11: an *in vitro* and *in vivo* study. *Biochemical Pharmacology*(64)**:** 1293-1303.

SAMHSA (2004). Clinical guidelines for the use of buprenorphine in the treatment of opioid addiction: A treatment improve protocol.

Satoh M, Minami M (1995). Molecular pharmacology of the opioid receptors. *Pharmacology and Therapeutics* **68**(3)**:** 343-364.

Saxena S (2010). *ATLAS of substance use: resources for the treatment and prevention of substance disorder*. France: World Health Organization (WHO).

Schmitz JM, Stotts AL, Rhoades HM, Grabowski J (2001). Naltrexone and relapse prevention treatment for cocaine-dependent patients. *Addictive Behaviors* **26**(2)**:** 167-180.

Schulz R, Faase E, Wuster M, Herz A (1979). Selective receptors for β-endorphin on the rat vas deferens. *Life Sciences* **24**(9)**:** 843-849.

Shaham Y (1996). Effect of stress on opioid-seeking behavior: evidence from studies with rats. *Annals of Behavioral Medicine* **18**(4)**:** 255-263.

Shaqura MA, Zollner C, Mousa SA, Stein C, Schafer M (2004). Characterization of μ opioid receptor binding and G protein coupling in rat hypothalamus, spinal cord, and primary afferent neurons during inflammatory pain. *The Journal of Pharmacology and Experimental Therapeutics* **308**(2)**:** 712-718.

Sheehan M, Elliott M (1993). *The Glaxo pocket guide to pharmacology*. 3rd edn. GlaxoWellcome: Herts.

Sheehan MJ, Hayes AG, Tyers MB (1988). Lack of evidence for ε-opioid receptors in the rat vas deferens. *European Journal of Pharmacology* **154**(3)**:** 237-245.

Shoaib M, Spanagel R, Stohr T, Shippenberg TS (1995). Strain differences in the rewarding and dopamine-releasing effects of morphine in rats. *Psychopharmacology* **117**(2)**:** 240-247.

Smissman EE, Makriyannis A (1973). Azodicarboxylic acid esters as dealkylating agents. *Journal of Organic Chemistry* **38**(9)**:** 1652-1657.

Smith CFC, Rance MJ (1983). Opiate receptors in the rat vas deferens. *Life Sciences* **33:** 327-330.

Spagnolo B, Calo G, Polgar WE, Jiang F, Olsen CM, Berzetei-Gurske I*, et al.* (2008). Activities of mixed NOP and μ-opioid receptor ligands. *British Journal of Pharmacology* **153**(3)**:** 609-619.

Spagnolo B, Carra G, Fantin M, Fischetti C, Hebbes C, McDonald J*, et al.* (2007). Pharmacological characterization of the nociceptin/orphanin FQ receptor antagonist SB-612111 [(-)-cis-1-methyl-7-[[4-(2,6-dichlorophenyl)piperidin-1-yl]methyl]-6,7,8,9 -tetrahydro-5H-benzocyclohepten-5-ol]: in vitro studies. *The Journal of Pharmacology and Experimental Therapeutics* **321**(3)**:** 961-967.

Spanagel R, Weiss F (1999). The dopamine hypothesis of reward: past and current status. *Trends in Neurosciences* **22**(11)**:** 521-527.

Stephenson RP (1956). A modification of receptor theory. *British Journal of Pharmacology* **11**(4)**:** 379-393.

Takemori AE, Ho BY, Naeseth JS, Portoghese PS (1988). Nor-binaltorphimine, a highly selective kappa-opioid antagonist in analgesic and receptor-binding assays. *The Journal of Pharmacology and Experimental Therapeutics* **246**(1)**:** 255-258.

Terenius L, Sandin J, Sakurada T (2000). Nociceptin/orphanin FQ metabolism and bioactive metabolites. *Peptides* **21**(7)**:** 919-922.

Testaferri L, Tiecco M, Tingoli M, Chianelli D, Montanucci M (1982). Selective dealkylations of aryl alkyl ethers and thioethers by sodium in HMPA. *Tetrahedron* **38**(24)**:** 3687-3692.

Thatcher DL, Clark DB (2008). Adolescents at risk for substance abuse disorders: role of psychological dysregulation, endophenotypes, and environmental influences. *Alcohol Research and Health* **31**(2)**:** 168-176.

Tkacz J, Severt J, Cacciola J, Ruetsch C (2012). Compliance with buprenorphine medication-assisted treatment and relapse to opioid use. *The American Journal on Addictions* **21**(1)**:** 55-62.

Toll L, Berzetei-Gurske IP, Polgar WE, Brandt SR, Adapa ID, Rodriguez L*, et al.* (1998). Standard binding and functional assays related to medications development division testing for potential cocaine and opiate narcotic treatment medications. *NIDA Research Monographs* **178:** 440-466.

Toll L, Khroyan TV, Polgar WE, Jiang F, Olsen C, Zaveri NT (2009). Comparison of the antinociceptive and antirewarding profiles of novel bifunctional nociceptin receptor/μ-opioid receptor ligands: implications for therapeutic applications. *The Journal of Pharmacology and Experimental Therapeutics* **331**(3)**:** 954-964.

Traynor JR, Nahorski SR (1995). Modulation by μ-opioid agonists of guanosine-5'-O-(3-[^{35}S]thio)triphosphate binding to membranes from human neuroblastoma SH-SY5Y cells. *Molecular Pharmacology* **47**(4)**:** 848-854.

Trigo JM, Martin-Garcia E, Berrendero F, Robledo P, Maldonado R (2010). The endogenous opioid system: a common substrate in drug addiction. *Drug and Alcohol Dependence* **108**(3)**:** 183-194.

UNODC (2010). *World Drug Report 2010* Vienna: United Nations Office on Drugs and Crime.

Uwai K, Uchiyama H, Sakurada S, Kabuto C, Takeshita M (2004). Syntheses and receptor-binding studies of derivatives of the opioid antagonist naltrexone. *Bioorganic and Medicinal Chemistry* **12**(2)**:** 417-421.

Van Dorpe S, Adriaens A, Polis I, Peremans K, Van Bocxlaer J, De Spiegeleer B (2010). Analytical characterization and comparison of the blood-brain barrier permeability of eight opioid peptides. *Peptides* **31**(7)**:** 1390-1399.

Varty GB, Lu SX, Morgan CA, Cohen-Williams ME, Hodgson RA, Smith-Torhan A*, et al.* (2008). The anxiolytic-like effects of the novel, orally active nociceptin opioid receptor agonist 8-[bis(2-methylphenyl)methyl]-3-phenyl-8-azabicyclo[3.2.1]octan-3-ol (SCH 221510). *The Journal of Pharmacology and Experimental Therapeutics* **326**(2)**:** 672-682.

Vauquelin G, Mentzer BV (2007). *G protein-coupled receptors: molecular pharmacology from academic concept to pharmaceutical research*. 1st edn. John Wiley & Sons, Ltd: Chichester.

Walsh SL, Preston KL, Stitzer ML, Cone EJ, Bigelow GE (1994). Clinical pharmacology of buprenorphine: ceiling effects at high doses. *Clinical Pharmacology and Therapeutics* **55**(5)**:** 569-580.

Ward SJ, Portoghese PS, Takemori AE (1982). Improved assays for the assessment of κ-properties and δ-properties of opioid ligands. *European Journal of Pharmacology* **85**(2)**:** 163-170.

Weiss F, Ciccocioppo R, Parsons LH, Katner S, Liu X, Zorrilla EP*, et al.* (2001). Compulsive drug-seeking behavior and relapse. Neuroadaptation, stress, and conditioning factors. *Annals New York Academy of Sciences* **937:** 1-26.

Westfall TD, Westfall DP (2001). Pharmacological techniques for the in vitro study of the vas deferens. *Journal of Pharmacological and Toxicological Methods* **45**(2)**:** 109-122.

WHO (2009). Guidelines for the psychosocially assisted pharmacological treatment of opioid dependence. Geneva: WHO Press.

Wnendt S, Kruger T, Janocha E, Hildebrandt D, Englberger W (1999). Agonistic effect of buprenorphine in a nociceptin/OFQ receptor-triggered reporter gene assay. *Molecular Pharmacology* **56**(2)**:** 334-338.

Yassen A, Olofsen E, Dahan A, Danhof M (2005). Pharmacokinetic-pharmacodynamic modeling of the antinociceptive effect of buprenorphine and fentanyl in rats: role of receptor equilibration kinetics. *The Journal of Pharmacology and Experimental Therapeutics* **313**(3)**:** 1136-1149.

Yin HS, Chen K, Kalpana S, Shih JC (2006). Differential effects of chronic amphetamine and baclofen administration on cAMP levels and phosphorylation of CREB in distinct brain regions of wild type and monoamine oxidase B-deficient mice. *Synapse* **60**(8)**:** 573-584.

Zaratin PF, Petrone G, Sbacchi M, Garnier M, Fossati C, Petrillo P*, et al.* (2004). Modification of nociception and morphine tolerance by the selective opiate receptor-like orphan receptor antagonist (-)-cis-1-methyl-7-[[4-(2,6-dichlorophenyl)piperidin-1-yl]methyl]-6,7,8,9- tetrahydro-5H-benzocyclohepten-5-ol (SB-612111). *The Journal of Pharmacology and Experimental Therapeutics* **308**(2)**:** 454-461.

Zaveri N, Jiang F, Olsen C, Polgar W, Toll L (2005). Small-molecule agonists and antagonists of the opioid receptor-like receptor (ORL1, NOP): ligand-based analysis of structural factors influencing intrinsic activity at NOP. *American Association of Pharmaceutical Scientists Journal* **7**(2)**:** E345-352.

Zaveri NT (2011). The nociceptin/Orphanin FQ receptor (NOP) as a target for drug abuse medications. *Current Topics in Medicinal Chemistry* **11**(9)**:** 1151-1156.

Zeilhofer HU, Calo G (2003). Nociceptin/orphanin FQ and its receptor - potential targets for pain therapy? *The Journal of Pharmacology and Experimental Therapeutics* **306**(2)**:** 423-429.

Zhao GM, Qian X, Schiller PW, Szeto HH (2003). Comparison of [Dmt^1]DALDA and DAMGO in binding and G protein activation at μ, δ, and κ opioid receptors. *The Journal of Pharmacology and Experimental Therapeutics* **307**(3)**:** 947-954.

Appendix I:

Definition for pharmacology parameters (Sheehan *et al.*, 1993)

EC_{50} The molar concentration of an agonist which produces 50% of the maximum possible response for that agonist.

ED_{50} Dose of drug which produces 50% of its maximum response effect.

IC_{50} The molar concentration which produces 50% of its maximum possible inhibition (for functional assay).

or

The concentration of competing ligand which displaces 50% of the specific binding of the radioligand (for receptor binding assay).

K_B The dissociation equilibrium constant for a competitive antagonist; the concentration which could occupy 50% of the receptors at equilibrium.

K_i The inhibition constant for a drug; the concentration of competing ligand in a competition assay which would occupy 50% of the receptors if no radioligand were present.

pA_2 A logarithmic measure of the potency of an agonist; the negative log of the concentration of antagonist which would produce a 2-fold shift in the concentration-response curve for an agonist.

pK_B A measure of the potency of a competitive antagonist; the negative log of the molar concentration which at equilibrium would occupy 50% of the receptors in the absence of agonist.

pEC_{50} The negative log of EC_{50}